CONDUCTANCE, TRANSFERENCE NUMBER AND ELECTROMOTIVE FORCE MEASUREMENTS OF POTASSIUM SOLUTIONS IN LIQUID AMMONIA AT-87°C:

Thesis for the Degree of Ph. D. MICHIGAN STATE UNIVERSITY
Gale Eugene Smith
1963

THESIS

LIBRARY
Michigan State
University

ABSTRACT

CONDUCTANCE, TRANSFERENCE NUMBER AND ELECTROMOTIVE FORCE MEASUREMENTS OF POTASSIUM SOLUTIONS IN LIQUID AMMONIA AT -37° C.

by Gale Eugene Smith

The details of conductance, transference number and electromotive force studies are given for solutions of potassium dissolved in liquid ammonia at -37.0°C. Conductance measurements are also described for <u>deutero</u>-ammonia solutions of potassium at the same temperature.

Two conductance cells and procedures are described. One of the cells was designed principally to improve upon the precision of the conductance data in the literature. Known quantities of solvent can be added with adequate stirring after each addition. The procedure is then reversed by removing known portions of the solvent to reconcentrate the solution. This procedure permits the determination of the amount of decomposition which occurs during the experiment, and allows the data to be corrected for this decomposition. The equivalent conductance at infinite dilution, Λ^2 , at -37.0°C was found to be 1042 cm² mho equiv-1 from a Shedlovsky analysis, and was computed to be 1103 at -33.5°. The concentration range investigated ranged from 0.00068 to 0.40 molar. Comparison of the potassium conductivities with published sodium conductivities suggest that the Λ^0 of the latter at -33.5° is nearer to 1040 than the accepted value of 1022.

A second conductivity cell and procedure is described which was designed to incorporate into a single experiment the ability to cover a large concentration range using only a small quantity of solvent.

This procedure was checked against potassium-ammonia solutions and applied to potassium <u>deutero-ammonia</u> solutions. The latter displayed conductivities 28 to 30% below those of ammonia at concentrations below 0.25 molar. A viscosity contribution appears to account for a decrease of about 21%. Λ° at -37.0° for <u>deutero-ammonia</u> solution of potassium is 856 and at -33.5° it is estimated to be 900.

Transference number measurements were made by the moving boundary method at -37.0°. Conductivity as well as titrimetric techniques are described for determining the concentration of the metal solutions in the cell. A complete description of the procedure and suggestions for the improvement of the apparatus are also given. These data combined with the conductance data showed the cationic conductance to decrease monotonically as the concentration increases, but the conductance of the anionic species goes through a minimum similar to the total conductance.

The cell used for electromotive force studies employed a constrained diffusion boundary across a fritted disk and conductivity cells for measuring the concentrations. The concentration range explored was from 0.000104 to 0.435 molar (average concentration in the two compartments).

The data obtained in this investigation were used to compute K_1 and K_2 for the following equilibria

$$K^{+} \cdot e^{-} \rightleftharpoons K^{+} + e^{-} \qquad K_{1} = \frac{(K^{+}) \cdot (e^{-})}{(K^{+} \cdot e^{-})} \quad f \neq^{2}$$

$$K^{+} \cdot e^{-} \rightleftharpoons \frac{1}{2} K_{2} \qquad K_{2} = \frac{(K_{2})^{\frac{1}{2}}}{(K^{+} \cdot e^{-})}$$

The treatment of the conductivity data failed to yield satisfactory constants. The emf data were used to compute activity coefficients with the aid of transference number measurements. These activity coefficients readily allowed the calculation of the constants: $K_1 = 4.3 \times 10^{-3}$ and $K_2 = 13.4$.

In a simple apparatus, transient colors were observed by the deposition of a potassium metal film onto ice which had been previously degassed. In regions thought to be of high metal content a coppercolored film appeared which changed to the familiar blue seen for metal-ammonia solutions as the reaction progressed and before all of the metal reacted with the water.

CONDUCTANCE, TRANSFERENCE NUMBER AND ELECTROMOTIVE FORCE MEASUREMENTS OF POTASSIUM SOLUTIONS IN LIQUID AMMONIA AT -37° C.

By

Gale Eugene Smith

A THESIS

Submitted to
Michigan State University
in partial fulfillment of the requirements
for the degree of

DOCTOR OF PHILOSOPHY

Department of Chemistry

331777

To my Mother and in memory of my Father

ACKNOWLEDGMENTS

The author wishes to express his sincere appreciation to Professor James L. Dye for his guidance, encouragement, and friendship throughout the course of this investigation.

He also wishes to extend his appreciation to Mr. Forrest Hood for the intricate glasswork used in this investigation as well as the acquisition of glassblowing techniques; to Mr. Frank Betts for his advice and to a colleague, Dr. Kenneth Vos, for his help in time of need.

Financial aid from the Atomic Energy Commission is gratefully acknowledged.

TABLE OF CONTENTS

CHAPTE	SR.	Page
I.	INTRODUCTION	1
II.	HISTORICAL	. 5
	A. Introduction	, 5
	B. Conductance	. 6
	1. Ammonia Solutions	. 11
	2. Conductivities in the Amines	. 13
	3. Inorganic Salts in Ammonia	. 14
	4. Inorganic Salts in Methylamine	. 15
	C. Transference Numbers	. 15
	D. Electromotive Force Measurements	. 17
III.	THEORY	. 21
	A. Introduction	. 21
	B. Conductance	. 21
	C. Transference Numbers	. 22
	D. Electromotive Force	. 29
IV.	EXPERIMENTAL	34
	A. Basic Apparatus and Procedures	. 34
	1. Basic Vacuum System	34

TABLE OF CONTENTS - Continued

HAPTER	Page
2. Helium Gas Purification	36
3. Ammonia Purification	37
4. Preparation of Ampoules of Metal	39
5. Preparation of deutero-Ammonia	45
6. Thermostat	48
7. Temperature Measurement	49
8. Circulating System and Bubble Remover	49
9. Conductance Bridge	50
10. Switching Network	51
B. Conductance Methods	54
l. Objective	54
2. Conductance Cell A	56 58 60 64 68 68 68 71 76
Volumetric Flask Calibrations	. 83
C. Transference Numbers	. 83
l. The Cell	. 83

TABLE OF CONTENTS - Continued

HAPTER	Page
2. Current Controller	87
3. Recommended Procedure for Transference Run	88
4. Comments on Individual Runs	97
D. Electromotive Force	100
l. The Cell	100
2. Procedure for EMF Run	105
3. Comments on Individual Runs	107
E. Metal Film Deposit on Ice	109
V. EXPERIMENTAL RESULTS	113
A. Conductance Data	113
1. Data from Cell A	113
2. Data from Cell B	130
3. Cell Constant Dependence upon Concentration	143
4. Temperature Coefficient	147
B. Transference Numbers	150
1. Typical Set of Experimental Data Analytical Results Data and Preliminary Results Corrections	150 151 151 153
2. Summary	156

TABLE OF CONTENTS - Continued

CHAPTE	R	Page
	C. Electromotive Force	158
VI.	DISCUSSION	169
	A. Conductance	169
	1. Results Using Cell A	169
	2. Amide Ion Conductance	170
	3. Results Using Cell B	171
	4. Calculation of \bigwedge^{o}	174
	5. Calculation of T	181
	6. Temperature Coefficient	181
	7. Ionic Conductances	182
	B. Transference Numbers	182
	C. Electromotive Force	186
	D. Calculation of K_1 and K_2 from Cationic Conductance	187
	E. Calculation of K_1 and K_2 from Activity Coefficients	192
	F. Activities and Thermodynamic Quantities	198
	G. Suggested Future Work and Concluding Remarks	205
REFEREI	NCES	210
APPENDI	CFS	216

LIST OF TABLES

TABLE Page
1. Summary of Equilibrium Constants for Solution of Metals in Ammonia and Methylamine
2. Summary of Conductance Determinations for Metal Solutions of Ammonia and Amines 8-9
3. Summary of Transference Number Data for Sodium-Ammonia Solutions
4. Switch Positions and Corresponding Electrode Connections
5. Comparison of Metal Content by Weight and by Titration
6. Calibrations of Volumetric Flasks 83
7. Conductance Data for Solutions of Potassium in Liquid Ammonia Using Cell A
8. Conductance Data for Solutions of Potassium in Liquid Ammonia Using Cell B
9. Conductance Data for Solutions of Potassium in Liquid deutero-Ammonia Using Cell B 138-141
10. Observed Data from Notebook for Runs 42-K-8 a and b 151
11. Comparison of Average Uncorrected Transference Numbers Using Concentrations from Conductance and Titration
12. Resistance and Concentration Data at Various Times During Runs 42-K-8 a and b
13. Summary of Corrections Applied to Transference Number Data

LIST OF TABLES - Continued

TABLE	ge
14. Summary of Corrected Transference Numbers 15	57
15. Total and Ionic Equivalent Conductances and Transference Numbers for Potassium-Ammonia Solutions at -37.0°C	60
16. Potentials from Concentration Cells with Transference for Potassium-Ammonia Solutions at -37.0°C and the Apparent Transference Numbers	67
17. Conductance Ratio of K-NH ₃ to K-ND ₃ Solutions and Viscosity Ratio of These Solutions	74
18. Selected Values of $K_1^{(a)}$, $K_1^{(t)}$ and K_2 Calculated from Cationic Conductance	91
19. Smoothed Data for Activity Coefficient Calculations of Potassium-Ammonia Solutions at -37.0°C	93
20. K_2 Required for Various Values of $K_1^{(t)}$	95
21. Comparison of Observed and Calculated Activity Coefficients for Dilute Potassium-Ammonia Solutions	96
22. Activity of Sodium and Potassium in Ammonia Over Entire Range of Solubility	01
23. Thermodynamic Functions for the Process: $M_{(s)} \rightarrow M_{(a m)}^{+} + e_{(a m)}^{-} \dots \dots$	04

LIST OF FIGURES

FIGURE	age
l. Equivalent conductance versus (molarity) ¹ for potassium in liquid ammonia	12
2. Anion transference number of sodium in liquid ammonia from paper of Dye, Sankuer and Smith	18
3. Schematic of a moving boundary	24
4. Schematic of volume changes in moving boundary	27
5. Basic vacuum system; ammonia and helium gas purification trains	35
6. Metal purification apparatus	40
7. Diagram of ampoule and ampoule-filling assembly	42
8. Apparatus for preparation of deutero-ammonia	46
9. Bubble remover for closed-loop circulating systems	50
10. Schematic of switching network for conductance cell B, emf cell, and modified transference cell	52
11. Diagram of conductance cell A	57
12. Diagram of stirring mechanism for use with conductance cell A	59
13. Schematic diagram of conductance cell A and associated apparatus	61
14. Diagram of conductance cell B	69
15. Schematic diagram of conductance cell B and associated apparatus	72

LIST OF FIGURES - Continued

FIGURE	Page
16. Resistance versus (frequency) showing dependence upon calibrating solutions	81
17. Cell constant versus specific conductance showing the variation of cell constant with calibrating solution and electrode surface	81
18. Diagram of transference cell and associated apparatus	84
19. Photograph of transference cell	85
20. Photographic enlargement of boundary	85
21. Suggested modification of boundary stopcock	97
22. Diagram of emf cell	-103
23. Apparatus to illustrate blue color of potassium metal film deposited on ice	111
24. Equivalent conductance versus (molarity) for CK-8 at -37.0°C	127
25. Equivalent conductance versus (molarity) for CK-11 at -37.0°C	128
26. Equivalent conductance versus (molarity) using data obtained from cell A	129
27. Comparison of smoothed values of equivalent conductance versus (molarity) from cell A with those obtained from cell B using cell constants determined with KCl.	142
28. Variation of cell constant ratio (k_B'/k_B) with square root of concentration	145
29. Equivalent conductance versus (molarity) for potassium solutions of ammonia and deutero-ammonia at -37.0°C	146

LIST OF FIGURES - Continued

FIGURE	Page
30. Resistance versus temperature from run CK-10	148
31. Solution resistance versus clock time for transference run 42-K-8 a and b	152
32. Anion transference number of potassium in liquid ammonia at -37.0°C	159
33. Anionic and cationic conductances for potassium- ammonia solutions at -37.0°C	161
34. The experimental emf data plotted in differential form and the resulting integral curve. Data are for potassium in ammonia at -37.0°C	163
35. Recorder tracing of potentials for run EK-2:: solution 29-a	168
36. Conductance and viscosity ratios between ammonia and deutero-ammonia solution versus (molarity)	175
37. Shedlovsky analysis of conductance data for potassium-ammonia solutions at -37.0°C and sodium-ammonia solutions at -33.5°C	178
38. Mean molar activity coefficient of potassium in liquid ammonia at -37.0°C	197
39. Activity of sodium and potassium in ammonia versus (molality) 2; standard state is pure solid metal. Data are at -35°C	202
40. A suggested Hittorf transference apparatus for closed systems	206

LIST OF APPENDICES

APPEND		Page
Α.	Schematic Diagram of Conductance Bridge	217
В.	Schematic Diagram of Current Controller	222
c.	Analysis of Error Entailed in the Successive Dilution Procedure Used with Cell B	224
D.	Derivation of Interdependence of $K_1^{(a)}$, $K_1^{(t)}$ and K_2 .	227

CHAPTER I

INTRODUCTION

Ammonia, some of its organic derivatives, a few polyethers, and a few other selected solvents are known to form true solutions with alkali metals, certain alkaline earth metals, and a few of the rare earths. The resulting solutions are blue in color, ranging from pale blue at about 1 x 10⁻⁵ molar to a very intense dark blue (if solubility permits). In the case of most metal-ammonia solutions (cesium excepted) a liquid-liquid miscibility gap occurs at higher concentrations. The more dense lower phase is dark blue; the upper phase, which is of a higher metal concentration, exhibits a beautiful bronze-colored metallic reflectance.

These ammonia solutions also exhibit a phenomenal volume expansion. For example, an approximate three molar solution of sodium shows the maximum increase of 43.4 ml per g atom of metal above the individual volumes occupied by the metal and solvent (1). At room temperature, a saturated lithium solution has a density lower than any other known liquid at this temperature (2).

Another striking property is their ability to serve as excellent conductors of electricity. Regardless of the concentration, the equivalent conductance of these solutions exceeds those of any other known electrolyte-solvent combination (2). For sodium, a plot of equivalent conductance, Λ , versus concentration displays typical electrolytic behavior, i.e., conduction by ions, for concentration up to 0.04 molar, where a minimum occurs. At infinite dilution, the equivalent conductance is 1022 cm^2 mho equiv⁻¹ (3). For concentrations above the

minimum (475 cm² mho equiv⁻¹), the equivalent conductance increases at an ever-increasing rate, until at saturation (4.96 molar; $^{n}NH_{3}/^{n}Na = 5.37$ at -33.5°C), $\Lambda = 1.016 \times 10^{6}$ cm² mho equiv⁻¹((4) this is the value obtained after correcting the densities of the solutions. It should be pointed out that the resulting equivalent conductance of sodium is considerably higher than that of potassium, while at one time these were thought to be about the same.). This is well within the region of electronic conduction of metals as illustrated by the atomic conductance of mercury at 20°C, which is 0.156 x 106 mhos or 1/6.5 that of the saturated sodium solution (2).

At low concentrations, magnetic suspectibility experiments show that the molar suspectibility approaches that of a free electron gas but falls to very low values as the concentration increases. A 0.5 molar potassium-ammonia solution is diamagnetic at -53°C as shown by a static field experiment (5).

Kraus postulated the first theoretical model:

$$Me + x(NH_3) \rightleftharpoons M^+ + e^- (NH_3)_x.$$
 [1.1]

With increasing dilution the equilibrium shifts to the right until the metal is completely dissociated into metal ions and electrons; the latter carrying about 7/8 of the current at infinite dilution. Metallic-type conduction results when the electron becomes free of its solvation sphere, as proposed by Kraus based on electromotive force data (6). At the conductance minimum, the postulated equilibrium should be shifted to the left. Both Me and e are paramagnetic, but magnetic suspectibility at this concentration is very low.

Two different models have since been postulated. The "cavity" model has the electron positioned in a "cavity" or "hole" in the solvent. The diamagnetic properties are explained by the pairing of spins of two electrons in the same cavity. The cavity model has now been

largely replaced by the "polaron" model, in which the electron polarizes the surrounding solvent molecules, thus creating a trapping potential for itself (1). The role of the positive ion is insignificant in these models.

The other model was first proposed by Becker, Lindquist and Alder (7). The constituents of this "cluster" model are the solvated electron, solvated metal ion, a monomer unit consisting of a central positive ion with an electron in an expanded orbital and a dimer (or higher polymeric units) held together by exchange forces. Equations [1.2] and [1.3] below illustrate the proposed equilibria.

Me
$$\stackrel{+}{=} M^{+} + e^{-} \qquad K_{1} = \frac{a_{M} + a_{e} - a_{M}}{a_{M}e}$$
 [1.2]

Me
$$M_1 = \frac{a_M + a_{e^-}}{a_{Me}}$$
 [1.2]
Me $M_2 = \frac{1}{2} M_2$ $M_2 = \frac{a_M e^{\frac{1}{2}}}{a_{Me}}$ [1.3]

Although these equilibria have been formulated from the cluster model, one should remember that the monomer species may well be an ion-pair involving an electron in a cavity. As yet, no experimental technique has been devised to distinguish between the two.

Equilibrium constants for these reactions obtained by various experimental techniques, are reported in Table 1 for several different metal solutions.

Table 1. Summary of Equilibrium Constants for Solutions of Metals in Ammonia and Methylamine

Solute	Solvent	Temperature	Method	$K_1 \times 10^3$	<u></u> K₂	Ref.
Na	NH ₃	-34°C	Conductance	7.23	27.0	3
Na	NH ₃	-37	Transference	9.2	18.5	8
Na	NH ₃	-37	Activity co-			
	_		efficient	9.6	23.0	9
K	NH ₃	-34	Magnetic Data	30	98	7
K	NH ₃	-34	"Polaron"	7.9	99	10
Li	CH ₃ NH ₂	-78	Conductance	0.058	5.42	11

This research was initiated to investigate similar equilibria for potassium-ammonia solutions by transference number and electromotive force measurements as previously applied to the sodium system (8,9). Because of discrepancies in the literature concerning conductivities of potassium-ammonia solutions, it was necessary to redetermine them in the concentration range of interest.

CHAPTER II

HISTORICAL

A. Introduction

Since 1864 when Weyl (12) first reported that alkali metals dissolve in liquid ammonia, numerous investigators have been attracted to these solutions because of their several anomalous properties. Hence many papers have been published as evidenced by about 750 entries in a bibliography on this and related fields compiled by Sankuer and Dye (13). Also, Lepoutre (14) has published an excellent bibliography on this topic including listings by subjects and by years.

The literature review will be confined primarily to the dissertation topic. Since this research is of an electrochemical rather than a structural nature, a discussion of the appropriate theoretical models as they apply to this work will be deferred to the Discussion. For other areas of investigation or a comprehensive review, the author wishes to refer the interested reader to several review articles: Yost and Russell, 1944 (15); Kraus, 1953 (16); Bingel, (in German), 1953 (17); Jolly, 1959 (2); Symons, 1959 (18); Evers, 1961 (19) and Das, 1962 (1). Special attention is invited to a series of papers by Leonello Paoloni, (in Italian), 1960, 1961 (20), and also to one by Birch and MacDonald (21) which was published in a journal with limited circulation. A review of the research prior to 1931 was written by Johnson and Meyer (22).

It is interesting to note that most of the investigations fall into two distinct time periods. The first was from 1898 to about 1935, dominated by the work of E. C. Franklin, W. C. Johnson, H. Moissan, Pleskov and Monozon, and especially by C. A. Kraus who showed remarkable experimental ingenuity. The second period started in 1946, when R. A. Ogg, Jr., (23) revived interest in these solutions practically overnight by reporting superconductivity at liquid air temperatures. Since then, a relatively steady stream of articles have appeared. Incidentally, the reported superconductivity was shown to be nonexistent.

B. Conductance

1. Ammonia Solutions

Cady (24) demonstrated that solutions of sodium in liquid ammonia were excellent electrical conductors with conductance values markedly greater than those of salts in the same solvent. In dilute solutions, the deepening of the blue color at the cathode indicated an increase in the metal concentration, but for concentrated solutions, material transfer was not observed. Franklin and Kraus (25) confirmed Cady's observation that these solutions conducted electricity without appreciable polarization at the electrodes.

Professor Kraus performed a series of experiments (26) to determine the nature of the conduction process. With special attention to the purity of the materials, the initial experiment confirmed Cady's observation. With a cell consisting of three compartments, he observed the deepening in color at the cathode and the disappearance of color in the vicinity of the anode. Upon reversal of the current, the clear space shifted its shape to a colorless wedge with an apex nearest the main body of solution. A colorless layer of a few tenths of a millimeter thickness surrounded the new anode. This layer appeared to be void of

ions indicated by a high resistance. A solution with only KNH₂ as solute was electrolyzed with similar effects appearing at the cathode.

As a further test, an experiment was made with potassium and potassium amide solutions which were separated by a narrow-diameter tubing. With the anode in the metal solution, a sharp boundary formed and moved in the direction of the anode. Upon reversal of the polarity, the boundary diffused. At higher metal concentrations, the boundary moved more slowly, and no concentration changes were noted at the anode. Thus, the conduction process was shown to be ionic with the positive metal ion considered identical to the positive ion from the salt. The negative ion was proposed as an electron surrounded by solvent. The representation is:

$$Me + x NH_3 \rightleftharpoons M^+ + e^-(NH_3)_x$$
 [2.1]

$$e^{-}(NH_3)_{x} \rightleftharpoons e^{-}_{free} + \times NH_3$$
 [2.2]

where en is the electron of high mobility separated from its solvation sphere.

Kraus (6) used concentration cells with transference to obtain relative transference numbers. The ratio of the fraction of current carried by the negative and the positive species approached 7 in very dilute solutions and increased to 280 at a concentration just below one normal. Transference number measurements (27) on salt solutions gave $\lambda_{Na}^{O} + = 130 \text{ cm}^{2} \text{ mho equiv}^{-1}$, hence λ_{-}^{O} is 910 cm² mho equiv⁻¹. Thus in dilute sodium solutions the equivalent conductance should approach 1040 cm² mho equiv⁻¹.

Table 2. gives a concise summary of the literature on the conductance of metal solutions in ammonia and amines. The temperature range, dilution limits, and references are given along with the equivalent conductance at infinite dilution and the temperature coefficient where determined.

Summary of Conductance Determinations for Metal Solutions of Ammonia and Amines Table 2.

		Temperature,		i	°<	Temperature	
Solvent	Solute	ان	Molarity Kange	ınge	77	Coefficient	Reference
NH3	Ľ	-33	0.0055 to	2.4			(28)
1		-38 to -70	2.5				(53)
		-13.2	0.00126	0.48	1665	ď	(30)
		-33.2	0.00126	0.48	1018	ď	(30)
		-53.2	0.00126	0.48	634	п³	(30)
	Z S	-13.2	0.00095	1.030	1695	ત્ય	(30)
		-33.2	0,00095	1.030	1036	αđ	(30)
		-53.2	0,00095	1.030	642	nd	(30)
		-33.0	0.000023	2.0			(28)
		-33.5	09.0	satd			(31)
		-33.5	0,00018	0.78	(026)	rd	(34)
		-48.5	0.00048	67.0	(650)	nd	(34)
		•	0,00055	0.49	(490)	rd	(34)
		•	0.169	7.2			(32)
		-33.5	3,63	4.96			(35)
		•	1		1022		(3)
		-33.5 to -78	0.008	0.62		nc	(36)
		-33 to +85	dilute			t,	(28)
		-33 to +50	conc		()	ሪን	(88)
		-77.7	0.00082	0.2608			(37)
	Na-K ^(d)	-33,5	0.000067	98.0			(28)
	×	-33	0.000102	9.0			(58)
		-33,5	0,00020	97.0		ď	(34)
		-33.5	1.4	satd			(31)
		-33.0 to -70	0,165	ထိ		ą	(33)
		-33,5	0,625	3, 12			(33)
		-33.5	3,51	60°5			(35)
		•		*** *** ***			

(36) (34) * (37)	(37) (36) (29)	(30) (30) (30)	*	(38) (39) (11)	(34) (34)	(34) (34)	(36)
nc	nc	તા તા તા		م			nc
1042		3350 2050 1200	856	228.3	159	.188 174	
1.06 0.18 0.40 0.21 (f)	0.998 ⁴⁷ 0.034 5.0	0.008 0.008 0.008	1, 18	16.69 0.6727 0.22	0.00720	0.00298	
0.04 0.00039 0.00068 0.00013	0.00266 0.003 0.04	0.00008 0.00008 0.00008	0.00044	0.0348 0.004355 0.00018	0.000135 0.0000629	0.000314 0.000098	0.0003
-33.5 to -78 -48.5 -37	-33.8 -33.5 to -78 -70	-13.2 -33.2 -53.2	-37	-22.8 to -78.3 -78.3	-33.5 -48.5	-33.5 -48.5	-28 to -128
	Cs	Ca	×	ដ	×	ဂ္ဂ	Na
			ND3	CH3NH2			CH ₃ NH ₂ (e) Na + NH ₃

a Logarithmic temperature coefficient calculated
b Non-differential temperature coefficient calculated
nc
No calculation reported

* This work

 $[\]frac{Na}{K} = 1.46$

^e $NH_3/CH_3NH_2 = 0.942$ f Concentrations given as dilutions at -33.8°C

Kraus (28) determined the conductance of dilute lithium, sodium, potassium and sodium-potassium solutions. This is the first quantitative indication of the anomalous conductance behavior. The sodium and potassium data have since been proven very reliable (3, this work) even though the data cannot be adequately corrected for changes in the accepted values for densities of solution and solvent. His use of both volume and weight analytical techniques would require the availability of the untreated experimental data before proper corrections could be made. Kraus indicated that the data on solutions of sodium were more reliable than those of potassium.

In a series of papers by Kraus and Lucasse (31, 32, 33) data are given on concentrated sodium and potassium solutions, intermediate concentrations for potassium solutions, and temperature coefficients of resistance for concentrated sodium and potassium solutions. Marshall and Hunt (4) recalculated the conductances using corrected volumes for the concentrated region. For a saturated solution of sodium the density at -33.5°C is 0.578 g 1-1 whereas Kraus and Lucasse had used the value 0.674 g l⁻¹ for lack of density data. With this correction the equivalent (atomic) conductance of sodium rises above that of potassium; it had previously been assumed that the conductances were the same in the concentrated region. From an extrapolated value of 1022 cm² mho equiv⁻¹ (3) at infinite dilution, the equivalent conductance of sodium solutions decreases as the concentration increases analogous to the behavior of other electrolytes in media of this dielectric constant. A minimum of 475 cm² mho equiv⁻¹ is reached at 0.04 molar, then the conductance increases at a rapid rate reaching 1.016 x 106 at 4.96 molar (saturation).

At about the same time, Gibson and Phipps (34) published their observations on conductivities of dilute sodium and potassium solutions. Their values do not have the internal consistency found by Kraus and

drop rapidly in dilute solutions either because of decomposition or some error in either the cell constant or concentration. * Volume-normal analytical procedures were used. Figure 1 gives a comparison between the data of Kraus (28) and those of Gibson and Phipps.

In connection with his thermoelectric studies, Lepoutre determined the conductivities of sodium and potassium solutions at -77.7° and of potassium solutions at -33.8°C. All concentrations are given as dilutions computed at -33.8°C which puts these data in a semi-quantitative category as far as the present investigation is concerned.

The only other available conductance data on potassium-ammonia solutions are those of Meranda (36). This experiment was designed for temperature studies on conductance and only two concentrations were studied. He also reported data for sodium and calcium solutions from -33.5 to -80°C and attempts to measure conductivities on frozen solutions. The latter gave inconsistent results and are barely acceptable even as trends. No temperature coefficient calculations were reported.

Superconductivity. In 1946, Professor R. A. Ogg, Jr., (23) cited the presence of persistent currents in frozen rings of sodium solutions in liquid ammonia. Since these were observed at liquid air temperatures (-180°C), this possibility of superconductivity at such a high temperature prompted immediate investigations by other workers (40,41). However, except for Hodgins (42), attempts to verify these persistent currents were unsuccessful. Hodgins observed positive indications for four trials out of some 115 experiments. Other investigators have suggested that the indications observed may have arisen from residual paramagnetic liquid oxygen clinging to the ring, the movement of the search coil in the earth's magnetic field, or the possible influence of neighboring apparatus.

A shift in the cell constant or a smaller shift in concentration has marked effects on the conductance curve as described in the Discussion.

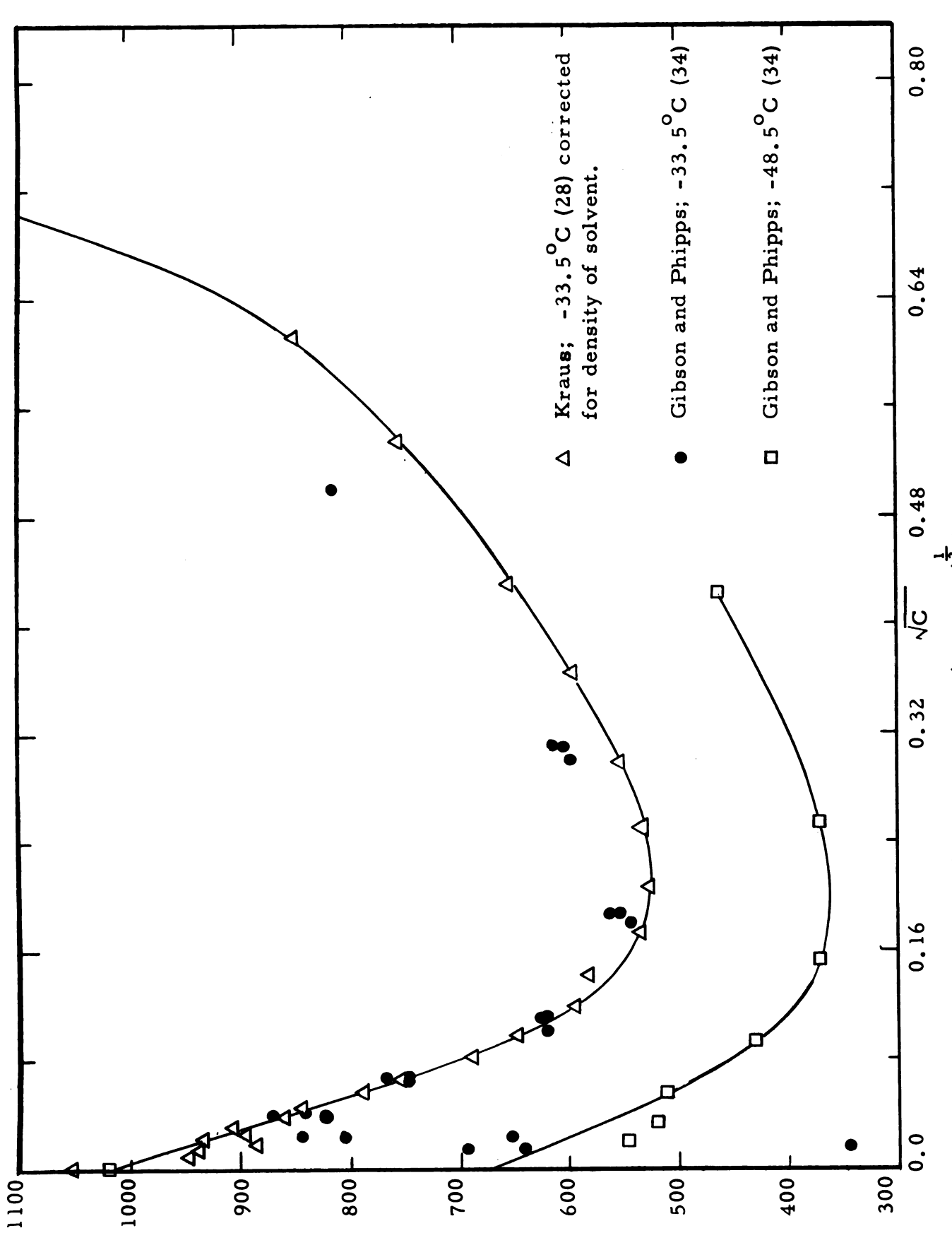


Figure 1. Equivalent conductance versus (molarity)⁷ for potassium in liquid ammonia.

Thermoelectric Behavior. Dewald and Lepoutre (43, 44, 45) have investigated the thermoelectric properties of metal-ammonia solutions and have shown the electron to have a large negative heat-of-transport. This can be accounted for by assuming a quantum tunneling process, rather than ionic or conduction-band processes, even at high dilution.

2. Conductivities in the Amines

The most extensive investigations have been in lithium-methylamine solutions by Evers et al. (11, 38, 39). This group has measured the conductivities of dilute solutions (1.8 x 10⁻⁴ to 0.22 molar) at -78.3°C, concentrated solutions (0.0348 to 16.69 molar) at -22.8°C and temperature coefficients for intermediate concentrations (0.004355 to 0.6727 molar) over the temperature range of -22.8 to -78.3°C.

Gibson and Phipps (34) investigated methylamine solutions of potassium and cesium at -33.5 and -48.5°C. They stated that lithium (in marked contrast with the above work) and sodium were not sufficiently soluble for satisfactory study. Meranda (36) reported the conductivity of a sodium solution using a mixture of ammonia and methylamine. (NH₃/Na = 53.09 and CH₃NH₂/Na = 56.35). The conductivity of this solution was 100 times smaller than that for the equivalent ammonia solution. Evers et al. (38) noted that for concentrations below 0.3 molar the conductances of lithium in methylamine, purified to remove ammonia, is about 10 times lower than that of the corresponding ammonia solution. The conductance of the saturated solution (5.26M) is 100 times below the saturated solution of sodium in ammonia.

Dewald (46) reported conductivities over a range of concentrations at room temperature for ethylenediamine solutions of sodium, potassium, rubidium, and cesium. His results show the earlier conductivity study of Windwer and Sundheim (47) using potassium in ethylenediamine to be incorrect.

For solution of metals in polyether, the only conductances reported are those of saturated solutions of potassium in 1,2-dimethoxyethane by Cafasso and Sundheim (48).

3. Inorganic Salts in Ammonia

An early paper by Kraus and Bray (49) gives an extensive listing of conductances of inorganic and organic salts in non-aqueous media measured in investigations prior to 1913. Where possible they have determined Λ^0 and the dissociation constant, K, through an empirical equation combining the mass-action law with an equation developed by Storch for strong electrolytes

$$\frac{Ca}{(1-a)C} = K + D(aC)^{m}$$
 ([2.3]

where $a = \frac{\Lambda}{\Lambda^0}$, C is the concentration, and D and m are constants which were determined from appropriate plots. The estimated error in Λ^0 for most salts is 1 to 3%. Most of the data were taken from papers by Franklin (50) or Franklin and Kraus (51, 52).

Hnizda and Kraus (53) used precision conductance methods to study salts in liquid ammonia at -34° C. These salts were sodium bromide, potassium bromide, potassium chloride and potassium iodide. The corresponding Λ° values are 314.45, 346.92, 348.13, and 344.55 cm² mho equiv⁻¹, and were determined using a Fuoss function.

The effect of sodium chloride on the conductance of sodium-ammonia solutions at -33°C has been calculated and experimentally verified by Berns et al. (54). The addition of salt depressed the conductance of the metal solution, but did not destroy the minimum in the curve. The experimental data used were those of Lepoutre (37).

One measurement was made by Meranda (36) on a sodium solution with sodium iodide added. The resulting two phases made it difficult to

obtain reproducible data but the conductivities of the solutions were less than those containing either sodium or sodium iodide alone.

One might expect either an additive behavior if the solutes were independent or a depression of the metal conductivity by a salting-out effect as found by Berns, but it is puzzling to find the conductivity below that of either solute.

4. Inorganic Salts in Methylamine

Fitzgerald (55) published data on silver nitrate, potassium iodide, lithium nitrate, lithium chloride, sodium nitrate and mercuric iodide in methylamine at -33.5°C and in some cases also at -15, 0, and 15°C. Franklin and Gibbs (56) have reported conductance values for potassium iodide and silver nitrate, Franklin and Kraus (57) for potassium iodide, and Gibson and Phipps (34) for cesium iodide at -33.5 and -48.5°C.

C. Transference Numbers

In his migration experiments, Kraus (26) formed a boundary between potassium and potassium amide solutions which is the basis of the moving boundary method of directly determining transference numbers. At that time, however, he was merely interested in showing the ionic behavior of these solutions and that the positive ions were the same in metal and in amide solutions.

It was not until 1957, that another attempt was made to determine transference numbers directly. Meranda (36) used a cell made from a U-tube with the two compartments separated by a glass-frit. After the preparation of potassium iodide solution in the cell, which was open to the atmosphere, a small piece of sodium, cut from a block, was added to the iodide solution in one arm. Current was then applied to the cell after cooling to -77°C. Many experiments were performed but few

gave satisfactory data. The values reported are 0.0047 and 0.012 for the anion, which gives 0.99 for the cation. The most frequent cause of failure was the mixing of the solutions, thus destroying the boundary. In 1904, Franklin and Cady (27) had listed the requirements necessary for a stable boundary in connection with their investigations on solutions of salts. These will be described in more detail later in the chapter on theory, but the one of importance here is the item requiring the following solution to be heavier if the boundary is rising. Meranda compounded his troubles by using a large diameter vertical boundary in a horizontal tube across which there existed two solutions with an appreciable density difference. Other significant errors, from this author's experience, can be expected from mixing the sodium and potassium iodide solutions together in the same compartment, the crude method of estimating concentrations, and the lack of a system closed from the atmosphere. Even with meticulous preparation and techniques, it is difficult to obtain reproducibility using the moving boundary method as experienced by the present investigator. The present results show the values obtained by Meranda to be in error by about 2000%.

A successful investigation using the moving boundary technique on sodium-ammonia solutions was performed by Dye, Sankuer, and Smith (8). The apparatus and procedures, which are also used for the potassium investigations reported here, are described in detail in the Experimental Chapter. Table 3 gives a summary of the reported results for sodium. The transference numbers are plotted in Figure 2 along with those calculated from the emf data of Kraus (6).

Of the two remaining methods for determining transference numbers, the Hittorf method involves determination of the material that has migrated between cell compartments. Except for solutions at least below 0.04 molar, material transfer is very small, and analysis would be difficult due to decomposition so this method does not

Table 3. Summary of Transference Number Data for Sodium-Ammonia Solutions (8)

Run Number	Average Molarity During Run	T_ Observed (includes solvent correction)	T_ After Volume Correction
28	0.01906	0.881	0.882
32	0.03948	0.895	0.897
25	0.04636	0.940	0.943
23	0.0806	0.918	0.922
29	0.1168	0.915	0.921
26	0.1427	0.933	0.941

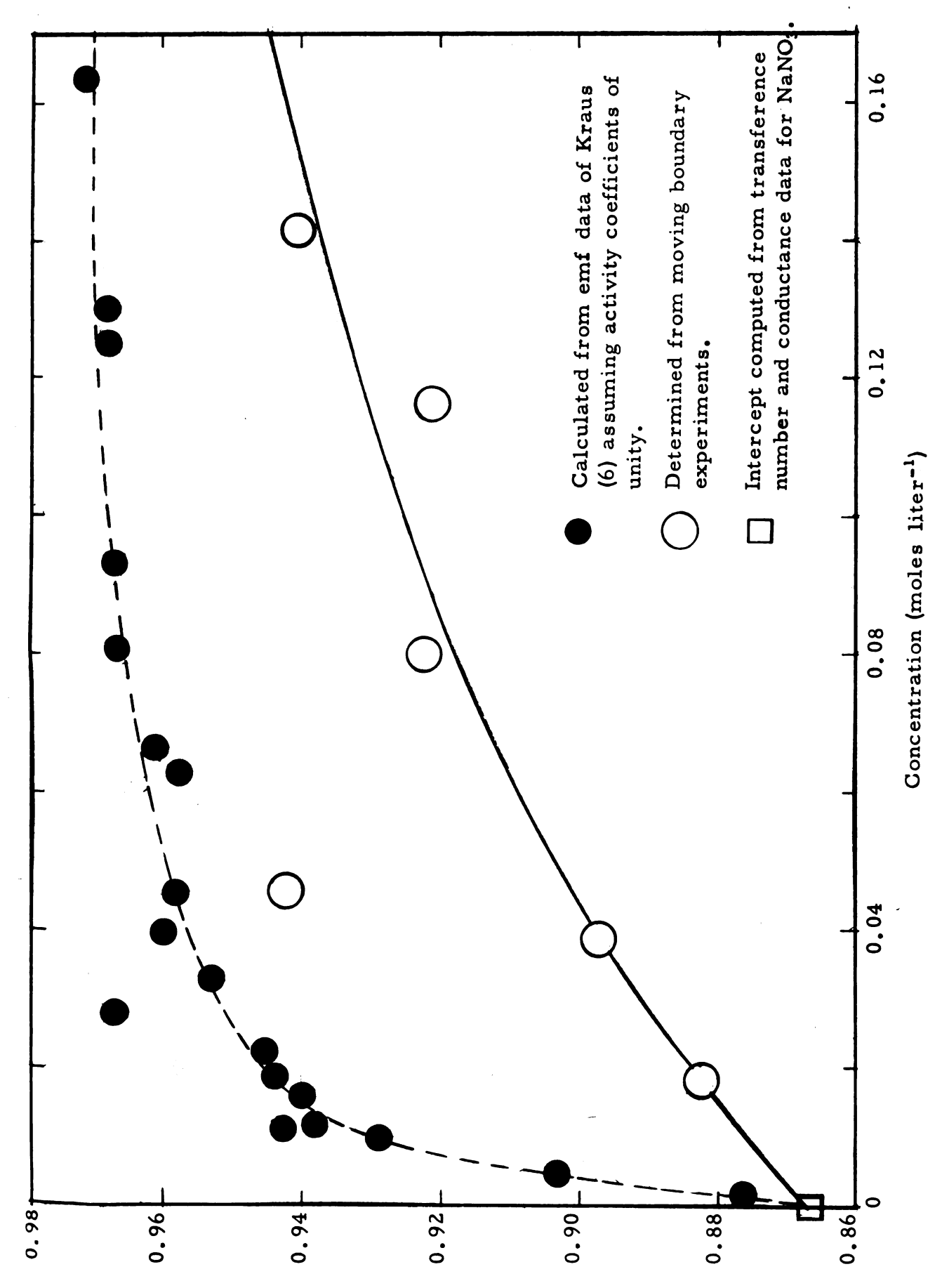
appear to be feasible. The other method employs emf measurements and would require an electrode reversible to the cation.

D. Electromotive Force Measurements

The emf measurements to be reviewed are those obtained using concentration cells with transference. For these solutions, no concentration cell without transference has been devised because such a cell requires reversible electrodes for both the cation and anion.

Concentration cells with transference require only one reversible electrode, and since platinum is reversible to the electron, this cell has been used by several investigators (6, 30, 58) to estimate the transference numbers of metal solutions making the assumption of unit activity coefficient.

Kraus (6) determined such apparent transference numbers in sodium solutions by using a cell incorporating a free diffusion junction. The two compartments containing the metal solutions with a concentration ratio of 1 to 2 were connected by a narrow tube. The solutions were kept separated by a glass rod ground to fit a conical seat in one



Anion Transference Number

Anion transference number of sodium in liquid ammonia from paper of Dye, Sankuer and Smith (8). Figure 2.

of the compartments. No lubricant could be used. By careful manipulation he was able to form the junction in the narrow connecting tube where mixing would be a minimum. In Figure 2 his results are compared with those obtained from the moving boundary method. The displacement can be attributed to the fact that the activity coefficient is not equal to one as assumed in the emf calculations. In the work of Kraus, the concentrations were determined volumetrically from calibration marks on the cell compartments and the weight of the metal determined at the end of a run. Concentrations were changed by completely withdrawing solution from one compartment and then allowing half of the solution from the other compartment to flow into the empty one. Kraus' data spans the concentration range 0.0024 to 0.870 molar at -33.5°C.

Fristrom (30) determined emf values for sodium solutions from 0.0004 to 0.263 molar and over an approximate temperature range of -8 to -73 $^{\circ}$ C. The smoothed data are reported as ratios of T_{e} -/ T_{Na} + versus (molarity) for the temperatures -13, -33 and -53°C. His cell design employed the free diffusion junction with the solutions forming the boundary in a Y-shaped capillary connecting the two cell compartments. The design was such that tilting the cell about thirty degrees would make or break the junction. Two tungsten electrodes were sealed into each cell compartment. They were used both as electron electrodes and conductance electrodes. Thus the concentration in each cell was determined by measuring the specific conductance. Fristrom found that the best results were obtained when electrode areas were large enough to allow low current densities thus minimizing effects from concentration polarization. A ratio of cell constant to electrode area of less than four to one was used. The oxide coating on the tungsten was removed by electrolyzing in dilute 0.5 normal sodium hydroxide.

Concentration was changed by removing a sample of the metal from the solution which had been deposited in a side tube.

For emf measurement of lithium in methylamine, Klein (58) used a cell employing a constrained diffusion junction. This junction was made by allowing the metal solutions to meet as they diffuse through a glass frit. Concentrations were determined from the total weight of methylamine and the calibration marks on the smaller of two cell chambers. The concentrations were changed by transferring solution or distilling solvent from one chamber to the other. Measurements were made at -78, -63.5 and -45.2 C and covered the concentration range 0.0132 to 0.567 molar. The potentials were measured on a recording potentiometer and approximately one hour was required to attain an equilibrium potential.

The transference numbers of a group of salts in ammonia were determined by Franklin and Cady (27) by the moving boundary method using an autogenic boundary. The salts investigated were: ammonium nitrate, ammonium iodide, potassium nitrate, sodium nitrate, sodium bromate, and silver nitrate for cation mobilities; ammonium nitrate, potassium nitrate, sodium nitrate, ammonium chloride, sodium chloride, ammonium bromide, sodium bromide, ammonium iodide, and potassium iodide for anion mobilities. At that time it was believed that the mobilities were independent of concentration and average mobilities were calculated. Fortunately however, data for individual experimental runs are given so that satisfactory interpolations may be made. The concentration range is from approximately 0.01 to 0.2 molar.

CHAPTER III

THEORY

A. Introduction

The theory of the electrochemical methods involved in this dissertation, to be described in this chapter, is fundamental and may be found in most references discussing electrochemistry (59,60,61). For convenience to the reader the equations to be used will be derived or at least presented with all terms defined.

B. Conductance

Faber (62) has given an excellent summary on the history and theory of conductance measurements so that only a summary of the equations and terms used in these investigations will be given.

At potential gradients below 10^5 volts per cm, and frequencies below 3×10^6 cycles per second, electrolytic solutions obey Ohm's law. Thus the relationship between the conductance (which is the reciprocal of the resistance, R) and other parameters is

Conductance =
$$\frac{1}{R} = \frac{A}{b \cdot 1} = L \cdot \frac{A}{1} = \frac{L}{k}$$
 [3.1]

where A is the area of the electrodes, 1 is the distance between the electrodes, k is the cell constant, and ρ is the specific resistance, which is the reciprocal of L, the specific conductance. The terms conductance and conductivity are synonymous in this work.

The equivalent conductance, Λ , is defined as the conductance of an amount of solution containing one equivalent weight of dissolved solute when measured between parallel electrodes which are one centimeter apart and large enough in area to include the necessary volume of solution. This quantity, which has units of cm² mho equiv-1, is calculated from the specific conductance by

$$\Lambda = \frac{1000 \text{ L}}{c^*}$$
 [3.2]

where c^* is the normality of the solution, which for this work is equal to the molarity, C or M, since a 1-1 electrolyte is being considered. The relationship between Λ and the mobilities, u_i , and the degree of dissociation, a, may be derived from the definition of Λ (60). For a binary electrolyte this is

$$\Lambda = a F \left(u_{+} + u_{-}\right)$$
 [3.3]

where F is the Faraday. The equivalent conductance at infinite dilution, Λ^0 , is obtained by extrapolation of a suitable function of the equivalent conductance and concentrations. Kohlrausch has shown Λ^0 to be the sum of individual equivalent ionic conductances, λ_i^0 , or for a cation and anion

$$\Lambda^{\circ} = \lambda^{\circ}_{+} + \lambda^{\circ}_{-}$$
 [3.4]

C. Transference Numbers

The transference number of an ion j is defined as

$$T_{j} = \frac{i_{j}}{\sum_{i} i_{i}}$$
 [3.5]

where $\,i_{j}^{}\,$ is the current carried by the ion of species $\,j\,$ and $\,\Sigma\,$ $\,i_{i}^{}\,$ is

the total current carried by all ionic species in the solution. Alternate expressions for transference number of ion j for a simple salt are

$$Tj = \frac{u_j}{u_j + u_i} = \frac{\lambda_j}{\lambda_j + \lambda_i}$$
 [3.6]

where u_j and u_i are ionic mobilities, λ_j and λ_i are ionic equivalent conductances and Λ is the total equivalent conductance.

There are three methods used for determining transference numbers in aqueous solutions: Hittorf, emf and moving boundary methods. The classical Hittorf method measures the migration of ions in a three compartmented cell by analysis of the contents of the electrode chambers. Such a method did not appear feasible for metal ammonia solutions since the prime carrier is the electron, and analytically it would be difficult to determine its concentration, especially in view of the decomposition reaction which would also occur.

The emf method requires two concentration cells: one with and the other without transference. The electrodes of the cell without transference must be reversible to both cation and anion. Presently, the only reversible electrode to K^{\dagger} ion is potassium amalgam whose manipulation in a closed system would seem to be less feasible than that of the moving boundary. In addition, the metals tend to be extracted from solution by mercury so that amalgam electrodes would not be suitable.

In this work, the transference numbers of the anionic species of potassium-ammonia solutions were determined by the moving boundary method.

Since the moving boundary technique is the most accurate method for determining aqueous transference numbers, several reviews have been written concerning its history and theory (60,61,63). The discussion here will be confined to the present investigation.

Consider Figure 3 in which a boundary a-a' is formed between

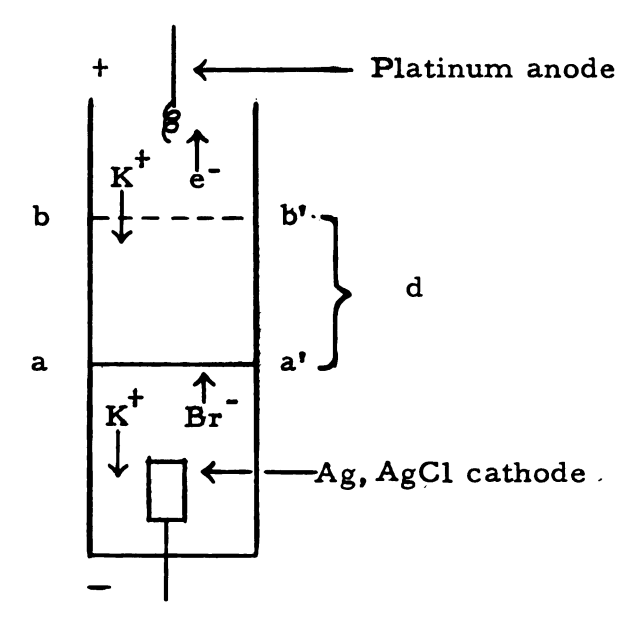


Figure 3. Schematic of a moving boundary.

the "indicating" or "following" solution of potassium bromide and the "leading" potassium metal solution. When a potential of the indicated polarity is applied across the cell, electrons and bromide ions migrate towards the platinum anode and K⁺ ions, which are common to both solutions, migrate toward the Ag, AgCl cathode. With the application of a steady current, i, for a given time, t, and with the mobility of the electron greater than that of Br⁻ ions, the boundary will ascend to some new position b-b'. This boundary is self-sharpening. If a Br⁻ ion crosses over into the metal solution the ion will encounter a lower potential gradient because of the lower specific resistance of the solution, and hence the ion will tend to drop back into its own environment. Likewise, a lagging electron will feel the effects of the higher potential gradient existing in the bromide solution and its velocity will increase.

If the boundary moves a distance d cm in t seconds the average velocity of the electron, v_- , will be d/t. The mobility, u_- , is defined as

$$u_{-} \equiv \frac{v_{-}}{X}$$
 [3.7]

where X is the potential gradient in volts cm⁻¹. Now

$$X = \frac{i}{AL}$$
 [3.8]

where i is the current in amperes, A is the cross-sectional area of the cell in cm^2 , and L is the specific resistance of the solution in mho cm^{-1} . In the previous section on conductance, the relationship between equivalent conductance, Λ , specific conductance, L, concentration, c^* , and mobility, u, was stated.

$$\Lambda = \frac{1000 L}{c^*} = F(u_+ + u_-)$$
 [3.9]

where F is the Faraday. Thus

$$L = \frac{c^* F(u_+ + \mu_-)}{1000}$$
 [3.10]

By combining these statements one obtains

$$u = \frac{d}{Xt} = \frac{AdL}{it} = \frac{Adc^* F(u_1 + u_2)}{1000 i t}$$
 [3.11]

The term Ad is the volume, v, swept out by the boundary. Since

$$T_{-} = \frac{i_{-}}{i_{+} + i_{-}} = \frac{u_{-}}{u_{+} + u_{-}}$$
 [3.6]

then substitution gives

$$T_{-} = \frac{c^* \quad v \, F}{1000 \, i \, t}$$
 [3.12]

In order to obtain a stable boundary, Kohlrausch (64) has shown that the concentration of the following solution must meet certain conditions. Since the electron and the bromide ion sweep out the same volume, rearrangements of equation [3.12] gives

$$\frac{T_{-}}{c^{*}} = \frac{v F}{1000 i t} = \frac{T_{Br}}{c_{Br}}$$
 [3.13]

where T_{Br}- is the anion transference number of the following solution of normality c*_{Br}-. Supposedly, the concentration of the indicator in the vicinity of the boundary automatically adjusts to that given by the Kohlrausch ratio. For aqueous solutions MacInnes and Smith (65) found this to be true if the following solution concentration was within three to eight per cent of the Kohlrausch ratio.

The following or indicator solution must meet these requirements:

- 1) The transference number of the indicator ion must be less than that of the leading ion, i.e., the mobility of the indicator ion must be less than that of the leading ion.
- 2) The density of the following solution must be greater than that of the leading solution since this is a rising boundary.
- 3) The solution must not react with the ion under investigation which is the highly reactive electron.
- 4) Some difference in the properties between the solutions must be present to indicate the boundary. In this case, the leading solution was an intense dark blue and the following solution was clear.

In addition, the current must be low enough to prevent heating, and consequently the vaporization, of the solution. Also the reaction at the electrodes must not introduce new ions which are faster than the ions traversing the tube.

The cathode compartment was completely filled with solution to facilitate the calculation of volume changes occurring between the boundary and the cathode. Referring to Figure 4, suppose that volume changes cause the average solvent molecule to move from x to x' as the boundary moves from a-a' to b-b'. If at the start of its motion the boundary is measured with reference to the point x and at the end with respect to point x' then the boundary will be with reference to a given quantity of ammonia instead of a fixed calibration point on the tube and thus the Hittorf transference number can be calculated.

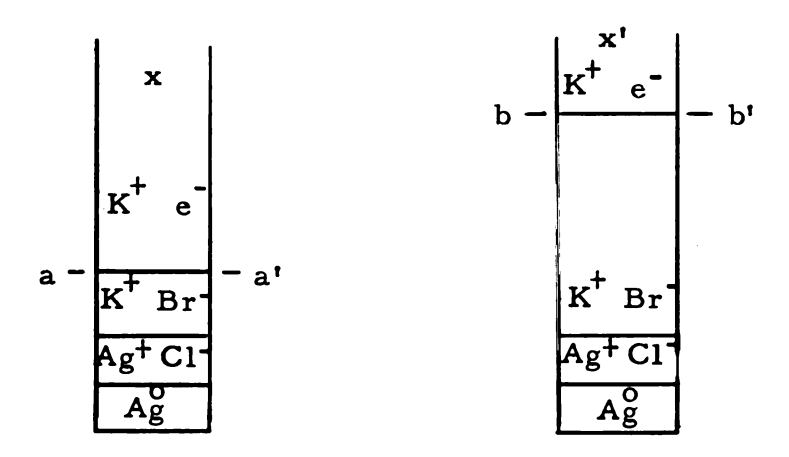


Figure 4. Schematic of volume changes in moving boundary.

Process:	<u>Δ V:</u>
Gain of 1 equiv of Ag by deposition	$\overline{\overline{\mathrm{v}}}_{Ag}o$
Loss of 1 equiv of Ag from AgCl solution	\overline{v}_{Ag}^{o} $-\overline{v}_{Ag}^{AgC1}$
Loss of l equiv of Cl from AgCl solution	- V _{Cl} -
Gain of l equiv of Cl in mixed KCl-KBr solution	V _{C1} , KBr
Gain of T ₊ equiv of K ⁺ across point x	$\mathbf{T_{+}\overline{V}_{K^{+}}^{K}}$
Loss of T_ equiv of e across point x	$-T_{\overline{V}}K_{\overline{e}}$
Gain of 1 equiv of K ⁺ as KBr across boundary	$\overline{\mathbf{v}}_{\mathbf{K^{\dagger}}}^{\mathbf{KBr}}$
Loss of 1 equiv of K as K	- VK+

The sum of the changes in Figure 4 is

$$\Delta V = \overline{V}_{Ag}^{o} - \overline{V}_{Ag}^{AgC1} - \overline{V}_{C1}^{AgC1} + \overline{V}_{C1}^{KC1} + T_{+}\overline{V}_{K^{+}}^{K} - T_{-}\overline{V}_{e^{-}}^{K} + \overline{V}_{K^{+}}^{KBr} - \overline{V}_{K^{+}}^{K}$$

$$[3.14]$$

Now

$$T_{+}\overline{V}_{K^{+}}^{K} = (1-T_{-})\overline{V}_{K^{+}}^{K}$$
 [3.15]

and assuming that

$$\overline{V} \frac{KC1}{C1} = \overline{V} \frac{KBr}{C1}$$
 [3.16]

then the net volume change becomes

$$\Delta V = \overline{V}_{Ag^{\circ}} - \overline{V}_{AgC1} + \overline{V}_{KBr} - T_{-}\overline{V}_{K^{\circ}}$$
 [3.17]

where ΔV is the volume change in liters per equivalent. Thus the corrected transference number $T_{\underline{i}}$ is equal to

$$T'_{-} = \frac{c^* \ v \ F}{1000 \ i \ t} - c^* \ \Delta V$$
 [3.18]

At low concentrations, Longsworth (66) has shown that an appreciable portion of the current is carried by ions resulting from the ionization of the solvent. This correction amounts to the additional term

$$\Delta T_{L} = T_{-}^{t} \frac{L_{0}}{L}$$
 [3.19]

where T_{-}^{t} is the true transference number and L_{0} and L are the specific conductivities of the solvent and solution, respectively. Thus the final expression for the calculation of the true transference number T_{-}^{t} is

$$T_{-}^{t} = T_{-} c^{*} \Delta V + T_{-}^{t} \frac{L_{0}}{L}$$
 [3.20]

D. Electromotive Force

The transference numbers may be determined potentiometrically by measuring the potentials produced across two cells, one of which involves transference of material across a liquid junction. A general representation of such a cell is

M, MX
$$\begin{vmatrix} A_{\nu_{+}}^{z_{+}} & X_{\nu_{-}}^{z_{-}}(C_{1}) \end{vmatrix} \begin{vmatrix} A_{\nu_{+}}^{z_{+}} & X_{\nu_{-}}^{z_{-}}(C_{2}) \end{vmatrix}$$
 MX, M [3.21]

where M, MX represents electrodes reversible to the X^- ion and concentration C_1 is greater than C_2 . Upon the passage of one Faraday of electricity through the cell, T_+ equivalents of salt will be transferred from C_1 to C_2 . The potential at the electrodes is E_+ .

The representation of a cell without transference is

M, MX
$$\mid A_{v+}^{z_{+}} \times_{v^{-}}^{z_{-}} (C_{1}) \mid A(Hg)_{x} - A(Hg)_{x} \mid A_{v+}^{z_{+}} \times_{v^{-}}^{z_{-}} (C_{2}) \mid MX, M$$
[3.22]

This cell requires that each of the electrodes be reversible to the corresponding ion constituents of the electrolyte. This usually limits the use of this cell to applications involving a combination of silver halide, hydrogen, or amalgam electrodes. A reversible transport of one equivalent of salt from concentration C_1 to C_2 occurs for each Faraday of electricity passed, with an electromotive force of E appearing at the electrodes. The ratio

$$T_{+} = \frac{E_{t}}{E}$$
 [3.23]

gives a direct measurement of the transference number. However, this number is a mean value and is only valid if it is constant in the concentration range C_1 to C_2 . If there is much variation then graphical methods must be used for fitting the data.

In metal-ammonia systems, Kraus (6), Fristrom (30), and Klein (58) have used concentration cells with transference to estimate transference numbers by assuming unit activity coefficient. If transference numbers are available from another type of measurement, then they may be combined with emf results from cells with transference for the calculation of activity coefficients.

The emf cell considered in this research may be diagrammed as

$$Pt | K(a_1) | K(a_2) | Pt$$
 [3.24]

The platinum electrodes are reversible to the electron which is the species leaving and entering the solution at the respective anode and cathode. The cell reactions are: for the left hand electrode

$$e_{(a_1)} \longrightarrow e_{\text{electrode}}$$
 [3.25]

and for the right hand electrode

$$e_{\text{electrode}} \longrightarrow e_{(a_2)}$$
 [3.26]

and the total reaction

$$e_{(a_1)} \longrightarrow e_{(a_2)}$$
 [3.27]

During the passage of one Faraday of electricity through the cell, T_{-} equivalents of negative ions (this being the solvated electrons, "free" electrons, or similar types of negatively charge species) are transferred from solution of activity a_{2} to a solution of activity a_{1} . Likewise, T_{+} or $(l - T_{-})$ equivalents of positive ion are transferred to the right. Thus

$$(1 - T_+)$$
 moles of e^- at $a_2 \longrightarrow e^-$ at a_1 [3.28]

$$T_+$$
 moles of K^+ at $a_1 \longrightarrow K^+$ at a_2 [3.29]

The net result from equations [3.27, 3.28, 3.29] is

$$T_+$$
 moles K at $a_1 \longrightarrow a_2$ [3.30]

The free energy increase is

$$\Delta G = T_{+} [(\mu_{K}^{+})_{2} - (\mu_{K}^{+})_{1}] + T_{+} [(\mu_{e}^{-})_{2} - (\mu_{e}^{-})_{1}]$$
 [3.31]

Since the transference number varies with concentration, one should consider that the concentrations of the solutions differ by a small amount G and G + dG. Then

$$dG = -T_{+} (d_{\mu K^{+}} + d_{\mu e^{-}})$$
 [3.32]

= -
$$T_+$$
 (RTd ln a_{K^+} + RTd ln a_{e^-}) [3.33]

$$= -2 T_{+} RT d ln a_{+}$$
 [3.34]

Substitution of

$$dG = -n F d E$$
 [3.35]

and rearrangement gives

$$\frac{dE}{T_{+}} = \frac{2RT}{F} \quad d \quad \ln a_{+}$$
 [3.36]

where a_± is the mean ionic activity of the potassium and electron ionic species.

Thus electrons move from the solution of higher to one of lower concentration. If during the transference process, the electrons carry along solvent molecules then an additional emf will result from moving solvent from a solution of higher to a solution of lower vapor pressure. This emf will be in the same direction as the emf produced by metal transfer; but, any solvation of the metal ion will not enter into this osmotic work since this ion does not lose its solvent at the electrodes.

Kraus (6) has shown this contribution to be

$$dE = m (1 - T_{+}) \frac{RT}{F} d ln \frac{p_{2}}{p_{1}}$$
 [3.37]

where m is the number of molecules of ammonia associated with each electron, $(l - T_+) = T_-$ is the number of equivalents of electrons transferred per Faraday of electricity passed through the cell, and p_2 and p_1 are the vapor pressures of the solutions.

In dilute solutions p_2/p_1 approaches unity since both approach the vapor pressure of pure solvent. At higher concentrations, p_2/p_1 may be considered to be near unity if the concentration ratio is not greater than about 2 to 1. Also at these concentrations, m is becoming smaller so that equation [3.37] may be neglected.

However, Kraus used this equation to calculate m for concentrated sodium-ammonia solutions and found that about a third of the negative species were not associated with solvent molecules; thus the "free" electron concept.

The transference number varies with concentration and, hence, with E; therefore, a reference concentration is selected corresponding to a reference transference number $(T_+)_{ref}$ and the substitution

$$\frac{1}{T_{+}} = \frac{1}{(T_{+})_{ref}} + \delta$$
 [3.38]

made. Integration of equation [3.38] between C_{ref} and C, where

the activities have been replaced by the corresponding stoichiometric mean molar activity coefficient, y, and concentration terms, gives

$$\frac{\mathbf{E}}{(\mathbf{T_{+}})_{ref}} + \int_{\mathbf{E}(\mathbf{C}=\mathbf{C}_{1}=\mathbf{C}_{ref})}^{\mathbf{E}(\mathbf{C}=\mathbf{C}_{2})} = \frac{2RT}{F} \left[\ln \frac{y_{+}}{(y_{+})_{ref}} + \ln \frac{C}{C_{ref}} \right]$$
 [3.39]

Rearranging and changing to logarithm of base 10

$$\log \frac{y_{\pm}}{(y_{\pm})_{ref}} = \log \frac{C_{ref}}{C} - \frac{F}{4.606 \text{ RT}} \left[\frac{E}{(T_{+})_{ref}} + \int_{0}^{E} dE \right] [3.40]$$

The integral $\int \delta dE$ is evaluated graphically. E is obtained from the graphical integration of $\Delta E / \Delta \log C$ versus $\log \overline{C}$ where

$$\frac{\Delta E}{\Delta \log C} = \frac{\Delta E}{\Delta \log \frac{C_2}{C_1}} \approx \frac{dE}{d \log C}$$
 [3.41]

and

$$\overline{C} = \frac{C_1 + C_2}{2}$$
 [3.42]

are from experimental data obtained from concentration cells with transference. The transference members are obtained directly from moving boundary experiments.

CHAPTER IV

EXPERIMENTAL

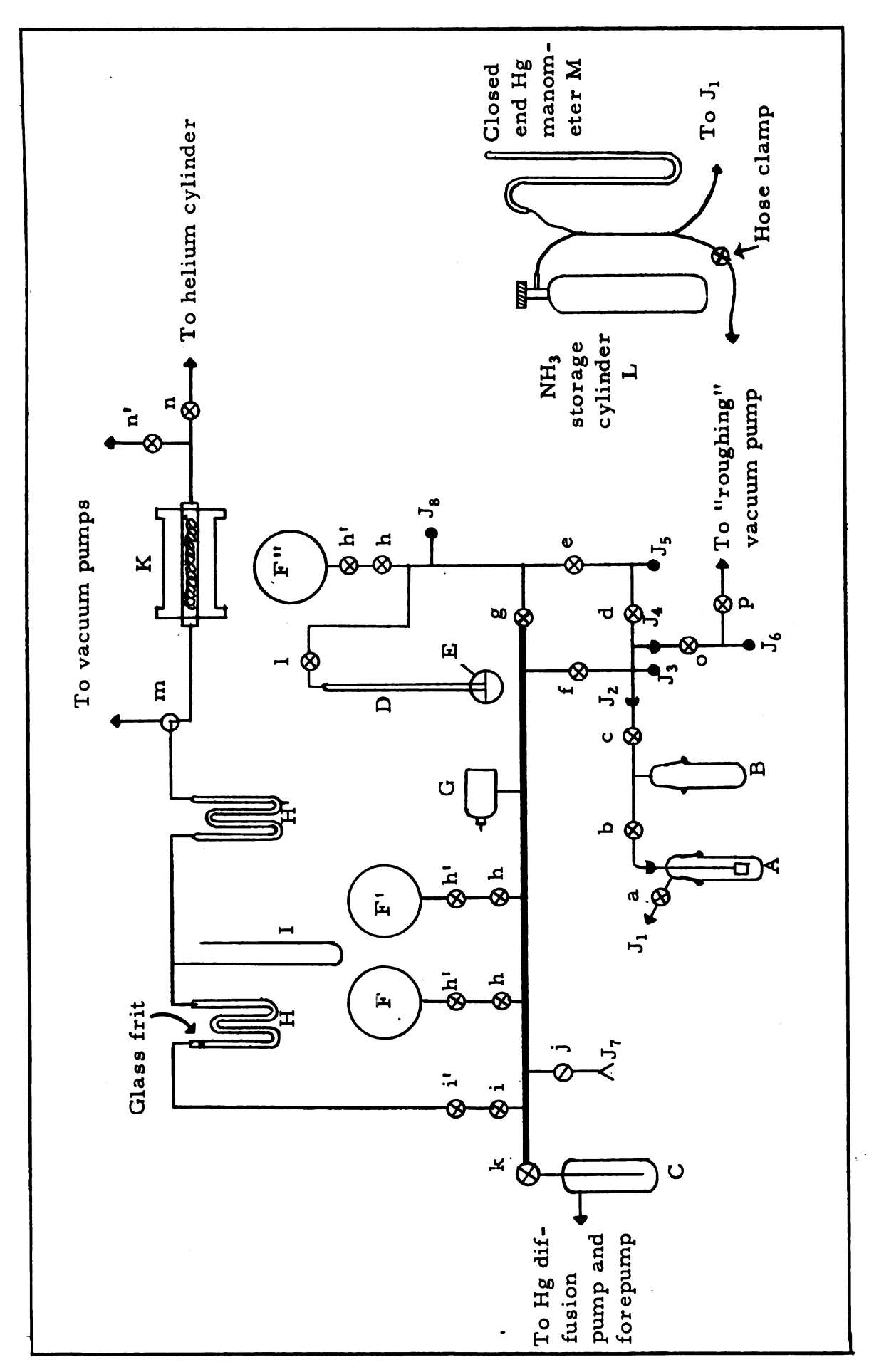
A. Basic Apparatus and Procedures

1. Basic Vacuum System

The basic vacuum system used in all three phases of this work is illustrated in Figure 5. A 20 mm manifold (bold line) was sealed to a two-stage mercury diffusion pump (Scientific Glass Apparatus Co.) through the liquid air trap C and a 15mm hollow-bore stopcock k.

The forepump was a two-stage Welch Duo-Seal vacuum pump (Series No. 1400). A Veeco RG-75P ionization gauge G in conjunction with a Consolidated Vacuum Corp. Model DPA-38 ion gauge controller was used to measure the pressure. High vacuum stopcocks were used throughout and were lubricated with Apiezon "N" grease except where they were exposed to cold surroundings or to the flow of ammonia solution in which case Dow Corning High Vacuum Silicone grease was used. Standard tapers and ball joints were sealed with Apiezon "W" wax ("black wax"), unless otherwise indicated.

The mercury manometer D was used to measure gas pressures up to atmospheric pressure and also served as a "blow-out" tube if the internal pressure exceeded one atmosphere. This manometer was used only when necessary. A line from the fume hood was connected to tubulation E which was sealed to the enclosed mercury reservoir.



Basic vacuum system; ammonia and helium gas purification trains. Figure 5.

2. Helium Gas Purification

Modified two-liter distilling flasks F, F' were used for the storage of the purified helium gas. The third storage vessel F" was added later for further convenience during transference runs since helium gas was not wasted by filling the manifold. Double stopcocks h, h' and i, i' retarded the diffusion of helium into the manifold.

The helium purification train H, I, H', K was evacuated, first through m and then connected to the manifold through i and i'. The traps H, H', filled with silica gel (Fisher Scientific, 14-20 mesh), were flamed with a torch. Glass wool plugs were used to confine the absorbent except for the indicated coarse sintered-glass frit. (Originally, an activated charcoal trap was installed in place of one of the present traps, H. This was replaced when it was brought to the investigator's attention that the coolant, liquid air, which becomes rich in liquid oxygen, could induce a violent explosion if it should come in contact with the charcoal through accidental breakage of the trap (67)). Tygon tubing connected the 3-way stopcock m to the combustion tube in the furnace K and from this tube to the helium cylinder through the pinchclamps n, n'.

During idle periods the train between i' and m was kept evacuated and that between n and m was filled with helium. When preparing the purified gas the latter section was flushed by evacuation and filling with gas through n and n' about four times before connection to the former section. A pressure greater than one atmosphere was maintained on the section to the right of stopcock m; m being used to regulate the rate of flow into the train proper.

Helium gas (Matheson, listed as 99.99% minimum purity) was passed at a slow rate (about 130 ml per minute) over Cu/CuO in a Vycor combustion tube heated to 600°C in a tube furnace K to remove carboneous matter, hydrogen, and oxygen. The gas then passed through

rem.

the 1

atmo train

After

warn

3. <u>A</u>

L of valve

distil

This

alcoho

as a t moist

which Care,

to pre-

tempe:

gas for The pr

kept ne

through

This se

from th

the two silica gel traps H, H' cooled by liquid air or liquid nitrogen to remove water and carbon dioxide. Thus purified, it passed through i and i' into the manifold and storage flasks F, F' and F".

When the open-end Mercury manometer I read one and one-half atmospheres one of the double stopcocks <u>h</u>, <u>h</u>' was closed and the train and manifold were evacuated through <u>n</u> allowing the traps to warm to room temperature to allow the release of absorbed gases. After evacuation the second stopcock was closed.

3. Ammonia Purification

Matheson anhydrous ammonia (listed purity 99.9% minimum) was distilled from the large shipping cylinder into a smaller steel cylinder L of 2500 ml capacity equipped with a Hoke-Phoenix metal diaphragm valve and charged with several grams of sodium metal (see Figure 5). This small cylinder was cooled by a Dry Ice-alcohol bath. (Usually the alcohol used in this and similar baths was methanol which had been used as a thermostatic bath fluid, but was no longer suitable due to a high moisture content. The resulting high viscosity caused poor stirring which resulted in large temperature gradients in the thermostat bath.) Care was taken to insure a vapor space above the liquid in the cylinder to prevent possible rupture by the expanding liquid as it warmed to room temperature. The cylinder was bled momentarily to remove any hydrogen gas formed from decomposition of the sodium in the sodium amide. The pressure during distillation, monitored on the manometer M, was kept near an atmosphere or just above to minimize diffusion of air through the rubber tubing. These lines were flushed by alternately evacuating to a mechanical pump and refilling with ammonia vapor. This set-up was used both in filling the steel cylinder and in distilling from this cylinder into the ammonia purification train.

Prior to condensing ammonia into the purification train, several grams of freshly cut sodium (J. T. Baker, lump, purified, dry packed) were placed in vessel A. This was melted and degassed through \underline{b} , \underline{c} , \underline{o} , and \underline{p} . After the initial degassing, the line was connected to the manifold (through \underline{f}) and evacuated until the pressure was below 5×10^{-6} torr.

Cooling baths consisting of Dry Ice-trichloroethylene mixture in Dewar flasks surrounded A and B. With b closed, ammonia was condensed into A through a. When A was full, a vacuum was applied to the solution through J1 to remove any hydrogen gas formed. With a closed and b open, the Dewar flask around A was lowered and the sodium-ammonia solution transferred into B from the vapor pressure build-up in A. The transfer was stopped before the solution reached the glass frit in A which was used to remove solids and slow the transfer. The bath around A was raised and b warmed to room temperature before closing to remove any ammonia left in the bore. Silicone grease was used here after several stopcocks were lost when they blew out (probably because ammonia vapor or solution dissolved in the Apiezon "N" grease and leaked into the vacuum back). The procedure was repeated until both vessels were nearly full. There was a tendency for ammonia to freeze in the frit, in which case a -40°C alcohol bath was placed around A for about a half-hour to melt the ammonia. The trap was then recooled with the -78° bath before opening b to prevent a sudden surge of solution through the frit.

Ammonia was distilled from B through \underline{c} into other parts of the system as needed. Usually, before distilling, a -40°C alcohol bath was placed around the vessel for several hours to facilitate the drying process. This bath also facilitates the distillation by serving as a heat exchanger and minimizes the danger of the pressure rising above one atmosphere. Before using, the vessel was opened to the rough vacuum (through \underline{c} , \underline{o} and \underline{p}) to remove decomposition gases.

4. Preparation of Ampoules of Metal

Freshly cut metal (below is the list of metals) was inserted in the assembly shown in Figure 6a and a tubulated cap sealed on with Apiezon "W" wax. After attaching a mechanical vacuum pump at the tubulation, the metal was melted using a soft torch flame; the melt ran through the constrictions into the lower tube. Most of the oxide remained at the first constriction. After cooling, the tube was sealed and removed at the lower constriction.

With an initial vacuum of 2 x 10⁻⁶ torr, the metal contained in this tube was distilled into six smaller ampoules in the apparatus shown in Figure 6b. This apparatus was cleaned with: (1) alcoholic KOH, (2) distilled water, (3) HF-HNO₃ and/or sulfuric acid-dichromate cleaner, (4) rinsed at least nine times with distilled water, (5) rinsed with de-ionized water, and (6) dried. These ampoules of metal were sealed at the constriction, removed and stored until needed.

The HF-HNO₃ cleaner was found superior to that of warm sulfuric acid-potassium dichromate from spectra studies on amine type solutions (46). The higher rate of decomposition observed with the latter cleaner is attributed to residual chromium oxide. The composition by volume of the new cleaning solution was:

2% acid soluble detergent

5% hydrofluoric acid

33% concentrated reagent grade nitric acid

60% distilled water.

Metals used in ampoules:

Sodium: The sample was cut from a larger piece of Baker's

Analyzed dry sodium which was stored in a vacuum

desiccator. All of the oxide coating was removed.

Potassium: The sample was from Mallinckrodt metal stored in light paraffin oil. The metal was freed of oil

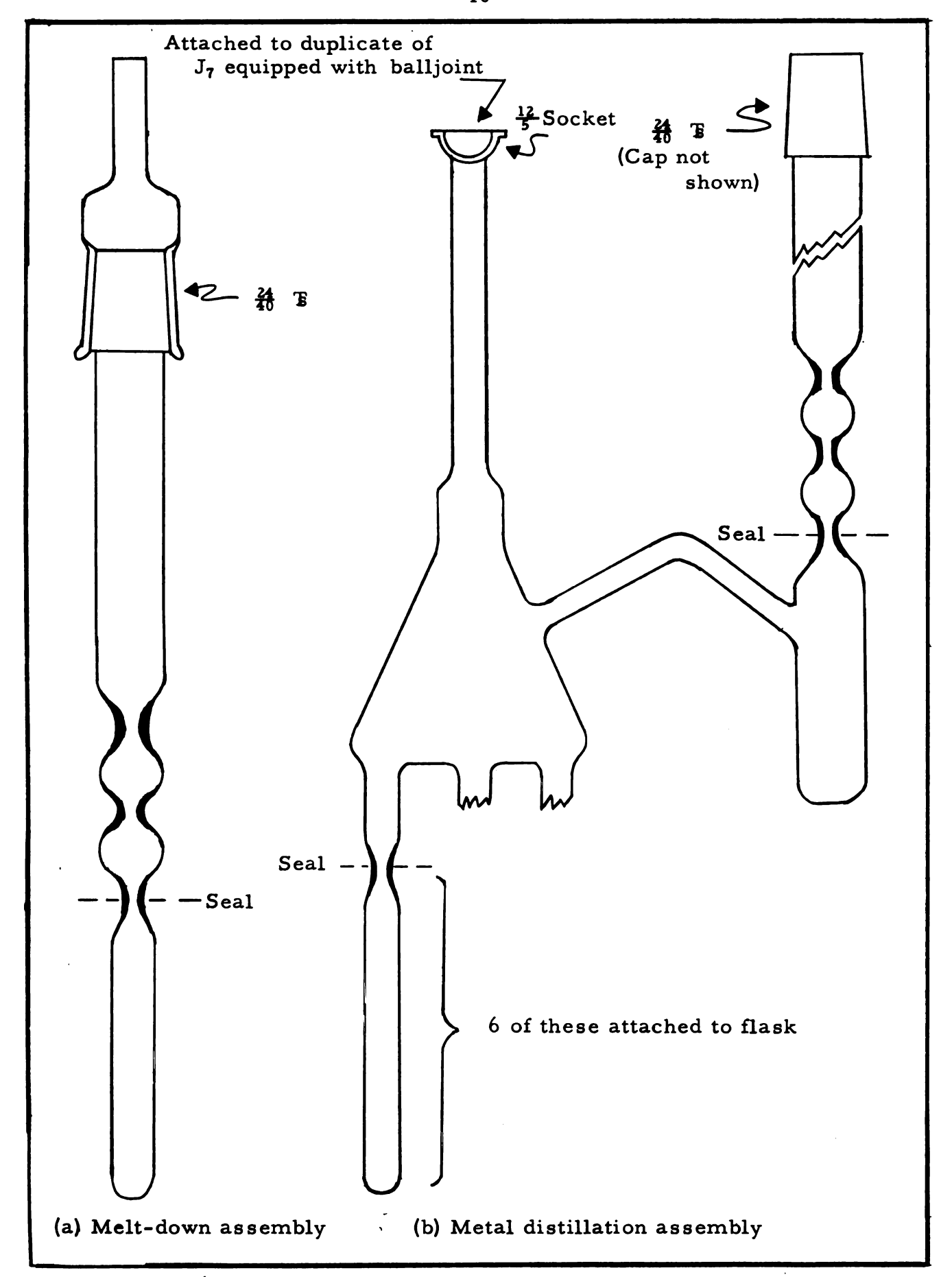


Figure 6. Metal purification apparatus.

with benzene and blotted dry with tissues. The sample was cut on all sides to expose fresh metal before inserting into the melt-down tube.

Rubidium and Cesium: For small (2 g) ampoules from Fairmount Chemical Co. (doubly distilled) the vial was frozen, broken, and dropped into O of the ampoule-filling apparatus (Figure 7b). This manipulation was performed under a plastic tent filled with a flowing stream of helium gas.

For the larger (25 g) ampoules of cesium the procedure above was followed, but first, the sample was broken into smaller ones by the apparatus in Figure 6b.

Small glass bulbs with attached stems (Figure 7a) were drawn from 10 mm Pyrex tubing previously cleaned with alcoholic KOH and sulfuric acid-dichromate cleaning solutions. These bulbs were then selected according to:

- 1. The stem diameters should be between 35 and 50 thousandths of an inch to insure an opening in the capillary large enough for the metal to flow through easily but small enough so that the capillary walls are of sufficient strength.
- 2. The bulb must be smaller than the inside diameter of a male 24/40 standard taper joint.
- 3. The weight of the bulb and stem should be less than 400 mg to reject those having excess glass which might not be easily broken when desired.
- 4. A sound test was made by dropping the bulb several inches onto a glass plate. Too high a pitch indicated the wall thickness of the bulb was too great to assure breakage.
- 5. Each ampoule was evacuated using a vacuum pump. If it was too fragile, it would implode, and hence, be discarded.
 For ease in testing, a glass tube drawn to a taper was inserted

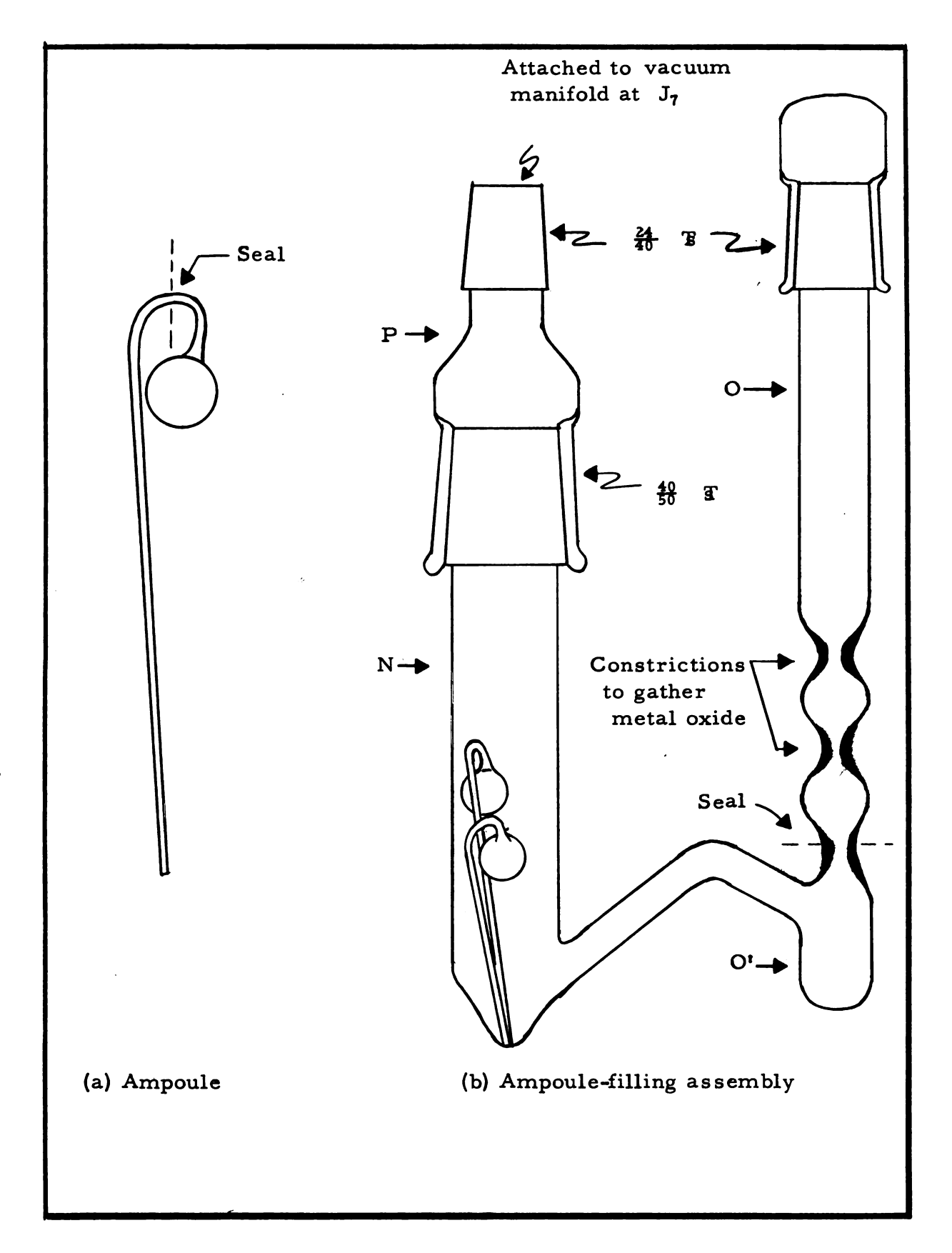


Figure 7. Diagram of ampoule and ampoule-filling assembly.

into a rubber stopper and the latter inserted into a tubing connected to the pump. The ampoule stem rested on the shoulders of the taper.

To facilitate keeping track of the ampoules used in a given assembly, a template was drawn in the notebook showing the length from the stem to the bend and from the bend to the bottom of the bulb. Care was taken to vary the size of the stems. If two stem lengths were nearly the same size, a notation was made about the bulb size or shape. Since the seal on the ampoule was made at the bend, this did not affect the length of the stem and made the template convenient to use.

The apparatus for filling the ampoules is shown in Figure 7b. After cleaning as previously described, six to twelve ampoules were cut to size, dried, and weighed. They were arranged in tube N so that the open ends were in the depression at the bottom. This unit was attached to the high vacuum system at J₇. A tube of metal was opened, inserted into O which was capped using Apiezon "W" wax. Immediate evacuation was effected and a heater placed under the part containing the ampoules. After a pressure of 2 x 10⁻⁶ torr was obtained, the metal was melted from the tube, the upper section was sealed and removed at the lower constriction and the metal was degassed by light flaming. The heater was removed after evacuating for 24 hours and after checking to see that a pressure of 2 x 10⁻⁶ torr would remain in this unit after being disconnected from the manifold for a period of 15 to 30 minutes. Then the metal was distilled over into the depression engulfing the stems of the ampoules. With the metal in the fluid state, purified helium gas was admitted through h, h' and j (Figure 5). This forced the metal into the ampoules. Stopcock k had been closed and taped to prevent popping. After pumping the helium gas out, an attempt was made to distill enough metal from O' over to cover the tips. Small amounts of helium gas (that between stopcocks h and h') were applied in hopes of forcing

metal into the capillary tube to form a seal. This seemed to work for roughly 30% of the ampoules. Only a few ampoules were ever lost because of "popping" from expansion of residual helium gas during the seal-off.

The manifold and assembly were filled with an inert gas from a commercial cylinder and the assembly N-P removed at J₇. With the adapter P removed, a stream of the inert gas was directed into the assembly through a small tube inserted halfway. The gas used at first was helium but in later preparations, argon was used and worked much better since it is more dense than air. The ampoules and stems were removed and sealed at the bend. If much gas were present in the ampoule there would be a tendency for a hole to be blown in the stem by the expanding gas. In such cases, a notation was made in the notebook for later reference. These samples were not used in the electrochemical experiments. The ampoules were placed in numbered beakers and the stems in correspondingly numbered test tubes. Originally, the stems were crushed in a mortar and pestle under water, transferred to a weighted sintered glass crucible and washed with deionized water. The crucible was dried and weighed. Later a more convenient and accurate method was employed. With the stem in the test tube, water was added and the test tube attached to an aspirator by a rubber stopper. The vacuum was broken through a "T" inserted between the aspirator and the stopper. This allowed the water to come in contact with the metal. Successive manipulations in like manner removed the metal and cleaned the stems. These stems were weighed directly after drying in a heated vacuum desiccator. The ampoules were washed with de-ionized water. A 5% solution of HF was used to remove any oxide present on the surface of the ampoule. The difference in weights between the filled ampoule and dried stem, and the empty ampoule gave the weight of the metal.

A semi-micro Mettler balance was used for later weighings thus assuring accuracy to \pm 0.1 mg. The ampoules were stored in numbered ten milliliter beakers in a compartmented plastic box. Vacuum corrections were applied to some of the more recently filled ampoules.

5. Preparation of deutero-Ammonia

O'Reilly (68) prepared <u>deutero</u>-ammonia (ND₃) by passing deuterium oxide vapor (D₂O) over magnesium nitride (Mg₃N₂) in an evacuated system. The ND₃ that evolved was condensed in a cold trap containing potassium metal. This method was tested by preparing ammonia, but appeared to be too slow for our purposes.

The apparatus finally designed is diagramed in Figure 8. More than the stoichiometric amount of Mg_3N_2 (Metal Hydride, Inc.) was placed in a liter flask C. The addition funnel B, equipped with double stopcocks, was filled with about 70 ml of D_2O (Isotopes Specialties Co., stated purity: 99.8%) through J_2 . With stopcocks \underline{b} and \underline{c} on the funnel closed, the water was degassed by evacuation through stopcock \underline{a} using a separate mechanical pump connected at J_1 . The degassing was done at room temperature because it would have been difficult to freeze the D_2O in the funnel. The stopcock bores were evacuated before filling the funnel with D_2O .

The column D was packed with alternated layers of glass wool plugs and two inch lengths of glass tubing. This, along with the attached Kjeldahl trap E, kept the powdery reaction products in C from entering the rest of the system and plugging up stopcock bores as in a previous trial.

The tower G was a 20 mm diameter tube with a glass wool plug in the bottom and several grams of Mg_3N_2 resting on top. The Mg_3N_2 was kept in place with several inches of loosely packed glass wool. The tower was cooled in a Dry Ice-alcohol bath. Its purpose was to convert any unreacted D_2O vapor.

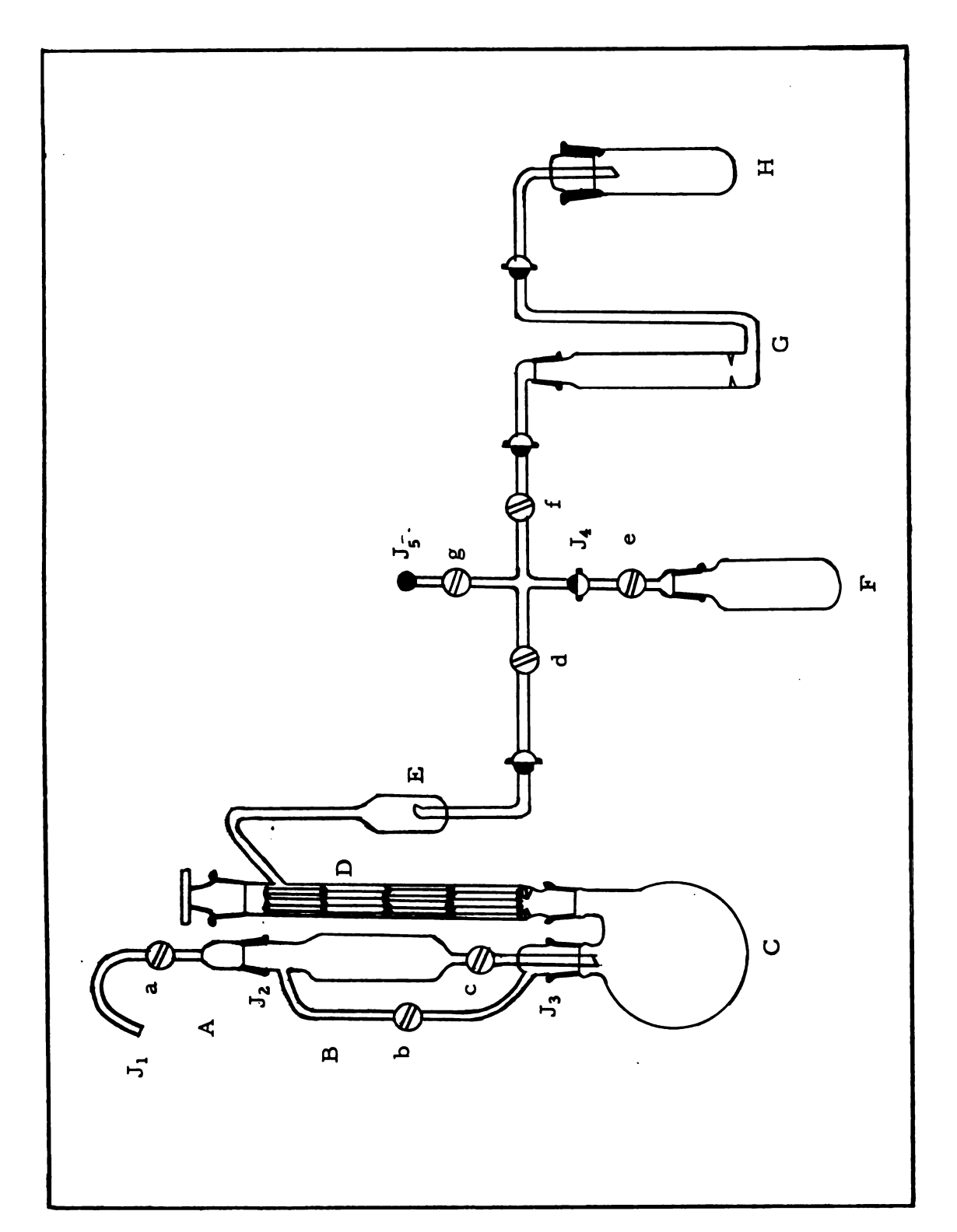


Figure 8. Apparatus for preparation of deutero-ammonia.

The condensation vessel H was cooled in liquid air. The storage vessel F, equipped with a demountable 24/40 adapter with attached stopcock e, contained several grams of sodium metal which had been previously degassed under vacuum. It was also cooled by liquid air.

After evacuation of the reaction and storage train to about 10^{-5} torr, an ice bath was placed around the reaction vessel C. With stopcock \underline{b} open, a half-dozen drops of D_2O were added through \underline{c} . The evolved ND_3 passed through \underline{d} , \underline{f} and G and was condensed in H. After all the D_2O had reacted, the reaction flask C was slowly warmed by a heating mantle. This apparently initiated a second step in the reaction (see equations [4.1] and [4.2] and the evolved ND_3 was condensed in H. When ND_3 evolution ceased, the heating mantle was replaced by a Dry Icealcohol bath and the Dewar flasks around traps G and H were removed. The ND_3 was in this way returned to C to convert any unreacted D_2O to ND_3 . The ND_3 was then transferred into the storage flask F through stopcock \underline{e} and condensed. Vessel C was flamed to liberate any residual ND_3 . With stopcock \underline{e} closed the flask was removed. The rest of the system was then disassembled, cleaned and reassembled before preparing another batch.

The HF-HNO₃ cleaning solution was used for glassware cleaning followed by rinses with distilled water. Apiezon "W" wax was used on the joints and "N" grease on the stopcocks. The system was evacuated through <u>g</u> which was connected to a vacuum manifold equipped with a two-stage mercury diffusion pump and a McLeod gauge.

The reaction is (69):

$$Mg_3N_2 + 6 D_2O \longrightarrow 3 Mg(OD)_2 + 2 ND_3$$
 [4.1]

An increase in yield may be obtained by heating the $Mg(OD)_2$ to recover D_2O for further reaction with Mg_3N_2 .

$$Mg(OD)_2 \longrightarrow MgO + D_2O$$
 [4.2]

An IR spectrum was recorded for each batch. If the spectra indicated the absence of ammonia, the product was distilled into a common storage vessel containing freshly degassed sodium metal.

6. Thermostat

The thermostat was constructed in this Laboratory by Professor J. L. Dye (8). Basically, it consists of a Pyrex cylindrical jar, 12 inches in diameter by 18 inches high, insulated on the bottom and side by a two inch layer of Foam-glass. The outside of the insulating layer was surrounded by a sheet-metal cylinder.

Double windows were left on opposite sides of the bath to permit observation of the boundary. The double window was made by cementing a Plexiglass box, open on the inside, to the glass jar. During a run, the space between the windows was continuously flushed with dry air. The air was passed through Drierite (anhydrous CaSO₄) and a liquid air trap before use.

Between the jar and the insulation was a copper sheet with openings for the window. To this sheet was soldered 1/4 inch refrigerating coils connected to a 1/3 hp compressor using Freon-22 gas. A second 1/4 hp compressor was also used with its evaporator immersed directly in the bath liquid.

The compressors ran continuously attaining an ultimate temperature of about -42°C. A 250 watt knife blade heater controlled by a variable autotransformer was used to balance most of the extra heat loss. A mercury regulator actuated an infrared lamp to provide the temperature control. The regulator was an H-B Instrument Co., No. 7530 "Red Top" which served as the sensor for a Fisher Scientific Model 30 Transitor Relay. In turn, this relay actuated a mercury plunger relay (H-B Instrument Co., No. 7550) which controlled the lamp.

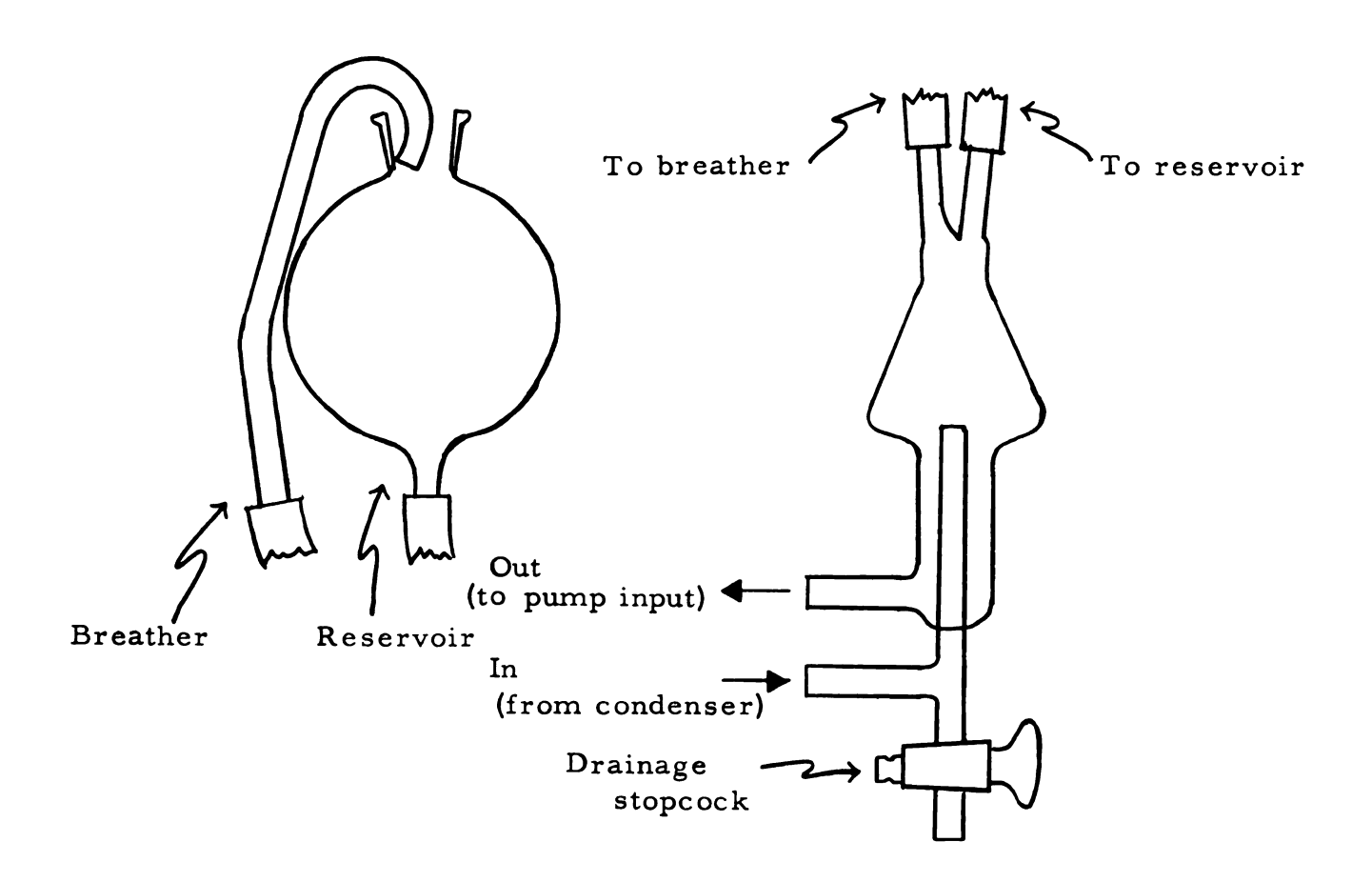
7. Temperature Measurement

The temperature measurements were made with a 25 ohm metal calorimetric platinum resistance thermometer and associated Mueller bridge circuitry. A calibration curve on this thermometer (Leeds and Northrup, Cat. No. 8160, Serial No. 1053280) was not available. However, it was compared over the range of use with a National Bureau of Standards calibrated glass platinum resistance thermometer (Leeds and Northrup, Cat. No. 8163, Serial No. 1016073).

The Mueller bridge (Leeds and Northrup, Type G-1, Serial No. 113758) was calibrated in international ohms. A Leeds and Northrup Type 2100 lamp and scale were used to read the deflection from the galvanometer (Leeds and Northrup, Type H.S., Serial No. 342371, Sensitivity 1.3 x 10-9 amp mm). About 15 small divisions corresponded to 0.01°C. The current to the bridge was maintained at two ma from a 10-turn potentiometer connected as a rheostat to a 1.5 volt dry cell.

8. Circulating System and Bubble Remover

The bubble remover was designed to remove air bubbles from the closed loop in the cold temperature circulating system. This system consists of a Gorman-Rupp No. 210 centrifugal pump, a 3/8 inch copper coil of 17 turns immersed in a Dewar flask containing Dry Ice and alcohol or acetone, and the make-up vessel to be cooled. With the bubble remover between the cooled vessel and the pump the bubbles would collect and separate from the circulating liquid. Fresh absolute ethanol was used as the circulating fluid. The diagram (Figure 9) is self-explanatory.



Top Unit: Reservoir Bottom Unit: Bubble remover

Figure 9. Bubble remover for closed-loop circulating systems.

9. Conductance Bridge

The conductance bridge was built by the author before starting the present research project. It was a duplicate (with minor improvements) of a previous bridge used in the Department (70). The oscillator, bridge, and detector amplifier sections were housed within a table model

relay cabinet. Associated equipment was the power supply chassis (with individual power supplies for the oscillator and detector circuits and a d-c voltage supply for the heaters of the first two stages of the detector circuit) and an oscilloscope (Heathkit Model 0-10). The basic oscillator circuit was a modified version of Heathkit Model AG-9 Audio Generator. In the output were five phase-shift networks for the frequencies: 400, 600, 1000, 2000, and 4000 cps. The detector amplifier was a three-stage circuit with five "Twin-T" filters (71), designed for the above frequencies, between the second and third stages.

The oscilloscope was used as the detector or comparator. A signal from the oscillator and one from the detector amplifier (which is the unbalance signal from the bridge) was applied to the horizontal and vertical inputs of the oscilloscope, respectively. By the proper settings of the phase controls, the resulting Lissajous figure can represent resistive balance by the closure of the loop and reactive unbalance by the tilt of the loop.

The bridge proper consisted of General Radio components mounted in a 22 gauge copper box ($12 \times 17\frac{1}{2} \times 6$ inches). Each segment of the bridge was isolated by an internal copper shield. The ratio resistors, shielded from each other, were enclosed in two concentric copper boxes. The intermost box was connected to the common terminal between the resistors, and insulated from the other shield with stand-off insulators. This "ratio box" was also situated in its own shielded compartment.

The complete circuit is described elsewhere (62), and also, may be found in Appendix A.

10. Switching Network

The switching network (Figure 10), or portions thereof, was used with conductance cell B, and emf cell and the modified transference cell.

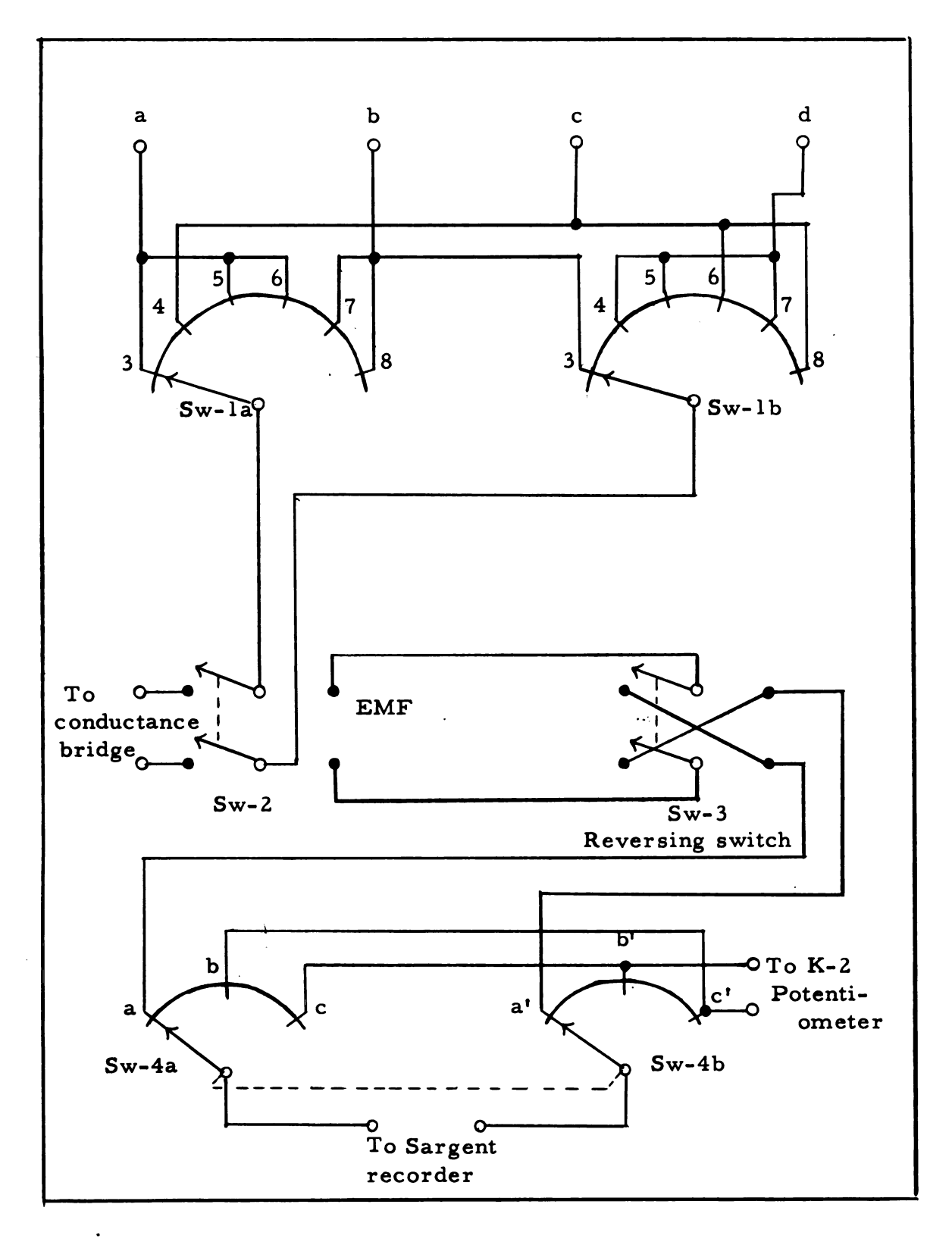


Figure 10. Schematic of switching network for conductance cell B, emf cell, and modified transference cell.

Switches Sw-1, Sw-2, and Sw-3 were mounted on a common board. Sw-4 was in a separate box. The switch manufacturers and switch characteristics are:

- Sw-1 a and b: Leeds and Northrup, Catalog No. 31-3-0-2, two-circuit, 12-position rotary switch.
- Sw-2 and Sw-3: Leeds and Northrup, Catalog No. 3294, DPDT pinch-type switch.
- Sw-4: A government surplus Cutler-Hammer, 5-circuit, 6-position enclosed rotary switch.

Number 22 insulated non-shielded wire was used for connections. The numbered switch positions on Sw-1 correspond to the dial plate used. The relationship between switch positions and electrodes for various cells are given in Table 4.

Table 4. Switch Positions and Corresponding Electrode Connections

Switch Position	Terminal Combinations	Emf Electrode Combinations	Cond. Cell	Modified Transf. Cell
3	a & b	a & b	2 & 3	1 & 2
4	c & d	c & d	•	-
5	a & d	a & d	1 & 2	1 & 3
6	а & с	a & c	-	-
7	b & d	b & d	1 & 3	2 & 3
8	ъ&с	b & c	-	-

B. Conductance Methods

1. Objective

In the present investigation, conductivity data on potassiumliquid ammonia solutions are desired for two reasons:

- Reliable conductance data would serve as a convenient tool for measuring concentrations by incorporating a conductance cell into each apparatus.
- 2. The calculation of ionic conductances can be made from total conductance and transference number measurements.

With these two items in mind, a literature survey reveals investigations by Kraus (28), Gibson and Phipps (34), Lepoutre (37), and Meranda (36). Lepoutre's more extensive tabulation is at -77.7°C. and his data at -33.8°C and those of Meranda's are not extensive enough to be useful to us. Comparison of the data of Kraus and of Gibson and Phipps, shown in Figure 1, indicates some discrepancy, but the work of Kraus would appear more internally consistent. Kraus (28) stated that the potassium data were more in doubt than those of sodium. Also in the calculations of Kraus, the densities of pure ammonia and of the solutions were taken as the same value, 0.674 g ml⁻¹. (The presently accepted value for pure ammonia is 0.6817 (72) at -33.2°C or 0.6828 (73) at -33.7°C. The value 0.6869 g ml⁻¹ at -37.0°C was used in this work.) The densities of the solutions were not known at that time, but they are now known to be very concentration dependent. Kraus' data is not amenable to correction since the added solvent was measured by volume and the solvent withdrawn was determined by absorbing in water and weighing.

It thus seemed desirable to redetermine the conductance of potassium-liquid ammonia solutions, primarily to see which data were more correct and, if possible, to improve upon the precision. More confidence in the data would result if some measurement of the amount of decomposition could be made. Conductance cell A was designed for this purpose. The temperature corresponded with our other experimental measurements so that it would not be necessary to make a temperature correction.

The design features incorporated into cell A were to achieve the following: to be able to stir the solution, to add a known amount of metal without introducing glass fragments, and, most important, to obtain a reliable estimate of the decomposition as a check on conductance data. The latter could be done by distilling ammonia into the cell to make successive dilutions and then reversing this technique by distilling known amounts of ammonia from the solution. If there were no decomposition the conductance curves should coincide, and if there were decomposition the difference in forward and reverse values could be used to correct the measurements.

This cell design was used in runs CK-1 through CK-11 and performed very well. One limitation was that only a narrow concentration range could be covered during a given run because each new addition of ammonia resulted in a smaller incremental change in concentration.

O'Reilly (74) estimated that the conductivity of potassium deutero-ammonia solutions would be approximately 20% below those of the ammonia solutions for the concentration range 0.15 to 0.50 molar at 25°C. This estimate was based on the Q values of the rf coil, coaxial line and sample during paramagnetic resonance absorption studies. As a short problem (actually it required six months!) it was thought of value to verify or dispute this statement. Because of the volume requirements of cell A and the expense of ND₃ it was necessary to design a new cell--cell B. The design for this cell stressed the desirability of covering a larger concentration range, and was based on that of Kraus (28). The most notable difference was the use of a

bulb cooled to a lower temperature than the thermostat to condense ammonia which was then vaporized to stir the solution, thus replacing a mercury Toepler pump used in Kraus' procedure. Also, the withdrawn ammonia was condensed and weighed in heavy-wall ampoules rather than absorbed in water.

2. Conductance Cell A

The Cell. The body of the cell N (illustrated in Figure 11) is an inverted 500 ml Erlenmeyer flask. The neck of the original flask becomes the cavity U which houses the stirring bar Z and to which the tubes Y, Y' to the electrode chambers X, X' are sealed. Prior to run CK-5 one of these arms, Y, entered the bottom of the cell body at the center. The motion of the stirring bar over this opening resulted in a fluctuating cell constant. Hence, the arm was moved to the side of the stirring chamber U. The stirring action was observed by dropping a few crystals of potassium permanganate into water; the motion of the solution through the electrode arms was satisfactory at low stirring speeds.

The electrodes were platinum balls formed by fusing no. 20 gauge wire. The lead ends of these electrode wires were silver-soldered to no. 20 gauge copper wires which served as leads. The electrode was sealed to the lead-glass portion of a 7 mm graded seal; the Pyrex portion was sealed to the end of the chamber. Thus the graded seal was inside the chamber. A 4 mm i.d. capillary W connected the two chambers X and X'. Hence, there were two current paths, that of the lower resistance probably being through the arms Y and Y', and the cell body.

Condenser. The condenser assembly O was attached to the cell body by means of a 34/45 standard taper joint. Apiezon "W" wax was used for sealing. A 7 mm glass tube wound as a spiral was surrounded by a glass cooling jacket.

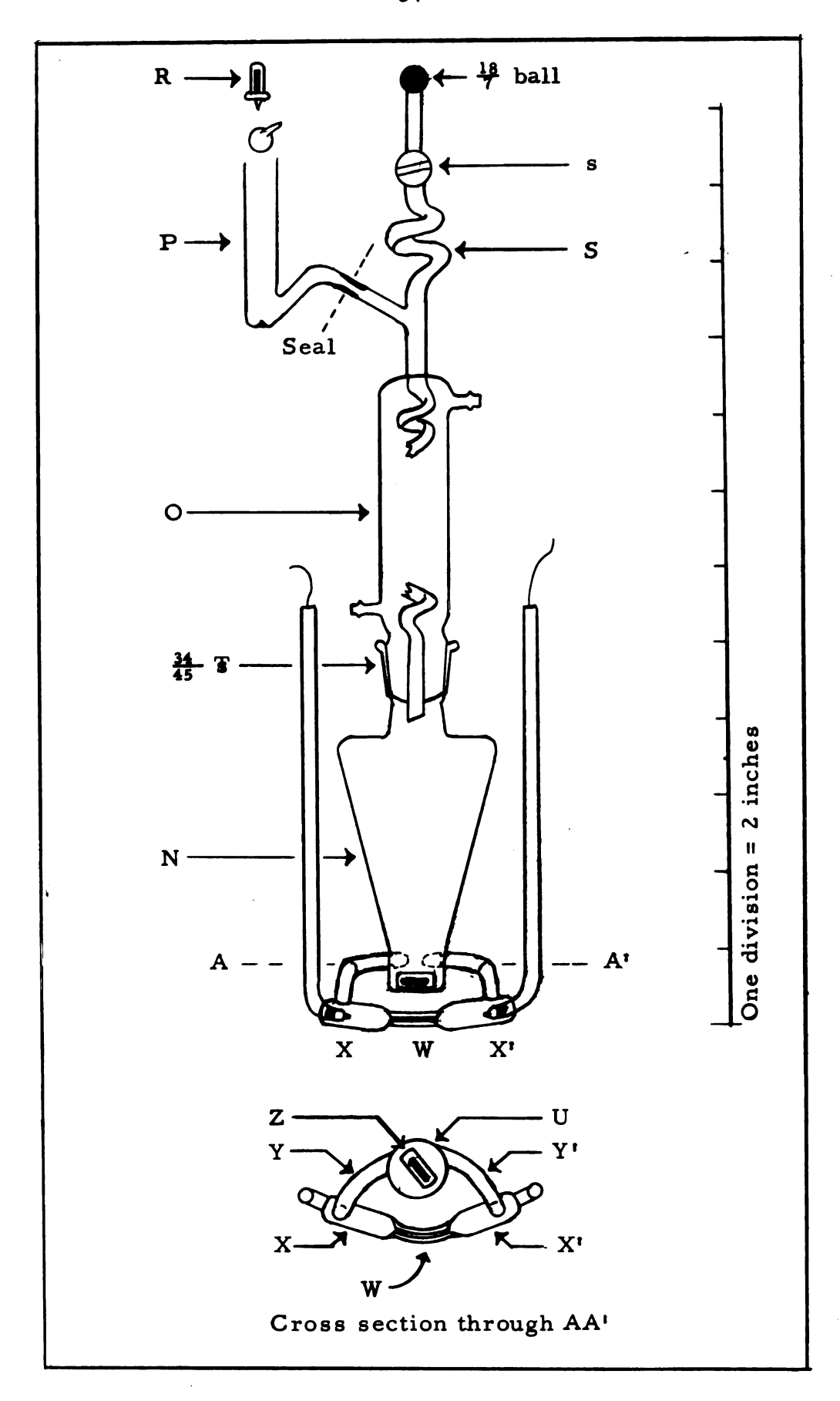


Figure 11. Diagram of conductance cell A.

The metal was introduced into the cell at the top of the condenser assembly through the distillation vessel P. This vessel was removed at the constriction when the metal had been distilled.

Originally, cold alcohol (-60 to -70°C) was circulated through the jacket using the closed loop cooling system. However, this resulted in refluxing the solution already in the cell and caused excessive splattering. This trouble was circumvented by adding the one turn spiral S and circulating the coolant from the thermostat through the jacket. The jacket temperature was estimated to be a degree or two above the thermostat, hence, preventing reflux action but still cold enough to avoid vaporization of the descending solution. The spiral S and the lines below it connecting to the condenser were wrapped with cheesecloth and aluminum foil shaped as a funnel. On these wrappings rested Dry Ice moistened with alcohol to aid heat transfer. This was effective in condensing the incoming ammonia which washed the metal into the condenser and on into the cell. If the ammonia condensation at the beginning was rapid, then approximately ten cubic centimeters of ammonia would flush the assembly so that blue solution was no longer evident by visual inspection. This small cold surface did not result in enough reflux action to cause any bouncing of the cell liquor.

Stirring Mechanism. To provide stirring action in cell A the internal stirrer must be actuated by an external stirring mechanism involving a magnetic field. Attempts to use the typical magnetic laboratory stirrer were unsuccessful at -37°C--the motor would freeze.

The mechanism shown in Figure 12 worked very well after rubber bands used as belts were replaced with spring belts. Rubber belts of Neoprene were also tried but became stiff and lost their elasticity at these temperatures. Two 3-step wooden pulleys were salvaged from a discarded ganged laboratory stirrer. No lubricants were used in the bearings. Sufficient play between the bearings and the collars on the

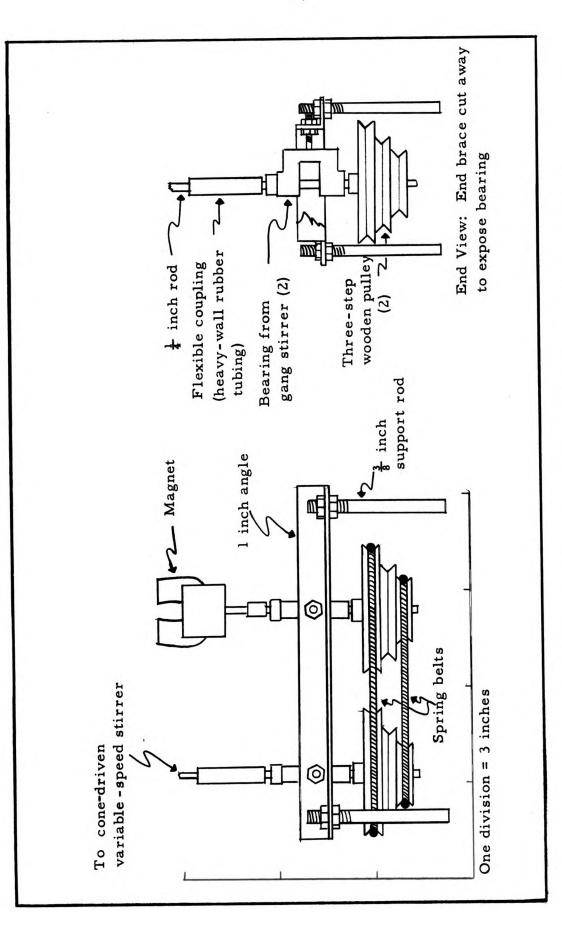


Figure 12. Diagram of stirring mechanism for use with conductance cell A.

shaft is necessary to allow for contraction upon cooling. A Cenco No. 78328 Alnico 5 horseshoe magnet was attached to the shaft situated below the cell. One end of a straight $\frac{1}{4}$ inch steel rod connected the shaft on the other pulley. A piece of heavy-wall rubber tubing served as a flexible coupling. The other end of the rod extended above the level of the bath liquid and was secured in the chuck of a Cenco No. 18803-1 variable speed cone-driven laboratory stirrer.

Typical Run Using Cell A. The cell, condenser and metal introduction assembly, distribution manifold Q, Kjedahl traps T, volumetric flasks V-2,-3,-5 and connecting tubes were cleaned with: (1) alcoholic potassium hydroxide solution, (2) rinsed with distilled water, (3) warm sulfuric acid-dichromate cleaning solution, (4) rinsed and soaked with distilled water, and (5) for the first three items, steamed for at least a half hour. The items were then dried.

The selected metal ampoule and glass enclosed magnetic breaker R were sealed in the metal introduction assembly P and this assembly was sealed to the condenser O as shown. With the stirrer (glass-encased magnet) in the cell, the condenser was attached to the cell using Apiezon "W" wax. The complete apparatus was attached to the manifold as J_7 and evacuated to a pressure of 2×10^{-6} torr. Infrared lamps were used for bake-out limiting the temperature to 150° C, the maximum allowable to avoid difficulty with graded seals, cracking, and wax softening. When the assembly could maintain a pressure of 1×10^{-5} torr for 30 minutes it was transferred to the thermostat and the remaining connections shown in Figure 13 were completed.

All components were evacuated to $\leq 1 \times 10^{-5}$ torr. With stopcocks \underline{s} , \underline{q} and \underline{g} closed, the bath cooling was started and the flasks V-2,-3, and -5 were filled from the storage vessel B (Figure 5) through \underline{c} , \underline{d} , \underline{e} , \underline{r} , and \underline{r} . A -40 C bath was used at B; Dry Ice-alcohol baths were used for the ammonia condensation. When the flasks were full,

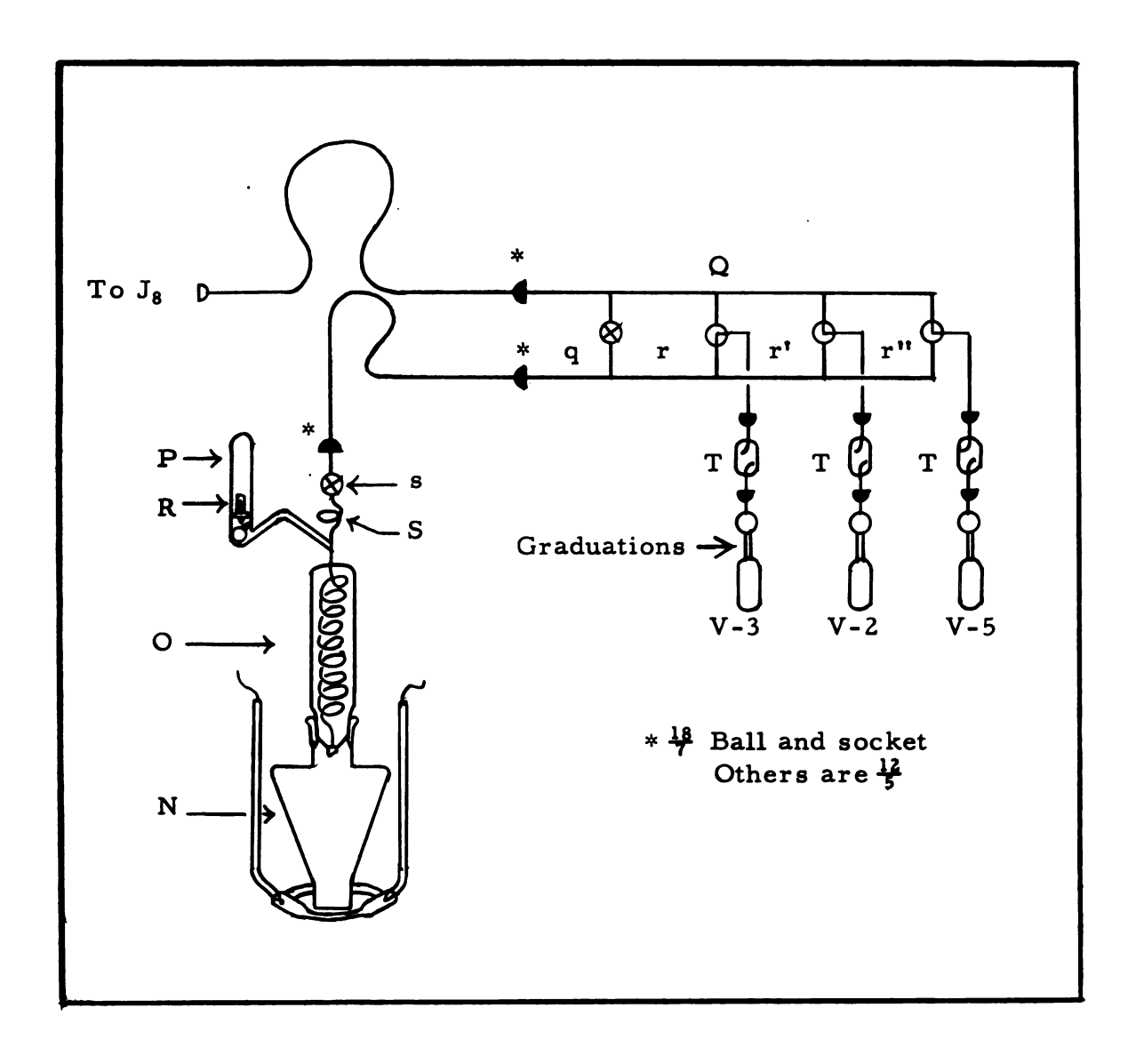


Figure 13. Schematic diagram of conductance cell A and associated apparatus.

the Dry Ice-alcohol bath was replaced with a -35 to -40°C bath. With the stirring of this bath to insure temperature equilibrium, the level of the ammonia was adjusted to the graduated portion, the stopcock closed and the level was recorded along with the reading from the platinum resistance thermometer. A very small piece of Dry Ice was added and the level again recorded when the resistance reading reached its previous value. This was repeated until two consecutive agreements were obtained. The flask was then stored at -78°C until needed. This procedure determined the amount of ammonia in the flasks.

With g opened, the distribution manifold was evacuated again. When the thermostat had reached controlling temperature, q and s were opened to the vacuum manifold and the cell pressure was observed to check for any possible leaks developed during cooling of the cell. With a pressure of less than 1×10^{-5} torr the ampoule was broken by raising the breaker with an external magnet and dropping it. Usually the presence of helium in the bulb drove the ion-gauge off scale, and it would take about fifteen minutes for the original vacuum to be reestablished. With s off, the metal was distilled from the vessel P by gentle heating. Because of the large mean-free-path the majority of the metal was deposited on the wall opposite the exit of the tube from the distillation vessel. This vessel was sealed off and removed at the constriction. The spiral was then wrapped with cheesecloth and a slurry of powdered Dry Ice in ethanol was used to saturate the wrapping. Ammonia vapor from the first flask V-3 (q closed and r opened to the lower manifold) was condensed on the metal and washed it down into the condenser and, hence, into the cell. This manipulation gave a quantitative transfer of the metal from the ampoule into the conductance cell proper.

When the addition was complete, resistance readings of the solution were recorded at 400, 600, 1000, 2000, and 4000 cps. Generally

the stirrer was operating during all measurements. When stable readings were obtained, another measured quantity of ammonia from the next flask was added. In the meantime, the previously emptied flask was being refilled and measured. The volume calibrations are given in Table 6, on page 83.

After six to eight additions the increment of change in concentration became too small to be useful. This cell was designed to permit concentrating the solution again after diluting it. This was accomplished by withdrawing a known amount of ammonia from the cell by condensation and measuring the volume in one of the flasks. After each withdrawal, a series of resistance readings was taken before proceeding to the next one. The last withdrawal removed all of the remaining ammonia from the cell. Because of the different flask volumes used, each flask had to be used the same number of times on withdrawal as on dilution to insure that the last increment of ammonia from the cell could be measured.

After completion of a run the apparatus was disassembled and the metal in the cell was converted to oxide by passing a stream of moist air into the cell and then washing the contents of the cell into a beaker. A drop of phenolphthalein in the condenser winding usually indicated that it was free of metal. The metal distillation vessel was opened and its contents were washed into a beaker, which also contained the washings from the condenser if the phenolphthalein test showed traces of the hydroxide.

Infrared lamps were used to evaporate the solutions to about 20 to 30 ml. The metal content was determined by titrating with standardized hydrochloric acid (standardized against Na₂CO₃) using a Beckman Model G pH meter. The equivalence point was determined from a plot of pH versus milliliters of acid. Although this method took longer than with an indicator it was more positive and permitted the end point

to be easily found. In general, weight of total metal from the two titrations agreed very well with the ampoule weight corrected for buoyancy (see Table 5). This substantiates the use of infrared heat lamps to concentrate the solutions and expel any residual ammonia.

Comments on Individual Runs for Cell A.

- CK-1: A Teflon stirring bar was used, thereby, reaffirming the reaction of alkali metals with polytetrafluoroethylene.

 The cell used had one of the exits to the electrode chamber entering the bottom of the cell. The condenser did not have the one turn spiral installed. Data were discarded.
- CK-2: A glass-encased stirring bar was used, but it cracked resulting in excessive decomposition of the solution. The cell mentioned above was used, but the make-up vessel from the transference apparatus replaced the condenser.

 The attempted procedure was to prepare the first solution outside of the cell and then transfer this solution into the cell.

 This was intended to introduce a quantitative solution with a known amount of metal but without introducing glass fragments. However, this method was too slow, and was abandoned.

 Data were discarded.
- CK-3: A broken graded seal was repaired and the cell constant redetermined to be 23.30 cm⁻¹ without the magnetic stirring bar. The glass-encased magnetic breaker chipped, but did not seem to affect the decomposition rate. Nine dilutions were made over a period of 81 hours. This was before the three flask distribution manifold and withdrawal techniques were devised.

Table 5. Comparison of Metal Content by Weight and by Titration

Run Number	Ampoule Weight Uncorrected Corrected	Weight Corrected	Weight in Condenser	Weight in Cell	Weight in Cell by Titration	Total Weight by Analysis	% Difference Between Columns 5 and 6
CK-3	0.0869	N.A.	N.A.	(0.0869)	0.07698 ^(a)	(0,0869)	12.4
CK-4	0,5067	N.A.	0.0042	(0, 5025)	0.4615 ^(a)	0.4657	8.5
CK-6	0690.0	N.A.	0.0024	(0,0666)	0.08488	0.08728	22.9
CK-7	0.14011	0, 1417	0,0044	0.1373	0.1373	0.1417	00.00
CK-8	0.40622	0.4078	0,0043	0.4035	0.4022	0.4065	0.32
CK-9	0.03471	0.03569	0,00169	0.03400	0.03301	0.3470	2.99
CK-10	0.14078	0.14124	0.0031	0.1381	0.1381	0.1412	00.0
CK-111	0.00782	0.00867	0.00116	0.00751	0.00693	0.00809	8.06
CK-12	0.8304	0.8314	0° 00800 (p)	0,8233	0.8232	0.8313	0.012
CK-14	0.4068	0.4080	0,0016 ^(b)	0.4064	0.4035	0.4051	0.72
CK-15	0.09367	0,09509	1	0.09509	0.09353	!	1.66
CK-16	0.2486	0.2497	:	0.2491	0.2477	!!	0.56

(a) These titrations were done with an indicator instead of pH meter.

N.A. Not available.

⁽b) Metal deposited above solution on first run which could not be returned to the solution.

- CK-4: Because of breakage, the cell was rebuilt with one of the side arms above the bottom of the cell by nearly the height of the stirring bar to prevent its being stuck in a side arm. The other side arm still entered through the bottom of the cell. The redetermined cell constant was 23.91 cm⁻¹. The cell was emptied after the first dilution so that the belt on the mechanical stirrer could be replaced. Because of bubble formation in the cell chambers, the cell was disconnected at the end of 6-D and tilted to remove bubbles. Helium gas, adjusted to one atmosphere pressure was used to cover the solutions.
- CK-5: The side arm entering the bottom was repositioned to the side of the cell. The cell constants were 22.19 cm⁻¹ with the solution height even with the top of the side arms, and 22.16 cm⁻¹ for solution heights above this. Six dilutions were made but it was determined that decomposition was excessive. Upon disassembly, a cracked stirring bar was found. Helium gas was used to adjust the pressure to one atmosphere. Data were discarded.
- CK-6: The cell and cell constants were the same as in run CK-5.

 The cell was disconnected and tilted to remove bubbles at the ends of dilution 1-D, 2-D and 4-D. Helium gas had been used to adjust the pressure to one atmosphere. A portion of the helium and hydrogen gases were removed on the withdrawal process by closing the stopcock above the condenser, reducing the ammonia vapor pressure nearly to zero by freezing the ammonia in the volumetric flask and evacuating this gas space by the high vacuum system.

- CK-7: The side arms and chambers were sloped so that bubbles would be discharged from this part of the cell. Cell constants were redetermined as 21.51 at the arms, and 21.50 cm⁻¹ for solution levels above the arm openings. Helium covering gas was used.
- CK-8: Same cell and cell constants as for CK-7. No covering gas was used. On 1-W, the three-way stopcock above a volumetric flask popped during a withdrawal. This could have allowed air to come in contact with the solution in the cell. Figure 24, in the next chapter, shows a large jump in ∧verifying this observation. It is interesting to note that after the initial decomposition the solution appeared to decompose at the same rate as before the admittance of air.
- CK-9: Same cell and cell constants as CK-7. Still some difficulties with bubble formation.
- CK-10: A 20% HF solution was used as a quick rinse in the cell clean-up procedure. The redetermined cell constants were 21.36 and 21.35 cm⁻¹. At the end of the run, a crack was observed in a graded seal; decomposition seemed rather high. Prior to the collection of resistance versus concentration data, resistance versus temperature data was recorded for five hours. The concentration was approximately 0.22 molar and the temperature range was from -37.1 to 46.9°C. No covering gas was used.
- CK-11: The graded seal was replaced. The redetermined cell constants were 21.15 and 21.14 cm⁻¹. Also cell constants determined with standard potassium chloride solution gave

essentially the same value. This was the most dilute run.

No covering gas was used. Because of the small amount of

metal, the possible error in analysis was somewhat higher.

Cell Constant Determination for Cell A. The cell constants were determined by the procedure recommended by Kraus (28). The calibrating solution was potassium iodide nearly saturated with iodine. The approximate amount of potassium iodide (usually for 0.05 molar solution) was mixed with iodine using a mortar and pestle. About 5 ml of boiling water were added and the solution filtered through a sintered glass funnel. The filtrate was made up to volume in a volumetric flask. If free iodine was present in the resulting solution, it was filtered off.

The specific conductance of this solution was determined by comparison with a Leeds and Northrup Type A conductance cell previously standardized with potassium chloride.

The standard solution of KCl contained 0.74532 g of recrystallized and fused reagent grade potassium chloride per 1000 g of solution in vacuo. The values of Jones and Bradshaw were used in the conductance equation:

$$\Lambda = 149.87 - 93.985 \sqrt{c} + 31.8 c \log c + 144 c$$
 [4.3]

where c = equivalents per liter (75). The comparison cell had a constant of 29.10₁ cm⁻¹.

Because of breakage of graded seals or rebuilding of the cell, the cell constant of the ammonia cell was determined several times as noted in the discussion on individual runs.

3. Conductance Cell B

The Cell. The cell is diagrammed in Figure 14. The notable features were: (1) three electrodes, hence, three pairs or combinations

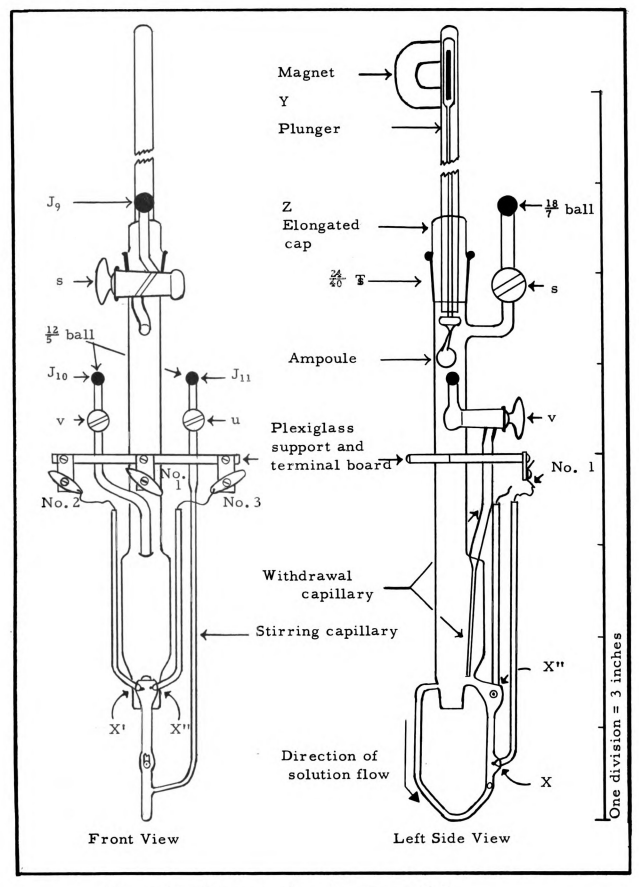


Figure 14. Diagram of conductance cell B.

to be called sub-cells, (2) provision for withdrawal of known amounts of solution, and (3) the use of vapor for stirring.

The upper body of the cell, made from 21 mm o.d. Pyrex tubing, was attached to 33 mm o.d. tubing. The lower end of the body was reduced in diameter and offset to be in line with the plunger. The 5 mm o.d. loop containing the electrodes entered the body about 2 cm above the bottom thus forming a well. The oval shape of the loop-body openings and the well served to retard glass ampoule fragments from entering the loop and obstructing the current flow.

The ball electrodes X, X', and X", which correspond to leads 1, 2, and 3 at the terminal board, were formed on no. 36 gauge platinum wire by melting. They were then sealed through 5 mm tubing and into the electrode chambers in the loop. X' and X" were separated by about 0.7 cm; X-X' and X-X", by about 4.5 cm. The platinum electrode wires were silver-soldered to lugs mounted on $\frac{1}{2} \times 1 \times \frac{1}{8}$ inch strips of laminated phenolic board. The other end of the lugs were soldered to the leads to the conductance bridge with rosin-core solder. Soldering was perferred over clips to minimize contact resistance. The phenolic strips were attached to the Plexiglass support with 6-32 brass machine screws. The three-sectioned Plexiglass support gave rigidity to the withdrawal and stirring capillaries and was not used for supporting the cell. The cell was supported just below the 24/40 taper by a three-fingered clamp.

The stirring capillary was 5 mm standard-wall tubing attached to a Pyrex No. 7544 - 2 mm stopcock. The withdrawal capillary was formed from 2 mm i.d. medium-wall capillary tubing of which a portion was drawn out to the taper mounted inside the cell. To keep the volume in the capillary small, it was sealed relatively close to a Pyrex No. 7546 - 2 mm stopcock. This type of stopcock has no bore to be filled with solution, permits only a small amount of solution to drain back

into the cell because it shears the flow, and provides sufficient volume to hold the vaporizing liquid ammonia. On withdrawal, the capillary was well rinsed, and thus, there was little danger that metal will be returned to the cell to change the concentration.

Typical Run Using Cell B. The apparatus shown in Figure 15 was cleaned as follows: (1) alcoholic potassium hydroxide solution, (2) rinsed with distilled water, (3) immersed in the HF-HNO₃ cleaning solution for periods not exceeding five minutes (preferably less-especially for the conductance cell), (4) rinsed and soaked in distilled water, (5) those items in contact with ammonia or solution such as the Kjeldahl traps, volumetric flasks, and cell were rinsed with concentrated or fuming nitric acid or concentrated hydrochloric acid to remove the last traces of detergent and then rinsed in distilled water, and (6) items were given final rinses with de-ionized water or if possible, attached to a steam generator and steamed for at least a half hour before drying.

The selected ampoule of metal was sealed to the glass plunger Y and suspended in the elongated cap Z by an external permanent magnet. Apiezon "N" grease was used on all stopcocks except \underline{u} and \underline{v} which were lubricated with high vacuum silicone grease. With socket caps on ball joints J_{10} and J_{11} the cell was attached to J_7 at J_9 , evacuated by a mechanical pump and then by the high vacuum system until a consistent pressure of less than 1×10^{-5} torr was attained.

The first several times that this cell was used, bake-out was attempted by using a soft flame or heat lamps. The last two runs did not include this bake-out because of suspicions that the Cenco Vacuum Wax 11455B used in the electrode tubes to stop minute leaks at the glass-to-metal seal might be fluid enough to flow through these leaks onto the electrode surfaces.

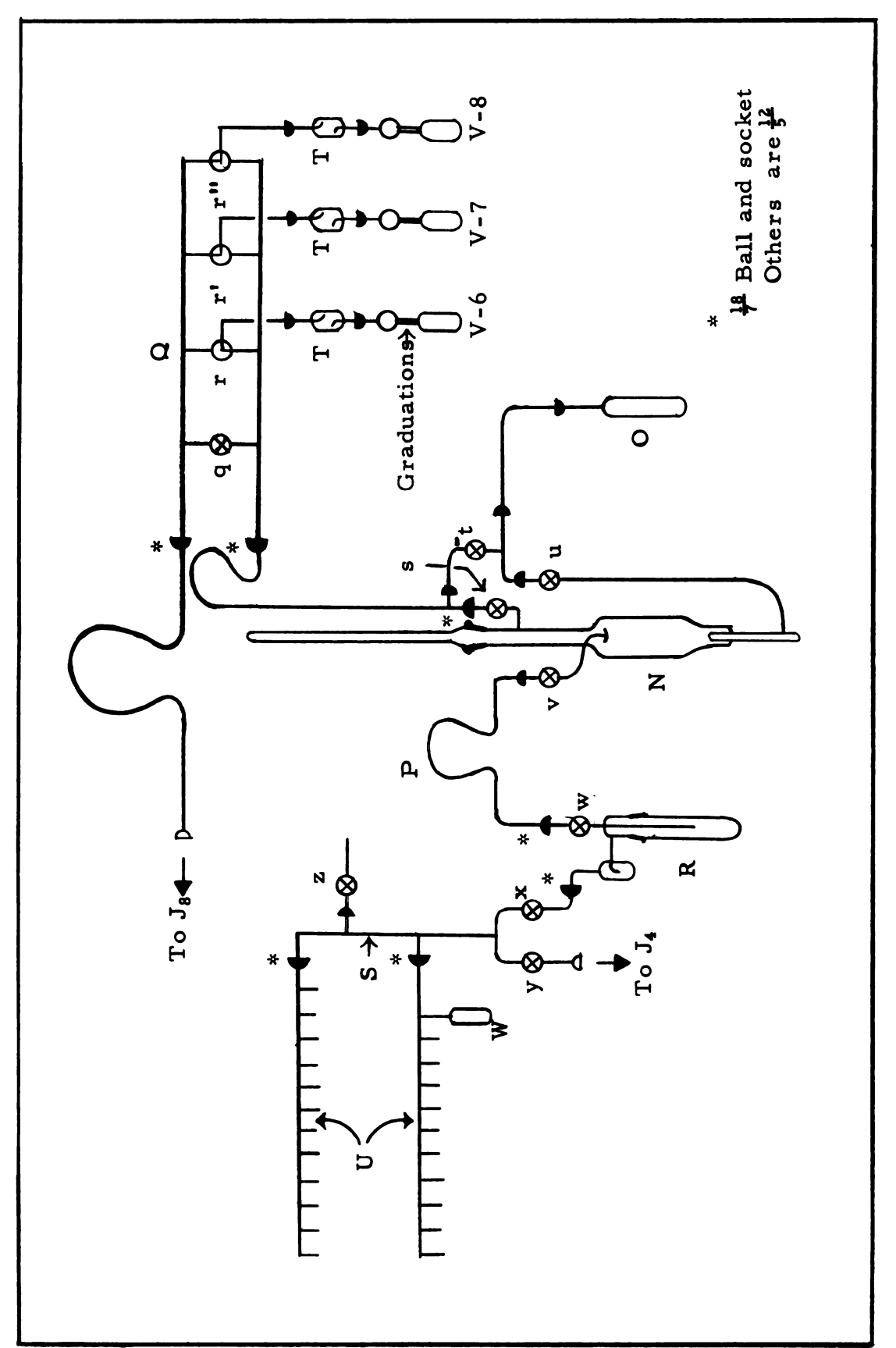


Figure 15. Schematic diagram of conductance cell B and associated apparatus.

The cell was transferred to the bath and the rest of the apparatus assembled as illustrated in Figure 15. Evacuation to less than 1×10^{-5} torr was effected before cooling was started. Temperature control of the bath could be established in less than two hours by auxillary cooling with a test tube, 2×16 inches, containing Dry Ice and enough alcohol to aid the heat transfer. After testing the cell for possible leaks resulting from cooling, \underline{s} , \underline{t} , \underline{u} and \underline{q} were closed and condensation and measurement of ammonia into the volumetric flasks V-6, -7, and -8 were accomplished as previously described for cell A.

The following procedure, used only on run CK-16, is recommended for rinsing the cell with pure solvent and measuring its specific conductance: Ammonia from the storage vessel B was condensed into a bulb of about 50 ml capacity attached at J₃. About 20 ml of ammonia from this bulb was then vaporized through d, e, q, t, and u to rinse the cell. This minimizes the danger of carrying metal in the vapor stream into the cell. Trouble of this type was encountered on runs CK-12, -14, and -15 when the rinse ammonia was condensed directly from the storage vessel. Once the cell has been contaminated from metal spray, it requires about eight cyclic rinses to lower the specific conductance enough to proceed with the run proper.

The cyclic rinses were performed by withdrawing solution down to the tip of the withdrawal capillary through \underline{y} into vessel R. This ammonia was then distilled back into the cell through \underline{x} , \underline{y} , \underline{d} , \underline{e} , \underline{q} , \underline{t} , and \underline{u} . Stirring of the solution was effected by closing \underline{u} and \underline{q} , opening \underline{s} and \underline{t} , and surrounding \underline{O} by a bath colder than -40° for 15 to 30 seconds. The vessel was then warmed, and when the solution in the cell began to rise in the stirring capillary \underline{u} was opened and \underline{t} or \underline{s} was closed. Proper manipulation of \underline{u} on the stirring tube is essential to prevent solution in the cell from being drawn or forced up the tube beyond the bath level, thus contaminating the solution or depositing metal which can not be reclaimed.

À

The bulb was then lowered and the solution stirred to rinse the bulb and plunger. With this recommended procedure the solvent conductance for CK-16 was less than 0.2×10^{-6} mho cm⁻¹ after the first rinse.

The ammonia in the cell was returned to the storage vessel B through the withdrawal network \underline{v} , \underline{w} , \underline{x} , \underline{y} and \underline{c} . Residual ammonia vapor was removed through \underline{q} and \underline{s} by connecting to the high vacuum manifold.

The ampoule was broken by releasing the plunger. When the cell pressure was less than 1×10^{-5} torr, \underline{q} and \underline{s} were closed and \underline{t} and \underline{u} opened. The condensation of ammonia from the first flask then commenced. A larger condensing surface is presented by bubbling the incoming vapor through the solution already present. The air stream from a hair dryer was used to hasten the transfer. With the transfer completed \underline{u} was closed and \underline{s} opened allowing the vapor above the solution outside the bath liquid to come to a temperature equilibrium. When the volumetric flask had reached room temperature \underline{r} was rotated 180° and filled with ammonia from storage vessel B and consequently measured as previously described. A check for leakage resistance to ground was made at this time.

Resistance readings at 400, 1000 and 4000 cps (also sometimes at 600 and 2000 cps) were recorded for all three cells. The solution was stirred by the technique described above and resistance values again determined. The second quantity of ammonia was then added from the next flask in line (V-7) and measurements were made by the above method. The flask calibrations are given in Table 6, page 83.

After the readings for the second addition had been made, about half of the cell solution was removed into the metal collector R. The recommended procedure involves surrounding R with liquid nitrogen.

With x closed, w and v were opened and solution was withdrawn,

taking extreme care that the level in the cell stayed above the tip of the withdrawal capillary. This prevented the withdrawal of any ammonia vapor from the cell which was suspected in run CK-12. By using liquid nitrogen for the withdrawal, the possibility of the cold solution vaporizing on reaching the warm areas of the withdrawal assembly and the resulting pressure build-up forcing a more concentrated solution back into the cell is minimized. This possibility of error could be checked at the completion of the withdrawal by stirring the solution and checking for a change in resistance. For CK-15 and CK-16, no resistance changes were observed.

The ammonia from the solution collected in R was distilled into a numbered heavy-wall glass ampoule W on one of the collection manifolds U. A bath colder than -40° was placed around R to aid the distillation and liquid nitrogen cools the ampoule. Before sealing the ampoule at the constriction, the space in the line, up to the withdrawal stopcock v, was exposed to the ampoule to essentially reduce the amount of ammonia vapor remaining in this segment to zero. In sealing the ampoule, the glass should be carefully annealed to relieve any strains. At room temperature, the pressure existing inside the ampoule is about ten atmospheres. Three ampoules of run CK-13 were lost when the tips blew off because if improper annealing.

The above procedure of adding known amounts of ammonia and withdrawing known amounts of solution was repeated until the resistance of the low conductance cell reached about 80,000 ohms.

After completing the dilutions, the ammonia remaining in the cell, and the ammonia vapor present in the lines connecting the lower manifold and that in the three volumetric flasks was condensed into two ampoules. This gave a check on total amount of ammonia used. The apparatus was then disassembled. The metal in the metal collection vessel R and line P was oxidized by an air stream. The washings

from these items and the cell were treated as described above to determine the total amount of metal.

As a margin of "safety," the sealed ampoules were first weighed at temperatures below -30° before being warmed to room temperature. After several hours at room temperature the ampoules were weighed using two independent trials to minimize weighing errors. They were then cooled to Dry Ice temperature, and a scratch was made on the tube which was then broken. A clean break is produced by simultaneously pulling and bending the tube. Only in a few cases were small chips. observed, and these were of negligible weight. Both the ampoule and the stem had been numbered before assembly with a vibrator marking tool. After the ammonia had evaporated, the ampoules and stems were dried at 130° for at least one hour, cooled to room temperature and weighed. A check is obtained after washing the ampoules and stems in distilled water, drying at 130° and cooling to room temperature. The two weights are averaged. The difference between the average weights gives the weight of ammonia withdrawn. The weight of ammonia added is determined by applying density-temperature data (73) to the readings recorded from measurements on the volumetric flasks.

Comments on Individual Runs with Cell B.

- CK-12: This was a potassium-ammonia run used to check the performance of the apparatus. The cell was cleaned with alcoholic-KOH and the HF-HNO₃ cleaning solution. Two rinses with pure ammonia from the storage vessel B gave a resistance of 6.3 x 10⁶ ohms or L = 0.87 x 10⁻⁶ mho cm⁻¹. Twelve dilutions were made. Some vapor may have been removed during the withdrawal process.
- CK-13: This was also a potassium-ammonia run. The cleaning procedure was the same as for CK-12. Two rinses were

made which gave $R = 33 \times 10^6$ ohms; $L = 0.17 \times 10^{-6}$ mho cm⁻¹. Twelve dilutions were made, but three of the ampoules of ammonia were lost so the data were discarded.

- CK-14: This was a potassium deutero-ammonia run, with the cleaning procedure the same as for CK-12. Spray, containing metal, was carried over into the cell; eight cyclic rinses were made after which R = 33 x 10⁶ ohms and L = 0.17 x 10⁻⁶ mho cm⁻¹. On the first dilution, some metal was deposited above the level of the solution in the stirring capillary.

 A total of eleven dilutions were made.
- CK-15: This was a deutero-ammonia run also, with the same cleaning procedure as above. Because of metal spray, seven cyclic rinses were made, with the ampoule and plunger being rinsed on the last one, which gave R = 14 x 10⁶ ohms, L = 0.39 x 10⁻⁶ mho cm⁻¹.
- CK-16: This was a potassium-ammonia run to replace that of CK-13; the same cleaning procedure was used. Rinses were taken from pure ammonia previously condensed in a small evacuated vessel from the sodium-ammonia storage vessel.

 Two rinses, including the ampoule and plunger on the last rinse, gave no detectable increase in conductance, which was for R = 33 x 10⁶ ohms: L = 0.17 x 10⁻⁶ mho cm⁻¹.

Cell Constant Determination for Cell B. The cell constants of all the cells were determined by comparison with a low-conductance cell used in aqueous conductance research. The constant for the latter cell and the method of calibration is specified on page 68. This method seemed to give satisfactory results and was not questioned until measurements were made on conductance cell B.

As previously described under the cell design, cell B was composed of two sub-cells for solutions of high conductance and one sub-cell for solutions of low conductance. The low cell (low conductance) gave consistently higher equivalent conductance values than the two high cells, which agreed within 0.3% for concentrations higher than 0.0016 M.

The values from the low cell were suspected to be in error because of the agreement between the other cells and also because of higher capacitance associated with this cell as noted from bridge readings.

However, the results from the low cell agreed quite favorably with the data of Kraus and with the results obtained with conductance cell A.

A possible explanation for this discrepancy might be the variation of the cell constant with solution resistance resulting from poor cell design.

The variations are probably not due to vacuum wax seeping through the glass-to-metal electrode seal because they were essentially the same for four different determinations.

As preliminary check, comparison solutions of three different concentrations of KI and I₂ were prepared. These were used to determine the constants of the cell at the completion of run CK-16 with the only cleaning being several rinses with de-ionized water. A plot of k (cell constant) versus specific conductance displayed a positive slope and changed quite rapidly at low concentrations.

Because of this behavior, more points were desired. The cell was cleaned by the procedure described in the experimental section. Two additional concentrations of KI-I₂ solutions were prepared; the approximate concentrations were: 0.0025, 0.01, 0.05, 0.1, and 0.5 molar in potassium iodide.

The thermostat was that used as the refrigerated bath but with distilled water as the bath fluid and a mercury regulator set at about 25°C to control the heat input of the infrared lamp. A current of air from the compressed air line was directed onto the liquid surface to produce

the cooling required to maintain proper temperature control. There remained a variation of $\pm 0.05^{\circ}$ during the complete cycle.

The cell constants using these solutions showed the same general trend as the previous determination but the values were inconsistent and not reproducible. Crystals of iodine were observed in several of the solutions.

Another set of solutions was prepared by making a stock solution of approximately equi-molar amounts of potassium iodide (slight excess) and iodine so that I₃ ion should be formed. But upon dilution, iodine precipitated from all solutions, and these were discarded.

Then a stock solution was prepared with a molar ratio of about 5 to 1 of potassium iodide to iodine. From this stock solution four other dilutions were prepared. All of these were free of iodine crystals when observed in a light beam. The electrodes were electrolyzed for several seconds in dilute potassium hydroxide solution and then rinsed thoroughly.

A frequency dependence was still observed. Generally, plots of resistance versus (frequency) possessed positive slopes with downward curvature, the percent change being greater at higher frequencies giving lower cell constants (see Figure 16). In a few cases, straight line extrapolations through all points could be made with positive slopes.

The graphs of cell constants versus specific conductance displayed the behavior described above, with a moderately large decrease in k at low concentrations. A smooth curve could be drawn through the points except for what appeared to be an inversion of the values at the two lowest concentrations. However, the change was too large to permit extrapolation. Rinsing and refilling with the same concentration gave reasonably reproducible results. After completing the most concentrated run, an attempt was made to check the cell constant by using more dilute solutions, but the results showed considerable scatter. At this

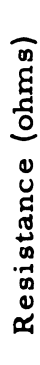
stage in the studies, there was fear that perhaps the calibrations of the other cells used for three years were in error.

The advantage of using KI-I₂ solutions is the depolarizing effect of I₃ resulting from the presence of I₂. The question to be answered was whether the inconsistent results obtained for cell B were due to polarization and/or poor cell design. Metal-ammonia solutions show very little polarization at electrodes as indicated by virtual absence of frequency dependence. Therefore, if the trouble were just with the use of KI-I₂, then the elimination of polarization and proper calibration with aqueous solutions should give a cell constant applicable to metal-ammonia work. In order to clarify the situation, KCl solutions of approximately 0.003, 0.05 and 0.1 molar were prepared and their specific conductances determined with the aqueous cell. These solutions, along with a standard 0.01 demal solution, were used to redetermine the cell constants for the transference and emf cells and for conductance cell A, which had previously been determined with KI-I₂ solutions, and to our great relief the agreement was quite satisfactory.

However, for cell B the values determined with KCl still varied (as much as 20% in the case of sub-cell 3). Plots of resistance versus (frequency) differed in character from those of KI-I₂ solutions as shown in Figure 16. In the case of sub-cell 3, the plot of k versus concentration resulted in a straight line. The values of k determined by KI-I₂ and KCl are shown in Figure 17.

It is apparent that when extrapolation is used, the two methods give the same value at infinite dilution. Also, it appears from Figure 16 that the same k might be obtained if extrapolation to infinite frequency could be made.

To further check this idea, the electrodes of cell B were platinized using chloroplatinic acid (76). Even a few seconds at one milliamp gave a black deposit. Cleaning by alternating current electrolysis in aqueous



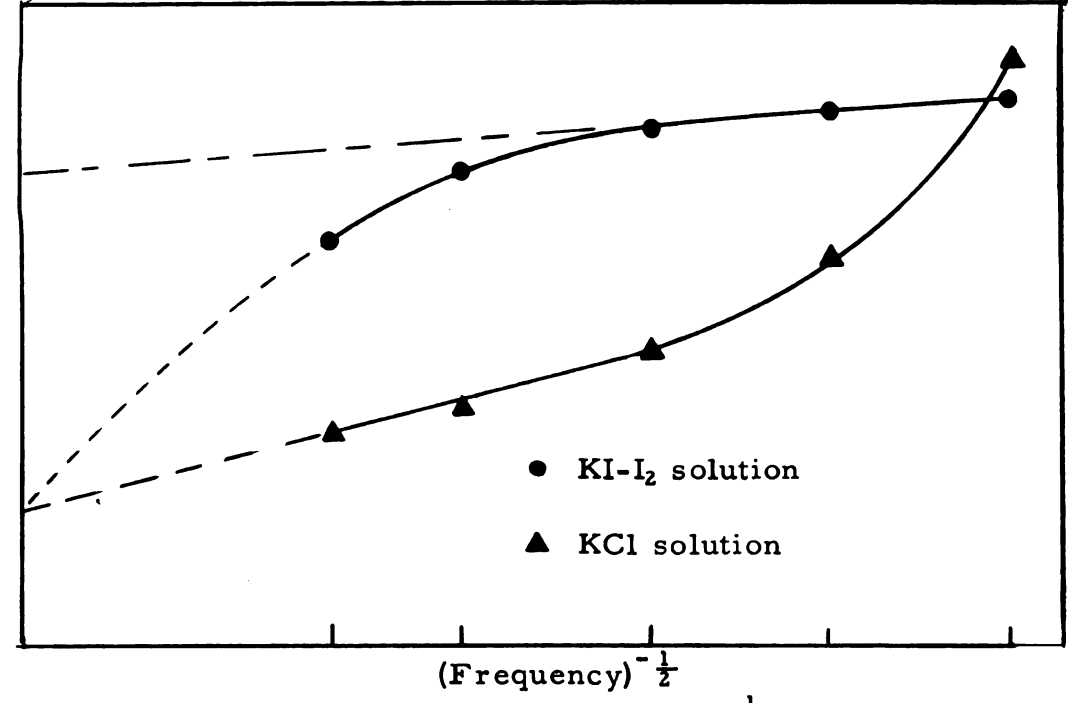


Figure 16. Resistance versus (frequency) dependence upon calibrating solutions.

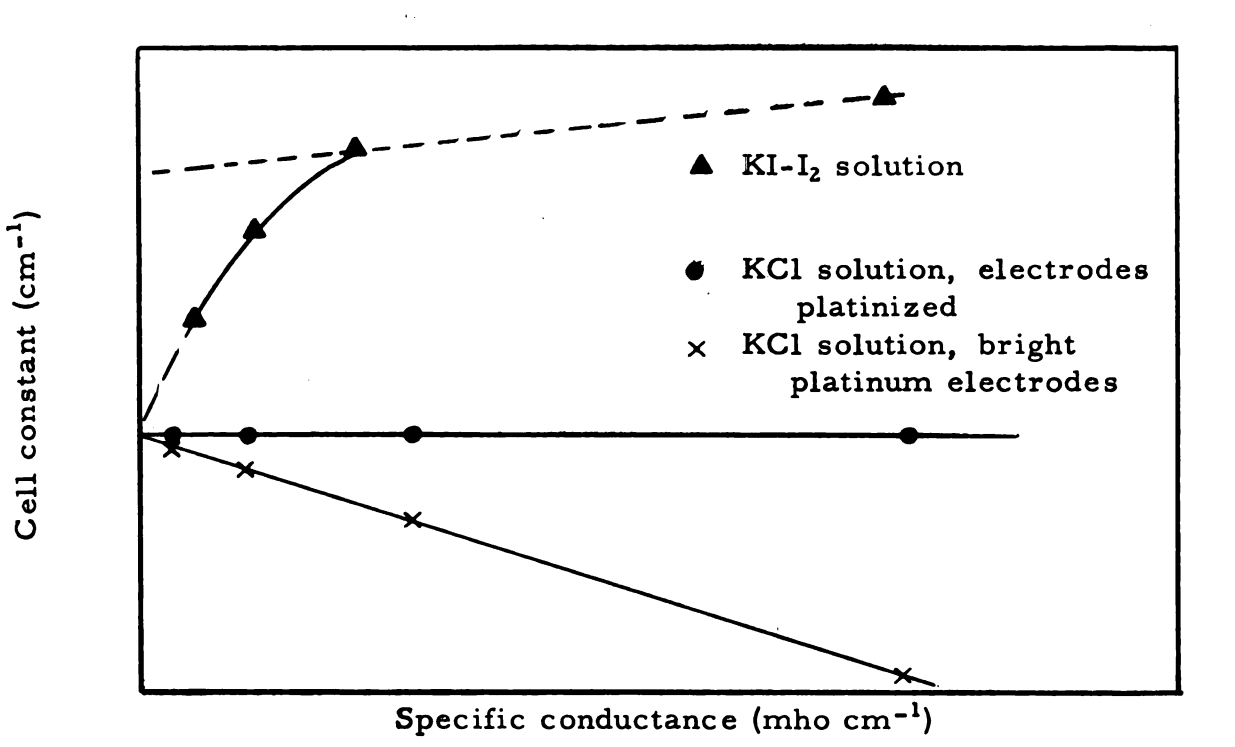


Figure 17. Cell constant versus specific conductance showing the variation of cell constant with calibrating solution and electrode surface.

potassium hydroxide solution removed the deposit. A new deposit was applied and the cell was rinsed with de-ionized water. The frequency dependence, as displayed by curves of R versus f was reduced only slightly at low concentrations. However, a plot of k versus concentration showed k to be independent of concentration—as should be the case for all good cells. Perhaps the reason for the difficulty with cell B is that the ball electrodes in this cell are smaller than in the other cells.

However, as will be seen in the next chapter, the cell constants for cell B thus determined were still not completely satisfactory.

There was a definite concentration dependence of the cell constant for the metal-ammonia solutions.

An appreciable amount of the frequency dependence of resistance may be removed in some cases. If the capacitance decades indicated a value higher than 400 pfd for the external capacitance, the method of Jones and Christian (77) was applied. They investigated the characteristics of cell design and its relationship to frequency dependence and polarization effects and derived the following equation

$$R_{s} = \frac{R_{p}}{1 + R_{p}^{2} C_{p}^{2} (2\pi f)^{2}}$$
 [4.4]

where:

 $R_n = resistance read from the bridge$

C_p = capacitance in 10⁻⁶ fd to balance the bridge

 R_s = resistance of the solution

f = frequency.

However, this equation does not correct for polarization resistance. For metal-ammonia solutions electrode polarization is usually negligible, but because of the small surface area it is possible that polarization effects were caused by appreciable current densities thus contributing to the curvature found in the R versus $f^{-\frac{1}{2}}$ plots.

Volumetric Flask Calibrations. Volumetric flasks numbers 2, 3, and 5 were calibrated with mercury by R. F. Sankuer (78). Flasks numbers 6, 7, and 8 were calibrated with triple-distilled mercury by the author. The volume was calculated from the average of two independent trials.

Table 6. Calibrations of Volumetric Flasks

Flask .	Calibration	Volume (ml)		
Number	Mark	25°C	-38°C	
2	0.3	31.58 ± 0.01	31.56 ± 0.01	
3	1.3	46.04 ± 0.02	46.01 ± 0.02	
5	1.7	48.79	48.76	
6	0.040	8.205 ± 0.000	$03 8.200 \pm 0.0003$	
7	0.080	8.469 ± 0.000	02 8.464 ± 0.0002	
8	0.080	8.529 ± 0.000	04 8.524 ± 0.0004	

The graduated portions on flasks 6, 7, and 8 were sections of 1/10 ml pipet with 1/100 ml graduated intervals. On flasks 2, 3, and 5, the graduated sections came from a 1 ml pipet with 1/10 ml graduated intervals. The small bulb above the graduated section aided the vaporization of ammonia.

C. Transference Numbers

1. The Cell

Except for the basic vacuum system (see Figure 5), the complete transference apparatus is diagramed in Figure 18. Figure 19 is a photograph of the cell corresponding to Figure 18. The photograph of the

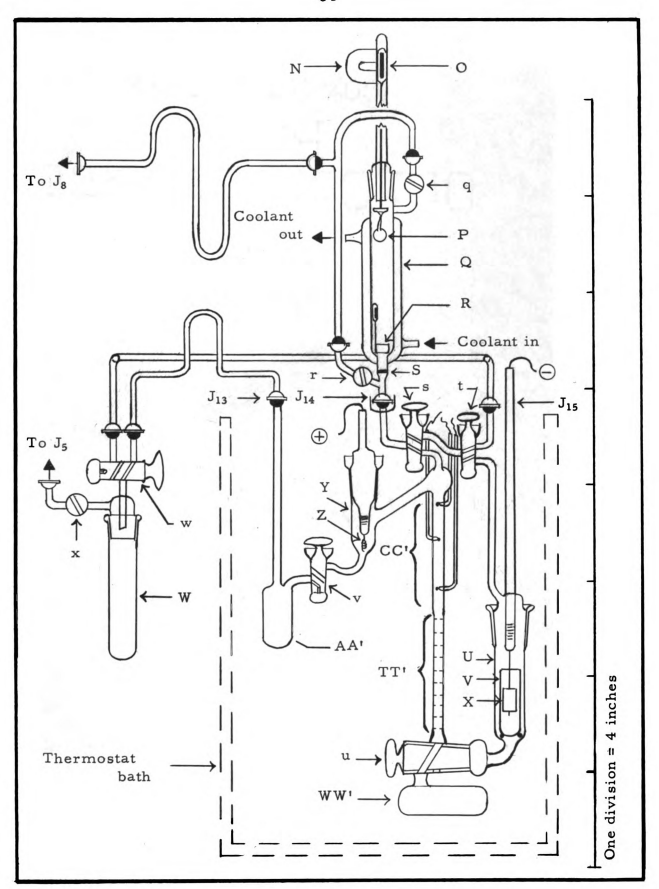


Figure 18. Diagram of transference cell and associated apparatus.



Figure 19. Photograph of transference cell.

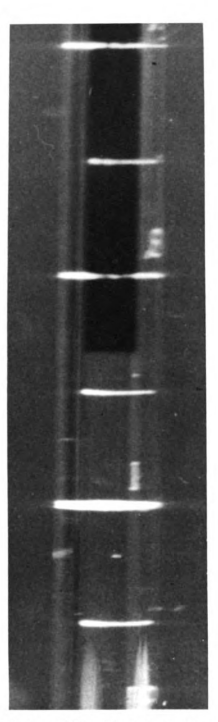


Figure 20. Photographic enlargement of boundary: top half is metal solution; lower half is salt solution.

rising boundary (Figure 20) illustrates its sharpness. Above the boundary is the dark blue metal-ammonia solution; below the boundary is the clear solution of the metal bromide in liquid ammonia.

The clear following solution (potassium bromide in liquid ammonia) filled the boundary stopcock <u>u</u> (Pyrex No. 7548, 6 mm bore) and cathode compartment U. The cathode X was made from two strips (12 mm width) of pure silver. One strip was corrugated and the other smooth. The ends of the two strips were squeezed and fused onto a no. 20 gauge platinum wire which was later sealed to the soft glass portion of a graded seal. A copper lead was silver-soldered to the other end of the platinum wire. The strips were wound concentrically into a cylinder of 12 mm diameter and their ends fused to the layer below. The AgCl coating was applied electrolytically. The cathode rested in a 16 mm o.d. x 55 mm cathode cup V which retained the solution and flakes of AgCl that were removed from the cathode in the presence of liquid ammonia.

The dark-blue leading solution was potassium metal dissolved in liquid ammonia. This solution filled the transference tube TT', conductance cell CC', and anode compartment Y. The anode Z was a spiral of no. 26 gauge platinum wire fused through soft-glass and attached to an extended 24/40 Pyrex taper (No. 6710) using a graded seal. For runs prior to 47-K-13, the conductance cell consisted of electrodes 1 and 2 which were no. 34 gauge platinum wire sealed through 3 mm Pyrex tubing and into the Pyrex transference tube. These electrodes were spaced 6.5 cm apart on opposite walls. The 3 mm tubing shielded the conductance leads from the bath liquid. Minute leaks at the wire seals were eliminated by partially filling the electrode tubes with Apiezon "N" lubricant. Because of difficulties to be discussed later, a third electrode of no. 36 gauge wire was installed opposite and 3.8 cm above the No. 2 electrode. The Apiezon "N" lubricant which showed signs of decomposition resulting from drying the cell in the oven, was removed and replaced with Cenco No. 11455 B vacuum wax which showed prior success in sealing

this type of leak in the emf and conductance cells. This wax was also used in the tube for electrode no. 3.

The transference tube was made from a two milliliter graduated pipet. The volume between marks was calibrated with mercury (78) before construction of the cell, and may be found in Table 10, page 151.

The graduated portion of the make-up vessel was a 100 ml Pyrex graduate. With the breaker cup R the volume was 12 ml less than the reading given by the graduated marks. (The cup occupied about 2 ml; the resting plunger without ampoule, occupied another 2 ml.) The graduate was enclosed by a 46 mm o.d. Pyrex jacket through which cold alcohol was circulated to condense the ammonia. To the bottom was sealed a 10 mm coarse glass frit S, and to the top a 24/40 female joint.

The stopcocks <u>s</u> and <u>t</u> were three-way stopcocks of 2 mm bore, each having a mercury well and vacuum back (Pyrex No. 7540). Stopcock <u>v</u> was of the same type but two-way (Pyrex No. 7500). The one, <u>w</u>, on the waste vessel W was a three-way high vacuum stopcock (H. S. Martin, M-30660, 4 mm). Stopcock <u>x</u> had an oblique 2 mm bore but not a vacuum back. A stopcock retainer (Emil Greiner Co.) assured proper seating for vacuum work.

2. Current Controller

The constant current source required for the determination of transference numbers by the moving boundary method, was constructed for investigations of aqueous solutions in this Laboratory. The circuit diagram appeared in Karl's thesis (79), and is repeated here for convenience and reference (Appendix B). The current is determined from the potential drop across a standard resistor connected in series with the cell and controller. This signal was compared in a Leeds and Northrup K-1 potentiometer, from which the unbalance was fed to a Brown "Electronik" 356358-1 amplifier used to drive a Brown 76750-3 balancing

motor. The motor was attached to a 10-turn multi-turn potentiometer which compensated for minor fluctuations not removed by the electronic current controller.

3. Recommended Procedure for Transference Run

The following preliminary manipulations are necessary before assembly in the thermostat:

- a) All the components illustrated in Figure 18 first received a preliminary cleaning operation by remaining in contact with alcoholic potassium hydroxide solution for one-half to one hour. The longer time was used for the transference cell to aid in the removal of the silicone lubricant.
- b) The cleaning was followed by several rinses with distilled water.
- c) The HF-HNO₃ cleaner was used next with the maximum time in contact with the glass limited to about two minutes. This cleaner appeared to attack the ground surfaces and the glass frit.
- d) After rinsing with distilled water, either nitric acid or hydrochloric acid was used to remove the last traces of detergent.
- e) The various items were then alternately rinsed and soaked in about six changes of distilled water and about the same number of changes of de-ionized water. Small items were steamed for at least a half-hour in preference to soaking. The steam was generated from de-ionized water in a one liter flask heated by a heating mantle.
- f) All items except the cell proper were dried at 120-140°C for twelve hours.

- g) The transference cell was suspended upside down and allowed to air dry. To avoid contaminating the grease with water, lint-free absorbent tissues (Kimwipes) were used to remove water droplets from the stopcock barrels and then the latter were warmed with a soft flame.
- h) The stopcock plugs were inserted using Dow-Corning High Vacuum silicone lubricant.
- i) Apiezon "W" was used to seal the standard taper containing the anode electrode to the cell.
- j) The surface of the silver cathode was cleaned in aqueous ammonia, rinsed, and electrolyzed in approximately 1N HCl solution. This solution was prepared from analytical reagent grade concentrated HCl and de-ionized water. A direct current of between 20 and 30 ma was applied long enough to give a 75% excess deposit over that required for a run and its duplicate (a complete run takes about four hours).
- k) The cathode assembly was recleaned by steaming. After drying at 120°C for several hours, it was attached to the cell using Apiezon "T" grease for the standard taper. The seal between stopcocks s and t is made with glass. The danger of striations developing at the standard taper can be minimized if the outer part of the taper is warmed and a slight pressure applied before making the glass seal.
- 1) The assembled cell was evacuated using a rough pump and checked for leaks with a Tesla coil. The cell was then transferred to the high vacuum manifold and evacuated to a pressure of 2 x 10⁻⁶ torr. The cell-to-manifold attachment was made between J₇ and J₁₃ and caps were applied to J₁₄ and J₁₅ so that the stopcock bores and backs could be evacuated.

The transference cell was placed in the thermostat, and assembly of the apparatus was completed as shown in Figure 18. The ampoule of metal P was attached to the plunger O using the smallest tip on the torch. The ampoule rested on an 18/7 socket during this operation. The plunger was suspended by an external magnet N taped with plastic electrical tape to the glass tube. The weighed sample of potassium bromide was transferred to the make-up vessel Q, the plunger assembly attached with Apiezon "T" lubricant and evacuation effected in quick succession. The potassium bromide used was Mallinckrodt analytical reagent recrystallized three times from de-ionized water. It was dried at 300° for at least two hours. The required weight of salt was calculated from the Kohlrausch ratio:

$$\frac{T_{Br^-}}{c_{Br^-}} = \frac{T_{e^-}}{c_{e^-}}$$
 [3.13]

T_{Br} is the transference number of Br from KBr estimated as 0.51 using aqueous solution values (80).

T_e- is the estimated transference number of the electron.

c___ is the concentration of KBr to be used.

ce- is the concentration of the metal solution.

An infrared lamp aided in the bake-out of the make-up vessel, KBr and glass frit. An occasional flaming of the frit was done with a small flame being careful not to heat the ring seal on the condenser above the frit. Aluminum foil was wrapped around stopcocks and joints to shield these items from the direct rays of the lamp. High vacuum silicone lubricant was used on stopcock <u>r</u> because its nearness to the cold thermostat makes Apiezon "N" grease too viscous to use.

When all items could maintain a pressure of less than 1×10^{-5} torr the cell was closed from the vacuum line and the thermostat cooling

started. The interior of the windows could be kept frost-free if the separate drying train for air was started prior to the beginning of the thermostat cooling. To accelerate the cooling rate, a large test tube containing Dry Ice and alcohol was inserted in the bath.

Upon reaching the controlling temperature, the cell pressure was rechecked. Usually this resulted in a better indication of the vacuum than previously noted because of the cold surfaces now present in the cell. If no leaks were present, the cell was shut off and the condenser cooling begun. The condenser was in series with a Gorman-Rupp No. 210 centrifugal pump, bubble remover, and copper heat-exchanger immersed in a Dewar flask containing Dry Ice-alcohol. With stopcocks q and s closed, ammonia was distilled from B through c, d, e and r into the make-up vessel. The incoming vapor kept the solution from running through the frit, effectively stirred the solution, and encountered a larger condensing surface as a result of bubbling through the solution. As the condensation neared the end, the rate of condensation was reduced and vessel B was not disturbed. Any disturbance usually resulted in vigorous bubbling in the make-up vessel with deposited KBr beyond the condensing surface. When the desired volumetric mark (90 ml mark is equivalent to 81 ml of solution; see earlier description) was reached in the make-up vessel, stopcocks r and c were closed and the condenser cooling stopped.

A Dewar flask containing liquid nitrogen surrounded trap W. At this stage the boundary-forming stopcock <u>u</u> was positioned with its bore connecting the graduated tube and waste vessel WW. Trap W was connected to <u>t</u> through stopcock <u>w</u>. Stopcocks <u>s</u> and <u>t</u> were closed. The pressure inside the make-up vessel was sampled through stopcocks <u>q</u> and <u>l</u> by observing the fall of the mercury level in manometer D (Figure 5). When the pressure was just short of one atmosphere, stopcock <u>q</u> was closed and <u>s</u> opened. The following

solution (KBr solution) filled the tubes to stopcock <u>t</u>. This stopcock, <u>t</u>, was turned to drain about 10 ml into trap W, and then it was quickly turned to allow the following solution to fill the "closed" side of the cell U. (Beware that it is not turned in such a direction as to expose the "evacuated back.") If the solution did not fill the cell within a minute or two, the manometer D was connected through <u>q</u> to relieve excessive pressure. When the back or closed side of the cell was full the excess solution was transferred into trap W. If the solution had not reached the thermostatic temperature, its expansion in the closed side could unseat the boundary stopcock <u>u</u>. As a precautionary measure, stopcock <u>s</u> was closed and <u>t</u> cautiously opened until a small bubble, about the size of a large pin head, developed in the closed side.

It was then necessary to rinse any KBr residue from the make-up vessel and connecting lines to the cell before the metal solution could be prepared. This was done by condensing fresh ammonia from B in the same manner as in the preparation of the following solution. On the first rinse about 20 ml was condensed and then transferred into trap W through s and t. In the same way, two more rinses of approximately 30 ml each were made. However, on these latter rinses, the ampoule and plunger were gently lowered and rinsed to remove any KBr that may have splashed onto them. The plunger with its ampoule was returned to the original position after each rinse. The ammonia for these rinses could be taken from either trap W or storage vessel B.

When the rinses were completed the lines containing ammonia vapor were evacuated through the rough pump and then connected to the high-vacuum manifold. When a pressure of less than 1×10^{-5} torr was reached the pressure in the front or leading solution side was checked. If these pressures were satisfactory, the cell was shut off from the manifold and stopcock \underline{u} positioned just a trifle beyond shut off from waste and with the top of the bore facing the nearer observation window.

The ampoule was broken by releasing the plunger. The ion-gauge often went off scale because of helium gas present in the ampoule. When less than 1×10^{-5} torr was again attained, the make-up vessel was closed from the vacuum manifold and cooling started. As before, ammonia from B, surrounded by a -40°C bath, was condensed to the desired mark in the make-up vessel. Stopcocks \underline{c} and \underline{r} were closed. It should be remembered that the plunger decreases the volume of the make-up vessel by about two milliliters and that an expansion of about two milliliters exists between solution at -70 and that at -40°C.

The metal solution was now ready for transfer into the cell.

For best results, the transfer must be made rapidly and smoothly.

Hence, the instructions are given in outline form:

- 1. Set stopcock t to waste W.
- 2. Turn off circulating pump.
- 3. Adjust helium pressure to one atmosphere up to the make-up vessel. When frost begins to melt, apply helium gas to the solution through q; leave connected to manometer D to relieve pressure.
- 4. Allow about 5 to 10 ml of solution to go to waste W through s and t. Control flow of solution with s.
- 5. Quickly but cautiously turn <u>s</u> to transference cell and fill tube until electrodes are covered; let set.
- 6. Drain solution from Step 5 into waste WW'; leave a small crack in the stopcock u.

Steps 7 through 11 should be done in quick succession.

- 7. Drain about 5 ml to waste W through s and t and quickly turn s to cell.
- 8. Allow some solution to flow through <u>u</u> into waste WW' and turn stopcock off.

- 9. Allow tube to fill--leave small bubble near s if possible.
- 10. Empty make-up vessel into trap W.
- 11. If no bubble is present, reconnect make-up vessel to cell until temperature equilibrates, <u>Careful</u>--solution may be sucked back into make-up vessel!
- 12. Evacuate make-up vessel (eliminates ammonia vapor).
- 13. Readjust helium pressure to just shy of one atmosphere; make sure make-up vessel is at room temperature.
- 14. Equalize pressures: (a) back side of cell; (b) then front side and maintain.
- 15. Check for resistance leakage to ground between an electrode and ground.
- 16. Measure conductance (resistance) versus time for about an hour.
- 17. Set calculated current on potentiometer of current controller.

 Use moving boundary equation and an estimate of 300 seconds between 0.1 ml marks.
- 18. Again equalize pressures as described in Step 14.
- 19. Leave make-up vessel connected to metal solution side. This will serve as a gas ballast; further discussion is given in the Results Chapter.
- 20. Turn large stopcock <u>u</u> connecting leading and following solutions and note any diffusion. There should be none if the pressures are the same.
- 21. Connect leads from the current controller and apply current.

 Note: The leads to the conductance cell must be disconnected from the bridge and should be suspended in mid-air to prevent leakage currents.

It took about an hour for the boundary to reach the first mark.

During this time a light with motorized blind was positioned at the window

behind the transference tube. A telescope was set up about four feet away from the front window to reduce parallax errors.

With the boundary about five minutes away from the first mark, one of the two calibrated stopwatches (A. R. and J. E. Meylan Co., Type 200B, 1/10 sec. graduation; KL6916 and KL6917) was started with reference to the time signal from the telephone company. As the boundary passed this mark the first watch was stopped, and simultaneously, the second one started. (The watches were mounted in such a manner that a hinged bar would actuate both watches simultaneously.) Also, the clock time as well as the time of metal solution transfer was recorded. The watches were activated as the boundary disappeared behind the calibration mark. After each time recording, the potentiometer was reset against the standard cell. When the boundary had passed the last mark the current was shut off, stopcock u was closed, current leads were disconnected, conductance leads attached and resistance versus time readings recorded for at least 15 minutes. The watches were stopped with reference to the telephone time signal. This gave a check against stopwatch malfunction since the sum of time intervals must equal the difference between the two time signals.

When adequate resistance <u>versus</u> time readings had been made to aid in correcting for the effects of decomposition, the solution level in the transference tube was lowered by means of stopcock <u>u</u>.

Adequate solution was drained into the waste vessel WW' until it could be assumed that the metal solution remaining in the transference tube was uncontaminated by KBr solution.

A duplicate run could then be made by repeating the above procedure starting with Step 15 (Steps 18 and 19 could be omitted).

After the necessary data had been obtained, the contents of the anode compartment were drained into the analysis vessel AA' through stopcock v. The helium gas was evacuated from the make-up vessel

and connecting lines by way of the manifold. The contents of waste vessel W were distilled into storage vessel B through x, d and c. The glass ammonia waste vessel, similar to vessel F in Figure 8, was attached at J₆ and evacuated by the rough pump. The contents of the transference cell, except for the analysis vessel contents were distilled into the evacuated vessel. The distillation was made by way of the make-up vessel and stopcocks q, e, d and o. This prevented potassium bromide and potassium solutions from reaching the stationary lines and leaving residual matter. Stopcocks s, t and u were rotated until no solution remained in the cell. With the stopcock on the ammonia waste vessel closed, all compartments of the cell except the analysis vessel were evacuated by the rough pump along with waste vessel W. With the pump off and stopcocks o, and e closed, the ammonia waste vessel was removed and its contents discarded. A heavy-wall ampoule attached to a socket joint was sealed to the position vacated by the ammonia waste vessel and evacuated. With a -40° to -45° C bath surrounding waste vessel W the contents of the analysis vessel were slowly distilled into W through w. When distillation appeared complete, the -40°C bath was replaced with a Dewar flask of liquid nitrogen to effect a quantitative transfer. The ammonia in W was then transferred by distillation into the ampoule through x, d and o with w closed. To assure quantitative transfer, the ammonia in the ampoule was frozen with liquid nitrogen, sealed, and removed at the constriction.

When the ampoule reached room temperature it was weighed, cooled and broken open. When the ammonia had evaporated, the ampoule and tip were dried, cooled and reweighed. The difference gives the weight of ammonia present in the analysis vessel.

With the refrigerators and heating circuits off, the apparatus was disassembled and removed from the bath before the bath liquid had a chance to warm up and create a safety hazard as a torch was required to soften the wax at the joints near the level of the bath.

The metal in the analysis vessel AA' was air-oxidized, dissolved in water and transferred with rinses to a 600 ml beaker. The ammonia was then expelled from the solution and its volume reduced by evaporation under a heat lamp. This technique and the analysis by pH titration using standard HCl solution is described under the procedures for conductance. The apparatus was then cleaned for the next run.

A suggested revision of the transference apparatus to minimize stopcock "popping" is illustrated in Figure 21. This will expose a large area of silicone lubricant to the following solution, but should not increase the decomposition rate since the metal solution is not exposed.

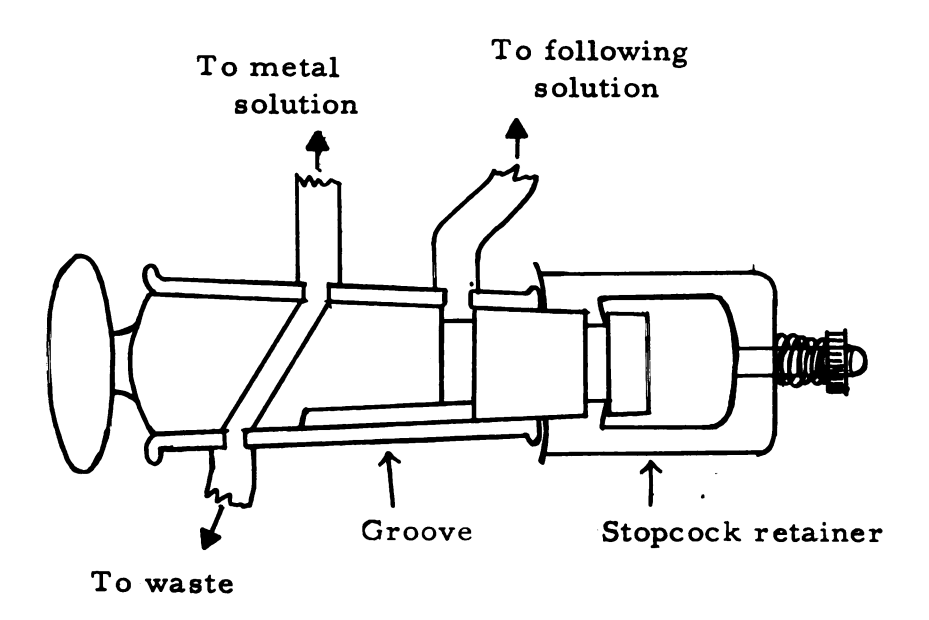


Figure 21. Suggested modification of boundary stopcock.

4. Comments on Individual Runs

35-K-1: One run was made which yielded data. Time between transfer of bromide and metal solutions was 12 hours. Only two rinses

were made; both included the ampoule. The cell contents were analyzed.

- 36-K-2: Unsuccessful; boundary-forming stopcock "popped" before any data could be taken.
- 37-K-3: Two runs were made; each yielded data. Time between transfers was 14 hours. Two rinses were made; both included the ampoule. The cell contents were analyzed.
- 38-K-4: One run was made which yielded data. Time between transfers was 18 hours. Three rinses were made, with the ampoule included in the last two. No analysis was made of the cell contents.
 - 39-K-5: Unsuccessful; boundary-forming stopcock "popped."
- 40-K-6: Two runs were made, each yielded data. However a number of "dark particles" were noted below the boundary on the "b" run. Time between transfers was 24 hours. Three rinses were made, with the ampoule included in the last two.
- 41-K-7: Unsuccessful. Heptane was substituted for ethanol as a bath fluid, but it picked up moisture and became so cloudy that the boundary tube was hidden from view.
- 42-K-8: Bath fluid changed to absolute ethanol. Two runs were made; each yielded data. Striations in boundary stopcock were prominent but no leakage resistances were detected. Time between transfers was $15\frac{1}{2}$ hours. Three rinses were made, with the ampoule included in the last two. The cell contents were analyzed.
- 43-K-9: Unsuccessful; boundary-forming stopcock "popped."

 Lower waste vessel appeared to be completely full.
- 44-K-10: One run was made but the boundary-forming stopcock "popped" before post-run conductance measurements could be made.

 Therefore the data had to be discarded. The diffusion of metal solution into the following solution was great because of unequalized pressures at the time the boundary was formed. Numerous "dark particles" were seen floating behind the boundary. Time between transfers was 17 hours.

Three rinses were attempted, with the ampoule included in the last two; however, on the last rinse, the ampoule broke. The ammonia was evaporated from the make-up vessel through the top. After evacuation to 5×10^{-6} torr, the normal metal make-up was started.

- 45-K-11: Two runs were made; each yielded data. Striations were present in the boundary-forming stopcock at the end of the run. Time between transfers was 11 hours. Three rinses were made, with the ampoule included in the last two. The cell contents were analyzed.
- 46-K-12: Two runs were made; each yielded data. Striations appeared in boundary-forming stopcock; a blue "muddy" color seemed to be below the boundary for the first 30 minutes after formation. This may have been a light reflection. Time between transfers was 11 hours. Three rinses were made with the ampoule included in the last two. The cell contents were analyzed.
- 47-K-13: Two runs were made; each yielded data. No appreciable striations were observed. Time between transfers was 15½ hours. Three rinses were made with the ampoule included in the last two. The cell contents were analyzed.
- 48-K-14: One run was made which yielded data. Striations were present in the stopcock. Time between transfers was 12 hours. Three rinses were made with the ampoule included in the last two. The cell contents were analyzed.
- 49-K-15: Two runs were made; each yielded data. A "black deposit" was observed on the silver wire of the silver-silver chloride cathode, which was funnel-shaped with flared end at top. Such a deposit could have appeared before and gone unobserved. Time between transfers was 11 hours. Three rinses were made with the ampoule included in the last two. The cell contents were analyzed.

D. Electromotive Force

1. The Cell

There are four methods (59) for forming the junction between two solutions for a concentration cell with transference. These are continuous mixture boundary, flowing junction, free diffusion junction and constrained diffusion junction. Fristrom (30) designed a cell using the free diffusion junction by allowing the solutions to come into contact in a Y-shaped capillary. Klein (58) used the constrained diffusion junction for his work with lithium metal in methylamine. Ease in manipulation of the cell and the possibility that solutions would mix through the capillary if the liquid levels were not the same prompted the use of the constrained diffusion type of boundary in the present work.

To test the reproducibilities of the emf values developed for the three types of cells: sharp junction, flowing junction and constrained junction, Guggenheim (81) used the cell:

Hg , HgCl | 0.1 N HCl | (C)KCl | 0.1 N KCl | HgCl , Hg.

He found no significant differences between the various types of junctions.

As a further check, Klein employed the cell:

Hg | HgCl | 0.1 N KCl | 0.1 N HCl | 0.2 N HCl | 0.1 N KCl | HgCl | Hg

in an apparatus using a flowing junction. The emfs from this apparatus, known to give highly reproducible data, agreed within 0.25% with those obtained using the same cell but forming the junction across a ten millimeter medium-porosity Pyrex fritted disk. Fluctuations of the same magnitude were observed in the cell

Hg | HgCl | 0.1 N KCl | 0.5 N KCl | 0.1 N Kcl | HgCl | Hg.

Thus the emf cell used in this work was based upon the design used by Klein.

Since the equivalent conductance <u>versus</u> concentration was used to determine concentrations in the transference runs, it would be convenient to incorporate conductance electrodes in the emf cell to measure concentrations rather than to depend upon volumetric techniques such as used by Klein.

The final design of the cell is shown in Figure 22. A model was built and tested with water to check the manipulations. The required manipulations, to be described below, could be performed; hence, the second and final cell body was constructed.

In summary the final design incorporated the following features:

- 1. Metal was distilled from the distillation vessel N into reservoir R. The vessel was removed by sealing at the constriction. This avoided glass fragments and added another purification step by distillation in vacuo.
- 2. Purified ammonia was condensed in the reservoir R. With stopcock s closed the cell was removed for manipulations.
- 3. The solution was poured from R into U and V and adjusted to about a 2 to 1 concentration ratio.
- 4. Tilting the cell introduced solution into the conductance cells X and Y. The solution concentration was determined from the resistance readings of electrodes "a" and "b" in cell X and "c" and "d" in cell Y.
- 5. Also with the cell in this tilted position, the two solutions form a junction at the glass frit T in the tube connecting the two chambers U and V. The potential developed across this frit may be measured by electrode combinations: a+c, a+d, b+c, and b+d.

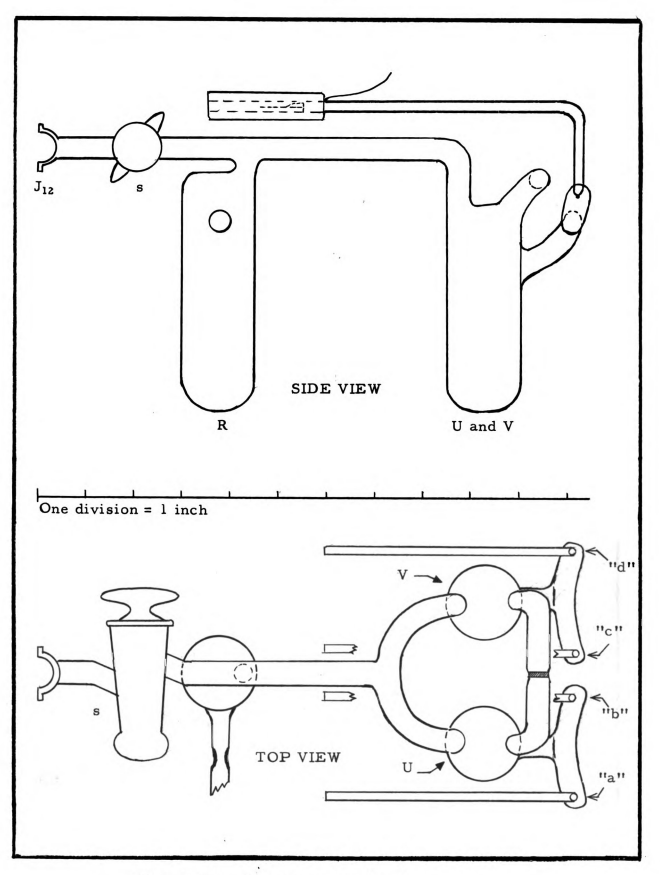


Figure 22a. Diagram of emf cell.

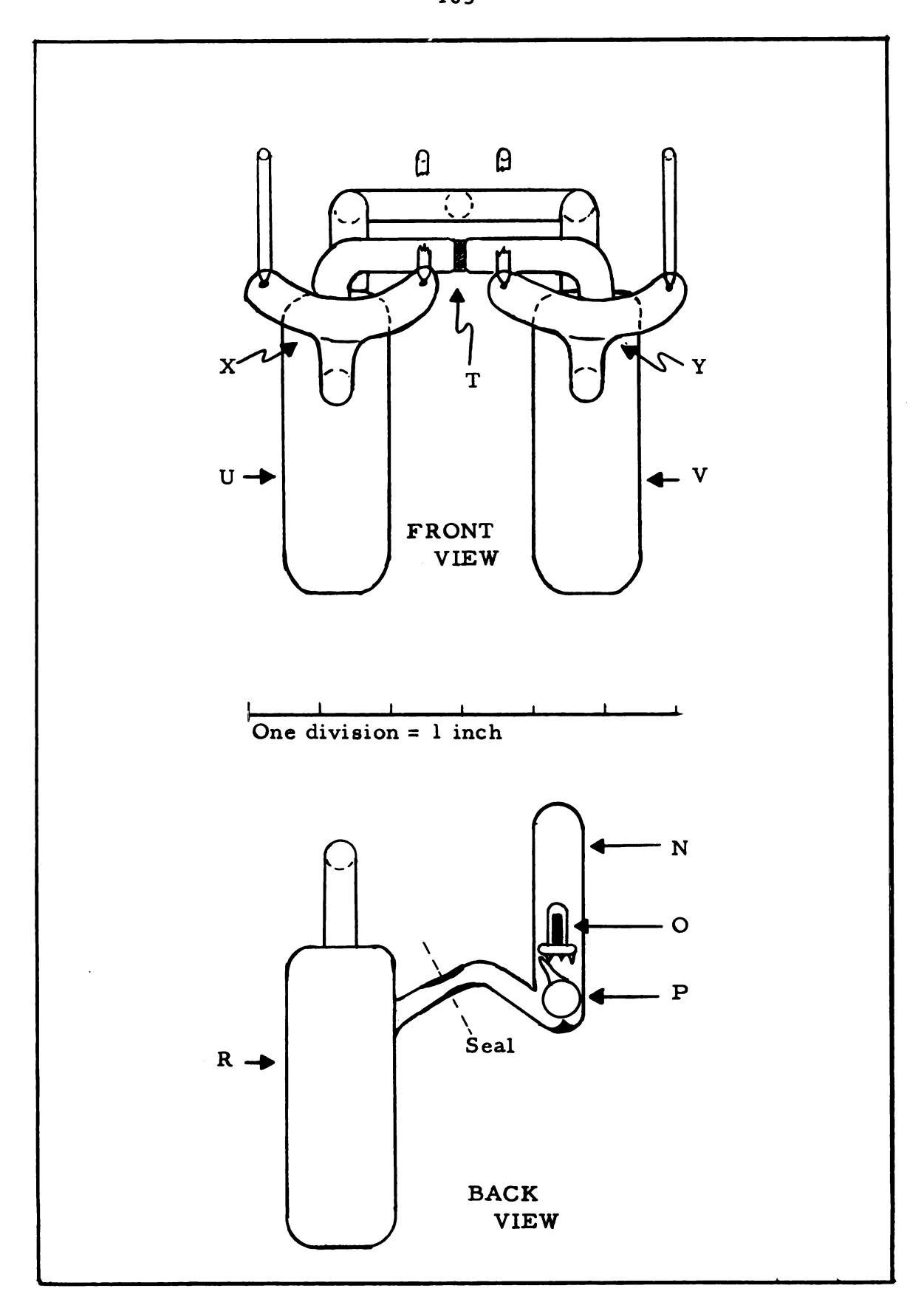


Figure 22b. Diagram of emf cell.

It was desired to use bright platinum electrodes; therefore, graded seals of soft glass-to-Pyrex would be necessary for a vacuum-tight seal. An attempt to purchase graded seals of 4 mm diameter was unsuccessful since commercially available grades are at least 3.5 cm in length and a grade of 1 cm was the maximum allowable size for the cell. The use of tungsten electrodes sealed directly to Pyrex was then attempted. In the process of cleaning the electrodes by the method of Fristrom (30) too high an alternating voltage from a variable transformer (Variac) was used and the tungsten dissolved in the dilute sodium hydroxide solution leaving only a cross-sectional area of the metal sheathed by a glass tube.

The tungsten electrodes were replaced with no. 36 gauge (0.005 in.) platinum wire. Cenco vacuum wax 11455B was melted into the electrode arms to seal any capillary leaks. A vacuum test on the manifold verified that the cell could maintain a pressure of less than 1 x 10⁻⁵ torr overnight. On runs after EK-2, the ends of the platinum wire were silver-soldered to no. 22 gauge insulated flexible wire at the electrode arms, and the latter wire was taped to the arm. Prior to EK-2, rosin-core solder was used, but was found to give questionable electrical connections with platinum wire. Because of the fine wire, very little trouble should result from heat conduction to the electrode surface, and hence, to the surrounding solution.

Originally, a Leeds and Northrup Model K-2 potentiometer was used to measure the emf. This proved inconvenient because it was too sensitive for the varying voltages present. The emf values were then measured on a recording potentiometer (Sargent, Cat. No. S-7215, Serial No. 129) and the K-2 potentiometer was used to calibrate the recorder. This recorder proved to have adequate sensitivity since there were still voltage fluctuations observable. The switching network is diagramed in Figure 10. The conductance portion of this

network was used in conductance measurements for runs CK-12 through CK-16 and transference runs 47-K-13 to 49-K-15. Sw-1 was used to select one of six available electrode combinations (see Table 4). The rotor leads went to switch Sw-2. This switch connected the selected electrode pair to either the conductance bridge or to the emf measuring circuit. Switch Sw-3 served as a polarity reversing switch before the input into the recorder. Switch Sw-4 selected the input signal to the recorder as either the unknown emf or a calibrating emf from the K-2 potentiometer.

2. Procedure for EMF Run

The recommended procedure for cleaning the cell is the same as that recommended for the transference cell. During the rinsing precedure, the cell is positioned such that water will seep through the frit. However, in all of these emf runs the warm sulfuric acid-dichromate cleaner was used since the alternate procedure was not known at this time.

If a cell constant determination was desired, the cell was partially filled with a solution of approximately 0.05 N potassium iodide-iodine solution. The cell was placed in an oil thermostat and resistance readings were recorded at five frequencies. The specific conductance of the comparison solution was determined by use of a low-conductance cell whose cell constant was determined with standardized potassium chloride solution (29.10₁ cm⁻¹; see cell constant determination under conductance cell A).

The previously cleaned metal distillation tube N was attached to the cleaned cell. The ampoule of metal P and glass-enclosed magnetic breaker O had been sealed inside. The ampoule should probably be rinsed with a 5% HF solution followed in quick succession with several rinses of de-ionized water. However, in all of these runs only the rinses with de-ionized water were used.

While still wet the cell was attached to the vacuum line at J_6 and pumped overnight on a rough pump. The apparatus was then connected to the high vacuum manifold and baked out using heat lamps and occasionally flaming with the torch until a pressure of 5×10^{-6} torr is reached. (Because of difficulties experienced at a later date with bake-out of the transference cell, it is recommended that the vicinity around the electrodes be kept cool to minimize the possibility of the wax seeping through minute passages and covering the electrode surfaces.)

The ampoule was broken using the glass-encased magnet and the metal distilled into the reservoir R after degassing for a short time. The various colors of thin films of metal indicated the absence of leaks. The distilling flask was sealed off and the cell re-evacuated. As a preliminary step, the sodium-ammonia solution in the storage vessel was maintained at about -45°C for at least three hours and the resulting hydrogen gas and other volatile impurities removed. Ammonia was then distilled into the reservoir until it was a little less than half full. The cell was shut off, disconnected from the system, and a ball joint inserted into the socket joint to prevent liquid and dirt from entering in case the cell needed to be reattached to the manifold.

The cell manipulations required for concentration changes and mixing were done in a large Dry-Ice-alcohol bath at -40°C or lower. Distillation from one cell chamber to another was accomplished by inserting the chambers into Dewar flasks. The Dewar flask surrounding the chamber into which ammonia was to be distilled contained Dry Ice and alcohol. The flask from which the ammonia was being distilled contained alcohol at a temperature of about -40°C to aid heat transfer. This also kept the ammonia vapor pressure below one atmosphere.

After changing the concentration, the solutions were mixed in their respective chambers with the aid of the large bath. The cell was

placed into the thermostat. After 10 minutes for temperature equilibration, the solutions were remixed by removing the cell from the bath and rocking it to alternately drain and fill the electrode chambers several times.

The cell was returned to the bath and resistance and emf readings recorded. The conductance measurements were made while the solutions made contact across the glass frit. Observations during cell constant calibrations showed that the electrode chamber was sufficiently separated from the bulk of the solution that no observable resistance difference was evident when the cell was tilted so that the solution in the conductance cell was: (a) separated from the bulk of the solution and junction tube; or (b) in contact with the bulk of the solution but not the junction tube, or (c) in contact with both bulk of the solution and the junction tube.

A check of resistance to ground of the electrode leads with the cell in the thermostat using methyl alcohol as the bath liquid gave infinite resistance on a Heathkit volt-ohmmeter.

A two-to-one concentration ratio should be maintained across the boundary. Once established, the next solution was made by draining equal amounts of solution from each chamber into the reservoir R. Then the ammonia was evaporated from the reservoir back into U and V. The solutions were mixed by gently shaking the cell in the manipulation bath before placing it in the thermostat. At least two sets of emf-conductance readings were taken before the next dilution, with the cell contents remixed between each set.

3. Comments on Individual Runs

<u>EK-1</u>: This first run gave varying, doubtful data. Fifteen different concentration pairs were made but for four of these the sign of the measured potentials was not compatible with the concentration

ratio. The measurement of resistance was hindered by a very distorted Lissajous figure of a "figure 8" shape and quite "hashy."

Most of this trouble, based upon later observations, is attributed to dirty electrode surfaces. Difficulty in measuring the cell constant using KI-I₂ solution supports this observation.

EK-2: The cell was cleaned with warm sulfuric acid-dichromate solution and rinsed several times with distilled water. When not completely full, the cell was positioned so that water would seep through the frit. After several rinses with de-ionized water the cell constants were determined with KI-I₂ solution as described in the conductance section for conductance cell A. The cell was rinsed several times with distilled water and then recleaned by the aforementioned procedure. Final rinsings were repeated over a period of several days. Bake-out consisted of using heat lamps and occasional flaming with a torch until a pressure of 2 x 10⁻⁶ torr could be maintained for four hours with the cell shut off from the manifold.

EK-3: Run EK-3 was attempted in the same way as EK-2 with the following exceptions. The flexible copper leads were silversoldered to the platinum wire to insure a better electrical connection than could be obtained with regular soldering. Since metal samples of over a half gram were not available, two ampoules were sealed in the distilling flask. The first one broke with ease but in attempting to break the second ampoule, pulverized glass from the first ampoule found its way into the reservoir R through the seal-off constriction.

The run was troublesome with inconsistent resistance measurements which involved electrode "d." After six dilutions this run was discontinued. Some "figure 8" pattern behavior was observed supporting this invisible electrode trouble. No visible malfunction of the electrode could be seen.

A larger G_1/G_2 ratio was used (approximately 2) which gave a much more stable voltage. However, a residual potential dependent upon the polarity was observed.

EK-4: The cell was rinsed with alcoholic-potassium hydroxide solution, distilled water, fresh chromic acid cleaning solution, and finally the electrodes were electrolyzed in sodium hydroxide solution using alternating current. After rinsing the cell thoroughly with deionized water the cell constant was determined with KI-I₂ solution. The cell was recleaned with alcoholic-potassium hydroxide solution to remove some silicone grease and rinsed thoroughly with distilled and de-ionized water.

EK-5: The same cleaning treatment as used for run EK-4 was used including the electrolysis of the electrodes in sodium hydroxide solution. The cell constant was not redetermined.

In order to keep the decomposition at a minimum when storing overnight the solution was frozen in liquid air. The ammonia vapor pressure was in this way decreased sufficiently so that it would not attack the potassium metal.

E. Metal Film Deposit on Ice

In 1924, Wolthorn and Fernelius (82) reported transient blue colorations formed at the interface of alkali metals as they dissolved in water before reaction took place. Positive results were obtained for lithium and potassium. A negative result was reported for sodium packed in the glass tube, but particles adhering to the side of the beaker did reveal slight blue tinges. No blue color was observed as sodium and potassium metals were rubbed on ice; also, for calcium in water. Lithium and sodium gave negative results when added to

methyl alcohol but potassium showed infrequent colorations in this solvent but was negative in ethyl alcohol.

Jortner and Stein (83) reported a spectrum for the reaction when potassium was distilled into a vessel at -10° C with water present at 0° C. The temperature did not exceed -5° C. A peak at 925 m $_{\mu}$ was observed. Freshly distilled metals showed blue colored solutions with methyl alcohol and ethyl alcohol at -40° C. Their postulated reactions were:

$$K \longrightarrow K_{(aq)}^{\dagger} + e_{(aq)}^{-}$$
 [4.5]

$$e_{(aq)}^- + H_{(aq)}^+ \longrightarrow H_{(aq)}$$
 [4.6]

$$^{2H}_{(aq)} \longrightarrow ^{H_2}$$
 [4.7]

and in the presence of oxygen:

$$e_{(aq)}^{-} + 0_{z} \longrightarrow 0_{z(aq)}^{-}$$
 [4.8]

These two interesting reports suggested another type of experiment: the distillation of a metal film onto ice.

The apparatus is shown in Figure 23. De-ionized water was placed in the flat bottom compartment; an ampoule of potassium metal and glass-encased magnetic breaker were sealed in the distillation tube. With the apparatus attached to J₆ (Figure 5), the water was degassed by successive freezings with liquid air, evacuations and thawings. When the water height was about 0.5 cm, it was frozen in liquid air. Evacuation and flaming were effected to remove residual water from other portions of the apparatus. The ampoule was broken, the evacuation stopped and the metal distilled onto the ice. The large mean-free-path allowed an appreciable quantity of metal to deposit on the ice. The deposit had the appearance of an unpolished piece of plated metal.

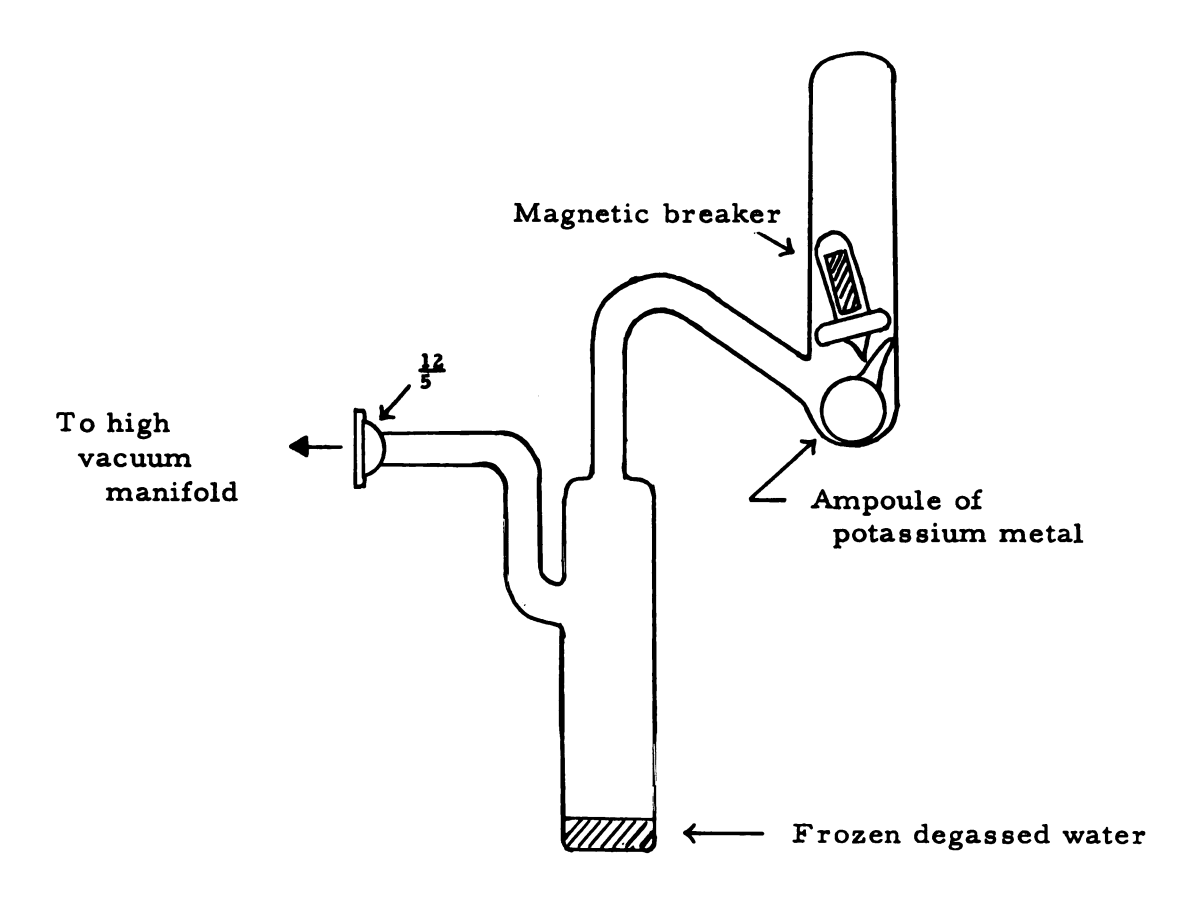


Figure 23. Apparatus to illustrate blue color of potassium metal film deposited on ice.

The liquid air was removed. As the ice warmed, a reddish copper color, which progressed toward the center, was observed on the surface of the ice. At the edge of the vessel, a dark-blue color appeared. By local warming with the finger tip, the colored area grew, then disappeared indicating the metal had completely reacted with the semi-fluid water.

Only one experiment was run. Because of the simple apparatus and short time involved, it would be most desirable to repeat the experiment using the other alkali metals with water, and alkali metals with other solvents, such as alcohols, ethers and amines, including tertiary amines. It would be interesting to verify or disprove the observations reported by Wolthorn and Fernelius. No blue colors have been observed with tertiary amines but they should be included in this experiment because the large surface area and high purity of the metal may sufficiently alter the experimental conditions.

It would appear, that with the aid of a rapid scan spectrophotometer, it would be experimentally feasible to record at least the reflectance spectra if not the absorption spectra of these systems by using a modification of this technique.

CHAPTER V

EXPERIMENTAL RESULTS

A. Conductance Data

A total of eleven experiments was: made on potassium-ammonia solutions using cell A. Of these, three were discarded because of equipment failure. Various corrections must be applied to the observed data. These include contraction of the volumetric flask, vapor space above the solution, decomposition, and density corrections on the solution, all of which are given in detail in the explanatory notes preceding Table 7.

With cell B, a total of five experiments was performed. Three were on potassium-ammonia solutions of which one was lost because of equipment failure. The other two were on potassium deutero-ammonia solutions. Discussion of the necessary corrections are in the explanatory notes preceding Tables 8 and 9.

1. Data from Cell A

Explanatory Notes for Table 7.

This table gives the experimental data and final corrected results for conductivities of potassium-ammonia solutions as determined by cell A.

- <u>Sub-run No.</u> This column designates the particular dilution or concentration under consideration.
- Elapsed time. This column gives the elapsed time in minutes from the start of the first dilution. This information is used in decomposition calculations.

nNH₃

This column gives the number of moles of pure ammonia added to the cell as determined from calibrated volumetric flasks. This includes a correction for contraction of the flask between the calibration temperature of 25°C and -38°C, the average temperature at which they were used. This was based on 96×10^{-7} degree⁻¹ for the coefficient of cubical expansion of Pyrex 7740 glass (84). The weight of ammonia was determined from the density of pure solvent at the measurement temperature. As an aid in determining the density of the solvent, the solvent density was plotted against the temperature over the range desired. Originally the data of Cragoe and Harper (85) were used but these were later corrected by shifting the curve 0.0005 density units to higher densities following publication of new density data by Hutchison and O'Reilly (73). Also, a small correction was applied for vapor present in the space (31.5 ml) above the solvent using the vapor pressure of ammonia at the measurement temperature. This vapor correction was made only if the flask was evacuated before filling. After transfer of the contents, an amount of vapor determined by the vapor pressure of the solution in the cell remained in the flask but this was taken into account as described under ncell.

nW NH3

This column gives the moles of ammonia withdrawn from the cell as measured by the volumetric flasks. The volume contraction, vapor space, and density corrections mentioned in connection with the preceding item were applied. After measurement, the ammonia was removed either by distilling into a waste vessel immersed in liquid air or through a roughing pump. In either case, the flask was considered to contain no residual ammonia vapor if it should be used in some subsequent withdrawal.

nNH₃ This column gives the calculated moles of liquid ammonia present in the solution. The representation is

$$n_{NH_3}^{cell} = \sum_{i=1}^{i} n_{NH_3}^{add} - \sum_{i=0}^{i} n_{NH_3}^{w} - (n_{NH_3}^{v})^{-37} - (n_{NH_3}^{v})^{25}$$
 [5.1]

where $n_{NH_3}^{add}$ and $n_{NH_3}^{w}$ are described above. The term $(n_{NH_3}^{v})^{-37}$ is the number of moles of ammonia vapor present in the vapor space of the cell below the level of the thermostat liquid. The volume of this space is that of the empty cell minus the volume of solution present in the cell. The ideal gas equation was used; the pressure of the vapor was taken as the vapor pressure (86) of the solution corrected from -35.0° to -37.0° . $(n_{NH_3}^{v})^{25}$ represents the moles of ammonia vapor present in other parts of the system whose temperature was taken as 25° C. These parts include the condenser, the lower section of the distribution manifold, connecting tubes, and from one to three volumetric flasks with associated Kjeldahl traps. The volume of a flask and accompanying trap was included in $(n_{NH_3}^{v})^{25}$ only if they contained vapor. The pressure of the vapor was taken as the vapor pressure of the solution.

metal present in solution after correction for decomposition.

A plot of Λ (uncorrected for decomposition) versus \sqrt{C} was made. Discontinuities in the curve would occur whenever a time lapse of several hours had occurred for a given solution. At least one and perhaps several of these lapses occurred whenever it was necessary to allow the solution to stand overnight or to fill volumetric flasks. From the duration of a given time lapse, the change in the number of moles of potassium required to match the Λ values was calculated. This allows the change in the

number of equivalents of potassium per minute to be calculated. Usually, the different time lapses for a given run would give essentially the same decomposition rate, $\Delta n/\Delta t$, thus indicating a zero-order reaction. For CK-8 it was necessary to use the initial and final readings for the run since $\Delta versus \sqrt{C}$ shows a sizeable discontinuity on the withdrawal segment probably resulting from momentary accidental exposure of the solution to the atmosphere. Figures 24 and 25 at the end of Table 7 illustrate typical uncorrected curves and the method of correction.

- This column gives the corrected concentration in g atoms of potassium per liter of solution. The mole ratio of potassium to ammonia (K/NH₃) was plotted against density of the solution using the data of Hutchison and O'Reilly (73) corrected to -33.2°C so that it would extend the curve of Johnson and Meyer (72) at the same temperature. The density for a given experimental solution was determined from this plot by calculating $n_{K}/n_{NH_{3}}^{cell}$. This density $\rho_{soln}^{-33.2}$, was multiplied by $\rho_{NH_{3}}^{-37.0}/\rho_{NH_{3}}^{-33.2}$ to obtain the density of solution, in which $\rho_{NH_{3}}^{-37.0}$ and $\rho_{NH_{3}}^{-33.2}$ are the densities of pure ammonia at -37.0° and -33.2°C, respectively. After determining the mass of solution from $n_{NH_{3}}^{cell}$ and n_{K} , the concentration was calculated.
- This column gives the square root of the normality listed in the previous column.
- Notes This column indicates the way in which the resistance values in the next column are chosen. The symbol "a" indicates that the resistance was obtained at infinite frequency from a plot of resistance versus (frequency) 1/2. The symbol "b" indicates that the lowest value of resistance, which occurred at 400 cps, was

chosen since the above plot yielded a negative slope. This behavior cannot result from polarization, so that the above extrapolation method is not valid.

- <u>R</u> This column gives the resistance in ohms corrected for lead resistances. (See previous paragraph for selection method.)
- This column gives the corrected equivalent conductance in cm² mho equiv⁻¹ at -37.0°C. This value has not been corrected for conductivity of the amide ion formed from the decomposition since the concentration of the amide ion is negligible. (See Amide Ion Conductance in Discussion Chapter.) The values of Λ are plotted in Figure 26 and the smoothed data are given in Table 15, page 160.
- Σ $n_{NH_3}^{add}$ and Σ $n_{NH_3}^{w}$ These are the summations of the moles of ammonia added and withdrawn, respectively. Ideally, they should be equal; therefore, the difference gives an indication of the precision of the manipulations and corrections. N.A. information is not available.
- Wt of metal (ampoule) This is the mass in grams of potassium metal in the ampoule (see ampoule preparation Chapter 4 for method). The volume of the ampoule was estimated from its dimensions. Buoyancy corrections were made on the assumption that the unfilled volume was completely evacuated and they also included corrections for the density of the metal. The symbol † indicates that a buoyancy correction was not made on this ampoule since the dimensions were not known.

- Wt of metal (titration) This is the mass of metal in grams calculated from the titration of the cell washings with standardized hydrochloric acid solution using a pH meter.
- Accepted wt of metal This is the accepted mass in grams of metal to be used in determining the concentrations of the solutions.
- $\frac{\Delta n}{\Delta t} \times 10^6$ This is the decomposition rate in equivalents per minute as described under n_{K} . N.A. information is not available.
- This is the cell constant. The value in parenthesis is used with the resistance values in parenthesis. This is for the cell with a small amount of solution in it.
- Solvent conductance For CK-11, a correction was made for the specific conductivity of the solvent; 0.215 x 10⁻⁶ mho cm⁻¹, which was determined at the beginning of the run.
- Additional Notes On run CK-8, (*) indicates that the rate of decomposition for the succeeding values was computed from the time the cell was momentarily opened to the atmosphere. A large drop in the conductance occurred after a stopcock "popped," possibly allowing a small amount of air into the system.

On run CK-3, the uncorrected ampoule weight was used since the titration value was uncertain. This was before the use of heat lamps, and the solution was heated directly to remove residual ammonia.

Table 7a. Conductance Data for Solutions of Potassium in Liquid Ammonia Using Cell A; Run No: CK-3

Sub- run No.	Elapsed time	add n NH3	w nNH3	cell ⁿ NH ₃	$^{ m n_{ m K}^{ m x}10^3}$	ပ	† Z	Notes	æ	<
1	155	1.272		1.241	2.096	08290.0	0.2604	. م	676.5	510.8
7	390	1,261		2.504		0.03368	0.1835		1376	505.6
٣	655	1.275		3.780		0.02233	0.1494	•	2013	521.3
4	830	1.275		5.056		0.01670	0.1292	•	2579	544.0
	1385			5.056		0.01670	0.1292		2593	541.1
S	1680	1.269		6.327		0,01335	0,1155		3125	561.6
	2240			6.327		0.01335	0.1155	 	3150	557.2
	2840			6.327		0.01335	0.1155	,,,,,,,,,,,,,,,,,,,,,,,,,,,,,,,,,,,,,	3158	555.7
9	3160	1,287		7.615		0.01109	0.1053		3670	575.6
	3240			7.615		0.01109	0,1053		3679	574.3
7	3620	1,281		8.898		0.009493	0.09743		4170	591.9
	4250			8.898		0.009493	0.09743		4192	588.7
∞	4580	1.277		10.176		0.008303	0.09112		4667	604.6
6.	4880	1.281		11.458	→	0.007374	0.08587	→	4981	637.9
tbath	-37.02°C	U		Wt of metal (ampoule):	tal (amp	-	0.0869 g			
Σ nNH3	11.478			Wt of metal (titration):	tal (titra		0.07698 g	k: 23.43 cm ⁻¹	m-1	
Σ nW ₃ 1	N. A.			Accepted wt of metal:	wt of m		0.08194 g	(averaged weight)	reight)	
				Δt		Į.	N. A.			

Table 7b. Conductance Data for Solutions of Potassium in Liquid Ammonia Using Cell A; Run No: CK-4

Sub- run No.	Elapsed time	add nNH3	n NH3	cell nNH3	nK×103	υ	C	Notes	æ	<
1-D	250	1,281		1,250	12.92	0.4050	0.6364	a or b	70.3	840.
2-D	455	1,275		2,527	12.89	0.2028	0.4503		187.5	629.2
3-D	615	1,276		3.804	12,86	0.1351	0,3676		314.5	562.9
4-D	715	1,275		5.081	12,85	0,1013	0,3183		444.9	530,7
	1285			5.081	12.77	0,1007	0.3173		467.	209.
5-D	1410	1,258		6.340	12.75	0.08067	0.2840		.009	494.
Q-9	1600	1,274		7,615	12,73	0.06708	0.2590		733.	486.
	1740			7.615	12.71	0.06699	0.2588		701.7	508.9
l - w	1940		1.287	6.327	12.68	0.08038	0,2835		570.5	521.6
2-w	2070		1,285	5.040	12.66	0.1006	0.3172		438.6	542.1
3-w	2180		1.278	3,761	12.65	0.1344	0.3666		307.1	579.5
4-w	2760		1.263	2.469	12.56	0.2023	0.4498		183.8	643.1
5-w	2920		1.262	1.205	12.54	0.4074	0.6383	→	70.6	832.
tbath	-37.10°C	ပ္ပ		Wt of me	Wt of metal (ampoule):	ule): †	0.5067 g	-		
Σ $^{add}_{NH_3}$	7.639	6		Wt of me	Wt of metal (titration):	ion):	0.4615 g	k: 23.92	23.92 cm ⁻¹	
$\Sigma _{NH_3}^{w}$	N.A.	_		Accepted	Accepted wt of metal: (a)	tal: (a)	0.5067 g	(a) See A	See Additional Notes	otes
•				$\frac{\Delta n}{\Delta t} \times 10^6$:	••	•	-0.1400	nugei	under 'Explanatory Notes''	ory Motes

Table 7c. Conductance Data for Solutions of Potassium in Liquid Ammonia Using Cell A; Run No: CK-6

Sub- run No.	Elaps ed time	add nNH3	w n/NH3	cell nNH3	$^{ m n_{K^{ m x}10^3}}$	U	C ST	Notes	æ	<
1-D	20	1,292		1,261	2,169	0.06905	0.2628	، م	(618.0)	520.0
	202			1,261	2,108	0.06711	0.2591		(658.2)	502.3
2-D	1050	1,282		2,545	2.077	0.03282	0,1812		1342,5	502.9
3-D	1350	1,265		3,811	2.051	0.02167	0.1472		1964.6	520.5
4-D	1510	1,273		5.086	2.036	0.01612	0.1270		2526.	544.2
	2025			5.086	1,990	0.01576	0.1255		2598.	541.2
5-D	2310	1,285		6.346	1,965	0.01248	0.1117		3125.	568.2
Q-9	2450	1,276		7.624	1,952	0.01032	0,1016	-	3635.	590.7
1 - w	3660		1.276	6.346	1.844	0.01171	0,1082		3250.	582.2
2-w	3790		1.274	5.071	1,833	0.01456	0.1207		2720.	559.5
3-w	3980		1.276	3.792	1,816	0.01928	0.1389		2146.	535.8
4 - w	4180		1,283	2,509	1.799	0.02886	0.1699		1509.	0.609
5-w	4330		1.274	1.233	1,785	0.05816	0.2412	→	(769.4)	495.2
tbath	-37.05°C)5°C		Wt of m	Wt of metal (ampoule):	-	0.0666 g			
αdd Σ ⁿ NH3	i is 7.673	. 22		Wt of m	Wt of metal (titration):		0.08488 g	k: (22.19 cm ⁻¹)	19 cm ⁻¹)	
Σ nW ₃	H ₃ N.A.	.		Accepte	Accepted wt of metal:		0.08488 g	22.1	22, 16 cm ⁻¹	
				$\frac{\Delta n}{\Delta t} \times 10^6$:	; ₉ 0	Ĭ	-0.0892			

Table 7d. Conductance Data for Solutions of Potassium in Liquid Ammonia Using Cell A; Run No: CK-7

											11
Sub- run No.	Elapsed time	add nNH3	nNH3	cell nNH3	$^{ m n_{K}^{x}10^{3}}$	υ	C 24	Notes	ж	<	
1-D	115	1.961		1.931	3,508	0.07291	0.2700	ત્ય	(578.0)	510.4	l
2-D	185	1.280		3,210	3.506	0.04391	0.2095	ą	9.686	494.9	
3-D	250	1.847		5.056	3.503	0.02789	0.1670	nd	1527.1	504.8	
4-D	315	1,969		7.027	3,501	0.02006	0.1416	q	2046.	523.9	
5-D	380	1.276		8,305	3.499	0.01698	0,1303		2359.	536.7	
Q-9	430	1.839		10,146	3.497	0.01389	0,1179		2789.	555.0	
	966			10.146	3.478	0.01381	0,1175		2815.	553.1	
l-w	1610		1,850	8.322	3,457	0.01674	0,1294		2380.	539.7	
2-w	1700		1,259	7.038	3,453	0.01977	0,1406		2074.	524.5	
	2240			7.038	3.435	0.01966	0,1402		2084.	524.9	
3-w	2360		1.867	5.169	3.431	0.02672	0,1635		1576.	510.5	
4-w	2460		1,970	3.200	3.427	0.04306	0,2075		983.7	507.7	
5-w	2560		1,269	1.930	3.424	0.07120	0.2668		(554.5)	544.8	
	2610			1,930	3.422	0.07116	0.2668	→	(554.0)	545.7	
tbath	-37.07°C	2°7		Wt of me	Wt of metal (ampoule):	ule):	0.1373 g				1
Σ $^{\mathrm{add}}_{\mathrm{NH_3}}$	1 10.172	72		Wt of me	Wt of metal (titration):	ion):	0.1373 g	k : (21.	: (21.51 cm ⁻¹)		
»u ⊠	N.A.	•		Accepted	Accepted wt of metal:	tal:	0.1373 g	21.	21.50 cm ⁻¹		
NH3	m			$\frac{\Delta_n}{\Delta_t} \propto 10^6$:	: 00	'	-0.0345				

Table 7e. Conductance Data for Solutions of Potassium in Liquid Ammonia Using Cell A; Run No: CK-8

		Name and Address of the Owner, where								
Sub- run No.	Elapsed time	add ⁿ NH ₃	nnH3	cell nNH3	$^{ m n_{K^{ ext{X}}}10^3}$	Ö	C 3	Notes	æ	\
1-D	96	1,862		1.832	10.271	0.2227	0.4718	a or b	(143.4)	673.6
2-D	185	1,281		3,112	10,258	0.1317	0.3629		281.2	580.6
3-D	305	1,858		4.969	10,239	0.08264	0.2875		490.8	530.1
4-D	360	1,281		6.252	10,231	0.06571	0.2563		635.0	515.3
5-D	450	1.865		8,119	10,217	0.05073	0,2252		835.6	507.2
	855			8,119	10,155	0.05042	0.2245		842.9	505.9
l-w	096		1.857	6.263	10,139	0.06499	0.2549		640.7	516.4
	115*			6.263	9.457	0.06062	0,2462		691.2	513.0
2-w	315		1.278	4.985	9,427	0.07621	0.2761		537.9	524.5
3-w	410		1.854	3, 129	9.412	0.1211	0.3482	·	311.6	569.8
4-w	661		1.278	1.850	9.374	0.2038	0.4514		160.7	657.0
	716			1.850	9,365	0.2036	0.4512	>	(161, 1)	655.7
			(1.862)							
tbath	37	-37.07°C		Wt of mo	Wt of metal (ampoule):	le): 0.4035)35 g			
$\sum_{n} \frac{add}{NH_3}$		8.147		Wt of m	Wt of metal (titration):	on): 0.4022)22 g	k: (21.51 cm ⁻¹)	(-1)	
Σ n NH3		8.129		Accepted	Accepted wt of metal:	al: 0.4022)22 g	21,50 cm ⁻¹	-1	
				사 ×	106:	-0, 1532	532	* See Additional Notes under "Explanatory Notes"	ial Notes un y Notes"	der

Table 7f. Conductance Data for Solutions of Potassium in Liquid Ammonia Using Cell A; Run No: CK-9

Sub- run No.	Elapsed time	add ⁿ NH ₃	w u s HN	cell ⁿ NH3	$^{ m n_{K^{ m x}10^3}}$	υ	C 2	Notes	ጸ	<
1-D	125	1.863		1.833	0.8425	0.01852	0.1361	- م	(2175)	533.9
2-D	200	1,271		3, 103	0.8414	0.01093	0,1045		3359	585.6
3-D	295	1.981		5,083	0.8401	0,006663	0.08163		4965	649.9
4-D	395	1,859		6.944	0.8387	0.004870	62690.0		6352	695.1
5-D	455	1.273		8.219	0.8379	0.004111	0.06412		7278	718.6
Q-9	543	1,965		10.186	0.8366	0.003313	0.05756	<u></u>	9658	749.8
l-w	290		1.970	8.217	0.8360	0.004104	0.06406		7292	718.3
	1060			8.217	0.8295	0.004072	0.06381		7348	718.6
2-w	1140		1,262	6.955	0.8282	0.004803	0.06930		6450	693.9
3-w	1260		1,851	5,105	0.8267	0,006531	0,08081		5071	649.2
4-w	1380		1,955	3, 148	0.8250	0.01057	0.1028		3479	584.7
5-w	1460		1,257	1.917	0.8238	0.01733	0.1316	→	(2305)	538.6
			(1.922)	•						
t bath	-37,	-37.08°C		Wt of m	t of metal (ampoule):		0.03400 g			
$\Sigma_{\rm nNH_3}^{\rm add}$		10.212		Wt of m	Wt of metal (titration):		0.03301 g	k: (2)	(21,51 cm ⁻¹)	
Σ nw NH2		10.217		Accepte	Accepted wt of metal:		0.03301 g	21	21.50 cm ⁻¹	
				$\frac{\Delta_n}{\Delta_t} \times 10^6$:	••	-0-	-0.01394			

Table 7g. Conductance Data for Solutions of Potassium in Liquid Ammonia Using Cell A; Run No: CK-10

Sub- run No.	E lapsed time	add nNH3	n NH3	cell NH3	$^{ m n_{K^{ m x}10^3}}$	υ	C 2	Notes	R	<
1-D	385	1.960		1.930	3,500	0.07277	0.2698	a or b	(570.7)	514.4
2-D	440	1,265		3,194	3.496	0.04401	0.2098	a or b	974.9	497.6
3-D	515	1.874		5.067	3.490	0.02772	0.1665	۰ م	1520.7	506.5
4-D	635	1.978		7.047	3.480	0.01989	0.1410		2041.5	525.9
5-D	170	1.270		8.319	3,469	0,01680	0.1296		2358.3	538.9
Q-9	830	1.845		10,166	3,464	0.01373	0.1172		2782.0	558.9
l - w	890		1.857	8,310	3,459	0.01677	0.1295		2358.5	539.8
	1340			8.310	3.422	0.01659	0.1288		2382.9	540.1
2-w	1400		1,282	7.028	3.417	0.01958	0.1399		2068.9	527.1
3-w	1440		1,958	5.071	3,413	0.02709	0.1646		1553.4	507.2
	1720			5.071	3,387	0.02689	0.1640		1564.7	507.2
4-w	1800		1,859	3,211	3,381	0.04244	0,2060	→	1014.6	495.8
2-w	1930		1,261	1.949	3,370	0.06939	0.2634	a or b	(603.8)	6.605
			(1.970)							
tbath	-37.02°C)2°C	Wt of m	Wt of metal (ampoule):	oule):	0.1381 g				
Σ nadd NH3	10, 192	192	Wt of m	Wt of metal (titration):	tion):	0.1381 g	차 :	k: (21.36 cm ⁻¹)		
Σ n NH,	10, 187	187	Accepted	ed wt of metal:	etal:	0.1381 g		21,35 cm ⁻¹		
	•		$\frac{\Delta n}{\Delta t} \times 10^6$: 9(-0.08211				

Table 7h. Conductance Data for Solutions of Potassium in Liquid Ammonia Using Cell A; Run No: CK-11

Sub- run No.	Elapsed time	add ⁿ NH ₃	n n NH3	cell nNH3	$^{ m n_{ m K}^{ m x}10^3}$	$C \times 10^3$	- KZ	Notes	æ	<
1-D	55	1.967		1.937	0.1765	3.675	0.06062	q.	(7740)	743.7
2-D	110	1.270		3.206	0.1759	2,213	0.04704		11764	812.0
3-D	165	1.860		5.065	0.1752	1,395	0.03735		17510	865.
	592			5.065	0.1740	1,386	0.03723		17600	866.5
4-D	: 325	1,969		7.036	0, 1733	0.9937	0.03152		23710	897.2
5-D	370	1.276		8.314	0.1728	0.8384	0.02896		27690	910.5
Q-9	420	1.848		10.164	0.172_{2}^{-}	0.6833	0.02614		33430	925 -
l-w	470		1,853	8.317	0.1718	0.8322	0.02885		27920	606
2-w	505		1.265	7.050	0.1712	0.9795	0.03130		24080	896.5
3-w	550		1.975	5.073	0.1706	1,356	0.03682		18035	864.3
4-w	615		1,856	3,215	0.1699	2,132	0.04617		12254	- ¹ •608
	1170			3, 215	0, 1633-	2.049	0.04527		12713	811.
5- &	1240		1,275	1.939	0.162	3,368	0.05803	→	(8469)	7414
			(1.963)							
t	-37.05°C)5°C		Wt of m	Wt of metal (ampoule):		0.00751 g			
Σ n NH,	1 10, 190	.90		Wt of m	Wt of metal (titration):		0.00693 g	k : (21.	: (21.15 cm ⁻¹)	
ν υ α ΝΗΥ	10.187	.87		Accepte	ed wt of metal:		0.00693 g	21.14	14	
				$\frac{\Delta_n}{\Delta_t} \times 1$	106:	-0.0	-0.01191	Solvent c	Solvent conductance = 0.215 x 10 ⁻⁶ mho cm ⁻¹	⇒ o cm ⁻¹

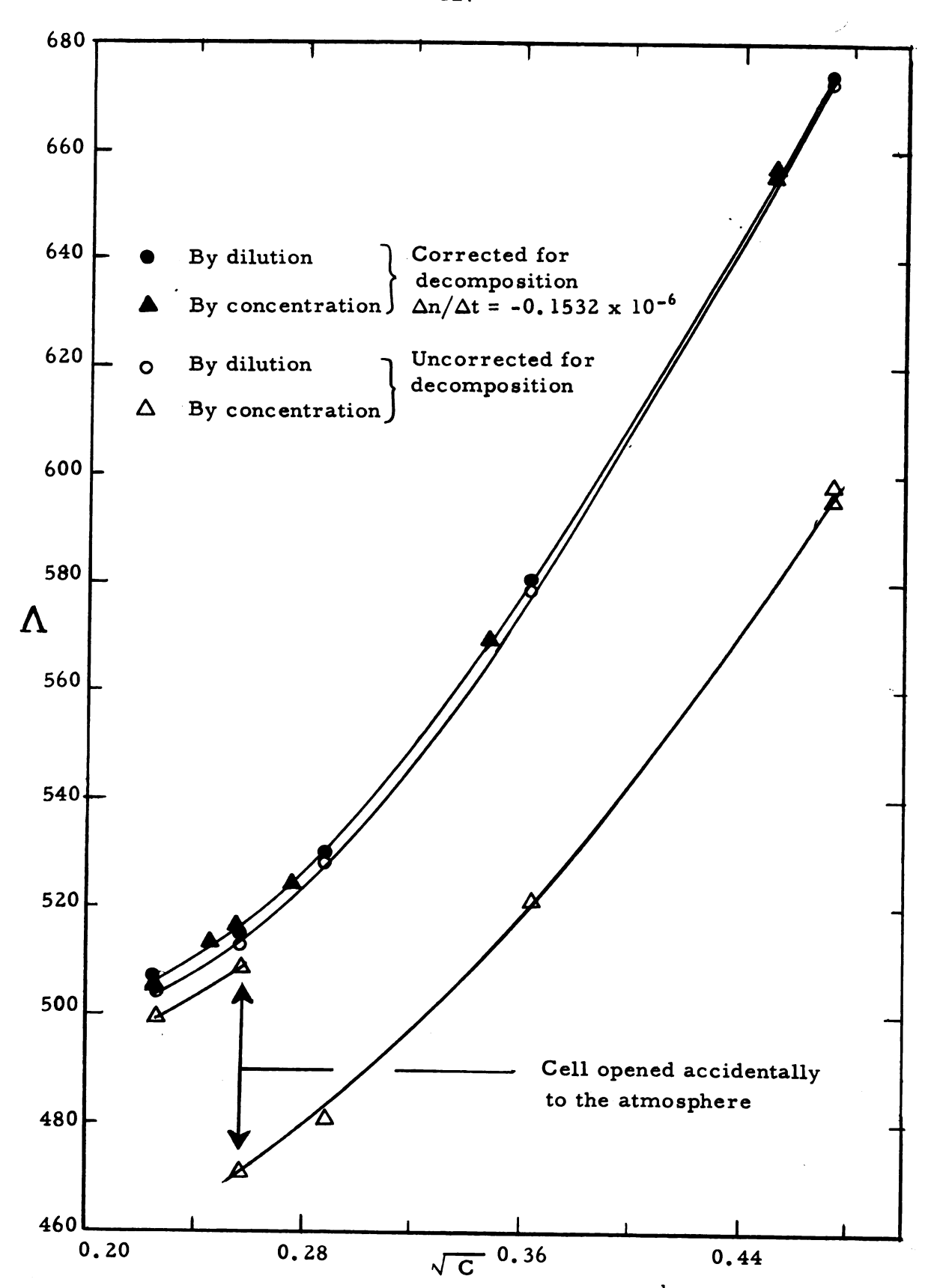


Figure 24. Equivalent conductance versus (molarity) for CK-8 at -37.0°C.

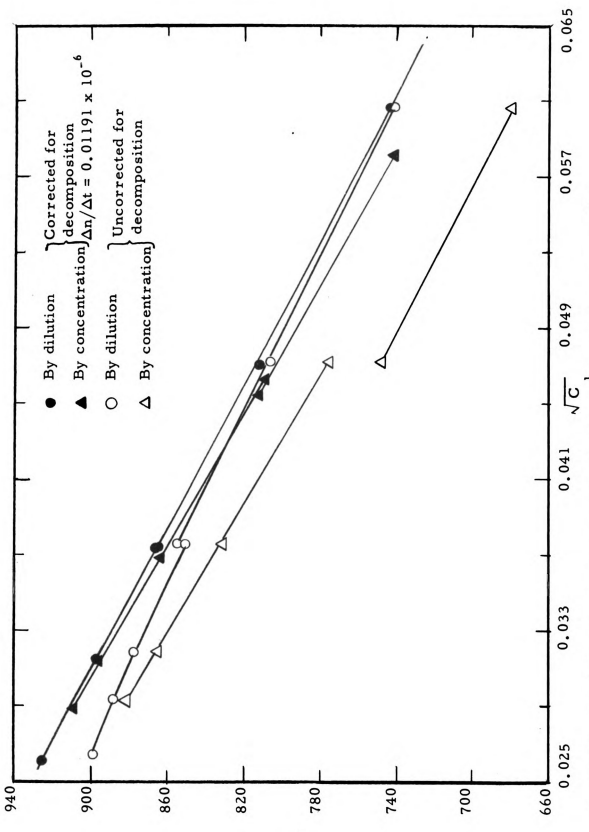
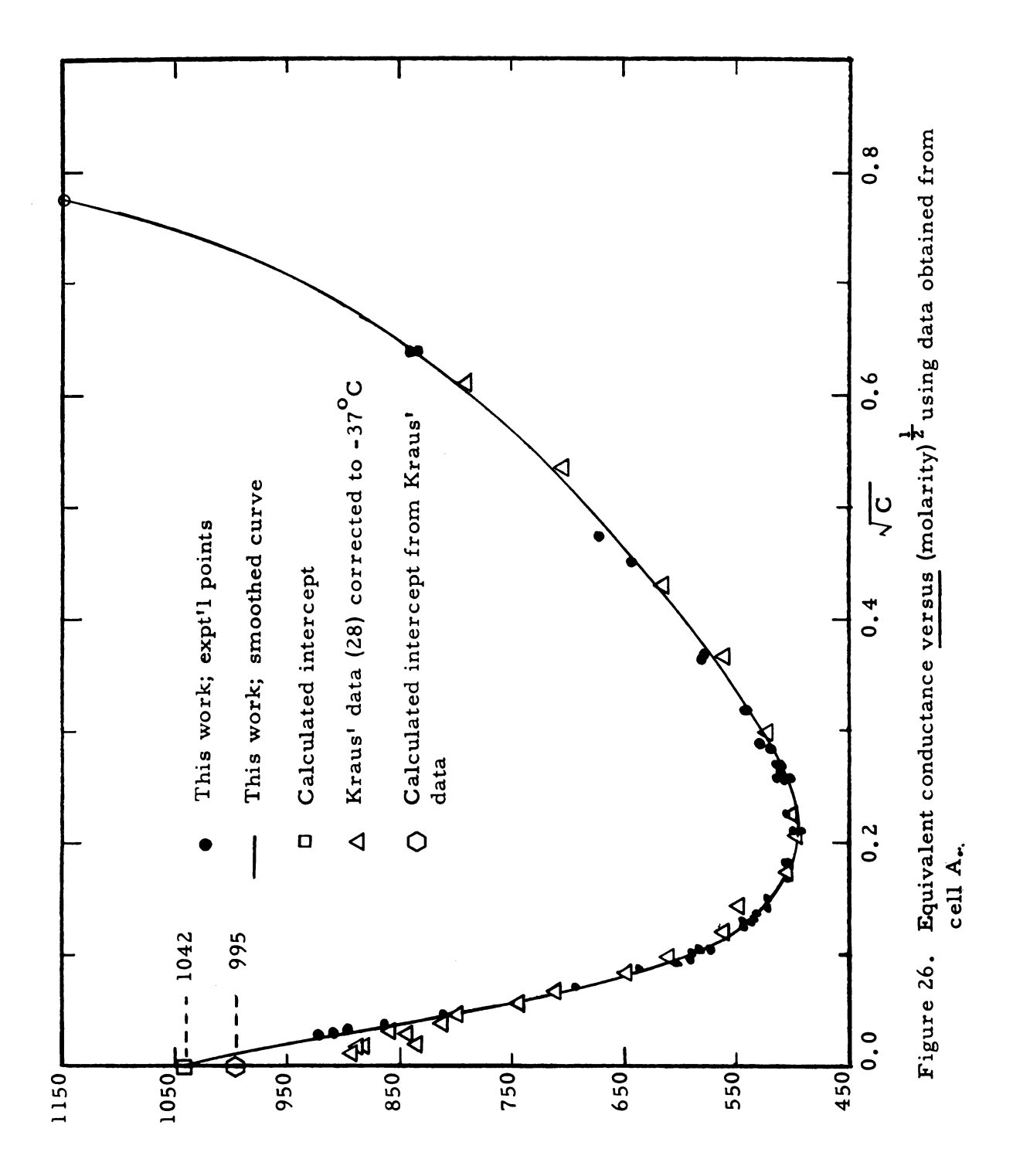


Figure 25. Equivalent conductance versus (molarity)² for CK-11 at -37.0°C.



The conductance values in Table 7 are plotted versus the square root of concentration in Figure 26. For comparison, the data of Kraus (28) corrected to -37.0° C with the temperature coefficient data of Kraus and Lucasse (33) have also been included. The value 995 for \bigwedge_{K}° was computed from data on solutions of sodium metal, and potassium and sodium nitrate. This value is lower than that calculated from a Shedlovsky analysis of the data obtained in the present investigation (1042). Both values are discussed further under "Calculation of \bigwedge_{K}° " in the Discussion Chapter.

A table of the smoothed values of \triangle may be found at the end of the transference results (Table 15). The maximum percent deviation from the smoothed data at any concentration was 0.8%, and the average deviation was 0.4%.

2. Data from Cell B

Explanatory Notes for Tables 8 and 9.

These tables give the experimental data obtained with conductance cell B. The conductivities of potassium solutions in ammonia are given in Table 8, and those of <u>deutero</u>-ammonia, in Table 9. Several of the column headings have the same significance as explained in the notes for Table 7.

Sub-run No. This column designates the particular dilution under consideration and is referred to as i in the following explanations.

This column gives the number of moles of pure ammonia added to the cell as determined from calibrated volumetric flasks. See notes preceding Table 7 for further explanations. For deutero-ammonia, the available density data (73) are at -33.7°C, which is taken into consideration in computing the correction ratio. The plot of density versus temperature for ND₃ was assumed to have the same slope as for NH₃.

nWNH3

This column gives the number of moles of pure ammonia withdrawn from the cell before the addition of new solvent as indicated by nadd for the same sub-run. The withdrawn ammonia was weighed in sealed heavy-wall ampoules at room temperature. The tip of the ampoule was then broken off, the ammonia evaporated. and the ampoule plus tip were reweighed after drying. The difference gives the mass of ammonia. Actually, solution was withdrawn from the cell into a metal collection trap from which the ammonia was distilled into the ampoule. Thus the ratio of the mass of ammonia removed and the mass left in the cell is the same as the ratio of the mass of solution removed and the mass remaining in the cell. No vapor corrections were required since the vapor pressure in the withdrawal system was reduced essentially to zero by cooling the ampoule in liquid air before sealing it off. The last value, if enclosed in parenthesis, is the amount of ammonia withdrawn from the cell following complete withdrawal.

This is the number of moles of liquid ammonia remaining in the cell. The method of computation is

$$n_{NH_3}^{cell} = \sum_{1}^{i} n_{NH_3}^{add} - \sum_{0}^{i} n_{NH_3}^{w} - (n_{NH_3}^{v})^{-37} - (n_{NH_3}^{v})^{25}$$
 [5.2]

where i is the sub-run in question. $(n_{NH_3}^V)^{-37}$ and $(n_{NH_3}^V)^{25}$ have the same interpretation as discussed in the notes preceding Table 7. The ideal gas equation was used, and the pressure in the system was taken as the vapor pressure of the solution at -37.0° C (86).

n_Kx10³ This column represents the number of equivalents of potassium metal present in the cell during the designated sub-run, <u>i</u>.

It cannot be corrected for decomposition as was done for cell A.

The calculation is

$$(n_{K})_{i} = X_{i}(n_{K})_{i-1}$$
 [5.3]

where

$$X_{i} = \frac{(n_{NH_{3}}^{cell})_{i-1} - (n_{NH_{3}}^{w})_{i}}{(n_{NH_{3}}^{cell})_{i-1}}$$
 [5.4]

in which (i-1) refers to the designated values for the previous dilution.

- <u>C</u> This column gives the concentration of the solution in g atoms of metal per liter of solution.
- $\frac{C^{\frac{1}{2}}}{C^{\frac{1}{2}}}$ This column gives the square root of the above concentration.
- Switch Position This column designates the particular cell in which the resistance value in the next column was measured. There were three electrodes, and hence, three possible cell combinations. The number refers to the switch position at which a given cell was connected.
- This column gives the resistance of the solution in ohms. The value listed has been corrected for lead resistances. Except for certain resistances for CK-16, the values listed are those observed at 1000 cps. If a plot of resistance versus (frequency) possessed a positive slope then the value at infinite frequency was taken; otherwise, the lowest value was selected. In most cases, the difference between the values at 400 and 1000 cps was negligible.
- This column gives the equivalent conductance in cm² mho equiv⁻¹ calculated by equation [3, 2] using the listed cell constants at the

- end of the table. These constants were determined using standard potassium chloride solution after platinizing the electrodes. The results are displayed in Figure 27, page 142.
- A^{adj} This column gives the equivalent conductance adjusted for the dependence of the cell constant upon concentration. (See section on "Cell Constant Dependence upon Concentration" for method used.) The results are plotted in Figure 29, page 146.
- tbath This is the temperature of the thermostat. The observed variations were within $\pm 0.05^{\circ}$ C.
- Σ n add and Σ n NH₃ These are the summations of the moles of ammonia added and withdrawn, respectively. The difference between them gives an indication of the precision of the manipulations and corrections.
- Wt of metal (ampoule), Wt of metal (titration), and Accepted wt of metal

 These have the same significance as described in the notes preceding Table 7.
- L x 10⁶ This gives the specific conductance in mho cm⁻¹ of a sample of solvent added to the cell and then withdrawn before the metal ampoule was broken. Conductance cell no. 3 was used in conjunction with a parallel resistor to measure the resistance. If several rinses were made, then the stated specific conductance is for the final rinse.
- k₃, k₅, and k₇ These are the cell constants for their respective cells as determined by standard potassium chloride solution after platinizing the electrodes. See section on "Cell Constant Dependence upon Concentration" for further revision of cell constants.

Table 8a. Conductance Data for Solutions of Potassium in Liquid Ammonia Using Cell B; Run No: CK-12

	•										
	687.1	599.0	9452	7							
	531.4 688.3	452.3 600.1	1149 9469	с го	0.08538	0.007290	0.1103	0.6106	0.3780	0.3415	6
	546.4 545.9	491.8 491.4	5089 5074	5	0.1286	0.01655	0.2656	0.6466	0.3515	0.3415	∞
	508.2 508.3	464.1 464.2	2549 2540	5 7	0.1871	0.03501	0.5715	0.6566	0.3340	0.3300	7
	514.8 514.3	479.3 478.9	1230.6 1227.1	5 7	0.2650	0.07023	1, 156	9099.0	0.3314	0.3432	9
134	582.0 582.6	557.2 557.0	511.3 509.6	5 7	0,3813	0.1454	2,363	0.6488	0.3280	0.3406	2
	734.5 734.0	722.2 721.7	189.4 188.8	5	0.5503	0.3028	4.878	0.6362	0.3841	0.3331	4
	1, 150 1, 150	1,150 1,150	58.1 58.0	5 7	0.7878	0.6207	11.06	0.6873	0.3115	0.3438	33
	7,600	7,600	4.6	5	1.088	1.184	21.05	0.6563	!	0.3413	2
	17,000 16,000	17,000 16,000	1.1	2 2	1.498	2.242	21.05	0.3163	;	0.3300	1
	$\Lambda^{ m adj}$	<	R	Switch position	C C	U	$^{ m n_{ m K}^{ m x}10^3}$	cell ⁿ NH3	n w NH ₃	add ⁿ NH 3	Sub- run No.

Continued

Table 8a - Continued

Sub- run No.	add _n NH3	, w n N H ₃	cell nNH ₃	$^{ m n_{K}^{ imes 10^3}}$	υ	- ₩	Switch position	ద	<	$\Lambda^{ m adj}$
10	0.3317	0,3551	0.5867	0.07861	0.003170	0.05630	8 2 6	N.A. 19321 19270	676.3	811.6
11	0.3413	0.3262	0.6018	0.02048	0.001373	0.03705	£ 50 ~	5297 42370 42480	682.5 712.0 707.6	912.5 912.8 907.1
12	0.3426	0.3418 (0.5885)	0.6026	0.008845	0.0005920	0.02433	4 23 3	12771 99600 100300	656.3 702.5 695.0	938.5 958.9 948.7
tbath	-37.06°C	2,9		Wt of meta	Wt of metal (ampoule):	0.8226 g	Cell	Cell constants	1 1 1 1 1 1 1 1 1	
Σ nadd		4.0606		Wt of meta	Wt of metal (titration):	0.8232 g	k3:	4.962 cm ⁻¹	m-1	
$\sum_{n}^{w}_{NH_3}$		4.0301		Accepted w	Accepted wt of metal:	0.8229 g	.;s	41.42 cm ⁻¹	m - 1	
				$L \times 10^6$ (solvent):	lvent):	0.347 mh	0.347 mho cm ⁻¹ k ₇ : 41.27 cm ⁻¹	41.27 c	m-1	

Table 8b. Conductance Data for Solutions of Potassium in Liquid Ammonia Using Cell B; Run No: CK-16

I				136					ı
$\Lambda^{ m adj}$	1300 1590 1610	796 826.4 827.2	655 657.2 659.5	571 570.5 572.0	515.2 514.7 516.0	497.2 497.4 497.7	518.1 514.2 513.3	565.0 564.0 565.5	
<	1300 1590 1610	757 818.2 819.0	610 639.3 641.5	523 542.8 544.2	466.7 480.6 481.8	443.1 456.8 457.0	455.3 466.6 465.8	489.6 504.5 505.8	
K	5.0 33.9 33.5	17.2 133.0 132.4	36.5 290.5 288.5	73.0 587.4 583.8	141.4 1146 1139	258.8 2096 2087	457.3 3724. 3717	776 6286 6247	
Switch position	25.7	2 2 2	2 2	25 %	2 2	25.3	8 W K	7 22 3	
aks O	0.8747	0.6169	0.4721	0;3604	0.2742	0.2080	0.1544	0.1143	
U	0.7652	0.3806	0.2229	0:1299	0.07519	0.04326	0.02383	0.01306	
$^{ m n_{K}^{ imes 10^3}}$	6.386	6.386	4.586	2.558	1.509	0.8691	0.4349	0.2477	
cell NH3	0.3183	0.6591	0.8168	6982:0	0.8054	0.8080	0.7350	0.7645	
n NH3	:	1	0.1858	0:3612	0.3228	0.3414	0.4037	0.3163	
add ⁿ N H ₃	0.3328	0.3416	0.3446	0;3313	0.3413	0.3440	0.3307	0.3458	
Sub- run No.	-	7	٣	4	ιń	9	~	∞	

Continued

Sub- run No.	add NH3	n NH3	cell nNH3	ⁿ K*10³	U	4 2	Switch position	&	<	$\Lambda^{ m adj}$	
6	0.3460	0.3388	0.7717	0.1379	0.007204	0.08488	253	1270 10290 10240	542.3 558.7 559.4	637.2 641.4 642.2	
10	0.3335	0.3232	0.7820	0.08017	0.004135	0.06430	8 is 6	2031 16370 16290	590.8 611.8 612.6	723.1 722.5 723.5	
	0.3435	0.3118	0.8137	0.04820	0,002389	0.04888	6 2 6	3277 26290 26180	633.7 659.7 659.7	808.0 809.4 809.4	
12	0.3446	0.3614	0.7969	0.02679	0,001356	0.03682	7 22 33	5602 44900 44700	653.2 680.2 680.7	870.1 869.3 869.9	13'
13	0.3293	0.4011	0.7251	0,01331	0,0007403	0.02721	w 20 L	10290 81900 81400	651.2 683.0 684.7	914.9 918.6 920.9	7
14	0.3421	0.3392	0.7280	0.007082	0.0003926	0.01981	8 2 C	19720 156700 155600	640.6 672.9 675.2	957.7 958.9 962.9	
15	0.3440	0.3236	0.7484	0.003934	0.0002121	0.01457	w 10 12	36260 289000 289000	644.5 675.2 672.8	979.6 982.4 978.9	
16	0.3299	0.3362 (0.7309)	0.7421	0.002167	0.0001178	0.01085		67900 556300 556300	619.5 631.2 629.0	975.7 943.6 940.4	
tbath D add D NH3 E NH3	d 5.4250 l ₃ 5.3974	oC 50 74	Wt of metal (ampowt of metal (titral Accepted wt of metal L x 106 (solvent):	Wt of metal (ampoule): Wt of metal (titration): Accepted wt of metal: L x 10 ⁶ (solvent):	0.24969 g 0.2477 g 0.24969 g 0.099 mho cm ⁻¹	o cm ⁻¹	Cell const k ₃ : 4.962 k ₅ : 41.42 k ₇ : 41.27	constants 1, 962 cm ⁻¹ 11, 42 cm ⁻¹ 11, 27 cm ⁻¹			

Table 9a. Conductance Data for Solutions of Potassium in Liquid deutero-Ammonia Using Cell B; Run No: CK-14

					13	38			1
Λ $\Lambda^{ m adj}$	7700	812	558.0 557.4	472.6 472.6	420.4	396.3 396.2	414.0 401.3 401.1	449.6 435.8 435.5	518.7 504.5 504.6
<	7700	812 811	549.8 549.2	454.9 454.9	395.5 395.3	365.6 365.5	364.8 364.8 364.6	390.3 390.2 389.9	439.6 437.9 438.0
æ	4°9 5°0	84.4	241.5 240.8	528.0 526.2	1093.8 1090.4	2201 2193	503.5 4220 4206	930.8 7771 7745	1693 14186 14134
Switch position	5 ~	2 2	5 ~	2 2	5 2	2 2	8 2 7	25.5	2 D B
C 2	1.088	0.7772	0.5586	0.4152	0.3094	0.2269	0.1640	0.1169	0.08166
υ	1.183	0.6041	0.3120	0.1724	0.09573	0.05147	0.02691	0.01366	0.006668
$^{ m n_{K}^{ imes 10^3}}$	10.36	10,36	5.476	3, 153	1.816	0,9491	0.4609	0.2353	0.1107
cell nNH3	0.3212	0.6641	0,6960	0.7332	0.7645	0,7457	0.6940	0.6987	0.6735
n NH3	:	i	0.3130	0.2952	0.3110	0.3649	0,3835	0.3398	0.3699
Sub add run ⁿ N H ₃ No.	0.3338	0.3436	0.3460	0,3324	0.3423	0.3461	0,3318	0.3445	0.3447
Sub run No.	7	7	က	4	2	9	7	∞	6

Continued

Table 9a - Continued

Sub- run No.	add ⁿ NH ₃	nNH3	cell ⁿ NH ₃	n _K ×10³	U	C Z	Switch position	Я	<	$\Lambda^{ m adj}$
10	0.3322	0.3588	0.6469	0.05174	0.003246	0.05697	w ro	3126 26220	489.0	608.8 584.3
							7	26140	486.5	583.8
11	0.3463	0.3948	0.5984	0.02017	0,001368	0.03699	3	6937	522.8	0.669
		(0.6017)					S.	57500	526.4	675.4
							7	58000	520	.299
tbath	-37.06°C	၂ ၁ွ	Wt of meta	Wt of metal (ampoule):	0.40644 g	89	Cell constants	tants		
$\sum_{\mathbf{n}} \mathbf{n}_{\mathbf{NH}}^{\mathbf{add}}$		37	Wt of meta	Wt of metal (titration):	0.4035 g	90	k3: 4.962 cm ⁻¹	cm-1		
Σ n α	3.7326	97	Accepted v	Accepted wt of metal:	0.4050 g	⊘0	k ₅ : 41.42 cm ⁻¹	cm-1		
; ; ;	2		$L \times 10^6 \text{(solvent)}$:	lvent):	0.109 n	0.109 mho cm-1	k_7 : 41.27 cm ⁻¹	, cm-1		

		:
		•
		: :
		:
		:
		;
		:
		: •
		:
		· ·
		•
		:
		:
		• •
		•
		:
		,

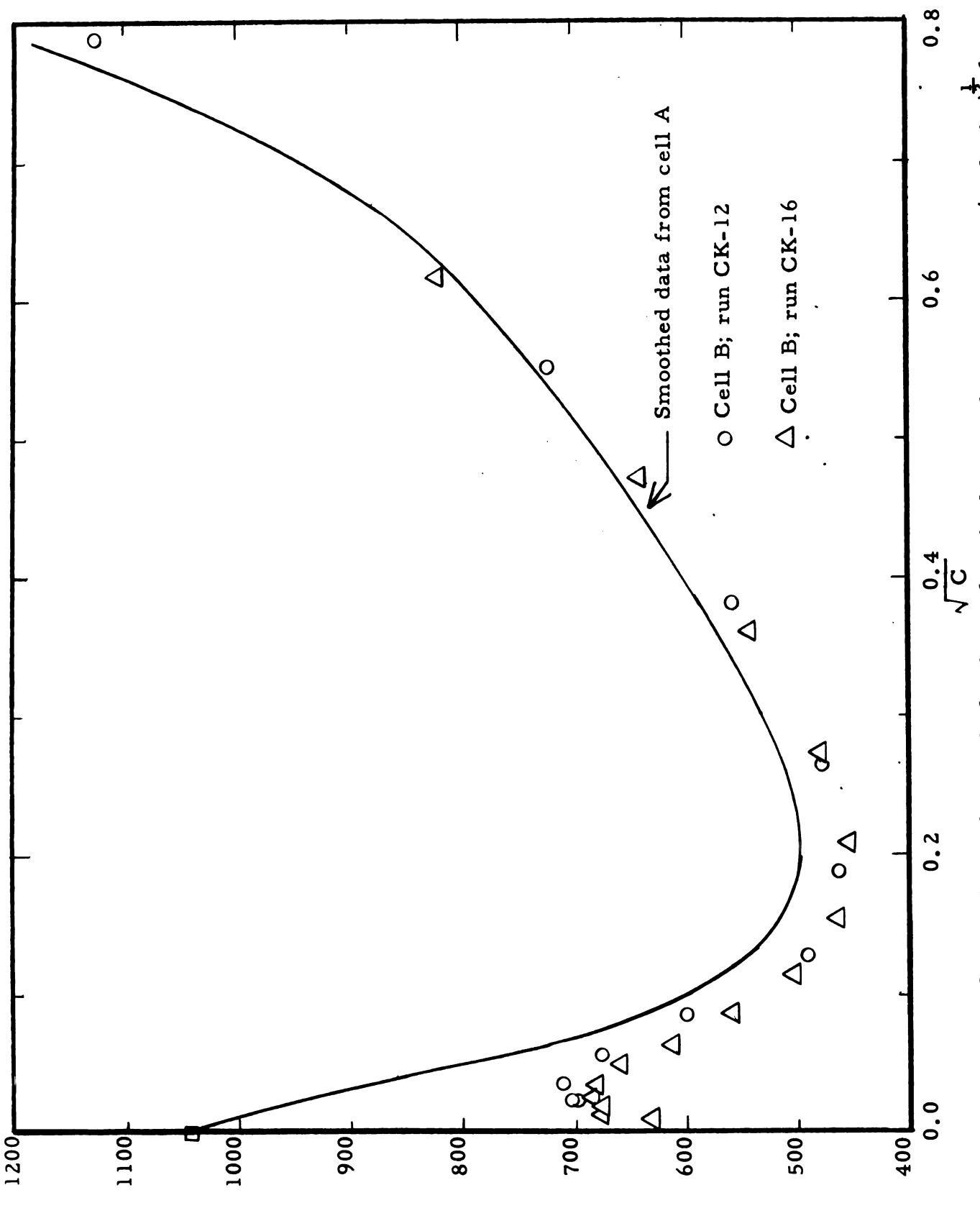
Table 9b. Conductance Data for Solutions of Potassium in Liquid deutero-Ammonia Using Cell B; Run No; CK-15

1				140)				
$\Lambda^{ m adj}$	532 540.6 545.2	448 442.6 445.5	399. 1 395. 2 396. 2	392.9 389.6 391.5	412.1 414.5 416.5	479.7 477.5 479.3	563.4 561.8 565.7	649.0 647.5 651.2	700
7	500 531.6 536.1	413 423.1 425.9	360.5 368.0 368.9	348.3 355.8 357.5	359.6 373.4 375.2	410.0 418.5 420.1	459.9 473.7 477.0	498.5 518.0 521.0	1
R	33.1 260.3 257.1	82.2 670.0 663.1	195.4 1598 1588	415.2 3392 3363	815 6552 6497	1493 12210 12120	2804 22720 22480	5335 42850 42450	
Switch position	6 2 7	25.3	2 2 2	2 2 2	2 2	2 2 2	827	253	
C 7	0.5472	0.3822	0.2654	0.1853	0,1301	0.09003	0.06203	0.04320	
υ	0.2994	0.1461	0.07043	0.03432	0.01693	0.008105	0.003848	0.001866	
$^{ m n_{K}^{ imes 10^3}}$	2.432	2.432	1,165	0.5499	0.2821	0.1328	0.06028	0.03072	
cell ⁿ NH ₃	0.3225	0.6683	0.6679	0.6486	0.6756	0.6646	0.6357	0.6680	
nn NH3	i	:	0.3482	0.3526	0.3161	0.3573	0.3630	0.3117	
add nNH3	0.3355	0.3465	0.3488	0.3333	0.3431	0.3463	0.3341	0.3440	
Sub- run No.	1	7	м	4	ω	9	2	œ	

Continued

Table 9b - Continued

Sub- run No.	add nNH3	nNH3	cell ⁿ NH ₃	$^{ m n_{ m K}}{ m x}^{ m 10^3}$	υ	C 7	Switch position	n R	<	$\Lambda_{ m adj}$
6	0.3448	0,3536	0.6592	0.01446	0.0008903 0.02984	0.02984	. 52 ~	10543 88900 85300	528.3 522.9 543.1	731.7 692.8 719.6
10	0.3328	0.3402 (0.6619)	0.6518	0.006997	0,0004357 0,02087	0.02087	e 20 F	21311 175000 173000	533.6 542.4 546.7	779.0 756.6 762.6
tbath 2 add 2 nNH3 2 nW	-37.05°C -37.05°C 3.4092 3.4046	D 7 9	Wt of metal (amp Wt of metal (titra Accepted wt of m L x 10 ⁶ (solvent):	Wt of metal (ampoule): Wt of metal (titration): Accepted wt of metal: L x 10 ⁶ (solvent):	0.09509 g 0.09353 g 0.09509 g	ho cm-1	Cell c k ₃ : k ₅ :	Cell constants k ₃ : 4.962 cm ⁻¹ k ₅ : 41.42 cm ⁻¹ k ₇ : 41.27 cm ⁻¹		141



Comparison of smoothed values of equivalent conductance versus (molarity) from cell A with those obtained from cell B using cell constants determined with KCl. Figure 27.

The adjusted values of equivalent conductance <u>versus</u> square root of concentration from Tables 8 and 9, are shown in Figure 29. The maximum deviation from the averaged curve at any value below 0.55 molar was 3%. The average deviation is 0.9%. In the concentration range 0.0006 to 0.0064 molar, run CK-12 deviates from CK-16 by as much as 6%. A table of smoothed values will not be given since only two runs were made in each solvent and the results lack the precision necessary to justify such a table.

3. Cell Constant Dependence upon Concentration

As mentioned in the experimental procedure, difficulty in determining the cell constants for cell B was attributed to poor electrodes or possibly cell design. If the ball electrodes were platinized, then a cell constant relatively independent of concentration could be determined with standard potassium chloride solution. However, bright electrodes were used for the metal solutions and comparison of the potassium-ammonia runs for cells A and B (Figure 27) shows a decided discrepancy.

There are two other possible sources that can give rise to this discrepancy. By overlaying the large plots of \triangle versus \sqrt{C} on an illuminated table, it was observed that the curves would coincide if the plot of cell B results was shifted to higher concentrations by an increment of 0.01 in the square root of the concentration. A vertical shift is also necessary which can be assigned to a constant error in the cell constant. This indicates that a reproducible error is present in the two ammonia runs made with cell B. This could be due to a miscalculation in either the amount of ammonia in the vapor phase, which is a sizeable fraction (2 to 4%) because of the small amount present as liquid (10 ml), or the amount of metal initially present as determined from the titration of the metal residue at the conclusion of a run.

The second possible systematic error is apparently inherent in the dilution technique. A small initial error in the solvent continues to grow in size after passing through a minimum. Further details are given in Appendix C.

Because of the difficulty in determining the cell constants and the relatively good reproducibility, it was assumed that the principal difficulty lies with an electrode phenomena. The procedure used to circumvent this difficulty was to determine the concentration dependence of the cell constants from the data obtained using cell B for potassium-ammonia solutions. The specific conductance of these solutions is known with precision from the results using cell A.

The concentration dependence of the ratio of the varying cell constant, k_B^i , to that determined from KCl, k_B^i , is shown in Figure 28. The adjusted equivalent conductance, Λ^{adj} , was calculated from

$$\Lambda^{\text{adj}} = \frac{k'B}{k_B} \Lambda \qquad [5.5]$$

where Λ is the equivalent conductance determined by the former cell constant. This ratio of cell constants was used to correct the Λ values in Tables 8 and 9 to the new values, Λ^{adj} .

In Figure 29, Λ^{adj} versus \sqrt{C} plots show very good agreement considering the difficulties encountered. The upper curve represents the smoothed data from cell A on ammonia solutions. Conductance values from run CK-16 are represented in two ways: those values which were used in computing the new cell constant are shown as solid squares, while the open squares represent values from the same run which were not used in the cell constant computation, and hence, may be considered independent of this determination. The values of run CK-12 agree well with those from cell A and from run CK-16 in cell B.

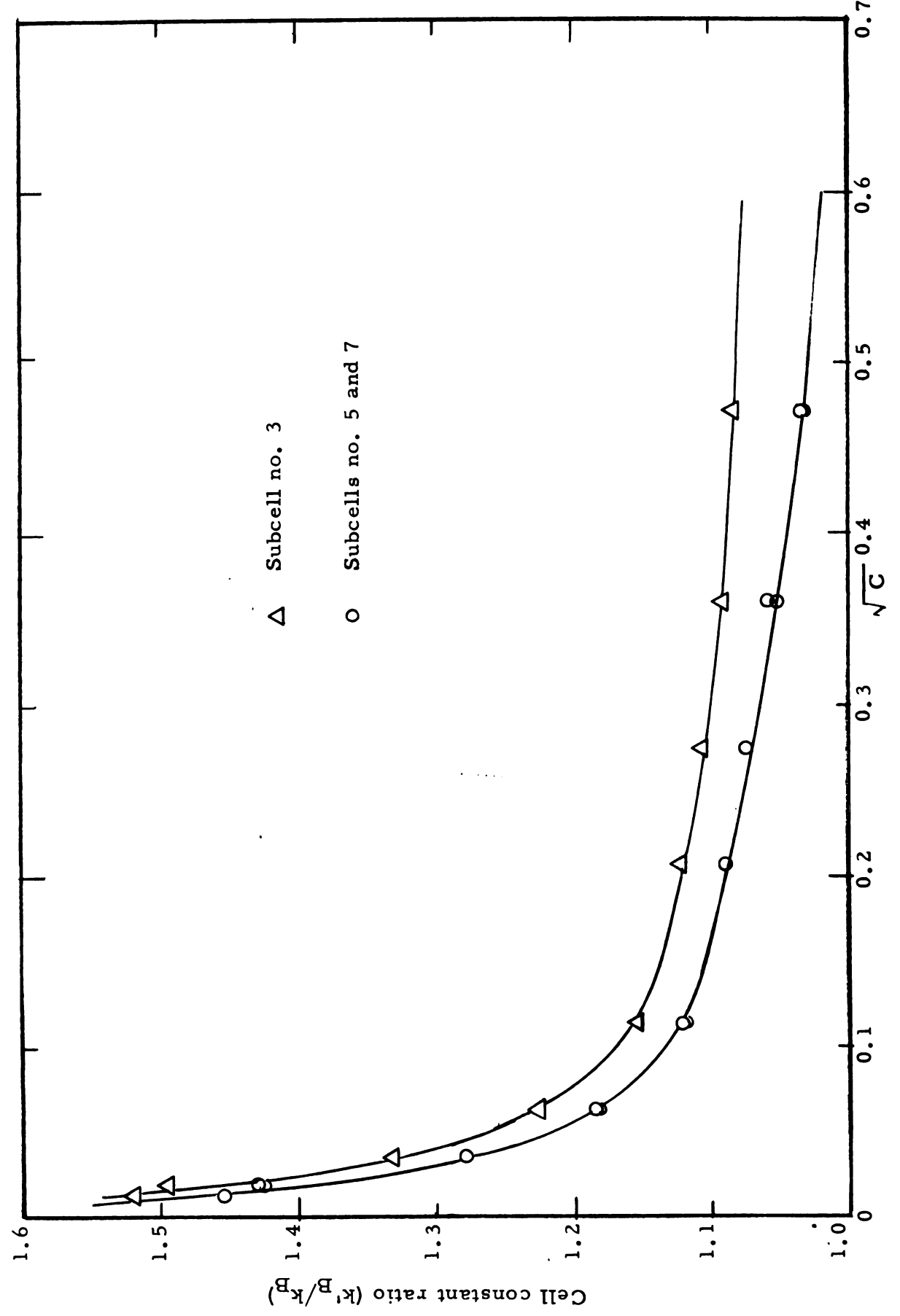


Figure 28. Variation of cell constant ratio $(k^t B/k_B)$ with square root of concentration.

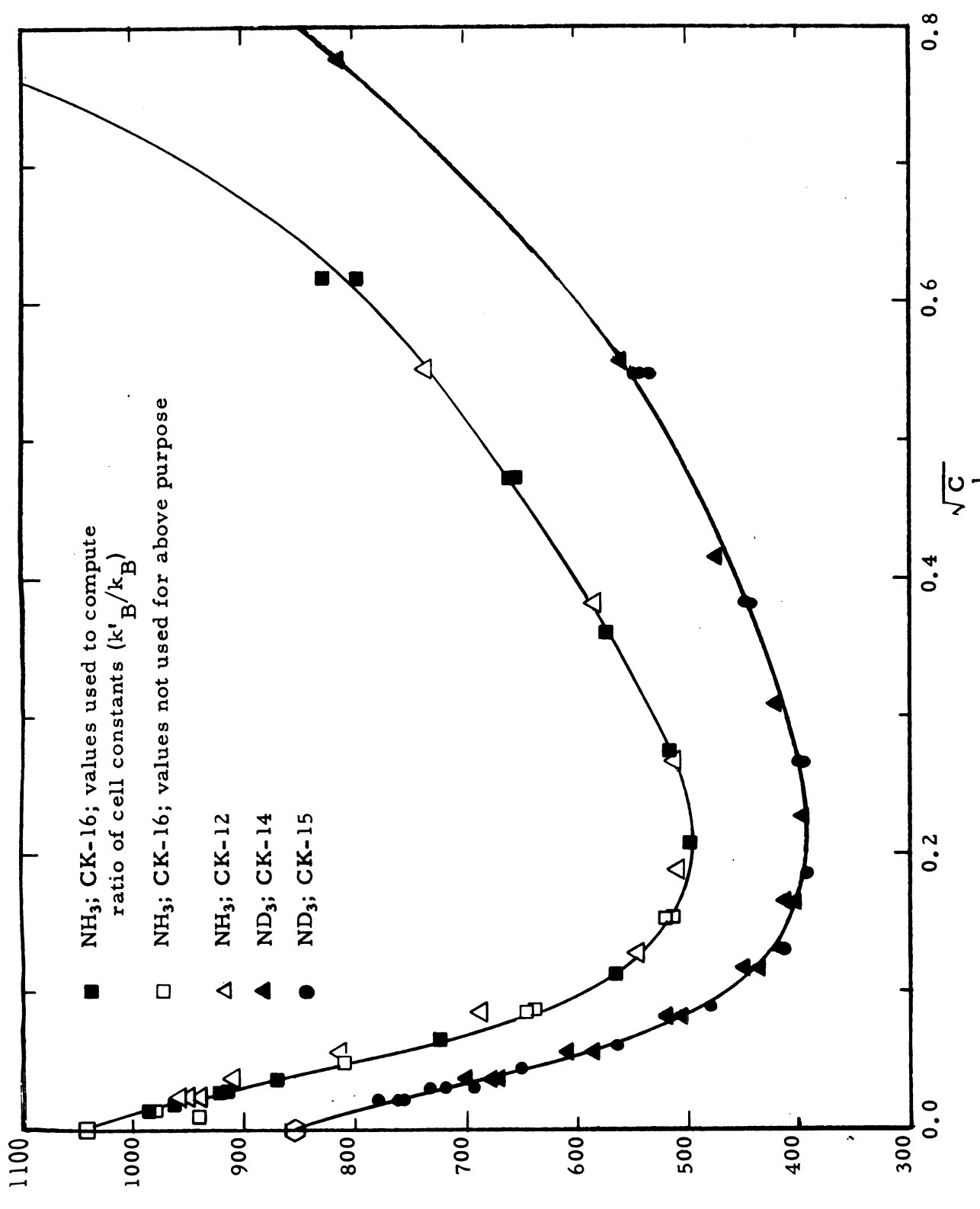


Figure 29. Equivalent conductance versus (molarity) $\frac{1}{2}$ for potassium solutions of ammonia and deutero-ammonia at -37.0 C.

The lower curve was drawn through the points obtained from runs CK-14 and CK-15 on deutero-ammonia solutions using the adjusted cell constants. Note that the data extrapolate well into the intercept determined from Walden's rule:

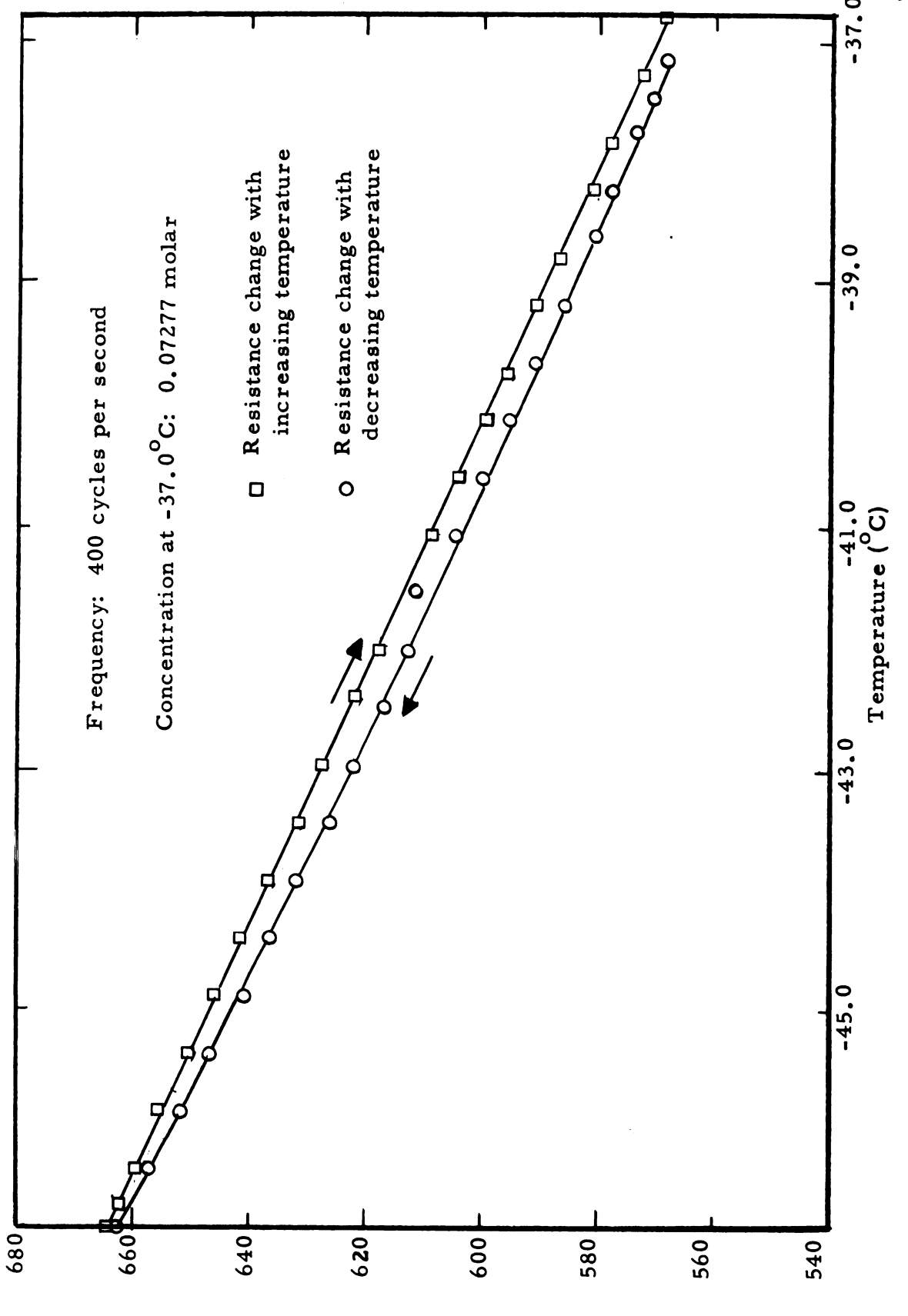
4. Temperature Coefficient

One observation was made on the variation of solution resistance with temperature. The run selected was CK-10 which had a concentration of 0.07277 molar at -37.0°C and the study covered the range from -37.0°to -47.0°C. The resistance is practically a linear function of temperature over this small range as shown in Figure 30. A displacement of the heating and cooling curves exists which can be attributed to a lag in the attainment of temperature equilibrium since the bath temperature was continually changing. The total elapsed time during the cooling and heating was 210 minutes.

The calculation of the temperature coefficient is as follows:

$$\Lambda = \frac{10^3 \text{k}}{\text{cR}}$$
 [5.7]

and



Resistance (ohms)

Figure 30. Resistance versus temperature from run CK-10.

$$c = n/V = n\rho 10^3/w$$
 [5.8]

where

 Λ = equivalent conductance

k = cell constant (21.36 cm⁻¹)

R = resistance in ohms

c = normality

n = equivalents

V = volume in liters

 ρ = density in g ml⁻¹

w = mass of solution in grams.

The variation of Λ and log R with temperature T can be obtained by expanding equation [5.7] by logarithms and differentiating this result and also equation [5.8] with respect to T.

$$\frac{1}{2.303} \wedge \frac{d\Lambda}{dT} = -\frac{10^{-3}}{2.303\rho} \cdot \frac{d\rho}{dT} - \frac{d \log R}{d T}$$
 [5.9]

and

$$\frac{d \log R}{d T} = \frac{1}{2.303R} \cdot \frac{dR}{dT}$$
 [5.10]

From the average of the data presented in Figure 30 and from density data of pure ammonia (73) one obtains the following values:

t (
$$^{\circ}$$
C) R (ohms) ρ (g m1 $^{-1}$)
-37.10 571.2 0.6870
-42.01 615.3 0.6930
-46.90 662.7 0.6988

Thus, $d\rho/dT = -1.20 \times 10^{-3}$ and dR/dT = -9.34. Now since the plots of both solution resistance and solvent density with temperature are essentially linear, the above values will apply to the solution at -37.10°C.

Hence d log R/dT = -0.0071 and d Δ /dT = 9.30. The value of d log R/dT obtained by Fristrom (30) on sodium solutions at this concentration was -0.0062 which occurs almost at the minimum observed in Fristrom's plot.

B. Transference Numbers

Fifteen transference number experiments were made on the potassium-ammonia solutions; four were discarded because of mechanical failures, the most common being the loosening of the boundary stopcock. Analyses of the cell contents were made on eight runs. The transport numbers computed using this method of determining the concentration were more consistent than those computed from concentrations derived from conductance measurements. For this reason, the analytical method of determining concentrations was accepted as more valid. This discrepancy is discussed later in this section. The conductance measurements were therefore used only to monitor the decomposition rate. Table 14, page 157, gives the results obtained from both methods. The conductance data used to determine the concentrations are the ones reported in the preceding section. A plot of log L versus \sqrt{C} facilitated the conversion of resistance readings to concentration values.

Experiment 42-K-8 is an example of a typical set of data and its treatment is as follows:

1. Typical Set of Experimental Data

Run No. 42-K-8

Bath temp: -37.08°C Cell constant: 25.75 cm⁻¹

See Figure 31, page 152, for plot of resistance versus time

Concentration of KBr: 0.042 molar Current for 42-K-8a: 2.700 ma

Current for 42-K-8b: 2,600 ma

Analytical Results

Ampoule No.:	K-39	Weight (uncorrected buoyancy):	0.2211 g
Weight of ammonia:	9.80 g.	Weight of metal (by titration):	0.0400 ₀ g
$\rho_{\rm soln}$ at -37.08 $^{\rm o}$ C	0.6864 g	Concentration:	0.0713 ₄ molar

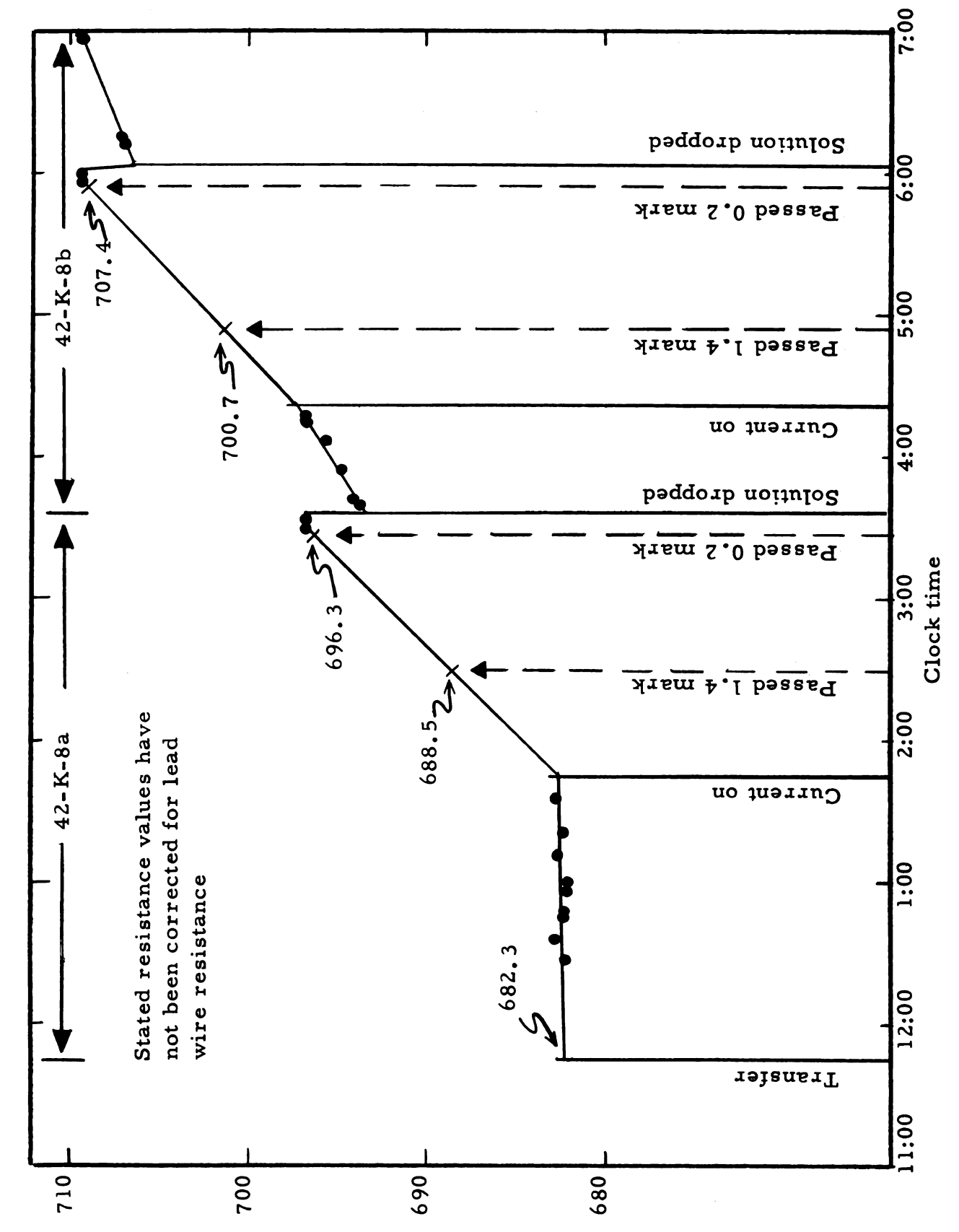
Concentrations determined by resistance measurements were obtained from a plot of log L versus \sqrt{C} after computing L from the cell constant and resistance readings.

Data and Preliminary Results

Table 10. Observed Data from Notebook for Runs 42-K-8 a and b.

Volume Interval	Volume (ml)	Run "a" Time [*] (sec)	Run ''b'' Time* (sec)
1.4-1,3	0.10095	302.8	271.6
1.3-1.2	0.10074	299.3	274.3
1.2-1.1	0.09981	304.8	281.2
1.1-1.0	0.09983	304.0	309.7
1.0-0.9	0.10008	296.7	285.1
0.9-0.8	0.10108	281.5	308.5
0.8-0.7	0.09803	270.7	287.6
0.7-0.6	0.10006	280.8	308.0
0.6-0.5	0.09973	280.5	297.0
0.5-0.4	0.09959	278.1	300.2
0.4-0.3	0.10085	281.5	303.1
0.3-0.2	0.10032	276.0	275.8

^{*}Time for boundary to traverse each volume increment.



Cell Resistance (ohms)

Figure 31. Solution resistance versus clock time for transference run 42-K-8 a and b.

Table 11. Comparison of Average Uncorrected Transference Numbers Using Concentrations from Conductance and Titration.

Interval	Volume (ml)	Time (sec)	Condu Molarity	ctance (a) T-	Titrat Molarity	
Run 42-K-	- <u>8a</u>			•	•	
1.4-0.8	0.6024	1789.	0.07113	0.8559	0.07134	0.8586
1.3-0.7	0.5996	1757,	0.07107	0.8667		.0.8702
1.2-0.6	0.5990	1738.	0.07100	0.8743		0.8786
1.1-0.5	0.5989	1714.	0.07094	0.8858		0.8909
1.0-0.4	0.5987	1688.	0.07088	0.8983	.	0.9043
0.9-0.3	0.5994	1673	0.07082	0.9067		0.9136
0.8-0.2	0.5987	1668	0.07075	0.9078	+	0.9155
	Average		0.07094	0.8851	0.07134	0.8902
Run 42-K-	-8b					
1.4-0.8	0.6024	1730	0.07010	0.9057	0.07134	0.8877
1.3-0.7	0.5996	1746	0.07005	0.8926	1	0.8755
1.2-0.6	0.5990	1780	0.07000	0.8742		0.8581
1.1-0.5	0.5989	1796	0.06996	0.8658		0.8504
1.0-0.4	0.5987	1786	0.06991	0.8695		0.8546
0.9-0.3	0.5994	1804	0.06986	0.8613	İ	0.8471
0.8-0.3	0.4984	1496	0.06984	0.8636	<u> </u>	0.8496
	Average		0.06996	0.8761	0.07134	0.8604

⁽a) Corrected for decomposition only.

Corrections

(1) Hittorf; correction for migration of potassium metal from anode compartment.

Total equivalents of electricity passed =

$$\frac{[(2.70 \text{ ma})(6000 \text{ sec}) + (2.60 \text{ ma})(5520 \text{ sec})] \times 10^{-3}}{96,493 \text{ coul equiv}^{-1}} = 0.317 \times 10^{-3} \text{ equiv}$$

⁽b) No corrections applied.

Equivalents of metal lost =

$$T_{+}$$
 (0.317 x 10⁻³) = (0.110)(0.317 x 10⁻³) = 0.0348 x 10⁻³ equiv.

Therefore the total amount of metal, n_K^0 , present in anode compartment before the current was turned on for run "a" is n_K^0 = equiv by analysis + equiv lost by migration

=
$$(1.023 + 0.0348)10^{-3} = 1.058 \times 10^{-3}$$
 equiv.

Thus the concentration is

$$C^{\circ} = 0.07376 \text{ equiv } 1^{-1}$$

(2) Decomposition during the period that the current was on.

Sub-run	Remark	Concentration	Time	$\frac{1}{c} \frac{\Delta c}{\Delta t} \%$
"a"	Current on 0.2 mark	0.07376		
	0.2 mark	0.07224	102 min.	0.0204 moles 1 min
"b"	Current on	0.07214		
	Current on 0.3 mark	0.07106	92 min.	$0.0164 \frac{\text{moles}}{1 \text{ min.}}$

See Table 12 for concentrations at various times during the run.

$$\frac{\overline{C}}{T_{-}^{c}} = (\overline{T}_{-}) \frac{\overline{C}}{\overline{C}} = (0.8902) (\frac{0.07266}{0.07134}) = 0.9067$$
 [5.11]

calculated from average values.

- (3) Solvent correction. This correction is negligible as discussed under Amide Ion Conductance in the Discussion Chapter.
- (4) Volume correction (see equation [3.8])

$$\Delta T_{-} = C \times 10^{3} (11.9 - 69.5 T_{-}) = -0.00371$$
 [5.12]

Table 12. Resistance and Concentration Data at Various Times During Runs 42-K-8 a and b

Remarks	Elapsed time (min)	(a Resistance (ohms)	(b) Concentration (molarity)	Concentration (c) (With Hittorf Corr.) (molarity)
At transfer	0	679.4	0.07184	0.07376
Current on	120	679.4	0.07184	0.07376
1.4 mark	164	685.6	0.07129	0.07309
0.2 mark	222	693.4	0.07060	0.07224
Solution dropped	231	690.5	0.07086	0.07256
Current on	277	694.5	0.07048	0.07214
1.4 mark	308	697.8	0.07022	0.07178
0.2 mark	369	704.5	0.06970	0.07106

⁽a) Corrected for lead wire resistance.

Thus
$$\overline{T}_{-}^{t} = \overline{T}_{-}^{c} - \Delta T_{-}$$

$$= 0.9067 + 0.0037 = 0.9104$$
 [5.13]

(5) Because of the large change in T_ from the value originally calculated, the Hittorf correction was twice recalculated using the newly determined T_ values. The final accepted value is

$$T_{-} = 0.9064 \text{ at} \cdot C = .07234$$

A summary of the various corrections for the "a" and "b" runs are given in Table 13.

⁽b) Calculated from conductance measurements.

⁽c) From titration; conductance measurements used only for determining decomposition rate.

Table 13. Summary of Corrections Applied to Transference Number Data

	42-K-8a		42-K-8b	
	C (molarity)	T_	C (molarity)	T_
Before corrections	0.07134	0.8902	0.07134	0.8604
First Hittorf correction (current applied)	0.07376		0.07214	
Decomposition	0.07266	0.9067	0.07142	0.8614
Volume change	0.07266	0.9104	0.07142	0.8648
Second Hittorf correction	0.07222	0.9048	Not calc	ulated
Third Hittorf correction	0.07234	0.9064		
			Not calc	ula

The molar volumes used for the volume correction were (in ml mole⁻¹): silver, 10.0 (87); silver iodide, 25.9 (55); potassium iodide, 27.8 (55); and potassium, 69.5 (73).

2. Summary

Table 14 gives a summary of all the transference experiments which yielded data. Included are the results obtained from computations using concentrations calculated from both conductance and analytical methods. The conductance values have been corrected for volume change at the cathode and for decomposition. The analytical results have been corrected for the migration of metal from the anode compartment (Hittorf correction), decomposition, and volume change at the cathode. Corrections usually necessary in aqueous solutions for the current carried by ionized solvent and, in this case, also for conduction by amide ion from decomposition products are negligible since the free amide ion concentration is suppressed by the large excess of potassium ions.

Table 14. Summary of Corrected Transference Numbers

Run	Cell Const.	By Condu	ıctance) By Titrat	tion
Number	cm ⁻¹	Molarity	T_	Molarity	Т_
35-K-1	25.82	0.02401	0.784	0.02756	0.900
37-K-3a	25.82	0.03849	0.774	0.04444	0.894
37-K-3b	25.82	0.03834	0.797	0.04373	0.910
38-K-4	25.75	0.03493	0.809		
40-K-6a	25.75	0.1322	0.845		
40-K-6b	25.75	0.1312	0.914		
42-K-8a	25.75	0.07094	0.889	0.07234	0.906
42-K-8b	25.75	0.06996	0.880	0.07196	0.871
44-K-10	25.75	0.1177	0.780		
45-K-11a	25.75	0.01596	0.857	0.01638	0.879
45-K-11b	25.75	0.01584	0.865	0.01619	0.883
46-K-12a	26.00	0.08245	0.661	0.1128	0.906
46-K-12b	26.00	0.08225	0.677	0.1115	0.919
47-K-13a	26.12	0.02636	0.574	0.04164	0.905
	41.20	0.02692	0.586		
40 75 101	16.13	0.01864	0.406	0.04300	0.035
47-K-13b	26.12 41.20	0.02652 0.02891	0.598 0.652	0.04109	0.925
	16.13	0.02891	0.632		
48-K-14	26.12	0.1191	0.832	0.1270	0.888
10 11 11	41.20	0.1218	0.851		3,000
	16.13	0.1220	0.852		
49-K-15a	26.12	0.1200	0.843	0.1261	0.886
	41.20	0.1195	0.839		
	16.13	0.1151	0.808		
49-K-15b	26.12	0.1198	0.845	0.1255	0.886
	41.20	0.1192	0.841		
	16.13	0.1144	0.806		

The experimental values for "a" runs where analyses of the cell contents were made are shown in Figure 32. For comparison with literature data an apparent T_ calculated from emf data as presented in the next section is also plotted. For this calculation the activity coefficient was assumed to be unity.

The calculation of T_{-}^{O} , which is 0.839, will be described in the Discussion Chapter. The smoothed curve for the transference experiments was calculated for the final corrected values of the "a" runs. These runs were felt to be a better representation of the transport phenomena than those of "b". A plot of T_{-} versus \sqrt{C} for the "a" runs showed a slight downward curvature at concentrations above 0.1 molar. Because of the uncertainty to be described below in the data at the higher concentrations, these runs were not included in a least squares treatment of the remaining six values. The intercept, T_{-}^{O} , was kept invariant. The resulting equation is

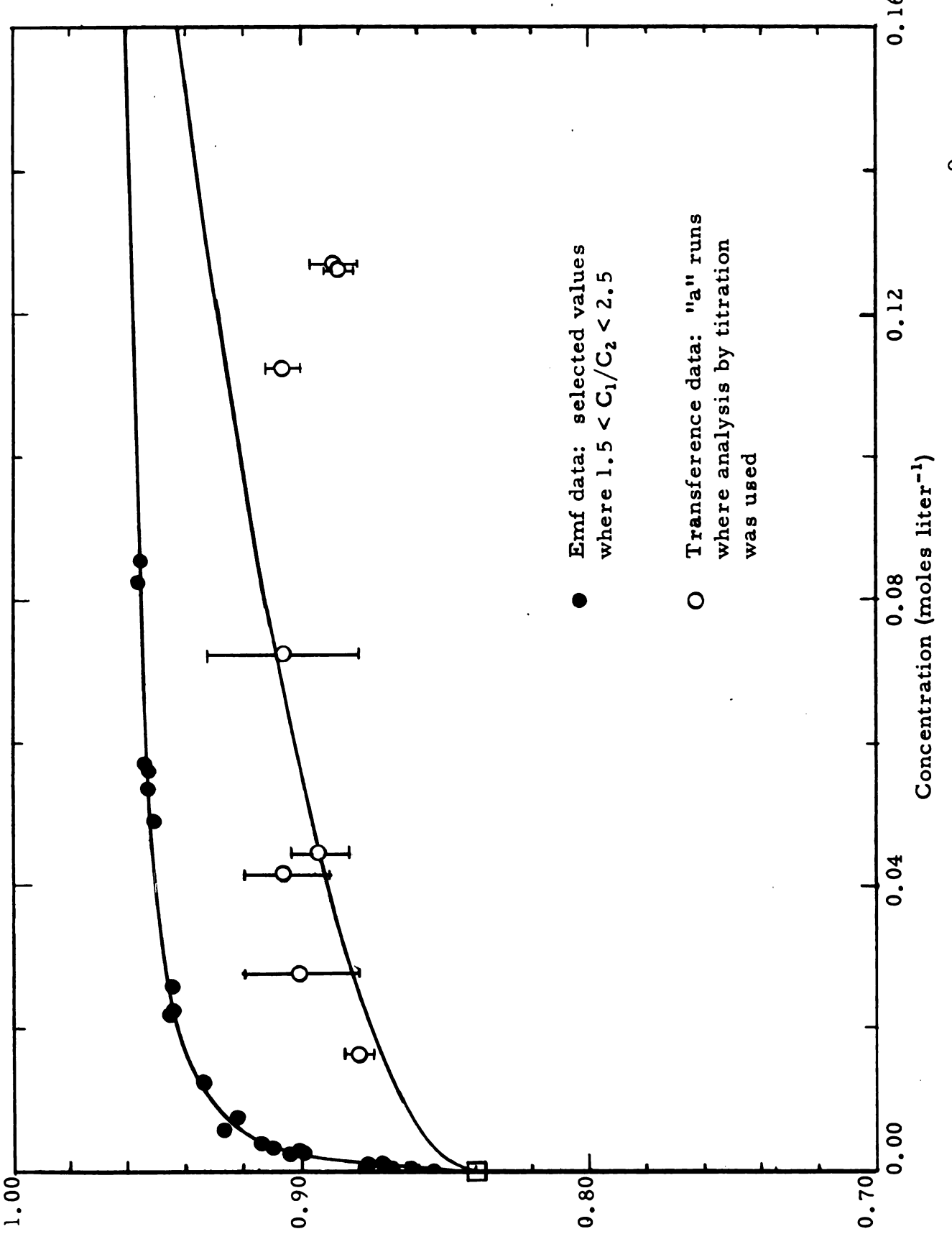
$$T = 0.839 + 0.258 \sqrt{C}$$
. [5.14]

This equation yielded the solid line in Figure 32.

Smoothed values of the equivalent conductance as determined by cell A are given in Table 15. Also included in Table 15 are the smoothed values of the experimentally determined transference numbers to the upper concentration limit of 0.16 molar, and the resulting smoothed values of anionic and cationic equivalent conductances. The concentration dependence of these conductances is displayed in Figure 33.

C. Electromotive Force

A total of five emf experiments were made using the cell design described in the previous chapter. Of these, two experiments, EK-1 and EK-2 representing 18 different concentration ratios, were discarded because of irregularities, and the remaining three (EK's -2, -4, and -5) comprised over 70 different concentration ratios.



H 1

Figure 32. Anion transference number of potassium in liquid ammonia at -37.0°C.

Table 15. Total and Ionic Equivalent Conductances and Transference Numbers for Potassium-Ammonia Solutions at -37.0°C

√c ,	С	$\Lambda^{(a)}$ cm² mho	T <mark>-</mark>	λ_ cm² mho	λ ₄ : cm² mho
(molarity)2	(molarity)	equiv-1		equiv ⁻¹	equiv ⁻¹
0.000	0.0000	1042.	0.839	874	168.
0.010	0.0001	1001.	0.841	842	159.
0.020	0.0004	957.	0.844	808	149.
0.040	0.0016	851.	0.849	723	128.
0.060	0.0036	742.5	0.854	634	108.
0.080	0.0064	655.5	0.860	563	92.1
0.100	0.0100	594.5	0.865	514	80.5
0.120	0.0144	554.6	0.870	482	72.2
0.140	0.0196	527.2	0.875	461	65.9
0.160	0.0256	510.5	0.880	449	61.2
0.180	0.0324	501.6	0.885	444	57.5
0.200	0.0400	497.8	0.890	443	54.5
0.220	0.0484	498.5	0.896	446	52.1
0.240	0.0576	502.6	0.901	453	49.9
0.260	0.0676	509.5	0.906	462	47.9
0.300	0.0900	530.3	0.916	486	44.4
0.350	0.1225	564.3	0.929	524	40.0
0.400	0.1600	602.3	0.942	568	34.8
0.450	0.2025	642.6			
0.500	0.2500	685.2			
0.550	0.3025	731.2			
0.600	0.3600	785.0			
0.650	0.4225	850.0			
0.700	0.4900	941.5			
0.750	0.5625	1072.			

Irregularities in run EK-3 were attributed to fragments from the glass ampoule entering the reservoir, and thus, into the cells. Erratic resistance readings from the conductance cells lent support to this conclusion. Because of the lack of an ampoule containing sufficient metal,

⁽a) The conductance data are smoothed values from cell A.
(b) The transference data are smoothed values determined by the movingboundary method.

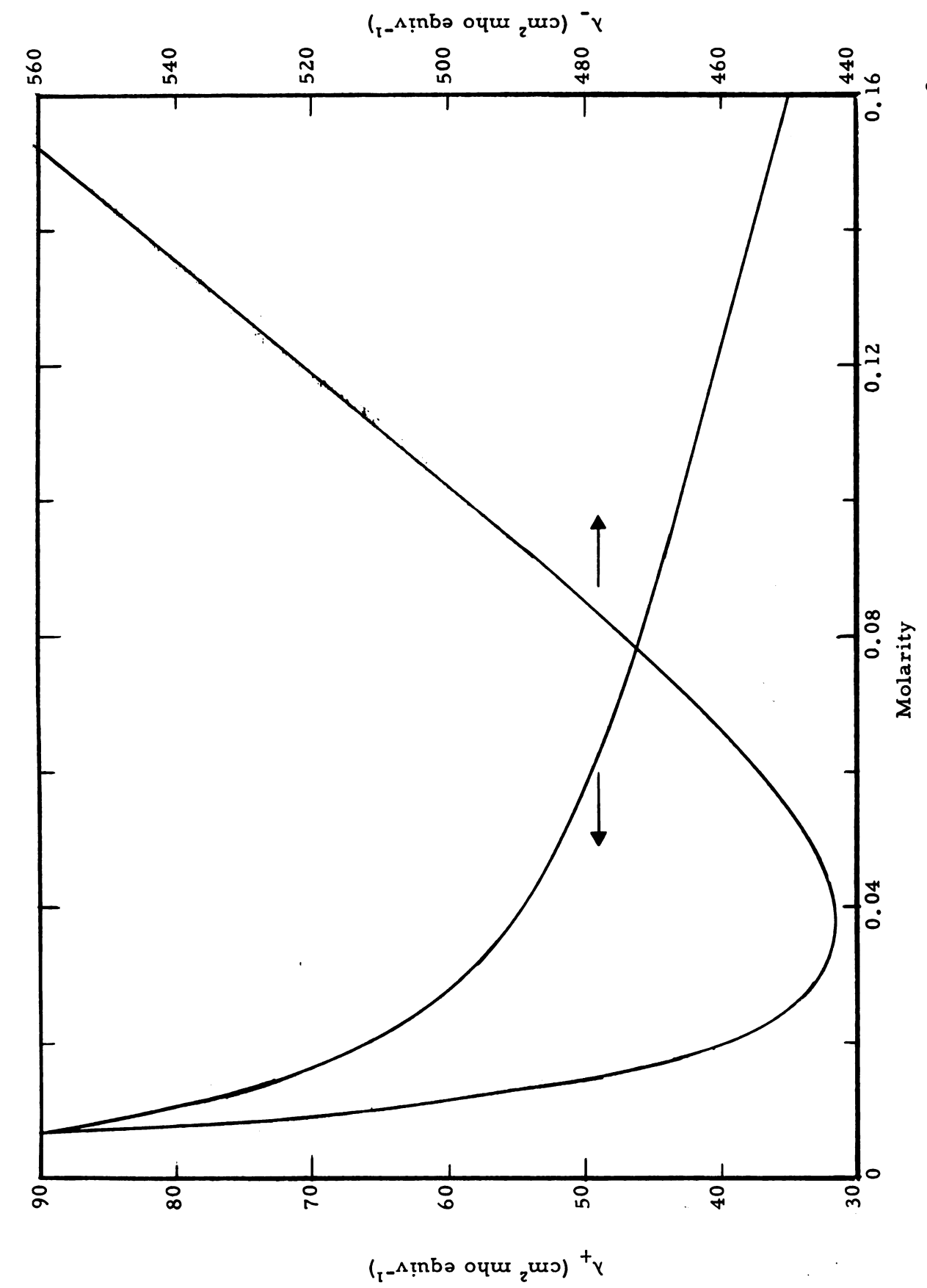


Figure 33. Anionic and cationic conductances for potassium-ammonia solutions at -37.0°C.

two ampoules were sealed into the distillation tube. One ampoule broke easily, but in attempting to break the second one, glass fragments from the first entered the reservoir.

An explanation of the erratic results of EK-1 is not readily available. From the possibility that the constants for the conductance cells were reversed, the values were recalculated, but the improvement was only slightly better, hence they were discarded.

Except for EK-1, plots of resistance <u>versus</u> (frequency) $^{-\frac{1}{2}}$ demonstrated negative slopes; hence, the lowest resistance value (usually at 400 cps, occasionally at 1000 cps) was used to compute the concentration. Positive slopes with negligible frequency dependence were obtained for EK-1. The concentrations were determined from a plot of log L versus \sqrt{C} using the conductance data at -37.0°C.

The emf data are for a number of pairs of solutions. To compute activity coefficients it is necessary to perform the integration described by Dye, et al. (9) so that emf values are obtained relative to a particular concentration. The approximation

$$\frac{\Delta E}{\Delta \log C} = \frac{\Delta E}{\log \frac{C_2}{C_1}} \approx \frac{dE}{d \log C}$$
 [5.15]

was used where ΔE represents the emf observed for a cell having metal concentrations of C_1 and C_2 , which are not widely different. A graph of $\Delta E_{\parallel}/\Delta \log C$ versus $\log \overline{C}$ was made, and graphical integration (88) was used to obtain E versus $\log \overline{C}$, where $\overline{C} = (C_1 + C_2)/2$. The original and integral curves are shown in Figure 34. A reference concentration corresponding to $\log C_{ref} = -2.20$ was chosen for several reasons. First, the concentration is high enough to be fairly insensitive to any errors in emf measurements but yet low enough so the laws for the

^{*}The integration method used is preferred for the construction of an integral curve along the entire path. This method of mean abscissas is seemingly lacking in many books which discuss integration.

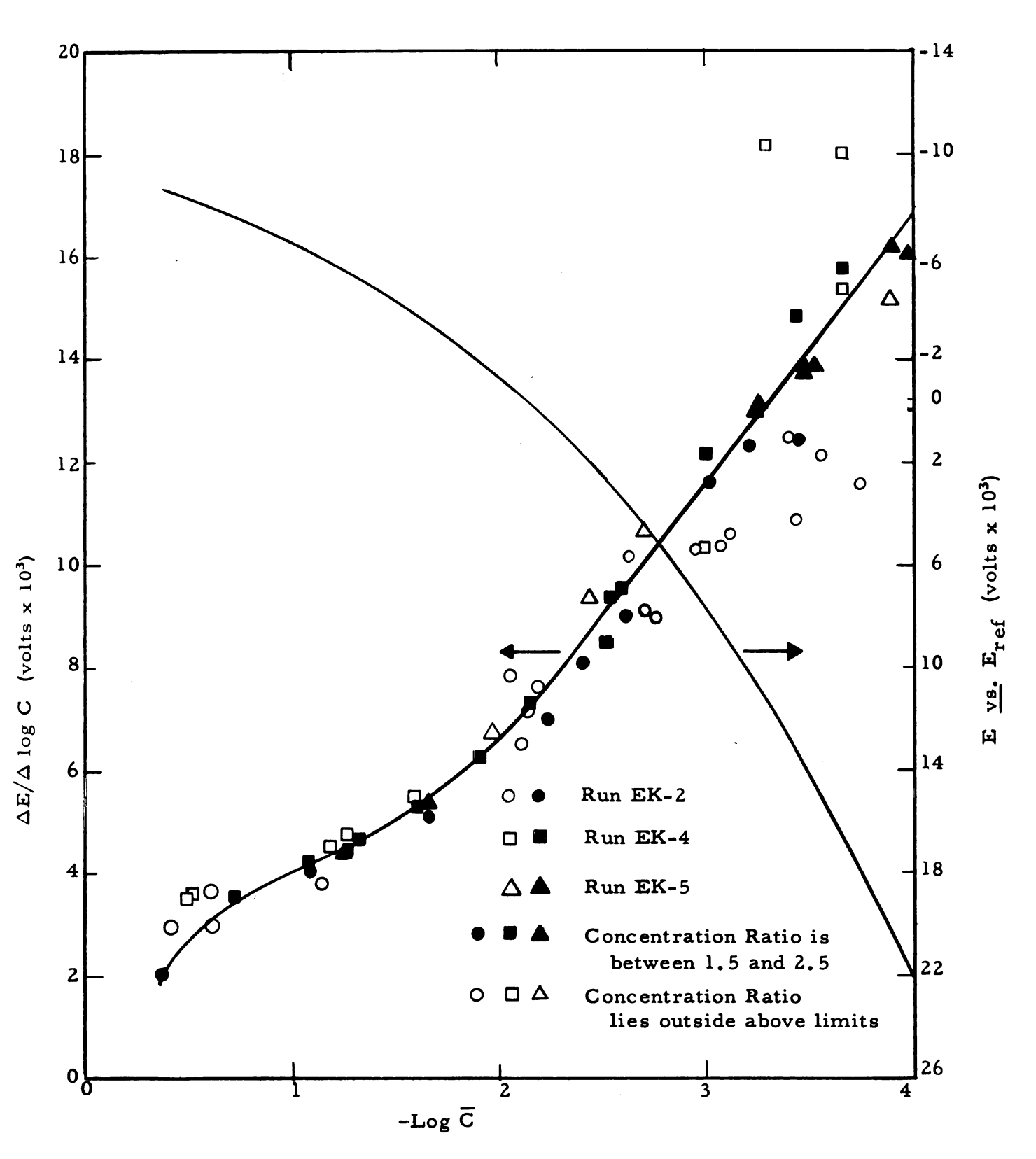


Figure 34. The experimental emf data plotted in differential form and the resulting integral curve. Data are for potassium in ammonia at -37.0°C.

behavior of dilute solutions can be applied to the reference solution. Secondly, it allowed a comparison with the results obtained for the sodium system (9). Utilization of this integral curve will be described in the next chapter.

The solid symbols designate those emf values for which the concentration ratio lies between 1.5 and 2.5. The closer the ratio is to one, the smaller the error because of differences in transference numbers and activity coefficients; however, the reproducibility becomes poor, probably resulting from small concentration gradients which have a relatively large effect when the concentrations are nearly equal. Above 2.5, the error from activity coefficients and transference numbers is probably significant.

The open symbols display the remaining data that lie outside the ratio limits. Generally they agree quite well although the scatter is greater.

Potentials for the various cell combinations were recorded, along with calibrating voltages, on the potentiometric recorder chart from which the interpolated readings are given in Table 16. A tracing from a typical run appears in Figure 35. The + or - designation of the switch position refers to the polarity setting of the switch. Switch positions 5 through 8 are four possible combinations of the potential measuring electrodes across the liquid junction. Positions 3 and 4 correspond to the electrodes serving as conductance electrodes in their respective conductance cells. As may be seen from the tracings, residual emfs were observed for the conductance electrodes, possibly from either thermal effects or concentration gradients in each cell. However, an average of the four potential values for a given polarity setting will give the true average potential existing across the junction.

Continued

Table 16. Potentials from Concentration Cells with Transference for Potassium-Ammonia Solutions at -37.0°C and the Apparent Transference Numbers.

R							
No.	$C_{1} \times 10^{3}$	$C_2 \times 10^3$	$\overline{C} \times 10^3$	-Log C	E x 103	$(\Delta \mathbf{E}/\log \frac{C_1}{C_2}) \times 10^3$	(t-/t+)
*9 - 6	0.144	•	0.104			16.0	4.85
5-7		•	0.104				4,54
5-16b*	•	0.0855	0.127	3.90	4.79	16.2	4.78
5-16a	0,196	•	0,131	3,88		15.1	5, 19
2-21	7.	•		3.73		11.6	7,10
7	7.	0,180		3,66		18.0	4.20
4-18*	0.294	•	0.217	3.66	5.04	15.7	4.96
2-18	.3	•	0.270	3,57		12.2	6.72
5-13*	4.	•	0.307	3,51	4.29	13.8	5.78
5,14*	•	•	0,334	3.48		13.7	5.84
2-20*	0.441	•	0,347	3,46	3.00	12.4	6,55
5-15	905.0	0.199	0,352	3,45		13,8	5.79
4-17*	4	•	0,363	3.44		14.7	5,38
	0.412	•	0.364	•	1.24	•	7.64
ı	0.471	•	0.397	•		12.4	6.52
4-15		•	0.512	3.29		18.2	4.16
5-12*	0,734	•	0.548	3.26		13.0	6.19
5-5*	•	•	0,585	•	5.16	•	6.20
2-11*	84	0.372	609.0	3,22	4.39	12.3	6.64
2-15	•	•	0.766		1.40	•	7.86
2-16	.97	0.702	0.834	3.08	1.47	•	8.05
2-10*	1,32	•	•		4.37	11.6	
4-14*	1,33	9.676	1.00	3.00	3.56	12.1	
4-16	1,10	•	1.01		0.770	10.3	8.25
2-12	1,26	•	1.09	2.96	1.37	10.3	8,12

Table 16 - Continued

2-8*	C ₁ ×10 ²	C ₂ x10°	$C \times 10^3$	-Log C	Ex 103	$(\Delta E/\log \frac{\zeta_1}{C_2}) \times 10^3$	(t/t_+) apparent
Ĭ	2,33	1,78	1.31		1,04	8.87	
ı	1.88	1.60	1.74		9	8.97	9.45
5-11	2.96	0.894	1.93		5.57		•
2-13	2.19	1,68	1.94		1.04	9.10	•
2-14	3.52	1,21	•		2	•	8.22
2-7*	3.02	1.85	2.44	2.61	6	0	9.38
4-25*	3,61	1,61	2.61		3,34	9.53	8.83
5-4	3.99	1.44	•		4.26	.5	8.78
4-13*	3.92	1.96	•		2.82	.3	•
4-26	3.46	2.70	3.08		0.907	8.48	10.0
5-10	6.17	1,29	•		6.37	9.36	•
2-6	5.24	2,65	3.94		2.40	8.09	10.6
2-5*	•	4.69	5.86		.1,22	6.94	· •
2-3	6.78	6.02	6.40		0.399	7.74	11,1
4-24*	9.10	5.28	7.19		1.72	7.29	•
2-4	11,35	3,36	7.36		3.81	7.21	12.0
4-12*	10,10	4.71	7.40	2, 13	2.42	7.30	11.8
2-30	9.03	6.43	7.73		0.954	6.47	13,5
2-2	90.6	8,56	8.81	2.06	0.197	7.87	10.9
5-3	16.5	4.97	10.7	1.97	3,50	6.71	13.0
4-11*	15.7	9.03	12.4	1.91	1,50	6.23	
5-9	14.8	10.4	12.6	1.90	0.972	7.	•
2-29*	28.1	15,5		1.66	1.32	0.	5.09
5-2*	28.3	16.2	22.3	1.65	•	٠,	•
2-26	34.4	12.3	23.2	1.63	2.37	5.29	16.7
4-23*	34.8	16.7	25.7	1.59	1.68	5.27	16.8
4-10	41.4	10.9	26.2		3,15	5.43	
4-22*	9.29	30.7	49.2	1,31	1.59	4.63	•

Table 16 - Continued

dun No.	$C_1 \times 10^3$	$C_2 \times 10^3$	$\overline{C} \times 10^3$	-Log C	E x 103	$(\Delta \mathbf{E}/\log \frac{C_1}{C_2}) \times 10^3$	(t/t_+) apparent
-7	73.7	34.1	53.9	1.27	1.49	4,46	20.0
9-:	90.4	18.4	54.4	1.26	3.27	4.72	18.8
8-	73.3	37.6	55.5	1.26	1.29	4.44	20, 1
5*	78.7	33.5	56.1	1.25	1.68	4.53	19.7
-1	73.9	40.1	57.0	1.24	1.17	4.40	20.3
6	102.6	29.7	66.2	1.18	2.42	4.49	19.9
:-25	84.4	60.7	72.5	1,14	0.546	3.74	24.1
28*	109.6	54.8	82.2	1.08	1.24	4.04	22.2
*81	114.	56.5		1.07	1.29	4.21	21.3
24*	248.	124.	186.	0.731	1.08	3,53	25.6
-21*	266.	119.	192.	0.717	1.27	3,58	25.2
3	202.	187.	194.	0.711	0.115	3,34	27.0
*4-:	260.	133.	197.	902.0	1.03	3.57	25.3
:-23	294.	224.	259.	0.586	0.345	2.92	31,1
-2	464.	144.	304.	0.517	1.81	3.56	25.3
-20	478.	177.	327.	0.485	1.50	3.49	25.9
:-22	438.	352.	395.	0.403	0.274	2.91	31,3
1*	556.	314,	435.	0.362	0.505	2,03	45.1
-1	Concentra	Concentration higher 1	than can be de	be determined with	h present cor	present conductivity data.	

 * Indicates that the ratio C_1/C_2 lies between 1.5 and 2.5. These runs were used in the activity coefficient calculations.

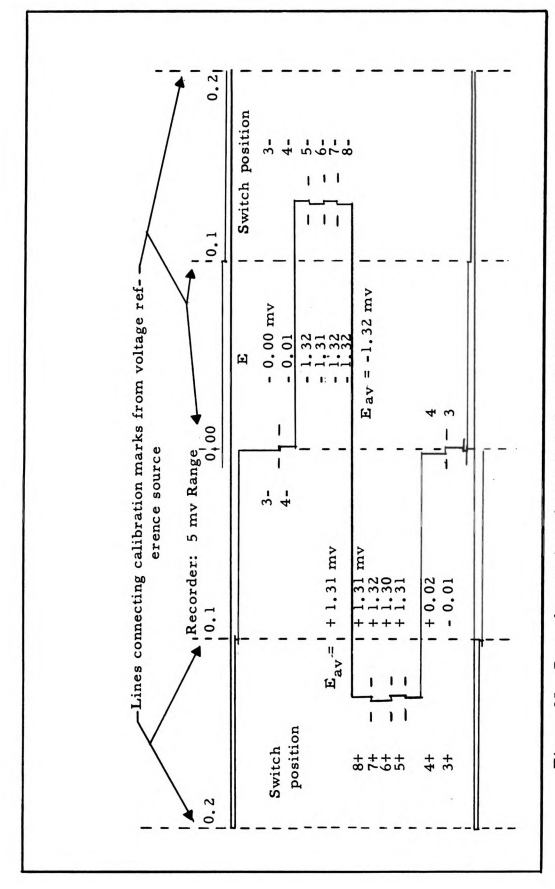


Figure 35. Recorder tracing of potentials for run EK-2: solution 29-a.

CHAPTER VI

DISCUSSION

A. Conductance

1. Results Using Cell A

As previously stated, it was desirable to redetermine the conductivities because of the reasonably large discrepancies between the data of Gibson and Phipps, and of Kraus which were internally more consistent. However, the two sets of data obtained by Kraus began to deviate below 0.004 molar.

The corrected conductivities of potassium-ammonia solutions determined with cell A show a higher degree of precision than those previously determined by other methods. This may be attributed to the ability to apply corrections for decomposition. The maximum percent deviation from the smoothed data at any concentration was 0.8% and the average deviation from the smoothed curve is 0.4%. The smoothed values are given in Table 15 and displayed in Figure 26.

Comparison with the values of Kraus adjusted to -37.0°C show agreement within 2% between the two sets of data for the concentration range 0.004 to 0.36 molar. Below 0.004 molar, Kraus' values show scatter and at infinite dilution differ by 4.5% from the present work. Above 0.40 molar the values from Kraus rise considerably above this work. The precision of our most concentrated solution (0.407 molar) is estimated at better than 1%. The data of Gibson and Phipps have not been adjusted to our working temperature, but a visual comparison (Figure 1) with those of Kraus shows their data to be higher.

2. Amide Ion Conductance

The data from cell A have not been corrected for conductivity of the amide ion formed from the decomposition since the concentration of this ion is suppressed because of the large metal ion concentration. This will be illustrated by an example.

The amide ion would have the greatest relative effect in dilute solution; therefore, let us consider run CK-11, solution 6-D, and the dissociation equilibrium for potassium amide. For

$$KNH_2 \iff K^+ + NH_2^-$$
 [6.1]

the dissociation constant (49) is given by

$$\underline{K} = \frac{[K^{\dagger}][NH_2^{-}]}{[KNH_2]} = 1.20 \times 10^{-4}.$$
 [6.2]

For the solution under consideration [KNH₂] = 2×10^{-5} moles 1^{-1} , [K[†]] = 6.8×10^{-4} moles 1^{-1} and $L_{K} = 0.632 \times 10^{-3}$ mho cm⁻¹, therefore,

$$[NH_2^-] = \frac{(1.2 \times 10^{-4})(2 \times 10^{-5})}{6.8 \times 10^{-4}} = 3.5 \times 10^{-6} \text{ moles } 1^{-1}$$
[6.3]

\$\Lambda_{\text{KNH}_2}\$ for this amide ion concentration, if no other ions were present, would be about 300 cm² mho equiv⁻¹; thus,

$$L_{KNH_2} = \frac{(300)(3.5 \times 10^{-6})}{1000} = 1.05 \times 10^{-6} \text{ mho cm}^{-1}$$
[6.4]

and

$$L_{K}^{\text{corrected}} = (0.632 - 0.0010)10^{-3} = 0.631 \times 10^{-3} \text{ mho cm}^{-1}$$

The resulting error is about 0.16% which is insignificant. The error is probably even smaller than this since $\Lambda_{\rm KNH_2}$ will be less than 300 at this total ionic strength.

3. Results Using Cell B

Conductance cell B was designed for small volumes of solution (~15 ml) since its primary use was for the determination of the conductance of potassium solutions in deutero-ammonia. To check its performance, regular potassium-ammonia solutions were used. The internal precision of the data is noticeably below that obtained for cell A. The maximum deviation from the smoothed data at any value observed below 0.55 molar was 3.0%. The average deviation was about 0.9%. Agreement between the cells for ammonia solutions was good up to 0.30 molar except for run CK-12 near 0.003 molar. At 0.42 molar the deviation between cells rose to 1.5%. Using cell B, run CK-16 agreed very well with the results from cell A from the lowest concentration up to 0.30 molar. These comparisons were made by superimposing the large plots (1 meter square) on an illuminated table.

For a few of the concentrated solutions, resistance readings were made with a d-c Wheatstone Bridge and galvanometer as well as the conventional a-c conductance bridge techniques. The resistance values were comparable if the d-c measuring circuit was closed only briefly and the direction of deflection was noted. If the circuit was energized for several seconds then electrolysis occurred and the readings were erratic.

There are apparently two major difficulties with this cell. The first can be attributed to poor electrode design. An attempt was made to keep the three electrode arms symmetrically located and as reasonably well separated as permitted by the physical size of the cell. The area of the electrode surface was smaller than that used for any of the other cells and is now thought to be too small to assure reproducible results.

The other contribution to the error is inherent in the dilution and withdrawal procedure used. A small error in computing the correct amount of ammonia in the vapor phase can become very sizeable after

tion remained in the small withdrawal capillary, it should have affected only the concentration previous to the first withdrawal and not succeeding dilutions provided the amount remained constant. This is true because the solution which remained in the capillary during a withdrawal was then transferred into the heavy-wall glass ampoule on the next withdrawal. It is, however, doubtful that unmixed solution remained in the capillary at all. Because of the reduced pressure in the cell during the beginning of the stirring process, the withdrawal capillary was probably emptied so that the entire solution reached a uniform composition.

When the cell constants for cell B were calculated using solutions of potassium in ammonia, then the extrapolated value of Λ° for potassium in <u>deutero</u>-ammonia solutions agreed with the predictions of Walden's rule using viscosity data. The extrapolated value is 856 at -37.0°C which gives 900 at -33.5°C from the Walden product.

The ratios of the experimental conductivities in the two solvents, and also the viscosity ratio of these solutions are given in Table 17. Run CK-16 was selected as representative of ammonia solutions since it agrees very well with the results from cell A. The ratios, $\Lambda_{\rm NH_3}^{16}/\Lambda_{\rm ND_3}^{14}$ and $\Lambda_{\rm NH_3}^{16}/\Lambda_{\rm ND_3}^{15}$, were then calculated from the deutero-ammonia solutions using runs CK-14 and CK-15. In the last two columns are the viscosities of potassium-ammonia solutions and the ratio of the viscosities of potassium solutions of deutero-ammonia to ammonia, respectively. These data are from O'Reilly (89) and have been corrected to -37.0°C from plots of log η versus 1/T. From the table, one observes that the conductivities of these solutions differ by about 28 to 30%. O'Reilly (74) had predicted a difference of 20% from observations on the Q values of his rf coil, coaxial line, and sample during paramagnetic resonance absorption studies at 25°C.

The results are plotted in Figure 36. A minimum is observed near the concentration of 0.04 molar where a minimum is also observed in the total conductance. Upon inspection, the "hump" appearing at $\sqrt{C} = 0.32$ for the ratio of run CK-16 to run CK-15 can be assigned to experimental error. A slight drop in the conductivity data for run CK-15 exists compared to the data from CK-14; this drop may be a result of an experimental error made at just one dilution.

Above 0.04 molar, one sees that as the concentration increases, the ratio $\Lambda_{\rm NH_3}/\Lambda_{\rm ND_3}$ increases, but the $\eta_{\rm ND_3}/\eta_{\rm NH_3}$ ratio at first decreases and then rises slightly. The difference in the conductivities between the two solvents can not be attributed to viscosity effects alone, or at least, not by the same relationship as expressed by Walden's rule (conductance-viscosity product). In this region it appears that the potential well for the electron is shallower in ammonia solutions than in deutero-ammonia solutions. By some unknown process the deuterium nucleus is presenting a slight hindrance to electronic conductance as the concentration increases.

At present, there is no logical explanation for the increase in the conductance ratio at concentrations below 0.04 molar. This may be an attribute of cell B, although the author feels that the indicated trend is experimentally correct and significant. The broken line indicates that the extrapolation to infinite dilution of the conductance ratios above 0.04 molar gives the viscosity ratio of the pure solvent.

The dielectric constant does not appear to be a contributing factor. Although the dielectric constant for <u>deutero</u>-ammonia is not known it is reasonable to assume the same value as for ammonia since the dielectric constants for water and heavy water are essentially the same, 78.54 and 78.25, respectively, at 25°C (90).

The data lacked the precision necessary to detect a possible shift in the conductance minimum between the ammonia and <u>deutero</u>-ammonia solutions. A shift in the conductance minimum to higher concentrations

Table 17. Conductance Ratio of K-NH₃ to K-ND₃ Solutions and Viscosity Ratio of these Solutions. Data are at -37.0°C.

$\sqrt{\frac{C}{C}}$ (molarity) ²	$\Lambda_{\mathrm{NH_3}}^{\mathrm{16}}/\Lambda_{\mathrm{ND_3}}^{\mathrm{14}}$	$\Lambda_{\mathrm{NH_3}}^{\mathrm{16}}/\Lambda_{\mathrm{ND_3}}^{\mathrm{15}}$	η _{NH} (centipdise)	$\eta_{\mathrm{ND_3}}/\eta_{\mathrm{NH_3}}$
0.00		.p. r	0.2657	1.218
0.02	••	1.228	0.2657	1.218
0.04	1,303	1.291	0.2657	1.218
0.06	1.296	1.296	0.2657	1.217
0.08	1.287	1.308	0.2656	1.217
0.10	1.282	1.297	0.2656	1.217
0.12	1.285	1.296	0.2655	1.216
0.14	1.282	1.296	0.2654	1.216
0.16	1.273	1.289	0.2653	1.216
0.18	1.267	1,283	0.2652	1.215
0.20	1.261	1,280	0.2650	1.215
0.22	1.258	1.284	0.2648	1.215
0.24	1,262	1,288	0.2646	1.214
0.26	1.264	1,293	0.2644	1.214
0.28	1,268	1,299	0,2641	1.214
0.30	1,272	1,308	0.2639	1.213
0.34	1.281	1,317	0,2632	1.212
0.38	1.287	1,322	0.2624	1.212
0.42	1,295	1.323	0.2617	1.209
0.46	1,307	1.329	0,2608	1.208
0.50	1.320	1.338	0.2598	1.207
0.55	1.334	1,349	0,2582	1.206
0.60	1.348		0.2562	1.206
0.65	1.354		0.2540	1.206
0.70	1.361		0.2514	1.207
0.75	1.379		0.2484	1.209
0.80	1.395		0.2450	1.211

has been found in methylamine solutions compared to ammonia solutions (11, 38).

4. Calculation of Λ°

There are several ways that Λ^{0} can be calculated for potassiumammonia solutions. These methods and the selected value will be discussed here.

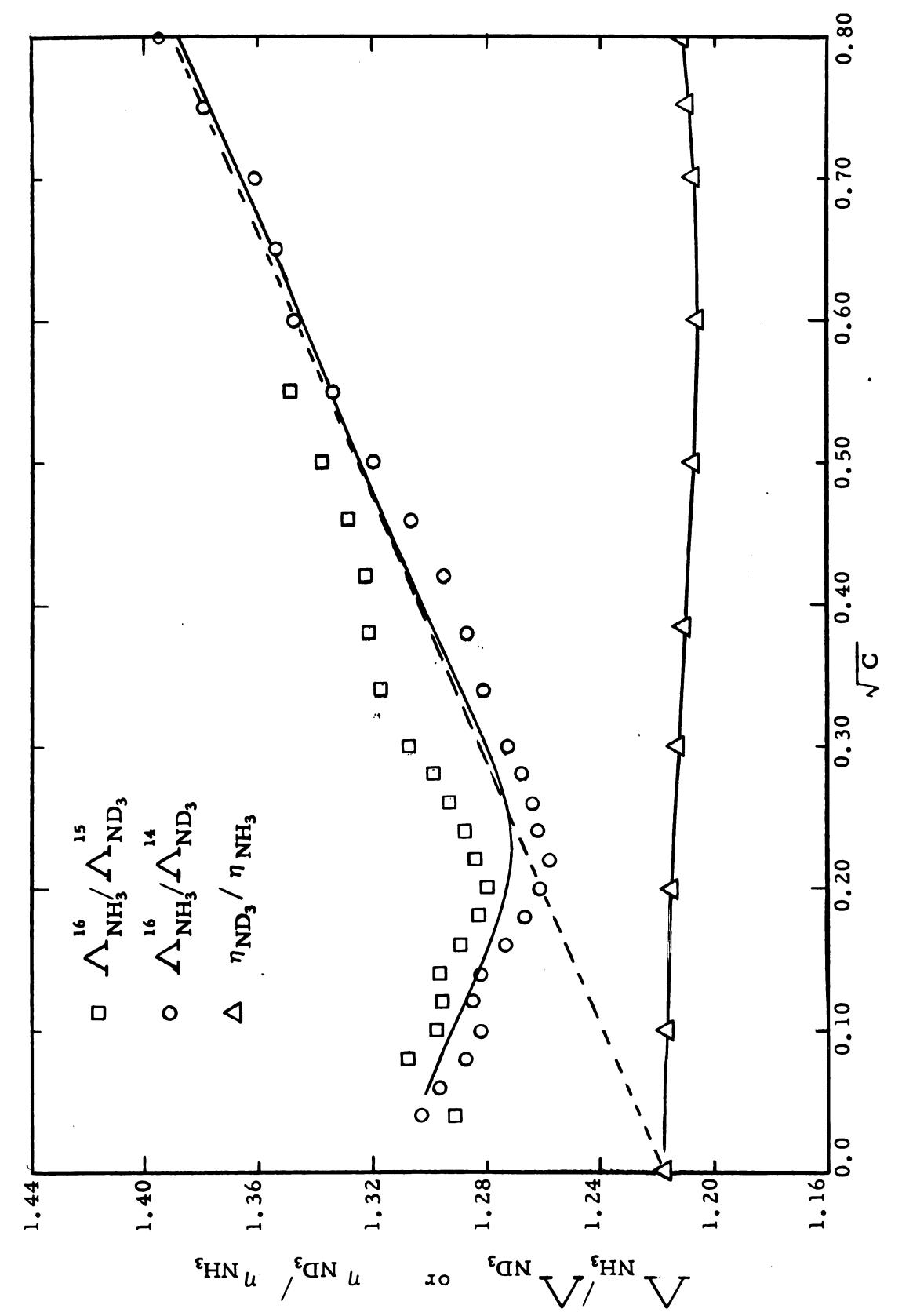


Figure 36. Conductance and viscosity ratios between ammonia and deutero-ammonia solutions versus (molarity) 7.

One way to arrive at Λ^0 is through some type of conductance function. The semi-empirical Shedlovsky function (91) represents the conductance for a hypothetical completely dissociated electrolyte over a wider range of concentrations than that covered by the limiting law (92). This function has been used successfully in the treatments of sodium-ammonia (3) and lithium-methylamine(11, 35) systems. As a first approximation it will also give a value for K_1 for the dissociation

$$K^{\dagger} \cdot e^{-} \rightleftharpoons K^{\dagger} + e^{-}; \quad K_{1} = \frac{a_{K} + a_{e}}{a_{K} + a_{e}} = \frac{C \alpha^{2} f^{2}}{(1 - \alpha)}$$
 [6.6]

where C is the concentration, a is the degree of dissociation defined below, and f is the activity coefficient calculated from the Debye-Hückel equation. Let

$$\alpha = \frac{\Lambda}{\Lambda^0} \quad S \quad (Z)$$
 [6.7]

where

S (Z) = 1 + Z +
$$\frac{Z^2}{2}$$
 + $\frac{Z^3}{8}$ + ... [6.8]
= $\left[\frac{Z}{2} + \sqrt{1 + (\frac{Z}{2})^2}\right]^2$

$$z = \sqrt[3]{(\Lambda^\circ)^{-\frac{3}{2}}} \sqrt{\Lambda^c}$$
 [6.9]

for D = 22.3, T = 236.11, and η = 0.264 centipoise. The Debye-Hückel equation gives f^2 :

$$\log f^{2} = \frac{-2 |z_{+}| z_{-} | A \sqrt{\alpha C}}{1 + Ba^{2} \sqrt{\alpha C}}$$
 [6.11]

where

$$z_{+} = z_{-} = 1$$

$$A = \frac{1.824 \times 10^{6}}{(DT)^{\frac{3}{2}}} = 4.776$$

$$B = \frac{50.29 \times 10^{8}}{(DT)^{\frac{1}{2}}} = 0.6931$$

$$a^{\circ} = 5.5 \times 10^{-8} \text{ cm (estimated)}.$$

The substitution of equation [6.7] into equation [6.6] yields the extrapolation function

$$\frac{1}{\Lambda S(Z)} = \frac{1}{\Lambda^{\circ}} + \frac{1}{K_1(\Lambda^{\circ})^2} C \Lambda f^2 S(Z) \qquad [6.12]$$

for the general Shedlovsky equation

Thus the intercept of a plot of $1/\Lambda S(Z)$ <u>versus</u> $C\Lambda f^2S(Z)$ gives $(1/\Lambda^0)^1$. An estimate of Λ^0 is obtained as the intercept from a plot of Λ^0 <u>versus</u> \sqrt{C} . This value of Λ^0 is used in the above equations to calculate $(1/\Lambda^0)^1$ which then serves as a new Λ^0 for the next iteration. The calculation is continued until a consistent value is obtained. The value of Λ^0 obtained in this way was 1042 cm^2 mho equiv⁻¹ and that of K_1 is 6.82×10^{-3} .

Figure 37 shows the extrapolation function. A smooth curve can be easily drawn through the points; it should be mentioned that the last five points are those of run CK-11. Although based upon one run, it is felt that these are fairly reliable because decomposition corrections were made as illustrated in Figure 25. It is unfortunate, however, that the dilution range was not extended.

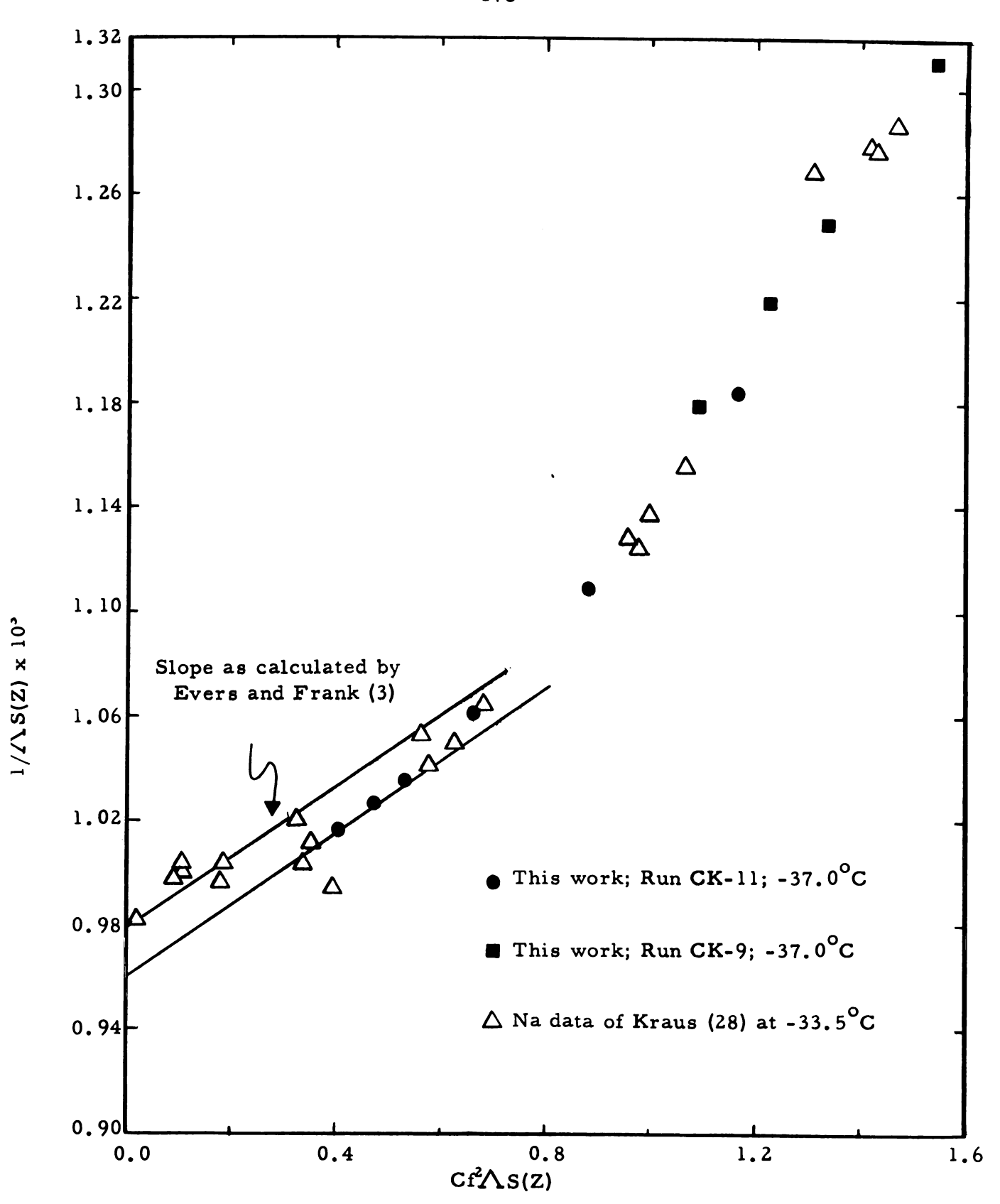


Figure 37. Shedlovsky analysis of conductance data for potassium-ammonia solutions at -37.0°C and sodium-ammonia solutions at -33.5°C.

Also illustrated in Figure 37, for purposes of comparison, is the Shedlovsky treatment of Kraus' sodium data (28) and the corresponding slope as determined by Evers and Frank (3). It is interesting to note that above $Cf^2 \Lambda S(Z) = 0.4$, the sodium data essentially coincide with those of potassium. Below this value, the curvature is appreciable and the scatter is greater, probably because of decomposition. Hence it is likely that the true value of Λ^0 for sodium-ammonia solutions lies closer to 1040 than 1022 cm² mho equiv⁻¹. Kraus calculated a value of 1040 from his emf data and λ^0_+ from salts. Recently, Paoloni (93) has made an estimate of the decomposition and also arrived at a value of 1040.

The potassium data of Kraus are too widely scattered in the dilute region to use the Shedlovsky treatment effectively, although a value of 1014 cm^2 mho equiv⁻¹ was calculated for \triangle° at -33.5°C.

From data on conductivities of salts, λ_{+}^{0} can be estimated. The most appropriate salt would be KNO3 since several investigators have published conductance data. Kraus and Bray (49), in re-evaluation of the conductance studies of Franklin and Kraus (51, 52) on salts, determined $\Lambda_{\text{KNO}_3}^{\text{o}}$ = 339 cm² mho equiv⁻¹ at -33.5°C. From their investigations of conductivities of alkali nitrates in liquid ammonia Monosson and Pleskov (94) reported $\Lambda_{\text{KNO}_3}^{\text{O}} = 338 \text{ cm}^2 \text{ mho equiv}^{-1} \text{ at } -40^{\circ}\text{C}$. This value has been adjusted to 331.1 at -40° or 351.0 at -34°C by Hnizda and Kraus (53) through the use of the Fuoss equation. Using the latter adjusted values and assuming a 1 % temperature coefficient for salts (53) one calculates for further calculations. Franklin and Cady (27) reported transference number data on several salts obtained by the moving boundary method using an autogenic boundary. Kraus and Bray (49) have treated these data, and consequently, published what they believed to be the best selected values. The theory of that day predicted constant mobilities for

ions as a function of concentration. A plot of T_+ versus \sqrt{C} for KNO₃ data at -33°C shows concentration dependence and gives $T_+^0 = 0.493$ by a least squares treatment discarding the highest concentration point which fell considerably below the others. From $T_+^0 = 0.493$ and $\Lambda_{KNO_3}^0 = 341$, one gets $\lambda_{K}^0 = 168$ at -37°C.

There are two values of \bigwedge° for sodium available for the computation of \bigwedge°_{K} . Let us first consider the currently accepted value of 1022 at -33.5°. Dye, et al. (8) have used the temperature coefficient data of Fristrom (30) to compute the values $\bigwedge^{\circ}_{Na} = 936$ and $\lambda^{\circ}_{e^{-}} = 811$ at -37.0°. This will give $\bigwedge^{\circ}_{K} = \lambda^{\circ}_{K^{+}} + \lambda^{\circ}_{e^{-}} = 168 + 811 = 979$ at -37.0°C. At -33.5°, one obtains by analogy these values: $\bigwedge^{\circ}_{Na} = 1022$; $\lambda^{\circ}_{Na^{+}} = 137$; $\lambda^{\circ}_{e^{-}} = 885$; $\lambda^{\circ}_{K^{+}} = 174$; and $\bigwedge^{\circ}_{K} = 1059$. The use of the temperature coefficient of Kraus and Lucasse yields $\bigwedge^{\circ}_{K} = 1001$ at -37.0°C. In aqueous solutions, the conductance-viscosity product for some large ions has been found to be independent of temperature over a large range (95). The use of this product on potassium solutions gives $\bigwedge^{\circ}_{K} = 1009$ at -37.0° computed from the temperature data of Kraus and Lucasse. The viscosity values used were: 0.253_2 at -33.5° and 0.265_7 at -37.0°C (89).

The newly suggested value of Λ_{Na}^{o} = 1040 at -33.5° gives these computed data at -33.5°C: λ_{e}^{o} = 903 from λ_{Na}^{o} = 137; and from λ_{K}^{o} = 174, Λ_{K}^{o} = 1077 which agrees with the value of 1078 recently suggested by Paoloni (93). Temperature adjustment to -37.0°C gives: by conductivity-viscosity product, 1026; by Kraus and Lucasse's data, 1018; and by Fristrom's data on sodium, 993.

All of the above values at -37.0°, which were from data at -33.5°, give low results compared to the experimentally determined $\Lambda_{\rm K}^{\rm o}$ (1042) from the Shedlovsky analysis. The same procedure for temperature adjustment as used above gives for $\Lambda_{\rm K}^{\rm o}$ at -33.5°C the following: by $\Lambda_{\rm H}$, 1093; by Kraus and Lucasse's data, 1103; and by Fristrom's data on sodium, 1123. For this work, the accepted value for $\Lambda_{\rm K}^{\rm o}$ is 1042 at -37.0°, and 1103 at -33.5°C. The latter value, computed from the temperature coefficient data of Kraus and Lucasse, was selected on the

basis that this temperature coefficient satisfactorily transformed Kraus¹ data (28) from -33.5 to -37.0 ^oC which, at the latter temperature, agrees very well with the experimental quantities found in this investigation.

5. Calculation of T.

From the Shedlovsky analysis of the experimental conductance data, $\Lambda_{\rm K}^{\rm o} = 1042$ at -37.0°C. As described above, $\lambda_{\rm K}^{\rm o} = 168$ which was obtained from KNO₃ data assuming no temperature dependence on the transference number. This gives $\lambda_{\rm e}^{\rm o} = 874$ and $T_{\rm o}^{\rm o} = 874/1042 = 0.839$.

6. Temperature Coefficient

The thermostat used in this work was designed for a specific temperature, hence, it is inadequate for studies involving a large range of temperatures such as the determination of the logarithmic temperature coefficient of resistance. However, one run, CK-10, was made at a concentration of 0.07277 molar (-37.05°C) over a ten degree range to provide a value to compare with the available data. The value of d log R/dT thus obtained was -0.0071. Fristrom (30) has shown that lithium and sodium solutions have nearly the same logarithmic temperature coefficient of resistance, and at this concentration his value is -0.0062. This is almost at the minimum in the plot of temperature coefficient versus concentration according to his measurements. The coefficient rises about 3×10^{-3} units upon dilution and remains nearly constant at concentrations lower than 0.03 molar. The value, which is -0.0062^{*} , at the lowest concentration (0.162 molar) investigated by Kraus and Lucasse (33) should lie near this minimum if Fristrom's data are correct;

^{*}The value at the lowest concentration reported by Kraus and Lucasse (33) is $\gamma = 1.42$, where $\gamma = (1/R_{-33.5})(\Delta R/\Delta t)$. If $\Delta R/\Delta t$ is assumed to be constant over the small range (12 degrees) investigated, then d log R/dT = (1/2.303 R) (dR/dT) \approx (1/2.303 R_{-33.5})($\Delta R/\Delta t$) = -0.0062.

the latter data gives -0.0056 at 0.162 molar. However, the adjusted data of Kraus using a constant temperature coefficient of -0.0062 agree very well with the data obtained in the present investigation. Except for this observation, there appears to be no reason why the coefficient for potassium should be different from sodium since those of lithium and sodium are essentially the same. The temperature coefficient for calcium (30), however, differs very markedly from the alkali metals, rising with a very steep slope from infinite dilution.

7. Ionic Conductances

The transference number measurements allowed calculation of ionic conductances. As shown in Figure 33, λ_{\bullet} goes through a minimum at 0.04 molar and increases at a rapid rate as the concentration increases. The onset of metallic-type conduction probably occurs below 0.04 molar. The cation conductance decreases monotonically with increasing concentration as would be expected from the increased percentage of potassium ions tied up in ion pairs and dimers. The transference data are not reliable above 0.12 molar; hence, the true cation conductance probably does not decrease as rapidly as shown above 0.12 molar.

B. Transference Numbers

The independent method of determining T_-^0 described above yielded a value of 0.839. A plot of T_- versus \sqrt{C} showed a small but definite downward curvature. However, because of the uncertainities in the experimental data this plot was assumed to be linear and was treated by the method of least squares to remove personal bias. With T_-^0 considered as an invariant point, the equation obtained is $T_- = 0.839 + 0.258$ \sqrt{C} . Only the data obtained from runs "a" where the concentrations were determined analytically are considered as valid representations of

the transference numbers. Most of the data obtained from conductance measurements were too widely scattered to even determine trends.

Only in later runs when the third electrode was installed did the concentration values from conductance agree favorably with those from analytical procedures.

The reliability of decomposition determinations is questionable since the plots of resistance versus time used to calculate the rates gave both positive and negative slopes for various runs. However, the resistances were used as recorded since the abnormal observations may be due to changing concentration gradients. As a check on uniform decomposition, the solution was dropped after each run, and in each case the resistance decreased only slightly indicating that the bulk of the solution above the conductance electrodes, and hence, at the boundary was reasonably stable.

For runs prior to 46-K-12, warm sulfuric acid-dichromate cleaner was used. Dye (96) showed that this cleaner leaves a residue which catalyzed the decomposition of his ethylenediamine solutions. He substituted a cleaner consisting of 2% acid soluble detergent, 5% HF, 33% reagent grade nitric acid, and the rest distilled water. This cleaner was used on all transference runs after 45-K-11 and on the conductance runs using cell B (CK-12 through CK-16).

The averaged values for all the transference number runs which yielded data are given in Table 14. When analytical results were used for concentration measurements, the averaged transference number was corrected for decomposition, Hittorf migration of metal from the anode compartment, and a volume change for the closed side of the cell using the molar volumes for Ag, AgI, KI, and K.

The last two runs, 48-K-14 and 49-K-15, gave low but very reproducible results. There are two possible explanations. The first explanation is that the cleaning procedure was changed. The apparatus

for potassium runs 46-K-12, 47-K-13, 48-K-14, and 49-K-15 was cleaned with the HF-HNO₃ cleaner, and the decomposition may have been less giving the low results for runs 46-K-12, 48-K-14 and 49-K-15. Decomposition at the boundary would give high results.

The second explanation is that the formation of hydrogen gas in the small enclosed space above the metal solution could have a tendency to force the solution downward, to fill minute spaces, particularly around the stopcocks. This would retard the boundary. This could have been avoided by keeping the cell connected to the gas ballast formed by the make-up vessel. For runs 47-K-13, 48-K-14 and 49-K-15 the stopcock connecting the cell to the make-up vessel was closed after equalizing the pressures in both halves of the cell. At the time, the investigator felt that with the make-up vessel connected, the motion of the boundary would be influenced by the expansion of the helium covering gas as the make-up vessel warmed. Thus disconnecting the make-up vessel from the cell would eliminate transferring to the boundary any fluctuations in gas pressure caused by temperature variations. However, the effect of hydrogen gas formed from the decomposition process was not realized at the time. It is now thought, even with temperature fluctuations, that the larger the volume of covering gas above the solution the smaller the effect on the boundary, particularly if this gas ballast could be maintained at a fairly constant temperature.

An approximate calculation can be made to show the effects of the formation of hydrogen gas in the closed side of the cell containing metal solution. From resistance readings on run 49-K-15, the decomposition rate is estimated at 9 x 10⁻⁴ moles 1⁻¹ hr⁻¹. The vapor space above the metal solution is approximated at 0.5 ml. To equalize the pressures in the two halves of the cell, helium gas was admitted until the pressure was about 95% of atmospheric pressure. Thus the gas volume of 0.5 ml contains helium gas at this pressure. The current was on for about

1-3/4 hours, and the volume occupied by the metal solution is estimated at 18.8 ml. From these quantities, one computes 29.6 x 10-6 moles of metal has decomposed which gives 14.8 x 10-6 moles of hydrogen gas. There are 24.5 x 10-6 moles of helium gas already present which gives 39.3 x 10-6 moles of non-condensible gases. If the pressure is to remain at one atmosphere then the occupied volume is 0.76 ml or an increase of 0.26 ml over the original available space. This volume increase must be taken up someplace or else the pressure would rise and since the solution is non-compressible, the most likely place is around the boundary stop-cock. This stopcock, because of its relatively large internal capacity, need not move much to provide the required space. This increase in the volume near the stopcock will be reflected to the boundary as a movement in the opposite direction to the ascending boundary, thus decreasing its speed.

Another way of viewing the situation is to calculate the pressure increase for the 39.3×10^{-6} moles of non-condensible gases confined to a volume of 0.50 ml. This pressure is 1.5 atmospheres, more than enough to move the boundary stopcock. Although there is a hydrostatic pressure outside from the bath fluid, there also exists a similar pressure inside the cell resulting from the solution. The conclusion is that the use of a closed stopcock in these latter runs was unfortunate and probably caused the low results observed.

Inspection of the T_ values in Table 14 calculated from conductance measurements shows the erratic behavior obtained. Leakage resistances between the cell and ground were always in excess of one megohm before and after a run except in those cases where the boundary-forming stop-cock was loosened. The possibility of foreign matter on the electrode surface was considered. However, a check of the cell constant at the completion of a run in which the cell was only rinsed with water would reproduce the cell constant to within about 2%. For the last three runs,

a newly installed third electrode served as a check. In two cases the reproducibility of the resulting three cells was good and agreed within 4% with the concentration determined analytically. The third case (47-K-13) displayed a marked difference and agreement with the analytical determinations is also poor. The enlargement of the electrode surface might help to reduce these discrepancies. The formation of the electrode surface by fusing platinum wire is now questionable since microscopic inspection on representative samples show minute surface imperfections.

For these reasons, the conductance data for determining concentrations were discarded in favor of the analytical results originally procured as a check on the concentration. It is unfortunate that analytical results were not obtained for several of the intermediate runs.

C. Electromotive Force

The data computed from the emf measurements are given in the discussion on activity coefficients which appears later in this chapter. The scatter present, particularly in dilute solutions, may result from concentration gradients or decomposition at the electrodes. As was mentioned previously, each electrode pair would usually give a different potential as well as a potential existing across the conductance electrodes. The average of the four readings gave a value free of these influences. It is now apparent that these fluctuations could have been reduced if each pair of conductance electrodes were made to serve as a potential electrode resulting in two, rather than four, potential measuring electrodes. This would present a larger effective electrode surface to the solution.

An interesting comparison can be made between the present emf investigation and that of Klein (58). In the present work, a small but noticeable decrease in potential was observed with time, but monitoring the conductance of each cell solution showed that the concentrations were approaching each other, and hence, the potential should decrease. Except for this observation, rapid equilibrium seemed apparent possibly limited only by thermal equilibrium.

On the other hand, Klein noted that the time required for the potentials to reach a constant value in lithium-methylamine solutions was usually about an hour. From the recent work of Dewald (46) there appears to be a slow dissociation step in the amine solutions that is not present, to any great extent at least, in ammonia solutions. The behavior noted during these emf measurements lend support to this dissociation hypothesis.

D. Calculation of K1 and K2 from Cationic Conductance

Equations [6.14] and [6.15] as originally formulated by Becker, Lindquist and Alder (7) were to describe their theory involving

$$M \rightleftharpoons M^+ + e^- {}_{1}\underbrace{K_{1}} = \frac{(M^+)(e^-)}{(M)}$$
 [6.14]

$$M \longrightarrow \frac{1}{2} M_2 \qquad K_2 = \frac{(M_2)^{\frac{1}{2}}}{(M)}$$
 [6.15]

solvated cations, solvated electrons, monomers and dimers. In the latter two species the valence electrons are suggested to exist in expanded orbitals outside the solvation sphere of the cation. The dimer unit is held together by exchange forces. However, these same equations could equally well describe a system where the monomer unit is actually an ion-pair and the dimer is a quadrupole formed from two ion-pairs. If this is the case, then it would be logical to include equilibria involving triple ions such as M⁺, e⁻. M⁺ and e⁻. M⁺.e⁻. These last two equilibria

as well as the two mentioned above are currently being investigated using a digital computer (97). The present work is limited to consideration of the equilibria expressed by equations [6.14] and [6.15]. The formation of ionic species suggests the feasibility of determining K_1 and K_2 from analysis of conductance data.

The mobility of the negative species is too high to involve solvent migration. Since a tunneling mechanism is suggested even in dilute solutions, the Fuoss-Onsager equation is not applicable for it requires the ionic species to move as a unit with a definite radius and a characteristic mobility correlated with λ_-^0 . The desired conductance function should describe the conductance of the free ions to permit calculation of the degree of dissociation of ion-pairs or monomers.

Such a theoretical function is not available for this system, but a suitable empirical one is that of Shedlovsky (91) which has also been used by Evers and Frank (3). Their derived function fitted the experimental data of Kraus (28) up to 0.04 molar (the minimum in the conductance curve). They were also able to calculate K_1 and K_2 for the dissociation and dimerization processes. A similar analysis has been useful in lithium-methylamine solutions (11).

In contrast to the sodium-ammonia system previously treated (8), this investigator has been unsuccessful in obtaining a reliable dissociation constant, K_1 , for dilute potassium-ammonia solutions through conductance studies alone. The determination of the dimerization constant, K_2 , was also unsuccessful. However, in combining the transference data with the emf data, both K_1 and K_2 were calculated without difficulty and the constants thus obtained fitted the experimental data very well up to a concentration of 0.1 molar above which reliable values of T_2 are not known.

In calculating Λ^0 by the Shedlovsky method, a "rough" estimate of K_1 can be obtained from conductance data only. This value was

6.82 x 10^{-3} . However, a complete Shedlovsky analysis, like that done by Evers and Frank, was not made. Such an analysis would correct this K_1 since the formation of dimers was not considered in determining Λ^0 .

Certainly a better way to obtain K_2 would be through magnetic evidence. Such an investigation was attempted in this laboratory (98), but available instruments were not adequate for the necessary quantitative measurements. Fortunately, several investigators have selected potassium-ammonia systems for magnetic studies. Freed and Sugarman (5) have used static methods to obtain the magnetic suspectibility. Becker, et al. (7) using data from Hutchison and Pastor (99) calculated the dimerization constant, K_2 , to be 99 at -33°C. From a plot of their values for -33°, 0° and 25° on semi-log paper, a value of 111 was obtained at -37°C.

The Shedlovsky function used is given in equation [6.13]. This equation

$$\Lambda = \Lambda^{\circ} - \frac{\Lambda}{\Lambda^{\circ}} (\alpha^* \Lambda^{\circ} + \beta^*) \sqrt{C_i}$$
 [6.13]

is applied to the individual ions and rearranged to give the conductance of the free sodium ion.

$$\lambda_{i} = \lambda_{i}^{\circ} - \frac{\lambda_{i}}{\lambda_{i}^{\circ} (a^{*} \lambda_{i}^{\circ} + \frac{\beta^{*}}{2}) \sqrt{C_{i}}}$$
 [6.16]

where

$$\alpha^* = 2.136$$
 at -37.0 °C with D = 22.3
 $\beta^* = 427.9$ with $\eta^\circ = 2.64 \times 10^{-3}$ poise
 $\lambda^\circ_{;} = 168$.

The degree of dissociation a is given by

$$\alpha = \frac{C_i}{C} = \frac{\lambda}{\lambda_i}$$
 [6.17]

where C_i is the concentration of the free ion, C is the total or stoichiometric concentration of the metal, λ_i is the free ion conductance, and λ is the measured conductance. From this equation one gets $C_i\lambda_i = C\lambda$. Values of $C_i\lambda_i$ were computed from equation [6.16] for chosen values of C_i , and a large graph of $\sqrt{C_i\lambda_i}$ versus $\sqrt{C_i}$ was made for convenience in determining C_i from the measured $C\lambda$. Experimental conductance and transference data gave λ for the corresponding C_i , and hence from the plot, the concentration of the free sodium ion C_i was determined.

Specifically the equilibria under consideration are

$$K^{+} \cdot e^{-} \rightleftharpoons K^{+} + e^{-}; \underset{(K^{+} \cdot e^{-})}{\underbrace{K_{1}}} = \frac{(K^{+})(e^{-}) f_{\pm}^{2}}{(K^{+} \cdot e^{-})}$$
 [6.18]

$$K^+ \cdot e^- \rightleftharpoons \frac{1}{2} K_2 \qquad K_2 = \frac{(K_2)^{\frac{1}{2}}}{(K^+ \cdot e^-)}$$
 [6.19]

where f_{\pm} is the mean molar ionic activity coefficient calculated from the Debye-Hückel equation

$$\log f_{\pm} = \frac{-A\sqrt{C_i}}{1 + Ba^0\sqrt{C_i}}$$
 [6.20]

where

$$A = 4.776$$

 $B = 3.812$
 $a^{0} = 5.5$

As was done for the sodium solutions (8), the second equilibrium is first neglected and an approximate or apparent equilibrium constant, $K_1^{(a)}$ is calculated. This is given by

$$K_1^{(a)} = \frac{C \alpha^2 f \pm^2}{(1 - \alpha)}$$
 [6.21]

Selected values of $K_1^{(a)}$ calculated by equation [6.21] are given in Table 18. The extrapolation of $K_1^{(a)}$ against molarity in dilute solutions should give an estimate of the "true" equilibrium constant, $K_1^{(t)}$.

Table 18. Selected Values of $K_1^{(a)}$, $K_1^{(t)}$ and K_2 Calculated from Cationic Conductance

С	Λ	T ₊	K ₁ (a)	K, for	K ₁ ^(t) x 10 ⁴	=
(molarity x 10 ²)		T	x 104	38	45	100
0.16	850	0.151	42.3		12.4	85.6
0.64	656	0.141	28.5	10.4	14.9	46.1
1.44	554	0.130	23.6	8.79	11.6	32.8
3.24	502	0.115	23.4	5.54	7.34	20.6
5.76	503	0.0990	25.1	3.54	4.78	13.8
9.00	530	0.0838	26.4	2.52	3.47	10.3

From $K_1^{(a)}$ and $K_1^{(t)}$, K_2 may be determined by the relationship

$$K_{2} = \begin{bmatrix} \underline{K_{1}}^{(t)} - \underline{K_{1}}^{(a)} \\ 2 (Ca \underline{f_{\pm}})^{2} \end{bmatrix} \qquad \underline{K_{1}}^{(t)}$$
 [6.22]

(The derivation is given in Appendix C). A series of $K_1^{(t)}$ values were used to calculate K_2 as a function of concentration. Ideally, a plot of the deviations for the various averaged K_2 for each $K_1^{(t)}$ would go through a minimum at the correct K_2 . However, such a minimum was not detected over the range of $K_1^{(t)} = 3.8 \times 10^{-5}$ to 10×10^{-5} . Thus suitable values of $K_1^{(t)}$ and K_2 could not be found from mobility considerations alone. This is not true, however, when the activity coefficients from emf data are considered as will be discussed.

As previously pointed out (8) a small error in T_{-} makes a large difference in the computed K_{2} .

The reliability of T_{-} is within a standard deviation of $\pm 1.4\%$ for molarities below 0.12, which is double that estimated for the sodium data (8). Above this concentration, the presented experimental evidence is in doubt, and we can only assume that T_{-} continues to increase, but probably not at as high a rate as shown.

E. Calculation of K_1 and K_2 from Activity Coefficients

With the aid of the transference measurements, the direct calculation of the activity coefficient ratio $y_{\pm}/(y_{\pm})_{ref}$ is feasible from potential measurements on concentration cells with transference. A suitable extrapolation would allow y_{\pm} to be evaluated. This coefficient, y_{\pm} , is the stoichiometric mean molar activity coefficient, and the ratio $y_{\pm}/(y_{\pm})_{ref}$ is obtained from equation [3.40].

The measured potentials are listed in Table 16. Figure 34 shows the resulting curve and also the integral curve of E with respect to the arbitrary reference concentration, 0.631 molar, for which $E_{ref} = 0$. The experimental data were plotted on a large graph (one meter square) upon which the integral curve was constructed. The values obtained by this integration are given in Table 19. It was also necessary to find the integral $\int \delta dE$ graphically, in which $\delta = \frac{1}{T_+} - \frac{1}{(T_+)_{ref}}$. The results of this integration, which was split-up into two sections on large graphs, are given in Table 19. The fifth column in Table 19 gives the calculated values of $y_{\pm}/(y_{\pm})_{ref}$. For aqueous solutions, the Debye-Hückel equation can be used to extrapolate $y_{\pm}/(y_{\pm})_{ref}$ to infinite dilution which then gives an approximate $(y_{\pm})_{ref}$. The process is recycled until $(y_{\pm})_{ref}$ remains constant. This treatment was tried with data from sodium solutions, but the curvature was too great for the extrapolation

lable 19. Smoothed Data for Activity Coefficient Calculations of Potassium-Ammonia Solutions at -37.0°C

C molarity x 10²)	т +	E (volt x 10 ³)	$- \int \delta dE$ (volt x 10 ³)	y±/(y±)ref	(1 mole^{-1})	đ	<u>K</u> (a) x 104
0, 158	0,151	5.50	1.54	1.583	0.603	0.862	41.7
0.251	0.148	3,43	0.684	1.404	0,535	0.819	37.2
0.398	0.145	1.61	0.169	1.202	0.458	0.754	33.9
0.631	0.141	00.00	00000	1,000	0,381	0.678	28.4
1.00	0.135	-1.40	0.184	0.8093	0,308	0.594	23.4
1.58	0.129	-2.65	0.764	0.6442	0,246	0.514	19.6
2.51	0.120	-3.75	1.78	0.504 ₈	0,192	0.439	16.6
3.98	0,110	-4.74	3.34	0.3934	0.150	0.375	14.3
6.31	0.0963	-5.67	5.78	0.3100	0,118	0.328	13,1
10.00	0.0795	-6.52	9.39	0.2479	0.0945	0.296	12.7
15.9	0.0582	-7.29	15.1	0.2057	0.0784	0.285	13.6
20.0	0.0456	-7.65	19,1	0, 1923	0.0733	0.292	15.2

to be reliable (9). The calculation was not performed for the potassium solutions. Instead $(y_{\pm})_{ref}$ was calculated from a at the reference concentration. As previously shown (9), K_1 and K_2 are "coupled"; that is, the data can be reproduced reasonably well over a range of values for K_1 if K_2 and $(y_{\pm})_{ref}$ are suitably chosen. Rather than adjust the constants for a "best fit," an independent method of calculating $(y_{\pm})_{ref}$ was used. If a represents the fraction of total metal that is present as ions, then

$$a = \frac{C_i}{C}$$
 [6.23]

and

$$y_{\pm} = \alpha f_{\pm}$$
 [6.24]

where f_{\pm} represents the mean molar activity coefficients of the ions present and is assumed to obey the Debye-Hückel equation in dilute solutions. For only the reference concentration a was determined from from conductivity data, the value being 0.668. This gives $(f_{\pm})_{ref} = 0.562$ from equation [6.20] and $(y_{\pm})_{ref} = 0.381$.

 K_1 and K_2 may now be calculated from the relative activity coefficients through successive approximations. From equation [6.21] an approximate value of $K_1^{(a)}$ was determined for each concentration and the corresponding $y_{\pm}/(y_{\pm})_{ref}$ calculated. An estimated a was used in equation [6.20] to calculate f_{\pm} which was then used in equation [6.24] to obtain a better value of a. The procedure was repeated until consistent values of a and f_{\pm} were obtained. The extrapolation of the $K_1^{(a)}$ values to infinite dilution gave an approximate $K_1^{(t)}$. These values of $K_1^{(t)}$ and $K_1^{(a)}$ were then used to obtain K_2 from equation [6.22]. Various $K_1^{(t)}$ values were used to give the most constant set of K_2 terms which was indicated by plotting the deviations from the average of each set of K_2 values. (see Table 20). Unlike the conductance treatment, a definite

minimum was obtained. The values thus determined are $K_1 = 4.3 \times 10^{-3}$ and $K_2 = 13.4$.

Table 20. K_2 Required for Various Values of $K_1^{(t)}$

C	$K_2 \text{ for } K_1^{(t)} =$			
x10 ²	39 x 10 ⁻⁴	43 x 10 ⁻⁴	50 x 10 ⁻⁴	
0.251	7.40	14.0	22.5	
0.398	9.36	13.2	18.9	
0.631	11.2	13.8	18.1	
1.00	11.7	13.8	17.3	
1.58	11.3	13.0	16.0	
2.00	11.0	12.6	15.4	
Average	10.4	13.4	18.0	
Deviation	±1.3	<u>+</u> 0,47	±1.8	

To check the validity of the two constants, they were used to compute y_± from equation [6.25] (see Appendix C) and f_± from

$$\alpha^2 = (1 - \alpha) \frac{K_1}{Cf_{\pm}^2 \left[1 + \frac{2}{K_1} (C \alpha f_{\pm} K_2)^2\right]}$$
 [6.25]

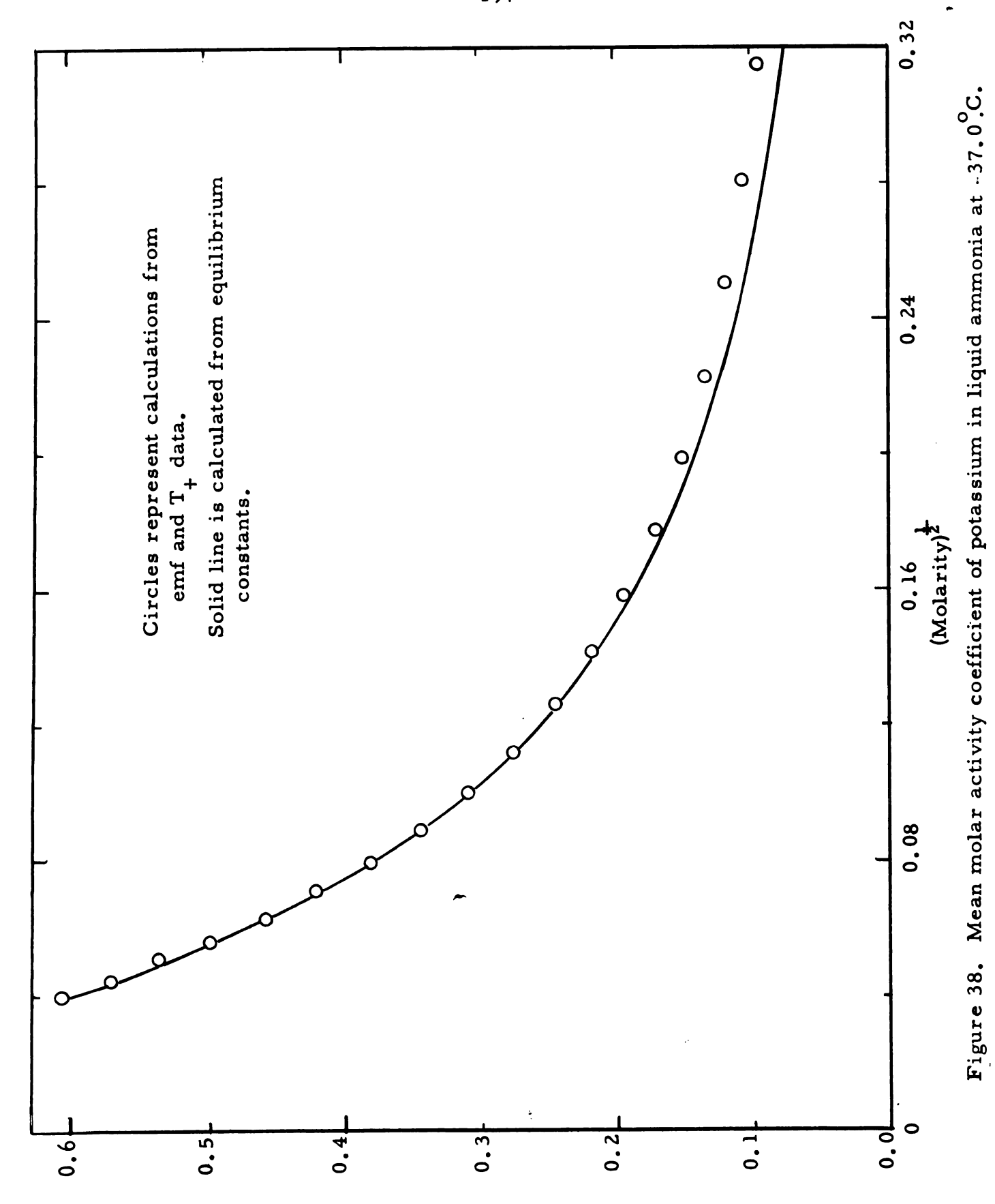
equation [6.20]. The results are given in Table 21 and plotted in Figure 38. The solid line represents the calculated values and the circles represent the smoothed activity coefficient curve obtained from emf and transference data. In contrast to the sodium system (9) the calculated and experimental values agree very well at low concentrations which attests to the validity of the method used in making the emf runs.

Table 21. Comparison of Observed and Calculated Activity Coefficients for Dilute Potassium-Ammonia Solutions

	y_{\pm} (1 mole ⁻¹)		
$M \times 10^2$	Calculated	Observed	
0.158	0.601	0.603	
0.200	0.566	0.571	
0.251	0.531	0.535	
0.316	0.495	0.496	
0.398	0.457	0.458	
0.501	0.420	0.420	
0.631	0.383	0.381	
0.794	0.346	0.343	
1.000	0,310	0.308	
1.26	0.276	0.276	
1.58	0.244	0.246	
2.00	0.214	0.217	
2.51	0.187	0.192	
3.16	0.162	0.170	
3.98	0.140	0.150	
5.01	0.121	0.133	
6.31	0.104	0.118	
7.94	0.0891	0.105	
.0.00	0.0761	0.0945	
12.60	0.0649	0.0856	

In the author's emf cell, the solution at the boundary and in the conductance cells was renewed with each concentration change. Thus, any bulk decomposition would be reflected in the conductance readings and was therefore taken into account. In Kraus' method for sodium solutions (6), the solutions were continually diluted and concentration errors resulting from decomposition could become rather sizeable for the most dilute solutions.

The only other data on potassium-ammonia solutions against which the K_1 and K_2 from this work can be compared are those computed from magnetic susceptibilities. Becker and co-workers (7) computed 30 x 10^{-3}



Mean Molar Activity Coefficient

for K_1 and 98 for K_2 at -34° and found K_1 reasonably independent of temperature. From extrapolation of their data, one determines K_2 to be 111 at -37°. Deigen (10) obtained 7.9 x 10⁻³ and 99, respectively, at -34°. All of these values of K_2 are considerably higher than determined here, 4.3 x 10⁻³ and 13.4 for K_1 and K_2 , respectively.

With the treatment used here, K_2 is more of a correction term used in the computation of K_1 than it is a true constant representing the dimerization equilibria. For this reason magnetic methods should give better values of K_2 . The comparison of the current results with those obtained for sodium (3,8,9) are a bit surprising. Both the dissociation constant and dimerization constant are lower for potassium solutions than for sodium solutions by about one-half in each case. The small K_2 value is unexpected from previous statements (8,19) which suggested the association would be higher for potassium than sodium. However, the dissociation constant for potassium is about 50% of that for sodium, thus on the basis of K_1 alone one finds a lower percentage of solvated potassium ions and electrons. The higher conductivity of potassium solutions compared with sodium is then due to the higher mobility of the positive species.

F. Activities and Thermodynamic Quantities

The range of activities may be extended by using the recent vapor pressure data of Marshall. At the time of the publication of the sodium-ammonia investigations (8, 9), there existed a large gap between the activity coefficient data and the available vapor pressure data of Kraus, Carney and Johnson (100). Dye, et al. used a curve matching technique to estimate the intermediate values. Since then the range of vapor pressure measurements has been extended by Marshall (86) not only for sodium solutions but also for solutions of lithium, potassium, rubidium,

and cesium in ammonia up to saturation. He has tabulated the mean molal activity coefficients relative to one molal solutions for the metal solutes obtained by a Gibbs-Duhem integration of the solvent activities. Division of the relative activities obtained from these values by the relative activity of the saturated solution gives the activities of the solutions with the pure metal as the standard state. The standard state for the present potassium-ammonia work, and also that for the previous sodium data, is the hypothetical, ideal, one molar standard state. For convenience in comparison these values were changed to the molal basis by use of (101):

$$m = \frac{C}{\rho - CM_2/1000}$$
 [6.26]

and

$$\gamma_{\pm} = y_{\pm} \left(\frac{\rho}{\rho_{o}} - \frac{CM_{z}}{1000 \rho_{o}} \right)$$
 [6.27]

where

ρ = density. The data are taken from Kraus, Carney and Johnson (100) for sodium-ammonia solutions, and from Hutchison and O'Reilly (73) for potassiumammonia solutions.

 ρ_0 = density of pure solvent = 0.6870 at -37.0°C (73).

M₂ = molecular weight of solute

C, m= concentrations expressed in molarity and molality, respectively

y₊ = mean molar activity coefficient

 γ_{+} = mean molal activity coefficient.

The matching of the vapor pressure data with those from emf is done by considering the activity ratio which must remain constant since

$$\frac{a_2}{a_2^7} = \frac{f_2/f_2^0}{f_2/f_2^{0^7}} = \frac{f_2^0}{f_2^0} = k = \frac{(\gamma \pm m)^2}{a_M}$$
 [6.28]

Thus

$$\log (\gamma_{\pm} m)^2 = \log k + \log a_{M}.$$
 [6.29]

The values of $(\gamma_{\pm}m)^2$ were plotted on the log axis <u>versus</u> molality on the linear axis of a sheet of semi-log paper, and the same was done for a_{Na} and a_{K} on another sheet using the same scales. Keeping coincidence in the concentration scales, the plots were adjusted vertically until the two sets of data could be connected by a smooth curve. The ratio of the readings from the two semi-log axes gives the value of k.

Table 22 and Figure 39 give the results of this calculation. The curve for potassium-ammonia solutions is divided because of the large range of activities. The sodium curve begins to show considerable "flatness" at its inflection point. This relects the fact that at -41.6°C for concentration in this region, a second liquid phase appears (102). The phase separation for potassium occurs at about -74°, although there has been some question raised concerning its existence (21,41). Observations of Vos (98) show conclusively that such phase separation does occur. The temperature of phase separation is low enough, however, so that it has little effect upon the activity curve at -37°C.

Because two different standard states are used, $(y_{\pm} m)^2 = k a_{M}$ gives the relationship between the states, where k is some constant determined by the relative free energies of the two standard states. For the process

$$K_{(s)} \longrightarrow K_{(am)}^{+} + e_{(am)}^{-}$$
 [6.30]

$$\Delta F_{+}^{O} = -RT \ln k \qquad [6.31]$$

where K[†] and e represent the hypothetical ideal one molal solution.

Table 22. Activity of Sodium and Potassium in Ammonia Over Entire
Range of Solubility

		Sodium		Potassium	
m	√ m	a x 10 ³	γ_{\pm}	a x 10 ³	γ_{\pm}
11.84	3.44	•		1000.	0.794
10.84	3.29	1000.	0.0306		
10.00	3.16	405.	0.0218	39.4	0.186
8.00	2.83	62.8	0.0104	2.13	0.0542
6.00	2.45	17.2	0.00726	0.211	0.0227
4.00	2.00	9.18	0.00794	0.0404	0.0149
3.00	1.73	8.15	0.0100	0.0235	0.0152
2.00	1.41	7.28	0.0142	0.0166	0.0192
1.50	1.22	7.53	0.0192	0.0140	0.0235
1.00	1.00	6.55	0.0269	0.0112	0.0315
0.800	0.894	5.84	0.0318	0.00951	0.0362
0.600	0.775	5.45	0.0408	0.00748	0.0428
0.400	0.632	3.90	0.0519	0.00525	0.0538
0.300	0.548	3.12	0.0619	0.00412	0.0637
0.200	0.447	2.23	0.0784	0.00281	0.0785
0.150	0.387	1.78	0.0936	0.00208	0.0907
0.100	0.316	1.37	0.123	0.00152	0.116
0.0585	0.242	0.849	0.166	0.000854	0.150
0.0232	0.152	0.371	0.276	0.000363	0.245
0.0116	0.108	0.182	0.387	0.000178	0.343
0.00365	0.0604	0.0334	0.527	0.0000432	0,535
0.00231	0.0481		r	0.0000219	0.603

Table 23 summarizes the thermodynamic quantities for the various standard states. The last column gives the values previously reported (9) for sodium-ammonia solutions obtained before the data of Marshall were available.

The estimation of the errors for the various steps in calculating the final result has been stated for sodium solutions (9) and for practical



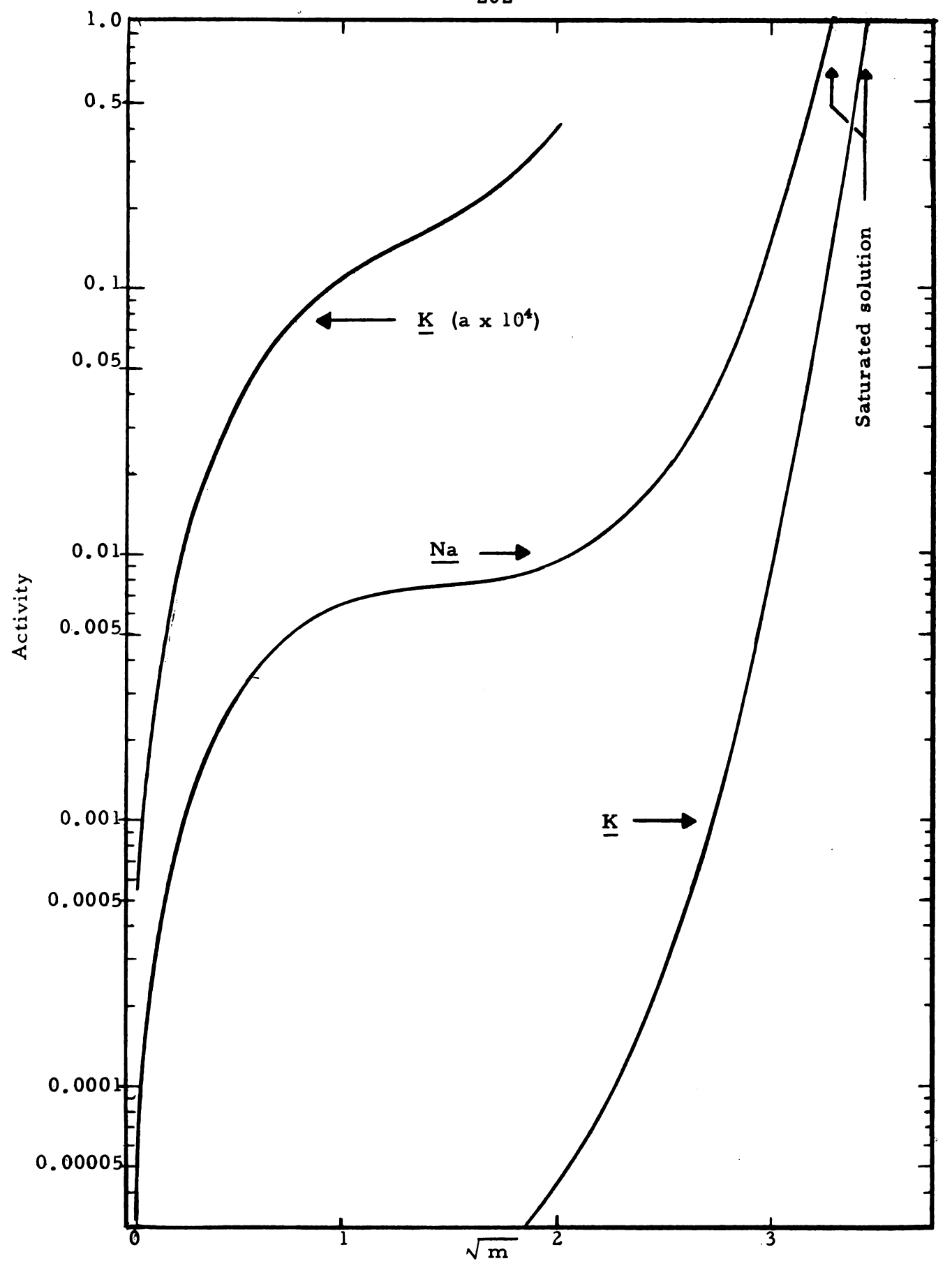


Figure 39. Activity of sodium and potassium in ammonia versus (molality) ; standard state is pure solid metal. Data are

purposes would also apply for the present investigation. The only error that would be significantly reduced is the matching with the vapor pressure curves since extended vapor pressure measurements were not available for the previous calculations. However, the error in T_{+} for potassium, is about double that for sodium. The probable error in T is ±1.2% which includes an estimate of concentration error. This reflects an error of $\pm 12\%$ in T_{\pm} compared with about 7% for sodium solutions. The error in $\Delta E/\Delta \log C$ is less than $\pm 3\%$ which gives an estimated error in $y_{\pm}/(y_{\pm})$ ref of from 1.4 to 8% between 0.01 and 0.35 M. The error in a nef is assumed to be the same as in T₊ (12%), which gives an error of 12% in $(y_{\pm})_{ref}$. The error in y_{\pm} or γ_{\pm} is estimated to be 13% at 0.15 m, the point of tie-in. Data are not available to estimate the error involved at the tie-in; however, certainly an extreme value would be $\pm 10\%$. This results in a maximum error in ΔF^{0} of ± 1.0 kcal mole⁻¹, the probable error being less. If the error in ΔH^{0} is \pm 0.1 kcal mole⁻¹, then the uncertainty in ΔS° is \pm 4 cal deg⁻¹ mole⁻¹.

The difference in free energies of solution for sodium and potassium solutions may be compared with the published difference in free energies for these same metals in their reactions with $H_{(am)}^{+}$ (103).

 $(\Delta F^{0})^{240^{0}}$ K(kcal mole-1)

$$K_{(s)} \longrightarrow K_{(am)}^{\dagger} + e_{(am)}^{-} \qquad -2.10$$

$$\frac{Na_{(am)}^{\dagger} + e_{(am)}^{-} \longrightarrow Na_{(s)}}{K_{(s)} + Na_{(am)}^{\dagger} \longrightarrow Na_{(s)} + K_{(am)}^{\dagger}} \qquad -1.03$$

$$K_{(s)} + Na_{(am)}^{\dagger} \longrightarrow Na_{(s)} + K_{(am)}^{\dagger} \qquad -3.13$$

$$K_{(s)} + H_{(am)}^{\dagger} \longrightarrow K_{(am)}^{\dagger} + \frac{1}{2} H_{2(g)} \qquad -46.1$$

$$\frac{Na_{(am)}^{\dagger} + \frac{1}{2} H_{2(g)} \longrightarrow Na_{(s)} + H_{(am)}^{\dagger}}{K_{(s)} + Na_{(am)}^{\dagger} \longrightarrow Na_{(s)} + K_{(am)}^{\dagger}} \qquad -3.4$$

This difference agrees with the published result within experimental error. This happy result lends credence to the complex treatments which have been described in this dissertation.

Table 23. Thermodynamic Functions for the Process: $M_{(s)} \rightarrow M_{(am)}^{+} + e_{(am)}^{-}$

Function	Potassium	Sodium	
		This Work	Dye, et al. (9)
ΔF_{m}^{o} ; kcal mole ⁻¹ hypothetical ideal, m = 1	-2.l ₀	1.03	-0.1
AFC; kcal mole ⁻¹ hypothetical ideal, C = 1	-1.74	1.39	0.3
ΔF _X ; kcal mole ⁻¹ hypothetical ideal, X = 1	1.78	4.91	3.8
ΔH ^O ; kcal mole ⁻¹ (103)	3.0	4.4	4.4
∆S [°] m; eu	21.3	14.0	18.7
∆S°; eu	19.8	12.6	17.1
∆S [°] X; eu	5.1	-2.1	2.5
o M ; eu (104)	13.7	10.8	10.8
o M ; eu (103)	25 . ₃	12.6	12.6
o e_ ; eu	9.7	12.2	16.9
hypothetical ideal, $m = 1$			

G. Suggested Future Work and Concluding Remarks

With the use of cell A as described, conductance studies should be extended to other metal-solvent systems since the techniques described allow correction for decomposition.

With larger electrodes installed in cell B, this cell should also be useful for conductance studies, particularly where a large dilution range is to be spanned or the quantity of solvent available is small (100 ml). However, one must keep in mind the multiplication of errors which arises when this dilution technique is used. The conductance procedures described in this dissertation would be suitable only for a reasonably volatile solvent.

It would be interesting to investigate the stability of lithiumammonia solutions. It seems likely that these solutions should be just
as stable as the other alkali metal solutions if pure lithium metal samples
could be prepared. The inability to distill this metal in glass hampers
the preparation of pure samples. If stable solutions can be prepared,
transference numbers, conductance, and electromotive force measurements should be made. From literature references, it appears that
these solutions are different enough from the other alkali metals to
warrant an extensive investigation. Lithium, because of its ion size, is
expected to have a larger number of solvent molecules tied up in its
solvation sphere than any of the other alkali metals.

Three suggested improvements on the transference number apparatus should allow one to obtain accurate transference numbers:

- (1) Install new electrodes with a larger surface area. Fused wire should not be used unless a pit-free surface can be assured.

 Leak-free seals without wax would be highly desirable.
- (2) Install a new boundary stopcock as shown in Figure 21. This should prevent "popping" of the stopcock before or during a run.

(3) Provide for a large gas volume above the metal solution, filled with purified helium gas. This gas ballast should be kept at constant temperature. This would probably greatly reduce the pressure build-up previously mentioned.

It may also be possible to devise a Hittorf transference number cell whose electrode chambers contain calibrated conductance cells for determining the concentration such as diagramed here. .

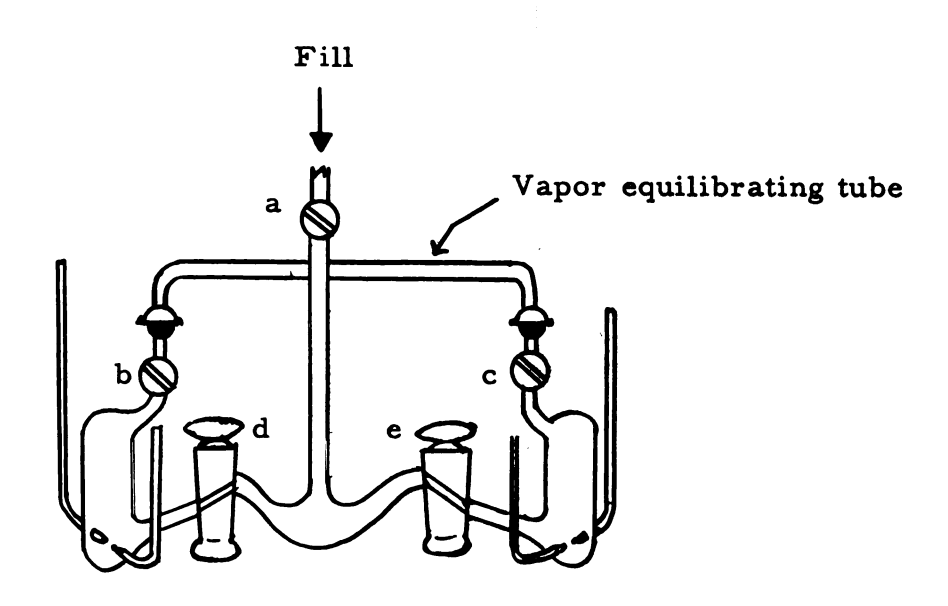


Figure 40. A suggested Hittorf transference apparatus for closed systems.

The cell would be filled with metal solution which is prepared in the make-up vessel of the transference apparatus. With <u>a</u> closed, the apparatus could be removed from the line to allow mixing of the solutions in the conductance cells. At the completion of the electrolysis, <u>d</u> and <u>e</u> would be closed and the conductivities measured. Pressure equilibrium would be maintained through b and c.

The present design of the emf cell and the method of manipulation would make this a convenient method of measuring emf values for other systems provided the solvent is sufficiently volatile to permit fairly rapid distillation from one compartment to another.

The success in obtaining blue and bronze colors by distilling potassium metal onto ice with the simple apparatus described (Figure 23) suggests a way of testing for metal solubilities for a multitude of metal-solvent combinations. Cesium metal, because it is easily polarized, would suggest itself as the first metal to try with solvents that have not previously shown colored solutions such as the secondary and tertiary amines, hydrocarbons, ethers, alcohols, etc. This should give us more insight into solvent-metal interactions required to permit solubility.

The investigation described here gives little, if any, insight into the conduction mechanism present in these solutions. In concentrated sodium solutions (1 to 5 molar), Farkas (105, 15) has explained the conductivity by quantum jumps of electrons between metal atoms. The theoretical equation fits the experimental data better as the concentration increases. Dewald and Lepoutre (45) have proposed that quantum tunneling also occurs even in dilute solutions. This is based on the negative heat of transport for the electron obtained from thermoelectric measurements.

It may be merely fortuitous, but Forsgard (106) has made the following comparisons concerning the ratios of ionic conductance in ammonia and in water (consider the metal as M[†]•e⁻):

$$\frac{\text{H}_2\text{O}}{\text{Λ o(\text{HC1})$}} = 2.8$$

$$\frac{\text{Λ o(\text{KC1})$}}{\text{$\Lambda$ o(\text{KC1})$}} = 2.8$$

$$\frac{\text{Λ o(\text{KC1})$}}{\text{$\Lambda$ o(\text{KC1})$}} = 4.8$$

$$\frac{\text{Λ o(e^-)$}}{\text{$\Lambda$ o(\text{K}^+)$}} = 4.9$$

$$\frac{\text{Λ o(e^-)$}}{\text{$\Lambda$ o(\text{Na}^+)$}} = 7.0$$

$$\frac{\text{Λ o(e^-)$}}{\text{$\Lambda$ o(\text{Na}^+)$}} = 6.9$$

$$\frac{\text{Λ o(\text{HC1})$}}{\text{$\Lambda$ o(\text{NaC1})$}} = 3.0$$

$$\frac{\text{Λ o(\text{Na})$}}{\text{$\Lambda$ o(\text{NaC1})$}} = 3.25$$

However, for methylamine solutions the ratios break down since $\Lambda_0(Cs)/\Lambda_0(CsI) = 4.2$ compared to $\Lambda_0(HI)/\Lambda_0(CsI) = 2.7$ for water. For sgard points out the possibility that the proton in aqueous solutions and the negative species in ammonia solutions have the same transport mechanism, similar to the "proton jump."

It is certainly safe to say that as more experimental data are obtained, the present models will be revised or replaced by newer ones. As an example, the recent spectra work by Gold and Jolly (107) and as interpreted by Gold, Jolly, and Pitzer (108) has replaced the "dimer" by an "ion quadrupole" of possibly square or rhombic configuration consisting of two solvated metal ions and two solvated electrons held together electrostatically. Their results have suggested the possibility that "triple ions" (e-\M^+\cdot e- or M^+\cdot e^-\M^+) may be important species which have previously been neglected. The effect of these "triple ions" is being considered in computations now currently in progress in this Laboratory. The proposed equilibria are

$$M^{\dagger} \cdot e^{-} \iff M^{\dagger} + e^{-}$$

$$e^{-} + M^{\dagger} \cdot e^{-} \iff e^{-} \cdot M^{\dagger} \cdot e^{-}$$

$$M^{\dagger} \cdot e^{-} + M^{\dagger} \iff M^{\dagger} \cdot e^{-} \cdot M^{\dagger}$$

$$M^{\dagger} \cdot e^{-} \iff \frac{1}{2} M_{2}$$

These equilibria give the solvated metal ion more significance than previous models. The metal ion upon solvation is certainly more bulky and immobile than the unsolvated electron. Hence the solvated positive ion could force the electron to fit the environment created by the positive species. The environment may include a "cavity," an expanded orbital, a smeared electron distribution on the protons of the ammonia molecules (21), or whatever may be proposed in the future.

REFERENCES

- 1. T. P. Das, "Structure and Properties of Metal-Ammonia Solutions" in Advances in Chemical Physics, I. Prigogine, Ed., Interscience Publishers, New York, 4, 303 (1962).
- 2. W. L. Jolly, "Metal-Ammonia Solutions" in Progress in Inorganic Chemistry, F. A. Cotton, Ed., Interscience Publishers, New York, 1, 235 (1959).
- 3. E. C. Evers and P. W. Frank, Jr., J. Chem. Phys., 30, 61 (1959).
- 4. P. Marshall and H. Hunt, J. Phys. Chem., 60, 121 (1956).
- 5. S. Freed and N. Sugarman, J. Chem. Phys., 11, 354 (1943).
- 6. C. A. Kraus, J. Am. Chem. Soc., 36, 864 (1914).
- 7. E. Becker, R. H. Lindquist, and B. J. Alder, J. Chem. Phys., 25, 971 (1956).
- 8. J. L. Dye, R. F. Sankuer, and G. E. Smith, J. Am. Chem. Soc., 82, 4797 (1960).
- 9. J. L. Dye, G. E. Smith, and R. F. Sankuer, J. Am. Chem. Soc., 82, 4803 (1960).
- M. F. Deigen and A. Tsvirko, Ukrain, Fiz. Zhur., 1, 245 (1956);
 C. A., 51, 5535e (1957).
- D. S. Berns, E. C. Evers, and P. W. Frank, Jr., J. Am. Chem. Soc., 82, 310 (1960).
- 12. W. Weyl, Ann. Physik, 121, 601 (1864).
- 13. R. F. Sankuer and J. L. Dye, <u>Selected Bibliography of Physico-chemical Properties in Liquid Ammonia and Related Solvents</u>, TID-3904, U. S. Atomic Energy Commission, Office of Technical Information, Washington 25, D. C., (1959).

- 14. G. Lepoutre, Solutions of Alkali Metals in Ammonia, Amines and Ethers. Systematic Bibliography, Catholic University of Lille, France.
- 15. D. M. Yost and H. Russell, Jr., <u>Systematic Inorganic Chemistry</u>, Prentice-Hall, Inc., New York, 1944, p. 139.
- 16. C. A. Kraus, J. Chem. Educ., 30, 83 (1953).
- 17. W. Bingel, Ann. Physik, 12, 57 (1953).
- 18. M. C. R. Symons, Quar. Revs. (London), 13, 99 (1959).
- 19. E. C. Evers, J. Chem. Educ., 38, 590 (1961).
- 20. L. Paoloni, Gazz. chim. ital., 90, 1682 (1960); 91, 121, 412, 518, 530, 787, 1063 (1961).
- 21. A. J. Birch and D. K. C. MacDonald, Oxford Science, 1948, 1.
- 22. W. C. Johnson and A. W. Meyer, Chem. Revs., 8, 273 (1931).
- 23. R. A. Ogg, Jr., J. Chem. Phys., 13, 533 (1945).
- 24. H. P. Cady, J. Phys. Chem., 1, 707 (1897).
- 25. E. C. Franklin and C. A. Kraus, Am. Chem. J., 23, 306 (1900).
- 26. C. A. Kraus, J. Am. Chem. Soc., 30, 1323 (1908).
- 27. E. C. Franklin and H. P. Cady, J. Am. Chem. Soc., 26, 499 (1904).
- 28. C. A. Kraus, J. Am. Chem. Soc., 43, 749 (1921).
- 29. J. W. Hodgins and E. A. Flood, Can. J. Research, 27B, 874 (1949); also J. W. Hodgins, Can. J. Research, 27B, 861 (1949).
- 30. R. M. Fristrom, Ph. D. dissertation, Stanford University (1949).
- 31. C. A. Kraus and W. W. Lucasse, J. Am. Chem. Soc., <u>43</u>, 2529 (1921).
- 32. C. A. Kraus and W. W. Lucasse, J. Am. Chem. Soc., <u>44</u>, 1941 (1922).

- 33. C. A. Kraus and W. W. Lucasse, J. Am. Chem. Soc., <u>45</u>, 2551 (1923).
- 34. G. E. Gibson and T. E. Phipps, J. Am. Chem. Soc., <u>48</u>, 312 (1926).
- 35. D. S. Berns, Ph. D. dissertation, University of Pennsylvania (1959).
- 36. F. R. Meranda, Ph. D. dissertation, Purdue University (1957).
- 37. G. Lepoutre, Ph. D. dissertation, Yale University (1953).
- 38. E. C. Evers, A. E. Young, II, and A. J. Panson, J. Am. Chem. Soc., 79, 5118 (1957).
- 39. A. J. Panson, Ph. D. dissertation, University of Pennsylvania (1957).
- 40. M. Nabauer, Z. angew. Physik, 1, 423 (1949); C. A. 43, 8780i (1949).
- 41. A. J. Birch and D. K. C. MacDonald, Trans. Faraday Soc., 44, 735 (1948).
- 42. J. W. Hodgins, Phys. Rev., 70, 568 (1946).
- 43. J. F. Dewald and G. Lepoutre, J. Am. Chem. Soc., 76, 3369 (1954).
- 44. G. Lepoutre and J. F. Dewald, J. Am. Chem. Soc., 78, 2953 (1956).
- 45. J. F. Dewald and G. Lepoutre, J. Am. Chem. Soc., 78, 2956 (1956).
- 46. R. R. Dewald, Ph. D. dissertation, Michigan State University (1963).
- 47. S. Windwer and B. R. Sundheim, J. Phys. Chem., 66, 1254 (1962).
- 48. F. Cafasso and B. R. Sundheim, J. Chem. Phys., 31, 809 (1959).
- 49. C. A. Kraus and W. C. Bray, J. Am. Chem. Soc., 35, 1315 (1913).
- 50. E. C. Franklin, Z. physik. Chem., 69, 272 (1909).
- 51. Reference 25, p. 277.
- 52. E. C. Franklin and C. A. Kraus, J. Am. Chem. Soc., 27, 191 (1905).
- 53. V. F. Hnizda and C. A. Kraus, J. Am. Chem. Soc., 71, 1565 (1949).

- D. S. Berns, G. Lepoutre, E. A. Bockelman, and A. Patterson, Jr.,
 J. Chem. Phys., 35, 1820 (1961).
- 55. F. F. Fitzgerald, J. Phys. Chem., 16, 621 (1912).
- 56. E. C. Franklin and H. D. Gibbs, J. Am. Chem. Soc., 29, 1389 (1907).
- 57. E. C. Franklin and C. A. Kraus, Am. Chem. J., 24, 83 (1900).
- 58. H. M. Klein, Ph. D. dissertation, University of Pennsylvania (1957).
- 59. S. Glasstone, An Introduction to Electrochemistry, D. Van Nostrand Company, Inc., Princeton, New Jersey, 1942.
- 60. D. A. MacInnes, The Principles of Electrochemistry, Reinhold Publishing Corporation, New York, 1961.
- 61. H. S. Harned and B. B. Owen, The Physical Chemistry of Electrolytic Solutions, 3rd ed., Reinhold Publishing Corporation, New York, 1950.
- 62. M. P. Faber, Ph. D. dissertation, Michigan State University, (1961).
- 63. D. A. MacInnes and L. G. Longsworth, Chem. Revs., 11, 171 (1932).
- 64. F. Kohlrausch, Ann. Physik, 62, 209 (1897).
- 65. D. A. MacInnes and E. R. Smith, J. Am. Chem. Soc., 45, 2246 (1923).
- 66. L. G. Longsworth, J. Am. Chem. Soc., <u>54</u>, 2741 (1932).
- 67. J. Taylor, J. Sci. Instr., 5, 24 (1928).
- 68. D. E. O'Reilly, Ph. D. dissertation, University of Chicago (1955), p. 172.
- 69. F. Ephraim, <u>Inorganic Chemistry</u>, translated by P. G. L. Thorne and E. R. Roberts, 5th ed., Interscience Publishers, Inc., New York, 1948, p. 619.
- 70. H. B. Thompson and M. T. Rogers, Rev. Sci. Instr., 27, 1079 (1956).
- 71. C. J. Savant, Jr., Electronics, 26, May 188 (1953).

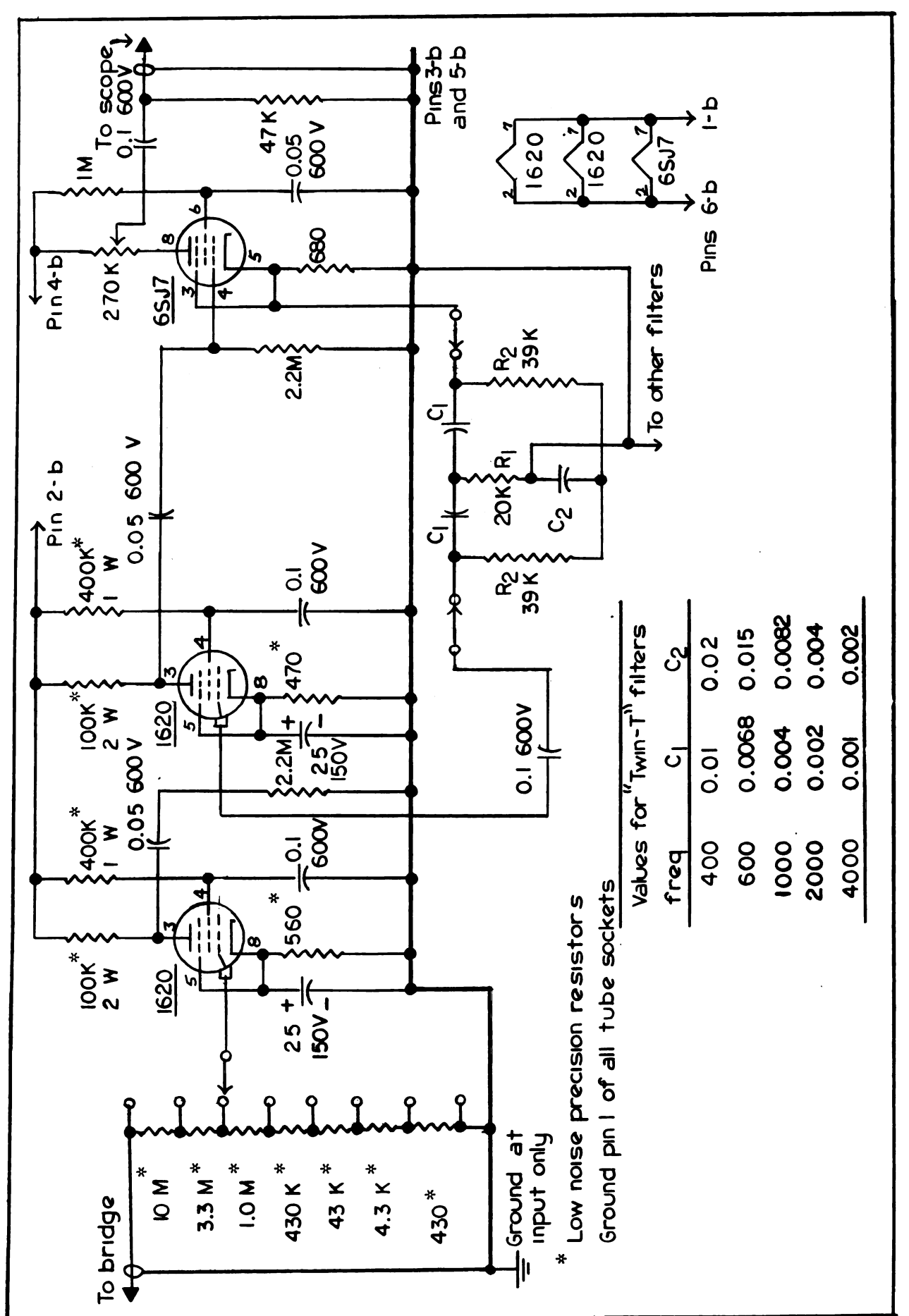
- 72. W. C. Johnson and A. W. Meyer, J. Am. Chem. Soc., <u>54</u>, 3621 (1932).
- 73. C. A. Hutchison, Jr., and D. E. O'Reilly, J. Chem. Phys., 34, 163 (1961).
- 74. Reference 68, p. 322.
- 75. Reference 61, pp. 179, 210.
- 76. G. Jones and G. M. Bollinger, J. Am. Chem. Soc., 57, 280 (1935).
- 77. G. Jones and S. M. Christian, J. Am. Chem. Soc., 57, 272 (1935).
- 78. R. F. Sankuer, this Laboratory, unpublished data.
- 79. D. J. Karl, Ph. D. dissertation, Michigan State University (1960).
- 80. Reference 61, p. 699.
- 81. E. A. Guggenheim, J. Am. Chem. Soc., 52, 1315 (1930).
- 82. H. J. Wolthorn and W. C. Fernelius, J. Am. Chem. Soc., <u>56</u>, 1551 (1934).
- 83. J. Jortner and G. Stein, Nature, 175, 893 (1955).
- 84. N. A. Lange, Handbook of Chemistry, 7th ed., Handbook Publishers, Inc., Sandusky, Ohio, 1949, p. 1641.
- 85. C. S. Cragoe and D. R. Harper, National Bureau of Standards, Scientific Paper No. 420, Government Printing Office, Washington, D. C., 1921, p. 287.
- 86. P. R. Marshall, J. Chem. and Eng. Data, 7, 399 (1962).
- 87. Reference 84, p. 267.
- 88. A. Willers, Practical Analysis, translated by R. T. Beyer, Dover Publications, Inc., New York, 1948, p. 149.
- 89. Reference 68, p. 38.
- 90. I. Kirshenbaum, Physical Properties and Analysis of Heavy Water, McGraw-Hill Book Co., Inc., New York, 1951, p. 36.

- 91. T. Shedlovsky, J. Franklin Inst., 225, 738 (1938).
- 92. Reference 61, p. 289, or Reference 61, 2nd ed., p. 189.
- 93. Reference 20, 91, 121.
- 94. A. M. Monoszon and V. A. Pleskov, Z. physik. Chem. 156A, 176 (1931).
- 95. Reference 59, p. 62.
- 96. J. L. Dye, private communication; see also reference 46, p. 19.
- 97. J. L. Dye, this Laboratory, current investigation.
- 98. K. D. Vos, Ph. D. dissertation, Michigan State University (1962).
- 99. C. A. Hutchison and R. C. Pastor, J. Chem. Phys., 21, 1959 (1953).
- 100. C. A. Kraus, E. S. Carney, and W. C. Johnson, J. Am. Chem. Soc., 49, 2206 (1927).
- 101. Reference 61, p. 12.
- 102. O. Ruff and J. Zedner, Ber., 41, 1948 (1908); C. A. 2,24863 (1908).
- 103. L. V. Coulter, J. Phys. Chem., 57, 553 (1953).
- 104. National Bureau of Standards, Circular 500, "Selected Values of Chemical Thermodynamic Properties," U. S. Government Printing Office, Washington, D. C., 1952, p. 447 for sodium; p. 483 for potassium.
- 105. L. Farkas, Z. physik. Chem., A161, 355 (1932); C. A. 27, 12 (1933).
- 106. F. C. Forsgard, Ph. D. dissertation, University of Pennsylvania (1954).
- 107. M. Gold and W. L. Jolly, Inorg. Chem., 1, 818 (1962).
- 108. M. Gold, W. L. Jolly, and K. S. Pitzer, J. Am. Chem. Soc., <u>84</u>, 2264 (1962).

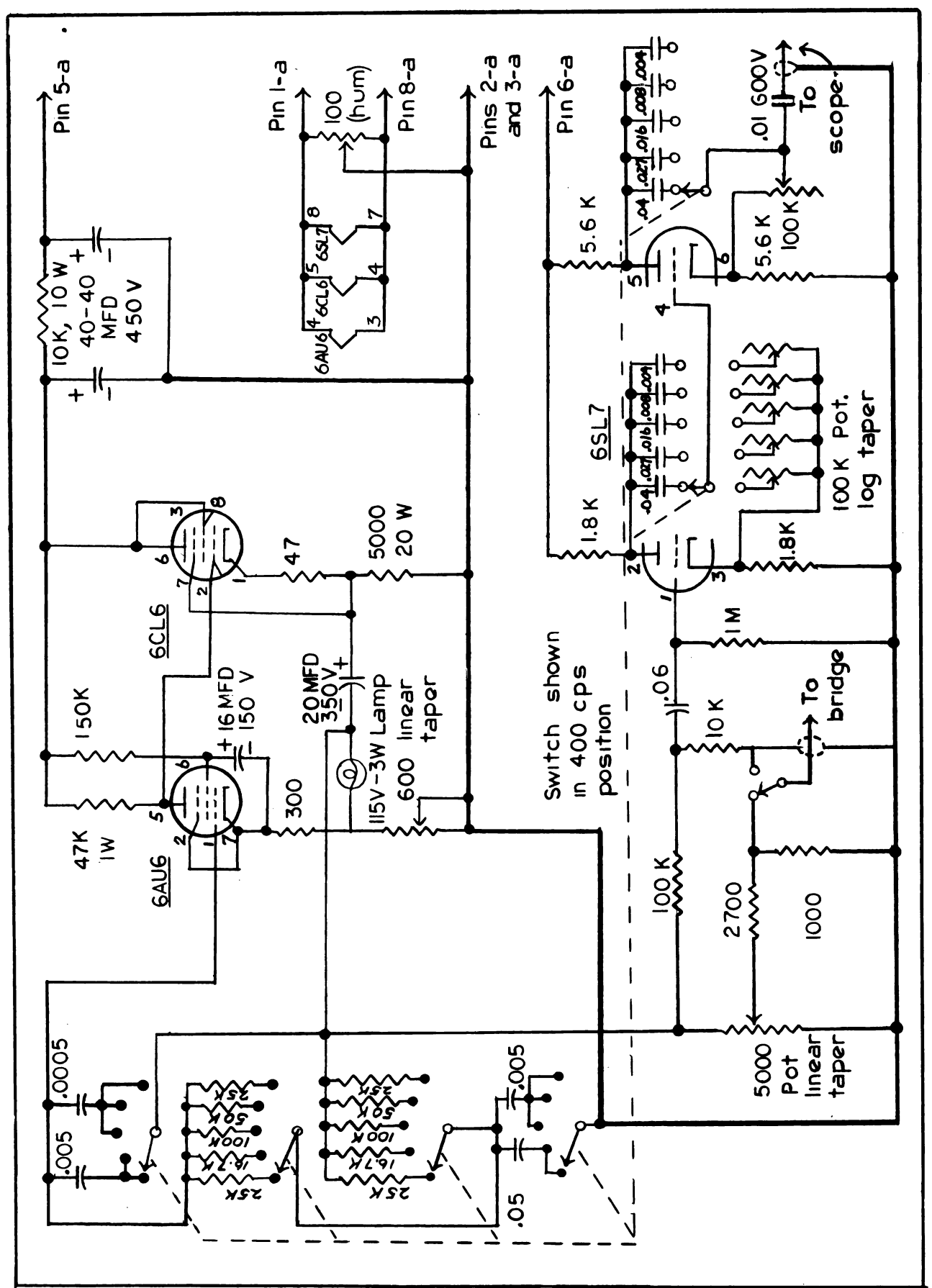
APPENDICES

APPENDIX A

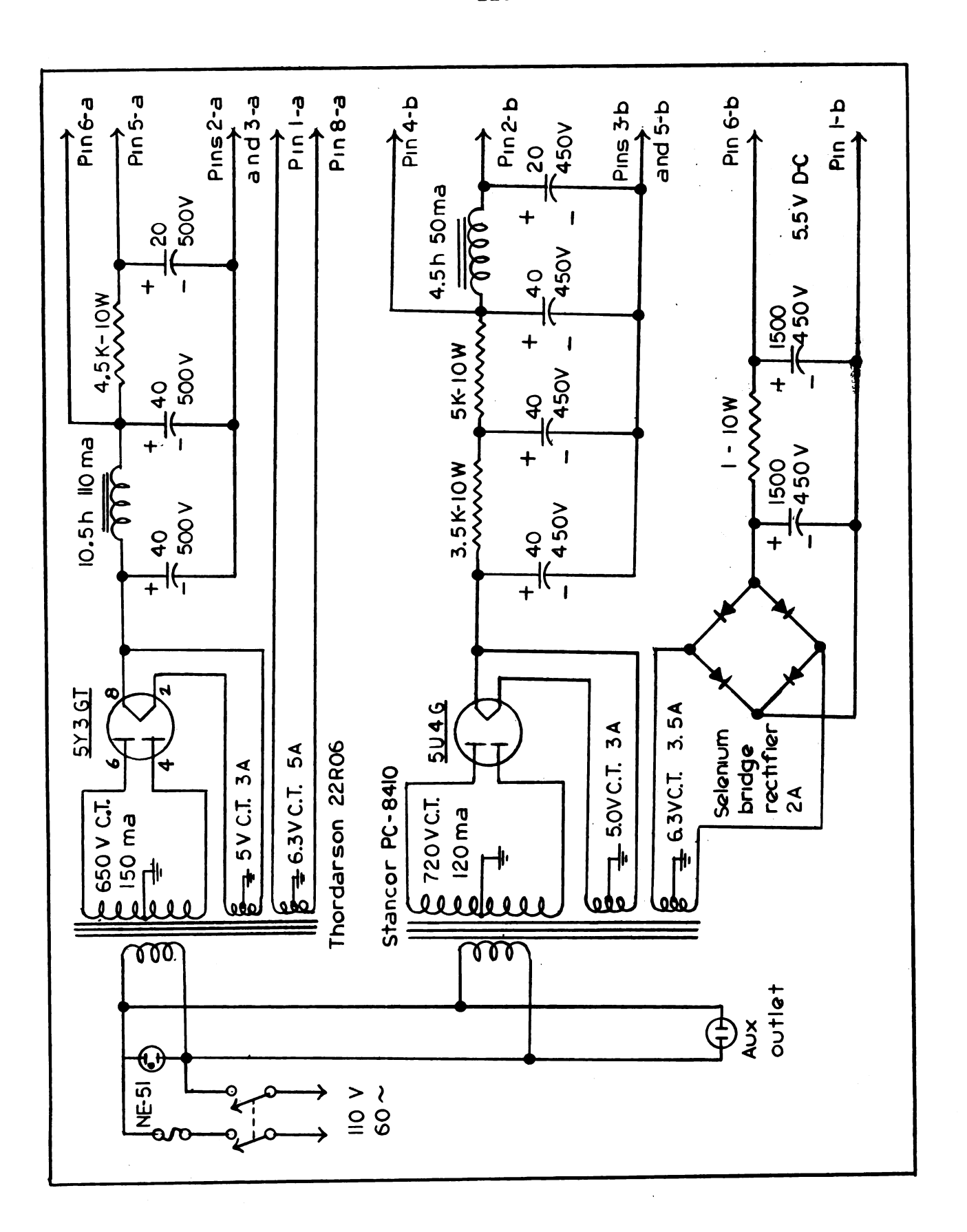
SCHEMATIC DIAGRAM OF CONDUCTANCE BRIDGE



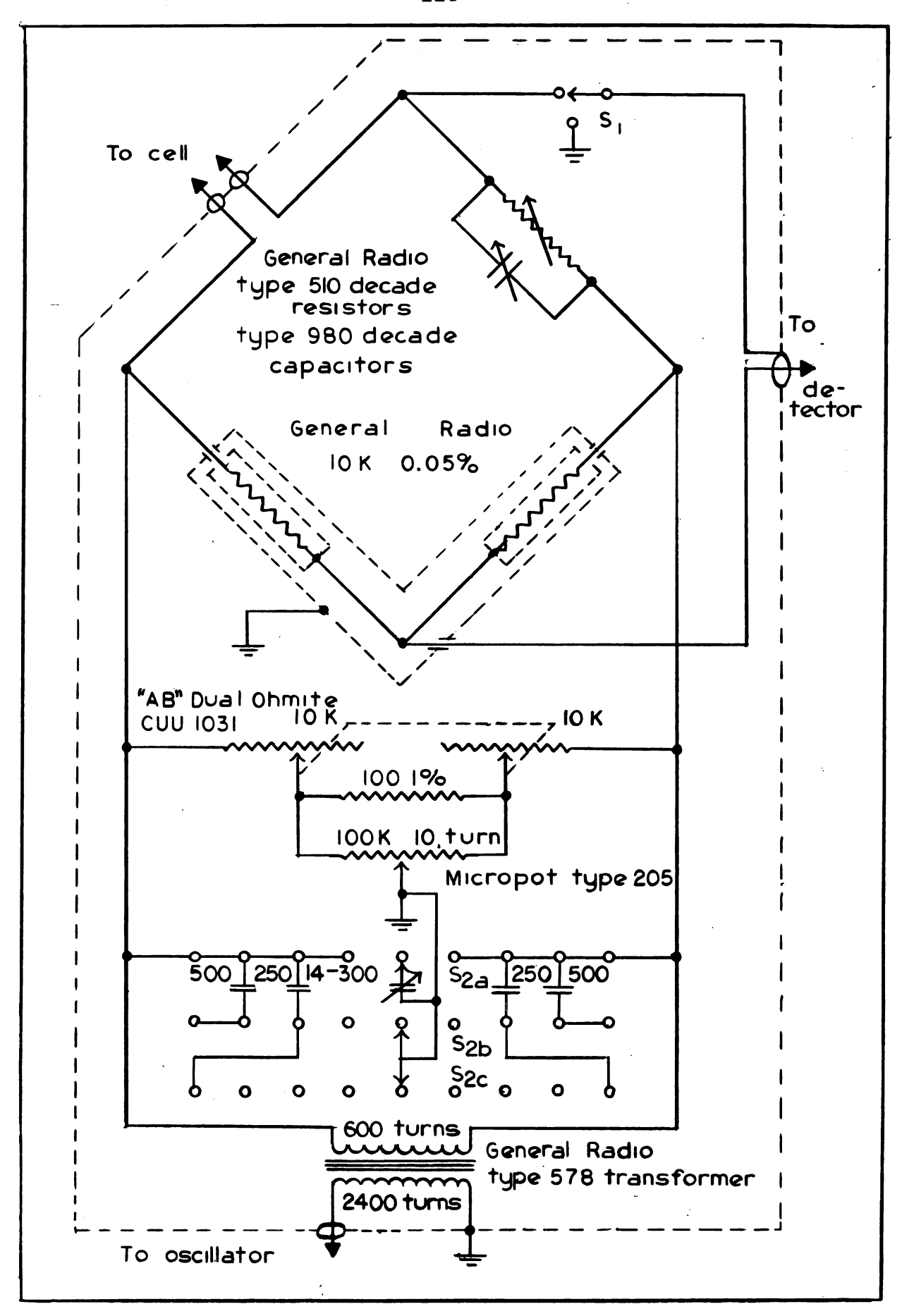
Conductance Bridge - Detector Circuit



Conductance Bridge - Oscillator Circuit



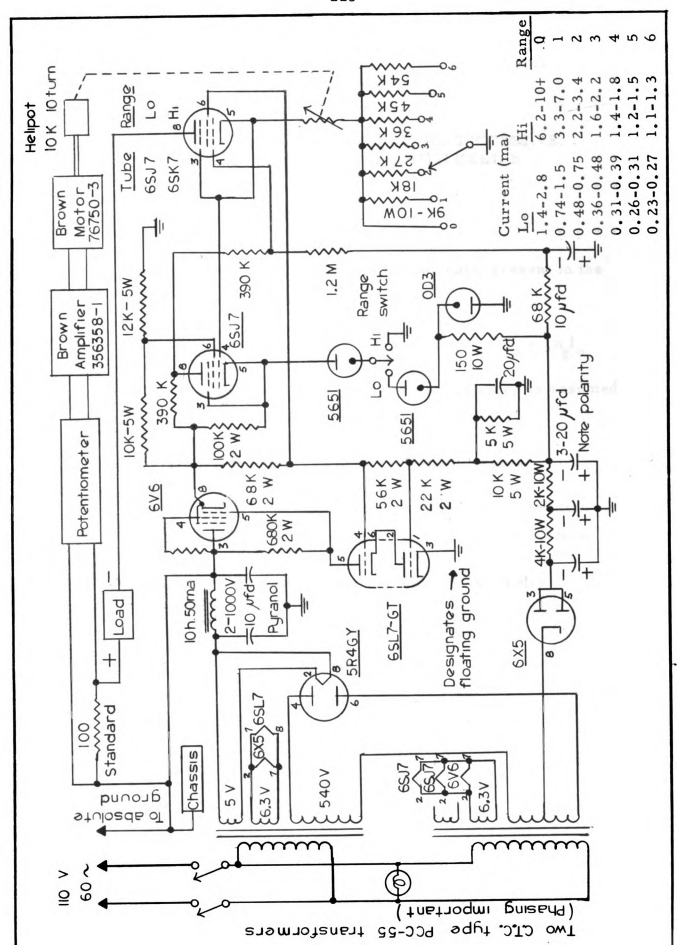
Conductance Bridge - Power Supply



Conductance Bridge - Bridge Circuit

APPENDIX B

SCHEMATIC DIAGRAM OF CURRENT CONTROLLER



APPENDIX C

ANALYSIS OF ERROR ENTAILED IN THE SUCCESSIVE DILUTION PROCEDURE USED WITH CELL B

Meaning of symbols used:

n = moles of liquid ammonia actually present in the cell originally

 $(n_T)_0$ = total moles of ammonia present = $n_0 + (n_g)_0$

 $(n_g)_0$ = moles of ammonia in gas phase which is assumed to remain constant = n_g

m = equivalents of metal originally present

n_i = moles of liquid ammonia in cell after addition of
 a_i moles of liquid ammonia on the ith dilution

w_i = moles of ammonia withdrawn from cell

 C_i = the concentration of the solution

For i = 0

$$C_0 = \frac{m_0}{n_0} = \frac{m_0}{(n_T)_0 - n_g}$$

$$C_1 = \frac{m_1}{n_1} = \frac{m_0}{n_0 + a_1} = \frac{m_0}{n_0} \left(\frac{n_0}{n_0 + a_1} \right)$$

For i = 2

Before the addition of ammonia for this dilution, a portion of the solution is removed which is equal to $(n_1 - w_1)/n_1$. The amount of metal remaining is

$$m_2 = (\frac{n_1 - w_1}{n_1}) m_1$$
.

The number of moles of ammonia present after the addition of a₂ moles is

$$\eta_2 = \eta_0 + a_1 + a_2 - w_1$$

Therefore,

$$C_2 = \frac{m_0}{n_0} \left(\frac{n_0 + a_1 - w_1}{n_0 + a_1} \right) \left(\frac{n_0}{n_0 + a_1 + a_2 - w_1} \right)$$

For i = 3

Proceeding in the same way as for i = 2:

$$m_{3} = m_{0} \left(\frac{n_{0} + a_{1} - w_{1}}{n_{0} + a_{1}} \right) \left(\frac{n_{0} + a_{1} + a_{2} - w_{1} - w_{2}}{n_{0} + a_{1} + a_{2} - w_{1}} \right)$$

$$n_{3} = n_{0} + a_{1} + a_{2} + a_{3} - w_{1} - w_{2}$$

$$C_{3} = \frac{m_{3}}{n_{3}} = \frac{m_{0}}{n_{0}} \left(\frac{n_{0} + a_{1} - w_{1}}{n_{0} + a_{1}} \right) \left(\frac{n_{0} + a_{1} + a_{2} - w_{1} - w_{2}}{n_{0} + a_{1} + a_{2} - w_{1}} \right)$$

$$\left(\frac{n_{0}}{n_{0} + a_{1} + a_{2} + a_{3} - w_{1} - w_{2}}{n_{0}} \right)$$

Assume as a good approximation,

$$a_1 = a_2 = a_3 = a = w_1 = w_2 = w_3 = w$$

Then

$$C_3 = \frac{m_0}{n_0} \left(\frac{n_0}{n_0 + a} \right)^3$$

For i = i

$$C_{i} = \frac{m_{o}}{n_{o}} \left(\frac{n_{o}}{n_{o} + a} \right)^{i}$$

Now if the original amount of liquid ammonia in the cell is in error by $\delta \eta_{\sigma}$ the the error in C_i , δC_i , is:

$$\delta C_i = -\frac{m_0}{(n_0)^2} \left(\frac{n_0}{n_0 + a} \right)^i \left[1 - \frac{ia}{n_0 + a} \right] \delta n_0$$

Or the relative error is

$$\frac{\langle C_i \rangle}{\langle C_i \rangle} = -(1 - \frac{ia}{n_0 + a}) \frac{\langle n_0 \rangle}{\langle n_0 \rangle}$$

The substitution $n_0 = a$ is made. This is not actually true since $(n_T)_0 = a$ but for this purpose the substitution is satisfactory. The result is

$$\frac{\delta C_i}{C_i} = -(1 - \frac{1}{2}i) \frac{\delta_{n_0}}{n_0}$$

APPENDIX D

DERIVATION OF INTERDEPENDENCE OF $K_1^{(a)}$, $K_1^{(t)}$ AND K_2

Let a_1 = fraction of total metal existing as ions a_2 = fraction of total metal existing as dimers

Then for the equilibria under consideration

$$K_1^{(a)} = \frac{\alpha_1^2 C^2 f_{\pm}^2}{(1 - \alpha_1)C}$$
 [A-1]

$$K_1^{(t)} = \frac{\alpha_1^2 C f^{\pm 2}}{(1 - \alpha_1 - 2\alpha_2)C}$$
 [A-2]

$$K_2 = \frac{(\alpha_2 C)^{\frac{1}{2}}}{(1 - \alpha_1 - 2\alpha_2)C}$$
 [A-3]

where $K_1^{(a)}$ is the apparent, and $K_1^{(t)}$, the true dissociation constants. Solving $K_1^{(a)}$ and $K_1^{(t)}$ for $(1 - \alpha_1)$ and α_2 , respectively, and substitution into the K_2 equation gives

$$K_2^2 = \frac{(K_1^{(t)} - K_1^{(a)})}{2(Caf_{\pm})^2} \cdot K_1^{(t)}$$
 [A-4]

where $a = a_1$.

The expressions for $K_1^{(t)}$ and K_2 are used in calculating y_{\pm} values. The equations [A-2] and [A-3] are combined and solved for a

$$\alpha = 1 - \frac{C\alpha^2 f \pm ^2}{K_1} \left[1 + \frac{2}{K_1} (C\alpha f \pm K_2)^2 \right]$$
 [A-5]

of

$$a^2 = (1 - a) \frac{K_1}{Cf_{\pm}^2 \left[1 + \frac{2}{K_1} (Caf_{\pm} K_2)^2\right]}$$
 [A-6]

The limits on convergence for the first expression became smaller as the concentration increased making the second expression advantageous.

CHEMISTRY LIBRARY